OPTIMIZATION FORMULATIONS FOR MULTI-PRODUCT NETWORKS

by

APOORVA M. SAMPAT

A dissertation submitted in partial fulfillment of
the requirements for the degree of

Doctor of Philosophy
(Chemical Engineering)

at the
UNIVERSITY OF WISCONSIN-MADISON
2020

Date of final oral examination: May 07, 2020

The dissertation is approved by the following members of the Final Oral Committee:

Victor M. Zavala, Associate Professor, Chemical and Biological Engineering
Brian F. Pfleger, Professor, Chemical and Biological Engineering
Thatcher W. Root, Professor, Chemical and Biological Engineering
Rebecca A. Larson, Associate Professor, Biological Systems Engineering

To my family.

ACKNOWLEDGMENTS

I am very fortunate to have people in my life who have inspired me to pursue education and enjoy the process of learning. To thank everyone who has played a part in my journey of learning, in two pages, is an impossible task. I apologize if I forget to thank someone here, but rest assured I am very grateful.

I want to begin by thanking Prof. Thatcher Root, Prof. Brian Pfleger, Prof. Rebecca Larson, and Prof. Victor Zavala for serving on my defense committee and giving me the opportunity to present my work.

I have been incredibly fortunate to have Prof. Victor Zavala as my academic advisor. He has taught me to think critically and ask questions that give insights to the problem. He has been very patient in teaching me how to clearly communicate my ideas, both written and oral, to a wide range of audience. Looking back at where this project started, I would have never anticipated the research accomplishments we have achieved. We have ventured into areas of agricultural systems, environmental engineering, mathematical optimization, game-theory, micro-economics, statistics, and machine learning. He has guided me to learn from these different areas, without getting lost in the non-essential details. I also have to mention the amazing group culture we have at Zavalab. It has been a joy being a part of a group that supports each other through academic and personal endeavors. Through the start of this group, Ranjeet Kumar and Jordan Jalving have been amazing batch-mates and friends. I will cherish the time we spent solving class assignments and later helping each other through research bottlenecks. I also want to thank Alex Dowling, Yankai Cao, Yicheng Hu, Sungho Shin and all group members and visiting students who joined later for creating a fun learning environment.

In the last five years, I have had the opportunity to collaborate with amazing researchers and graduate students. From my first year I started working with Prof. Rebecca Larson and her team including Dr. Mahmoud Sharara and Dr. Horacio Aguirre-Villegas, who introduced me to the area of agricultural systems. This work would not have been possible without their expertise and insights to the subject. In the second year, Yicheng Hu joined our lab and expanded this project. Specifically his GIS plots, many of which are included in this dissertation, still amaze me by the economic and geo-spatial insights they provide. I also started working with Prof. Mariano Martín and Edgar Martín in my second year. They have been amazing friends and colleagues in providing me the data for various nutrient and energy recovery technologies. The following summer, I worked with Dr. Gerardo Ruiz-Mercado at the U.S. Environmental Protection Agency. He taught

me about policy design and made me think about the project from the perspective of different stakeholders. During this time, we also began an intra-university research project - INFEWS. The discussions we had during these meetings have been crucial to the project. In my penultimate year, I enjoyed working with Dr. Victor M. Saucedo, Remya Pushpangatha Kurup, and Kawa Chiu at Genentech. They taught me to address the operational challenges of industry through mathematical optimization models.

During the course of my graduate studies, I also learned another skill - taekwondo. The Taekwondo Club at the University of Wisconsin-Madison has played a huge role in helping me maintain my sanity through the rigorous demands of graduate school. I have met some of the most amazing people through this club. One of the most memorable times of my stay in Madison has been training with the club and preparing for collegiate nationals (including running by Lake Mendota, hill sprints, and climbing Van Vleck stairs in the freezing winters). I want to thank Master Park, James, Evan, Micah, Emma, Scott, and Alice for coaching me and encouraging me to participate in local and national tournaments. I am also thankful to the club for providing me the opportunity to experience leadership roles through my appointment in the executive board and instructors board.

I have made incredible friends in Madison during the last five years. Ranjeet has been a great friend and always provided sound advice to both my personal and professional challenges. Saurabh, Jordan, Ashwin, Sandy, and Coogan have been amazing friends who made my stay in Madison so much enjoyable. When I first arrived in Madison, Clark and Kaitlin helped me transition to the life in U.S. They invited me to numerous personal and social events to foster cultural exchange. I had most fun in Madison when Carol and Renke were visiting our lab. Over a short period of time, they became very good friends of mine.

I would have never had the opportunity to purse my graduate studies in Madison, had it not been for my undergraduate alma mater - Institute of Chemical Technology, Mumbai (ICT). Here, I was exposed to fours years of well-rounded chemical engineering curriculum. Professors J.B. Joshi, Ashwin Patwardhan, Sunil Bhagwat, Aniruddha Pandit, Ravi Mariwala, and Anand Patwardhan inspired me to pursue research as a career and ignited in me a sense of curiosity for chemical engineering. I also made life-long friends at ICT who continue to support me even after almost a decade.

Last and certainly not least, I want to thank my family for their unwavering support and unconditional love. My parents, sister, and grandparents have been my biggest cheerleaders through good and bad times. I am thankful beyond words for their presence in my life.

Apoorva M. Sampat
Madison, WI
May 2020

CONTENTS

LIST OF FIGURES

LIST OF TABLES

ABSTRACT

Multi-product network models are routinely used to evaluate the economic and environmental performance of infrastructure networks such as electricity and biomass supply chains. Several models in the literature deal with different types of systems, constraints, and study areas. Unfortunately, these models are usually developed on a case-by-case basis. This lack of coherence limits systematic comparisons (benchmarks), collaboration and sharing of data sets, analysis of solution properties, and development of software implementations. Our work provides a coherent way to model multi-product networks.

The key research accomplishment of this work is the development of multi-product network models that aid decision-making. When multiple stakeholders are involved, the final solution is often derived by qualitative discussions. This work provides quantitative tools to drive those decisions and achieve an optimal compromise solution. From a modeling perspective, this work has developed mathematical frameworks to: (i) model supply chains in a coherent manner, (ii) derive economic interpretations of supply chains, and (iii) allocate resources amongst multiple stakeholders in a fair manner.

We apply these modeling frameworks to a case study for organic waste management in the Upper Yahara watershed region in the state of Wisconsin, U.S. Excessive amounts of phosphorus have accumulated in this area, primarily due to livestock manure and the heavy use of agricultural fertilizers. Rain and snow melt often wash these nutrients into waterways, which lead to the blue-green algae blooms in the Yahara lakes. Our modeling abstraction captures the complex product dependencies in this setting and provides insights into policy decisions that can drive waste processing and reduce phosphorus runoff.

1

INTRODUCTION

1.1 Multi-Product Networks

Multi-product networks form the basis of a variety of infrastructure networks such as gas, electric, water, transportation, communications, and biomass supply chains. These networks involve products that are transported to spatially dispersed facilities to be transformed into intermediate and final products that are delivered to final destinations. These networks have been extensively modeled in the literature on a case-by-case basis to account for different types of systems, constraints, and study areas. This case-specific approach has rendered a lack of coherence, thus making it difficult to systematically analyze these networks and develop software implementations.

Similar observations have been made in other fields such as chemical process synthesis and planning and scheduling, where innovations in modeling abstractions (e.g., disjunctive programming formulations (Raman and Grossmann, 1994) and state-task networks (Kondili et al., 1993)) have spurred the development of formulations with stronger theoretical properties, a wider range of applications and more efficient solution strategies (Yeomans and Grossmann, 1999). We seek to establish general modeling abstractions for multi-product networks, by merging concepts from interdependent infrastructure net-

works and supply chains.

The agricultural industry is an important application area of supply chain models. Models have been recently developed for biomass-to-fuels supply chains for the conversion of food crops to biodiesel (You and Grossmann, 2008a,b; Mele et al., 2011; Giarola et al., 2011; Zamboni et al., 2009; Akgul, O., Zamboni, A., Bezzo, F., Shah, N., & Papageorgiou, 2010; Corsano et al., 2011), cellulosic biomass to biodiesel (Alex Marvin et al., 2012; Ekşioğlu et al., 2009; Čuček et al., 2010; Huang et al., 2010; Leduc et al., 2010; Dal-Mas et al., 2011; Santibañez-Aguilar et al., 2011; Akgul et al., 2012; Chen and Fan, 2012; Chen, 2014), cellulosic biomass to general biofuels (Parker et al., 2010; Tittmann et al., 2010; Bowling et al., 2011; Kim et al., 2011a,b; Papapostolou et al., 2011; You and Wang, 2011; Walther et al., 2012), algae to biofuels (Avami, 2012), and biomass to energy (Elia et al., 2011; Dunnett et al., 2007; Dawoud et al., 2007; Burak Aksoy, Harry Cullinan, David Webster, Kevin Gue, Sujith Sukumaran, Mario Eden and Jr., 2011; Čuček et al., 2012). Recent studies have also pointed out the need to model complex interactions over a wider range of products that include food, water, and energy resources (Garcia and You, 2016; Čuček et al., 2014).

Our work identifies these issues and answers three important research questions about multi-product networks:

1. Does there exist a single modeling abstraction?
2. What is the inherent value of products?
3. What makes a resource allocation fair?

We provide mathematical analysis of these questions and apply our findings to the problem of organic waste management in the state of Wisconsin, US. Excessive amounts of phosphorus have accumulated in this area, primarily due to livestock manure and the heavy use of agricultural fertilizers. Rain and snow melt often wash these nutrients into waterways, which lead to the blue-green algae blooms in the Yahara lakes. Our modeling abstraction captures the complex product dependencies in this setting and provides

insights into policy decisions that can drive waste processing and reduce phosphorus runoff.

1.2 Organic Waste Management

Urban, agricultural, and food sectors produce significant amounts of organic waste (mostly in the form of livestock waste, food waste, and biosolids from wastewater processing). To give some perspective, the dairy sector in the U.S. State of Wisconsin is a 43 billion USD enterprise that manages 1,270,000 dairy cows (University of Wisconsin-Extension, 2015; USDA National Agricultural Statistics Service (NASS), 2014) and provides 29 billion gallons of milk and 2.8 billion pounds of cheese annually. A single dairy cow produces approximately 6,800 gallons of manure per year and the entire sector generates 8.7 billion gallons of manure per year (USDA - National Agriculture Statistics Service, 2018; State of Wisconsin - Department of Agriculture, Trade, and Consumer Protection, 2018). Moreover, it is estimated that 30% of all dairy food products supplied by the sector are wasted (Cuéllar and Webber, 2010). Waste management operations (collection, processing, and disposal) are becoming increasingly troublesome and costly due to ever increasing volumes of waste streams, their highly distributed nature, and their complex bio-physico-chemical composition. When left untreated, organic waste releases excess nutrients, chemicals, and biological agents to the soil, surface and ground waters, and emissions to the atmosphere, ultimately disrupting natural ecosystems. Nutrients in livestock waste and biosolids such as phosphorus and nitrogen accumulate in surface water bodies (e.g. lakes, ponds) triggering algal blooms and degrading the quality of water resources (Belsky et al., 1999; Hoagland and Scatasta, 2006). Decreased water quality ultimately impacts health and socio-economic activities that are fundamental for some regions (e.g., tourism, real estate, swimming, sailing, fishing). To give some perspective, in the State of Wisconsin, the estimated annual phosphorus (P) input from livestock manure application as fertilizer is 103 million pounds while the input from synthetic fertilizers is

96 million pounds (Bundy and Sturgul, 2001). The total estimated P removed from crop production (corn grain, silage, hay, and soybeans) is around 150 million. Consequently, the accumulation is on the order of 50 million pounds per year. From this surplus, it is estimated that nearly 3 million pounds of P are lost to water bodies through runoff. P surplus arises because manure is often over applied as a fertilizer by farmers in order to match crop nitrogen needs and/or because farmers might have insufficient land base available for manure application. Moreover, farmers usually have an incentive to overapply fertilizer in order to mitigate risk associated with weather, soil conditions, and crop yields (Sheriff, 2005). In several areas of the state, the amount of P accumulated in the soil has reached levels that can cover crop P needs for 20 years. This accumulation of P increases nutrient loses contributing to the diverse environmental and human health impacts across the region (State of Wisconsin - Department of Natural Resources, 2016). Current management of livestock manure is not sustainable and scalable, endangering the economic prospects of the dairy industry. In addition, organic matter contained in livestock waste, food waste, and wastewater generates harmful and odorous pathogens and gases (e.g., methane and ammonia) that leak to the atmosphere. For instance, landfills were the third largest anthropogenic source of methane in the U.S. in 2016 (accounting for 14% of the total methane emissions (U.S. Environmental Protection Agency, 2018).

1.3 Outline

This dissertation is structured as follows:

Chapter 2 – Modeling Abstraction. This chapter introduces the modeling abstraction that coherently captures the inter-dependencies in a multi-product network. We use this model consistently through this dissertation to answer questions about multi-product networks.

Chapter 3 – Technologies for Nutrient Recovery. The applicability of our modeling framework is demonstrated through the problem of phosphorus runoff in the Upper Yahara watershed region, WI. This chapter provides a review of the nutrient processing technologies for phosphorus recovery.

Chapter 4 – Policy Design: Environmental Regulations and Incentives. This chapter provides a mathematical framework to account for external impetus such as federal and state incentives that can drive the processing of products in a multi-network supply chain.

Chapter 5 – Coordinated Management and Inherent Value of Products. This chapter provides a stakeholder perspective to multi-product network which helps in revealing the inherent value of products. We present a coordination framework that enables handling of complex interdependencies between products and locations in the network.

Chapter 6 – Quantifying Economic Impacts of Phosphorus Runoff. This chapter introduces the concept of treating the environment as one of the market players. We quantify the environmental impact of phosphorus runoff and utilize this value for market for organic waste processing. We combine this analysis with the coordination framework from previous chapter to activate the market for organic waste processing.

Chapter 7 – Fairness Measures for Decision-Making and Conflict Resolution. This chapter provides mathematical foundations for allocating resources amongst stakeholders in a fair manner. It sets the foundation for answering how the environmental cost estimated in the previous chapter should be distributed amongst stakeholders.

Chapter 8 – Conclusions and Future Directions. This chapter provides a summary of the major contributions of this dissertation. Specific areas for improvement for future research are also identified.

2

MODELING ABSTRACTION

2.1 Introduction

Multi-product supply chain networks involve a set of products that are transported to geographically dispersed facilities to be transformed into intermediate and final products that are delivered to final destinations. These models are used to identify optimal facility types, sizes, and locations (network design) as well as to identify optimal resource allocation strategies (network management/operation) (Bloemhof-Ruwaard et al., 1996; Guillén-Gosálbez and Grossmann, 2009; You et al., 2012; Kim et al., 2008; Neiro and Pinto, 2004; Papageorgiou et al., 2001; You et al., 2009; Grossmann, 2004). Coupled infrastructure networks (e.g., gas, electric, water) as well as chemical supply chains are important application areas. The presence of *product transformations* is a key feature that distinguishes these models from those arising in other domains such as multi-commodity network flows (Hu, 1963).

In this chapter, we present optimization formulations for multi-product supply chain networks. The formulations use a general multi-product network representation that considers a set of technologies placed at a set of nodes and under which a set of products undergo transformations. Interactions between products are captured by using a *hierar-*

chical graph that maps products at each node using a transformation matrix and that maps network nodes using transportation paths (arcs). The proposed graph abstraction combines modeling concepts from supply chain and infrastructure network modeling. With this we seek to provide a formal and general representation that can cover a wide range of settings existing in the literature (which tend to be developed on a case-by-case basis). For instance, the formulations presented in (Bowling et al., 2011; Hugo and Pistikopoulos, 2005; Kalaitzidou et al., 2015; You et al., 2012) capture interactions between multiple products but no general representation is provided. Our abstraction also makes an explicit distinction between in-network (derived) product flows and out-of-network source (supply) and sink (demand) product flows. This feature can be used to couple boundaries of different systems and to derive internal prices (for intermediate products) in a more systematic manner, compared to existing models (Alex Marvin et al., 2012; An et al., 2011; Balaman and Selim, 2014; Kim et al., 2011b). Our graph abstraction resembles that used in p-graphs (Varbanov and Friedler, 2008; Lam et al., 2010) in which nodes are interpreted as technologies (unit operations) that transform products. The p-graph abstraction enables the use of graph-theoretical strategies to identify feasible pathways between products and feasible network topologies (i.e., superstructures) (Varbanov and Friedler, 2008) as well as to design supply chains (Čuček et al., 2010). Our proposed abstraction extends this work by using a general optimization setting that includes more complex sets of constraints and objectives. In particular, we show how to use the formulations to capture conflicting priorities on different metrics and geographical network locations. We demonstrate the applicability of the proposed framework by using a case study in the State of Wisconsin in which we seek to design supply chains to process organic waste from a set of concentrated animal feeding operations (CAFOs) to mitigate point phosphorus (P) and methane emissions.

The chapter is structured as follows. In Section 2.2 we introduce the proposed multi-product network abstraction. In Section 2.3 we discuss how this framework can be used to derive high-level optimization formulations. In Section 2.4 we apply the proposed frame-

work to case studies that seek to perform P and biogas recovery from agricultural organic waste across the State of Wisconsin. The paper closes in Section 2.5 with conclusions and directions for future work.

2.2 Multi-Product Network Modeling

We consider a network (a graph) that comprises a set of nodes $\mathcal{N}$, links (arcs) $\mathcal{L}$, products $\mathcal{P}$, sources $\mathcal{S}$, sinks $\mathcal{D}$, and technologies $\mathcal{T}$.

Associated with each source $i \in \mathcal{S}$ there is a supply flow $s_i \in \mathbb{R}_+$, product type $p(i) \in \mathcal{P}$, maximum offered capacity $\bar{s}_i \in \mathbb{R}_+$, location $n(i) \in \mathcal{N}$, and supply cost $\alpha_i^s \in \mathbb{R}_+$. Associated with each sink $j \in \mathcal{D}$ there is a demand flow $d_j \in \mathbb{R}_+$, product type $p(j) \in \mathcal{P}$, maximum requested capacity $\bar{d}_j \in \mathbb{R}_+$, location $n(j) \in \mathcal{N}$, and demand cost $\alpha_j^d \in \mathbb{R}_+$. We use attributes to define the nested sets $\mathcal{S}_{n,p} \subseteq \mathcal{S}_n \subset \mathcal{S}$ with $\mathcal{S}_n := \{i \mid n(i) = n\}$ (i.e., all suppliers attached to node n) and $\mathcal{S}_{n,p} := \{i \mid n(i) = n, p(i) = p\}$ (i.e., all suppliers of product p attached to node n). We follow a similar reasoning to define the nested sets $\mathcal{D}_{n,p} \subseteq \mathcal{D}_n \subset \mathcal{D}$.

Associated with each link $\ell \in \mathcal{L}$ there is a flow $f_\ell \in \mathbb{R}_+$, product type transported $p(\ell) \in \mathcal{P}$, maximum capacity $\bar{f}_\ell \in \mathbb{R}_+$, transportation cost $\alpha_\ell^f \in \mathbb{R}_+$, sending (source) node $n_s(\ell) \in \mathcal{N}$, and receiving (destination) node $n_r(\ell) \in \mathcal{N}$. The transportation cost captures operational costs associated with the movement of a unit of flow from the source to the destination node. The set $\mathcal{L}_n^{in} := \{\ell \mid n_r(\ell) = n\}$ is the set of all flows entering node $n \in \mathcal{N}$, the set $\mathcal{L}_n^{out} := \{\ell \mid n_s(\ell) = n\}$ is the set of all flows leaving node $n \in \mathcal{N}$. We also define the nested subsets for entering flows $\mathcal{L}_{n,p}^{in} \subseteq \mathcal{L}_n^{in} \subseteq \mathcal{L}$ where $\mathcal{L}_{n,p}^{in} := \{\ell \mid n_r(\ell) = n, p(\ell) = p\}$ is the set of flows entering node n and carrying product p and we note that $\cup_{p \in \mathcal{P}} \mathcal{L}_{n,p}^{in} = \mathcal{L}_n^{in}$. We use similar definitions to construct subsets $\mathcal{L}_{n,p}^{out} \subseteq \mathcal{L}$. The notation and node-level interactions are sketched in Figure 2.1.

Associated with each technology $t \in \mathcal{T}$ there are transformation (yield) factors $\gamma_{t,p} \in \mathbb{R}$, a reference product $p(t) \in \mathcal{P}$, processing capacity $\bar{\xi}_t \in \mathbb{R}_+$, processing (operating)

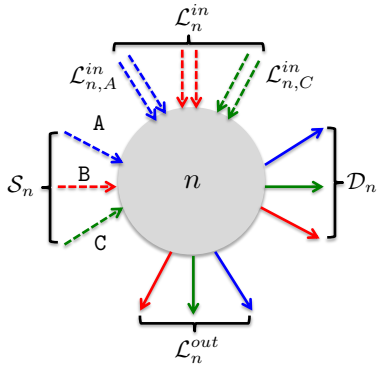

Figure 2.1: Sketch of input and output flow sets into node n for products A, B, C.

cost $\alpha_t^{\xi} \in \mathbb{R}_+$, and location $n(t) \in \mathcal{N}$. Transformation factors represent units of product p consumed/generated per unit of reference product $p(t)$ consumed/generated in the transformation technology. We use the convention that $\gamma_{t,p} > 0$ if product p is generated in the technology t, $\gamma_{t,p} < 0$ if product p is consumed in the technology, and $\gamma_{t,p} = 0$ if product p is neither produced nor consumed in technology. Moreover, we use the convention that $\gamma_{t,p(t)} = -1$ (i.e., one unit of reference product is consumed to produce/consume other products). For each technology we also define an extent of transformation $\xi_t \in \mathbb{R}_+$, which is the total amount of $p(t)$ processed.

Using these basic definitions we impose the following product balances at each node $n \in \mathcal{N}$ in the network:

$$\left(\sum_{i \in \mathcal{S}_{n,p}} s_i + \sum_{\ell \in \mathcal{L}_{n,p}^{in}} f_\ell\right) - \left(\sum_{j \in \mathcal{D}_{n,p}} d_j + \sum_{\ell \in \mathcal{L}_{n,p}^{out}} f_\ell\right) + \sum_{t \in \mathcal{T}_n} \gamma_{t,p}\, \xi_t = 0, \ (n,p) \in \mathcal{N} \times \mathcal{P} \qquad (2.2.1)$$

The first term in parenthesis is the total input flow for product p (given by supply flows and links entering the node). The second term in parenthesis is the total output flow of product p (given by the demand flows and links leaving the node). The third therm is the generation/consumption flow of product p. The notation and network-level interactions are sketched in Figure 2.2.

The total input flow of the reference product $p(t)$ for technology $t \in \mathcal{T}_n$ in node n are

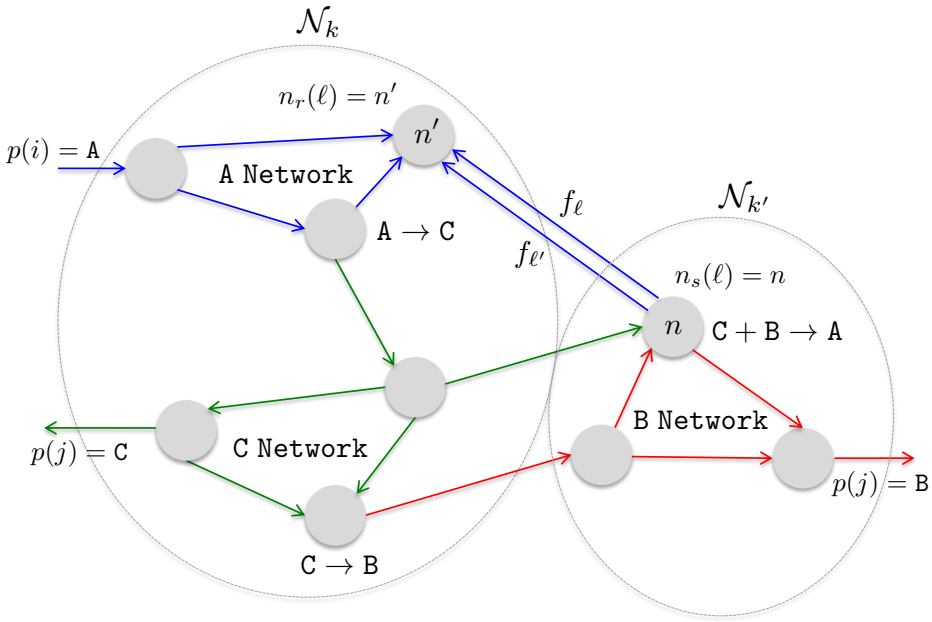

Figure 2.2: Sketch of multi-product network coupling and notation.

modeled as (for simplicity, assuming only one technology at a node):

$$\left(\sum_{i \in \mathcal{S}_{n,p(t)}} s_i + \sum_{\ell \in \mathcal{L}^{in}_{n,p(t)}} f_\ell \right) = \xi_t, \quad n \in \mathcal{N}. \tag{2.2.2}$$

We note that equations (2.2.1) and (2.2.2) can be combined to give:

$$\left(\sum_{i \in \mathcal{S}_{n,p}} s_i + \sum_{\ell \in \mathcal{L}^{in}_{n,p}} f_\ell \right) - \left(\sum_{j \in \mathcal{D}_{n,p}} d_j + \sum_{\ell \in \mathcal{L}^{out}_{n,p}} f_\ell \right) + \gamma_{t,p} \left(\sum_{i \in \mathcal{S}_{n,p(t)}} s_i + \sum_{\ell \in \mathcal{L}^{in}_{n,p(t)}} f_\ell \right) = 0$$

$$(n, p) \in \mathcal{N} \times \mathcal{P} \tag{2.2.3}$$

From these expressions it becomes clear that individual product networks couple at the nodes. We can also see that the transformation factors $\gamma_{t,p}$ measure the strength of the coupling between networks (by setting $\gamma_{t,p} = 0$ we decouple the networks). The balance

for reference product $p(t)$ can also be expressed as:

$$(1+\gamma_{n,p(t)})\left(\sum_{i\in\mathcal{S}_{n,p(t)}} s_i + \sum_{\ell\in\mathcal{L}^{in}_{n,p(t)}} f_\ell\right) - \left(\sum_{j\in\mathcal{D}_{n,p(t)}} d_j + \sum_{\ell\in\mathcal{L}^{out}_{n,p(t)}} f_\ell\right) = 0,\ n\in\mathcal{N}. \tag{2.2.4}$$

We can thus see that $\gamma_{n,p(t)} \geq -1$ must hold. Capacities on flows, sources, sinks, and processing technologies are given by:

$$0 \leq f_\ell \leq \bar{f}_\ell,\ \ell\in\mathcal{L} \tag{2.2.5a}$$

$$0 \leq s_i \leq \bar{s}_i,\ i\in\mathcal{S} \tag{2.2.5b}$$

$$0 \leq d_j \leq \bar{d}_j,\ j\in\mathcal{D} \tag{2.2.5c}$$

$$0 \leq \xi_t \leq \bar{\xi}_t,\ t\in\mathcal{T}. \tag{2.2.5d}$$

We highlight some key features of the proposed abstraction. The products can be interpreted as primary or derived products such as natural gas, electricity, sensor information, raw and derived chemical products, pollutants, water, or stream of different quality that come from the network boundary (i.e., out-of-network) or from the network (i.e., in-network). Products induce a hierarchy of primary, secondary, and final products at the nodes (e.g., biomass to biodiesel to carbon dioxide) directly from the transformation factors $\gamma_{n,p}$ or implicitly through the network. The supply flows s_i are *out-of-network* suppliers while $\gamma_{t,p}\xi_t$ (with positive $\gamma_{t,p}$) are *in-network* supply flows. In other words, out-of-network supplies are not produced at the nodes but enter the system for its boundaries. Similarly, d_j are out-of-network demands while $\gamma_{t,p}\xi_t$ (with negative $\gamma_{t,p}$) are in-network demands. Technologies (pieces of equipment or entire facilities) at a node perform physico-chemical transformations (e.g., chemical plants, separators, power plants, heat exchangers, biodigesters, storages, compressor, pumps). The transformation factors can be used to specify chemical reactions (induced or due to degradation), split factors, or storage efficiencies to model losses or gains due to interactions with the environment.

In-network production flows $\gamma_{t,p}\xi_t$ are expressed as a function of the reference prod-

uct and are defined by $\gamma_{t,p}$ (i.e, units of p produced per unit of reference product $p(t)$). For nodes that do not perform transformations we set $\gamma_{t,p} = 0$ and they become simple transportation/transshipment nodes. The cost factors for suppliers, demands can be interpreted as *offering prices* for products at different locations (nodes) and we note that there might be multiple suppliers and demands of the same product to a single node. Cost factors for production flows can be used to capture offering/supply costs for products in different technologies (e.g., different technologies can generate a product at different costs). Cost factors for flows can be interpreted as offering prices for transportation services for a given link (or can be used to capture other features such as transportation delays). We note that multiple links can exist between nodes with different transportation costs (to reflect the possibility that different types of transportation or links of the same type are available). We thus seek to highlight that the proposed modeling abstraction is general and flexible.

2.2.1 *Degrees of Freedom*

We define $N = |\mathcal{N}|$, $L = |\mathcal{L}|$, $P = |\mathcal{P}|$, $S = |\mathcal{S}|$, $D = |\mathcal{D}|$, and $T = |\mathcal{T}|$ (where $|\cdot|$ denotes the cardinality of the set). The total number of variables is given as follows: for flows f_ℓ is L, for sources s_i is S, for sinks d_j is D, and for processed input flow ξ_t is T. This gives a total of $T + L + S + D$ variables. The total number of equations is: for node balances (2.2.1) is $N \cdot P$. This gives a total of NP equations. The total number of degrees of freedom is $T + L + S + D - NP$. Consequently, these many variables need to be specified for the network to be fully defined.

If we define a source and a sink per node and per product (i.e., $S = D = NP$), and a technology per node (i.e., $T = N$), the number of degrees of freedom is $N + L + NP + NP - NP = N + L + NP = N(P + 1) + L$. Consequently, in addition to specifying all the flows, we need to specify $N(P + 1)$ sinks or sources for the system to be fully defined. In the single product case (i.e., $P = 1$), we would need to specify the $2N$ sinks or sources in

addition to the flows to fully define the system. We also note that the number of flows connecting the nodes can be extremely large. For instance, if we consider that a flow can exist between any pair of nodes, for every product, and in every direction, but no self-flows are allowed (i.e., $f_\ell = 0$ for $n_s(\ell) = n_r(\ell)$) we have $L = 2N(N-1) \cdot P$ flow variables. This shows a quadratic growth in complexity with the number of network nodes. For instance, a network with $O(10^2)$ nodes has $O(10^4)$ possible flows.

2.2.2 *Transportation Nodes and Decoupled Networks*

For a given product p, the balance equation at node n with no generation/consumption ($\gamma_{t,p} = 0$) is:

$$\left(\sum_{i \in \mathcal{S}_{n,p}} s_i + \sum_{\ell \in \mathcal{L}^{in}_{n,p}} f_\ell \right) - \left(\sum_{j \in \mathcal{D}_{n,p}} d_j + \sum_{\ell \in \mathcal{L}^{out}_{n,p}} f_\ell \right) = 0, \quad n \in \mathcal{N} \tag{2.2.6}$$

The node becomes a simple transportation node for product p. The case with $\gamma_{t,p} = 0$ for all $t \in \mathcal{T}_n, n \in \mathcal{N}$ and $p \in \mathcal{P}$ indicates also that there is no product transformation at any node, and the balance equations become:

$$\left(\sum_{i \in \mathcal{S}_{n,p}} s_i + \sum_{\ell \in \mathcal{L}^{in}_{n,p}} f_\ell \right) - \left(\sum_{j \in \mathcal{D}_{n,p}} d_j + \sum_{\ell \in \mathcal{L}^{out}_{n,p}} f_\ell \right) = 0, \ (n,p) \in \mathcal{N} \times \mathcal{P} \tag{2.2.7}$$

This indicates that the individual product networks decouple, as is the case of multi-commodity network flow models (i.e., the proposed representation can capture this case as well). This situation also arises in electrical, gas, and electrical network models when interdependencies are ignored.

2.3 Optimization Formulations

We now illustrate how to incorporate the proposed framework into high-level optimization problems of interest in network design.

2.3.1 *Network Operations*

The resource allocation problem is a classical problem in supply chain optimization that seeks to capture operational performance (in the form of economics, environmental, or social objectives). To define this problem using the proposed notation, we consider supply cost, demand cost, generation/ consumption cost, and transportation cost for each element of the network:

$$\phi_j^d = \alpha_j^d d_j,\ j \in \mathcal{D} \tag{2.3.8a}$$

$$\phi_i^s = \alpha_i^s s_i,\ i \in \mathcal{S} \tag{2.3.8b}$$

$$\phi_\ell^f = \alpha_\ell^f f_\ell,\ \ell \in \mathcal{L} \tag{2.3.8c}$$

$$\phi_t^\xi = \alpha_t^\xi \xi_t,\ t \in \mathcal{T}. \tag{2.3.8d}$$

This gives rise to the multi-objective allocation problem:

$$\min \{\phi_j^d, \phi_i^s, \phi_\ell^f, \phi_t^\xi\} \tag{2.3.9a}$$

$$\text{s.t. } (2.2.1), (2.2.5). \tag{2.3.9b}$$

This formulation seeks to capture inherent trade-offs between revenue collected from individual sources, cost incurred by sinks (consumers), revenue/costs of in-network suppliers/consumers (technology provides), and revenue of transportation providers. Here, we assume that each supplier, demand, flow, and technology provider represents a different objective. This allows us to capture natural conflicts among network locations. Consequently, this problem can be interpreted as a market clearing problem (Pritchard

et al., 2010; Zavala et al., 2017).

In summary, the statement of the network operation problem is: Given a set of products ($\mathcal{P}$), sources ($\mathcal{S}$), sinks ($\mathcal{D}$), nodes ($\mathcal{N}$), and technologies ($\mathcal{T}$) the goal is to determine an optimal allocation of flows (f_ℓ), product supplies (s_i), demands (d_j), and product processing (ξ_t) that is a Pareto optimal solution of the problem (2.3.9).

Prioritization

Traditionally, a compromise (Pareto) solution for the multi-objective problem is found by maximizing the social welfare function:

$$\phi = \underbrace{\sum_{j\in\mathcal{D}} \phi_j^d}_{\phi_d} + \underbrace{\sum_{i\in\mathcal{S}} \phi_i^s}_{\phi_s} + \underbrace{\sum_{\ell\in\mathcal{L}} \phi_\ell^f}_{\phi_f} + \underbrace{\sum_{t\in\mathcal{T}} \phi_t^\xi}_{\phi_\xi}. \tag{2.3.10}$$

This formulation implicitly seeks to maximize the demand served while minimizing supply and transportation costs (recall that cost coefficients for in-network and out-of-network flows are negative). One can easily show that the solution of this problem is a Pareto optimal solution of problem (2.3.9). Moreover, the coefficients α_i^s, α_j^d, α_ℓ^f, α_t^ξ are used to prioritize different node locations and often have natural economical interpretations (i.e., offering prices).

We also note that a solution of the social welfare problem is a Pareto optimal solution of the aggregated problem:

$$\min \{\phi^d, \phi^s, \phi^f, \phi^\xi\} \tag{2.3.11a}$$

$$\text{s.t. } (2.2.1), (2.2.5) \tag{2.3.11b}$$

in which we capture trade-offs between *total* supply, demand, transportation, and production costs. It is also well-known that a Pareto optimal solution to this problem can be found by using an ϵ-constrained method. In this approach we solve problems of the

form:

$$\min \phi^d \tag{2.3.12a}$$

$$\text{s.t. } (2.2.1), (2.2.5) \tag{2.3.12b}$$

$$\phi^s \leq \epsilon^s,\ \phi^f \leq \epsilon^f,\ \phi^\xi \leq \epsilon^\xi. \tag{2.3.12c}$$

where $\epsilon^s, \epsilon^f, \epsilon^\xi$ are threshold values. We note that we have picked (arbitrarily and without loss of generality) the demand cost as the cost to be minimized. It is also possible to derive ϵ-constrained formulations by using the individual node costs but this would result in an extremely large number of threshold values to be specified. Because of this, it is often difficult to identify threshold values under which a feasible solution exists.

Multi-Stakeholder Prioritization

In certain settings, the coefficients α_i^s, α_j^d, α_ℓ^f, α_t^ξ do not have well-defined values. This can be because markets for certain products (e.g., agricultural or food waste) are not well-established or because different decision-makers (e.g., government agencies or facility managers) attribute different importance to different geographical locations. In such cases, it is possible to rely on *opinions* from multiple stakeholders that seek to express their priorities and to use such opinions to identify compromise solutions for the multi-objective problem (2.3.9).

Consider the situation in which a stakeholder $\omega \in \Omega$ prioritizes the total cost vector $\phi = (\phi^d, \phi^s, \phi^f, \phi^\xi)$ by using the weight vector $\mathbf{w}_\omega$ to construct the scalar function $\mathbf{w}_\omega^T \phi$. The optimal solution for this stakeholder is thus given by:

$$f_\omega := \min \mathbf{w}_\omega^T \phi \tag{2.3.13a}$$

$$\text{s.t. } (2.2.1), (2.2.5). \tag{2.3.13b}$$

Here, f_ω is the optimal objective for the stakeholder ω given her/his priority vector and

represents the situation in which the stakeholder is *most satisfied*. Stakeholders, however, will naturally disagree on how to prioritize the different objective functions. Consequently, we define a dissatisfaction function that will measure how dissatisfied is stakeholder $\omega \in \Omega$ with an alternative solution that is not optimal for her/his priorities (i.e., it is not the solution of (2.3.13)). The dissatisfaction function is given by $d_\omega = \mathbf{w}_\omega^T \phi - f_\omega$. A compromise solution for the stakeholders can thus be found by minimizing a measure of the dissatisfactions d_ω, $\omega \in \Omega$. Dowling et al. (2016) propose to use the conditional value at risk (CVaR) as a *collective dissatisfaction measure* that we seek to minimize. The resulting problem is given by:

$$\min \ \ \nu + \frac{1}{\beta \mid \Omega \mid} \sum_{\omega \in \Omega} [d_\omega - \nu]_+ \tag{2.3.14a}$$

$$\text{s.t. } (2.2.1), (2.2.5). \tag{2.3.14b}$$

where $\beta \in (0, 1]$ is a probability level and ν is the value at risk. One can show that this problem minimizes the worst dissatisfaction when $\beta \to 0$ and it minimizes the average collective dissatisfaction when $\beta = 1$. Moreover, one can show that the solution of the CVaR problem are Pareto optimal for (2.3.9).

In the proposed setting, the stakeholders prioritize supply, demand, generation, and transportation costs. The multi-stakeholder framework, however, is general and can also be used to find compromise solutions for stakeholders prioritizing individual nodes (or regions) and products. We also highlight that the computation of the compromise solution does not require the computation of the Pareto set (which is intractable when many objectives are considered). On the other hand, this approach cannot identify the shape of the Pareto set, as is done is traditional multi-objective optimization and dimensionality reduction methods (Miettinen, 2012; Copado-Méndez et al., 2014).

The multi-stakeholder setting discussed here can be seen as a quasi-cooperative decision-making framework in which stakeholders have their own individual priorities expressed through via the weights $\mathbf{w}_\omega$. A compromise solution for the stakeholders is found cen-

trally (in a cooperative manner) by solving the CVaR minimization problem. We note that this approach yields a Pareto efficient solution while a fully decentralized approach (in which stakeholders do not reveal their priorities) does not. In particular, a decentralized setting often finds a game-theoretical equilibrium (e.g., a Nash equilibrium) which is not Pareto efficient. For more information on different decision-making settings arising in supply chains the reader is referred to Garcia and You (2015).

2.3.2 *Network Design*

In addition to finding optimal allocation for resources, we often seek to identify optimal locations for different types of technologies (and associated capacities) to enhance operational performance. This problem is often referred to as the facility location or supply chain design problem.

Under the proposed modeling abstraction, we use the binary variable $y_t \in \{0,1\}$ to indicate that technology $t \in \mathcal{T}_n$ is installed at node n. Each technology $t \in \mathcal{T}_n$ has a set of transformation factors $\gamma_{t,p}$, reference product $p(t)$, capacity $\bar{\xi}_t$, and investment cost $\alpha_t^I \in \mathbb{R}_+$. The transformation factors $\gamma_{t,p}$ capture the consumption/generation of products $p \in \mathcal{P}$ in technology $t \in \mathcal{T}_\mathcal{N}$ and represent the amount of product p that is consumed/generated per unit of reference product $p(t)$ consumed/generated.

We express the balance equations that capture all the possible technologies to be installed at node $n \in \mathcal{N}$ as:

$$\left(\sum_{i\in\mathcal{S}_{n,p}} s_i + \sum_{\ell\in\mathcal{L}^{in}_{n,p}} f_\ell\right) - \left(\sum_{j\in\mathcal{D}_{n,p}} d_j + \sum_{\ell\in\mathcal{L}^{out}_{n,p}} f_\ell\right) + \sum_{t\in\mathcal{T}_n} \gamma_{t,p}\,\xi_t = 0,\ (n,p) \in \mathcal{N}\times\mathcal{P} \tag{2.3.15}$$

We now introduce the logic that only one technology can be installed per node:

$$\sum_{t\in\mathcal{T}_n} y_t \leq 1,\ n \in \mathcal{N}. \tag{2.3.16}$$

The processed flow of technology t is bounded by the capacity of the installed technology:

$$0 \leq \xi_t \leq \bar{\xi}_t, \ t \in \mathcal{T}_n, n \in \mathcal{N}. \tag{2.3.17}$$

The capacities for the sources and sinks are given by:

$$0 \leq s_i \leq \bar{s}_i, \ i \in \mathcal{S} \tag{2.3.18a}$$

$$0 \leq d_j \leq \bar{d}_j, \ j \in \mathcal{D} \tag{2.3.18b}$$

In certain situations it is also of interest to consider the possibility of installing different types of technologies to transport products (e.g., a gas pipeline or a roadway). If we define the set of candidate transport technologies $\mathcal{T}_\ell$, such a problem can be formulated in a straightforward manner by using the following set of constraints:

$$0 \leq f_\ell \leq \bar{f}_t \cdot w_{t,\ell}, \ t \in \mathcal{T}_\ell, \ \ell \in \mathcal{L} \tag{2.3.19}$$

where the binary variable $w_{t,\ell} \in \{0, 1\}$ indicates that technology t is used in link ℓ. The flow is bounded by the technology capacity $\bar{f}_t$ and is zero otherwise.

Investment costs in design problems can easily be expressed in terms of the binary variables $y_t, w_{t,\ell}$. The design problem can thus be cast as the following multi-objective mixed-integer linear program (MILP):

$$\min \quad \{\phi^I, \phi^d_j, \phi^s_i, \phi^f_\ell, \phi^\xi_t\} \tag{2.3.20a}$$

$$\text{s.t.} \quad (2.3.15) - (2.3.19). \tag{2.3.20b}$$

Here, the function ϕ^I captures total investment costs and $\phi^d_j, \phi^s_i, \phi^f_\ell, \phi^g_{n,p}$ capture operational costs/performance at every node. As before, we can compute compromise (Pareto) solutions for this problem by using prioritization (e.g., social welfare), multi-stakeholder formulations, or ϵ-constrained methods.

We highlight that the one-technology-per-node assumption is not as restrictive as it sounds because one can consider multiple technologies to be installed at the same geographical location by defining multiple nodes at the same location and by setting transportation costs between those nodes to zero.

In summary, the problem statement for the network design problem is as follows: Given a set of products ($\mathcal{P}$), sources ($\mathcal{S}$), sinks ($\mathcal{D}$), candidate locations ($\mathcal{N}$), and candidate technologies ($\mathcal{T}$) the goal is to determine the optimal locations (y_t) for siting these technologies, product flows (f_ℓ), and resource allocation (s_i and d_j) that is a Pareto optimal solution of problem (2.3.20).

2.4 Case Studies

We illustrate the applicability of the proposed modeling framework by using case studies arising in the context of livestock organic waste management from concentrated animal feeding operations (CAFOs). Organic waste generated at U.S. CAFOs (manure) is estimated to be 300 million tons per year, which represents twice the amount of waste produced by the entire U.S. human population. A single dairy cow generates 20 tons/year of waste (MacDonald et al., 2009) and there are 9 million (USDA NASS (United States Department of Agriculture, National Agricultural Statistics Service)) dairy cows in the U.S., which roughly translates to 180 million tons of waste generation each year. When organic waste is applied directly as fertilizer, it promotes P accumulation in the soil, which can be lost as runoff to surface waters and trigger eutrophication. Eutrophication in turn leads to algal blooms which degrade water quality and disturb ecosystems. One strategy to mitigate eutrophication is to prevent P accumulation in an area of interest (i.e., balance P generation and intake from crops). This can be achieved by separating excess P from the waste and transporting it to P-deficient areas inside or outside the are of interest. Another environmental issue associated to manure is the emission of greenhouse gases (GHG) (methane and nitrous oxide) and of pathogenic bacteria. Capturing

methane from waste (biogas) through anaerobic digestion provides an avenue to mitigate these issues. The U.S. Environmental Protection Agency (EPA) AgSTAR program reports that about 8,000 U.S. farms could support biogas systems, providing about 1,670 MW of electricity (enough to power one million homes) and reducing methane emissions by 1.8 million metric tons (in carbon dioxide equivalent this corresponds to taking 6.5 million cars off the road).

The development of biogas and P recovery technologies has been historically difficult. According to the American Biogas Council, there are only 247 digester farm installations in the U.S. A small number of P-recovery installations are also in operation. A reason for this is that deploying manure processing technologies is economically and logistically challenging. In particular, farms are highly dispersed geographically, which makes it challenging to balance economies of scale and transportation costs. Another issue is the need to capture the priorities of multiple stakeholders, which will seek to prioritize certain geographical regions (e.g., those with a higher concentration of P or those that are near to urban areas and watersheds) or that will seek to prioritize certain environmental objectives over others (e.g., water quality over GHG emissions).

We use the proposed framework to determine optimal technology layouts for recovering P (in the form of struvite) and biogas from the dairy waste in the State of Wisconsin. Specifically, we seek to design a supply-chain network to process the organic waste of the 100 largest dairy farms (ranked by the number of animal units) in the state [1]. These farms act as sources of waste and also serve as candidate locations for installing the technologies. In Figure 2.3 we present the CAFO locations and the stream total P concentration in different regions of the state.

Our studies seek to highlight conflicts that arise in these complex supply chain design studies and to highlight the insights that can be gained with the proposed framework. We consider the following specific cases:

- P recovery analysis (without geographical priorities).

[1] http://dnr.wi.gov/topic/AgBusiness/data/CAFO/cafo_all.asp

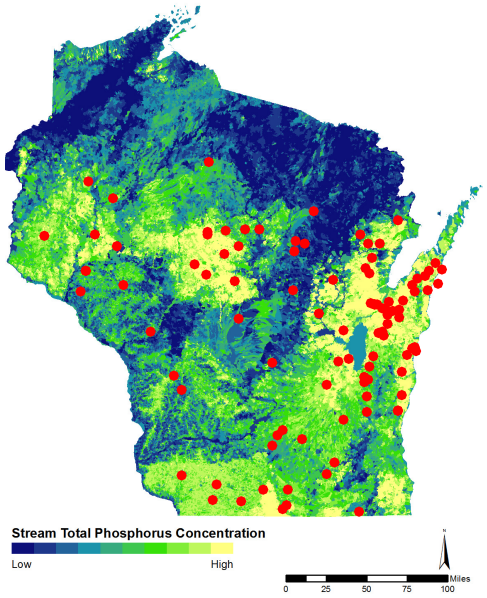

Figure 2.3: P concentration in the State of Wisconsin along with CAFOs locations (adapted from U.S. Environmental Protection Agency (2014)).

- P recovery analysis (with geographical priorities).
- P and biogas recovery analysis (with stakeholder priorities).

In summary, the scope of these case studies can be summarized as follows: given the data on 100 largest dairy CAFO locations (representing both the sources $s \in \mathcal{S}$ of waste and candidate locations $n \in \mathcal{N}$), candidate technologies ($t \in \mathcal{T}$), their corresponding reference products ($p(t)$), and transformation factors ($\gamma_{t,p}$), the goal is to identify Pareto optimal solutions for the placement of these technologies (y_t) and the product flows f_ℓ (corresponding to waste, struvite, digestate, and biogas) across the State of Wisconsin. This is achieved by maximizing the total amount of struvite recovered (Section 2.4.1), by maximizing struvite recovered by including geographical priorities (Section 2.4.2), and by minimizing the collective stakeholder dissatisfaction associated to different priorities on water quality and GHG impacts (Section 2.4.3).

2.4.1 *P Recovery Analysis*

We consider three capacity variants for a P recovery technology in the form of struvite (magnesium ammonium phosphate $NH_4MgPO_4 \cdot 6H_2O$). Recovering P as struvite has the dual benefit of mitigating eutrophication and providing an alternative source to phosphate rock (obtained from mining). In Figure 2.4 we present a simplified flowsheet for a fluidized bed reactor (FBR) technology used for recovering P as struvite. These reactors are commercialized by nutrient management companies such as Ostara (http://ostara.com). The capacity of the system considered is expressed in terms of the total amount of waste from animal units (AUs) that it can process. We consider processing capacities for 500, 1,500, and 3,000 AUs. A waste generation rate of 80 lbs/AU/day [2] is used to calculate the net waste generated by a farm, where AU denotes the number of animal units at each location. AU is a standard unit used in calculating the relative grazing impact of different kinds and classes of livestock. It is defined as an animal equivalent of 1000 pounds live weight. To provide a reference, a single dairy cow weighs about 1,400 pounds or 1.4 AUs. In the study area, there are 280,567 AUs, which generate a total waste of 22,445,360 lb/day (about 10 million metric tons of waste per day).

The FBR technology takes waste as input to generate struvite and digestate as output products. We thus have the set of products $\mathcal{S} := \{\texttt{Waste}, \texttt{Struvite}, \texttt{Digestate}\}$. A recovery percentage of 6.47% for struvite from waste (on a per-mass basis) has been considered. This value is obtained by assuming that 90% of P (Cusick et al., 2014) present in the waste is recovered in the form of struvite. The generated digestate is used as a bedding material at animal farms and is assumed to represent the rest of the waste not recovered. The yield factors are summarized in the transformation matrix:

[2] https://www.nrcs.usda.gov/wps/portal/nrcs/detail/null/?cid=nrcs143_014211

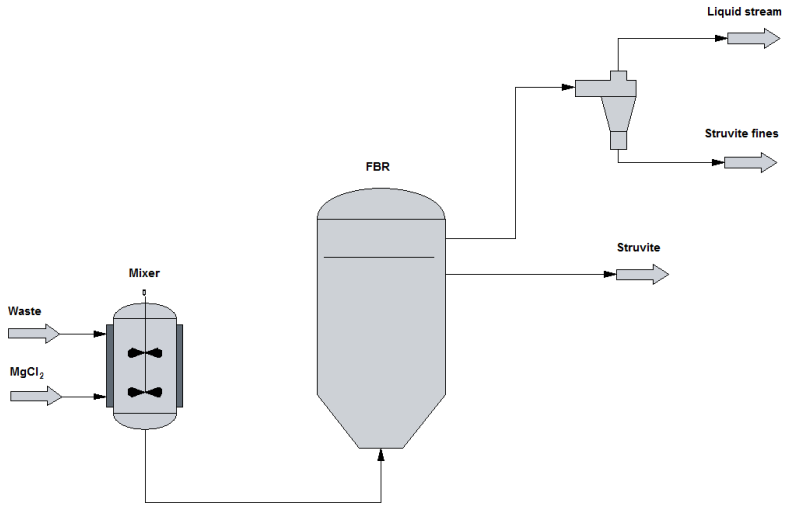

Figure 2.4: Schematic of fluidized bed reactor process for recovery of P as struvite.

$$\begin{bmatrix} \texttt{Technology} & \texttt{Waste} & \texttt{Struvite} & \texttt{Digestate} \\ \texttt{Str\_I} & -1 & 0.0647 & 0.9353 \\ \texttt{Str\_II} & -1 & 0.0647 & 0.9353 \\ \texttt{Str\_III} & -1 & 0.0647 & 0.9353 \end{bmatrix}$$

The capacities and investment costs for the technologies are given by:

$$\begin{bmatrix} \texttt{Technology} & \bar{\xi}_t(\text{kg/day}) & \phi_t^I(\text{USD}) & p(t) \\ \texttt{Str\_I} & 18,143 & 364,000 & \texttt{Waste} \\ \texttt{Str\_II} & 54,431 & 704,000 & \texttt{Waste} \\ \texttt{Str\_III} & 108,862 & 1,070,000 & \texttt{Waste} \end{bmatrix}$$

The investment costs have been calculated by sizing the equipment units involved in the FBR process and then applying cost estimation techniques for the overall project (Walas, 1990; Peters et al., 1968). We consider a nominal design with a flow rate of `Waste` of 1kg/s. The investment costs corresponding to the capacity equivalent of 500, 1500 and 3000 AUs (i.e., 0.21, 0.63 and 1.26 kg/s of `Waste`, respectively) are then estimated by using the *six-tenths-factor rule*, which captures economies of scale (Peters et al., 1968). The equipment units involved in the overall process are a mixing vessel, FBR, dryer, heat exchanger and a

hydrocyclone. The mixing vessel is used to make the waste uniform in composition. The cost of this vessel is estimated at USD 28,930, which includes the material and agitator cost. The chemical formation of struvite occurs in the FBR according to the reaction:

$$Mg^{2+} + NH_4^+ + H_nPO_4^{n-3} + 6H_2O \rightarrow MgNH_4PO_4{\cdot}6H_2O + nH^+$$

The FBR is designed using bed design parameters reported in Jordaan (2011) and kinetic rate constants reported in Nelson et al. (2003). Using these values, we use standard design procedures (Kunii and Levenspiel, 1991) to estimate an equipment cost of 7,225 USD. For the heat exchanger, dryer, and hydrocyclone we have estimated investment costs of 1,916 USD, 121,014 USD, and 18,535 USD, respectively. The total equipment costs add up to 177,620 USD. The physical plant cost (which includes cost of pipes, equipment construction, buildings and site development) is calculated by multiplying the total equipment cost by a factor of 3.15 (Peters et al., 1968). The value obtained is then scaled up by a factor of 1.4 to obtain the total investment cost of 783,303 USD. This value is used to estimate the investment costs for the technology capacities.

The cost of transporting waste (via hauling trucks) is assumed to be 0.08 USD/km/-ton (Paudel et al., 2009). For this case study, a value of 0.16 USD/km/ton is used in order to account for the two-way travel of the hauling trucks. The transport cost ϕ_ℓ^f factors in the distance traveled (in km) by the flows f_ℓ between the associated sending and receiving nodes. The per-unit transportation cost of digestate and struvite has been assumed to be same as that of transporting waste (i.e., the products use the same mode of transportation). The reference product is organic waste ($p(t)$ = `Waste`) for all the technologies (because these differ only in capacity).

We perform trade-off analysis among the conflicting objectives of maximizing total struvite recovered (denoted as $\phi_{\texttt{str}}$) while minimizing total investment and transportation cost (denoted as $\phi = \phi^I + \phi^f$). The cost is expressed on a per-day basis. We constrain this total cost by a budget level ϵ. In our analysis, we report percentage of unprocessed

manure that remains in the system (denoted as $r_{\texttt{Waste}}$). We also report the total number of technologies installed $\sum_{t\in\mathcal{T}} y_t$ and the average transportation distances for the waste (denoted as $h_{\texttt{Waste}}$) and struvite (denoted as $h_{\texttt{str}}$). Each farm has the option to treat the waste that it generates on-site or to transfer it to other locations. We use a common collection point for struvite at the boundary of the state in order to estimate the costs associated to shipping the recovered P out of the state (outside the network boundary) and with that prevent P accumulation in the state. This is modeled by defining a single demand for struvite at the collection point.

Table 2.1 summarizes the results of the trade-off analysis and Figure 2.5 presents Pareto solutions for different budget levels. As expected, when the budget is unconstrained (we set the budget to a large value of 500,000 USD/day), the optimal supply chain consists of siting as many technologies as possible (101 facilities are installed) in order to treat all the waste present in the system (i.e., no waste is left untreated). As a result, the transportation costs and hauling distances are allowed to be arbitrarily large. This indicates that the model cannot distinguish between different locations and that the solution is degenerate (i.e., the same amount of struvite can be recovered regardless of the location). This degeneracy becomes evident when we reduce the budget to 70,000 USD/day. In this case, we obtain the same amount of struvite but the transportation costs are reduced by an order of magnitude. As we constrain the budget further, the investment cost remains the same but network flows are re-routed and transportation cost is reduced, indicating that there is some inherent flexibility in the supply chain that can be used to mitigate transportation costs. A further reduction in the budget value causes a fast increase in the amount of waste left unprocessed (a fast decrease in the total amount of struvite recovered). Interestingly, because the total mass of struvite recovered in each technology is just 6.47% of the total waste processed, it is *more economical to process the waste locally (at the source node) and then transport struvite to the collection point*. This is reflected in the average transporting distance for struvite $h_{\texttt{str}}$, which is much higher than that for waste $h_{\texttt{Waste}}$.

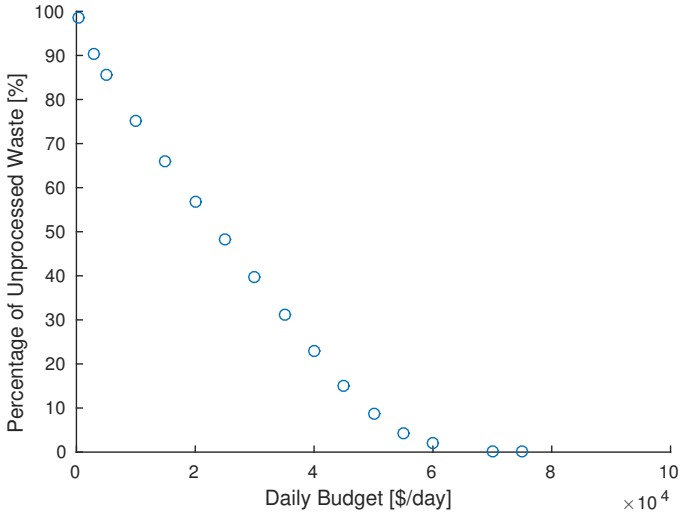

Figure 2.5: Pareto curve for daily budget (daily cost) and percentage of unprocessed waste.

Table 2.1: Trade-off analysis results for struvite recovery study (without geographical priorities).

Budget (USD/day)	ϕ^I (USD)	ϕ^f (USD/day)	Total Tech. Sited	$\phi_{\mathtt{str}}$ (kg/day)	$r_{\mathtt{Waste}}$ (%)	$h_{\mathtt{Waste}}$ (km/day)	$h_{\mathtt{str}}$ (km/day)	ϕ^f_{waste} (USD/day)	ϕ^f_{str} (USD/day)
500,000	102.95×10^6	485,898	101	6.59×10^5	0.00	34.97	170.02	448,014	37,281
70,000	102.61×10^6	55,944	100	6.59×10^5	0.00	47.86	144.69	18,557	37,387
55,000	102.27×10^6	40,991	100	6.30×10^5	4.43	22.81	346.16	5,342	35,649
45,000	93.60×10^6	32,179	96	5.59×10^5	15.13	7.21	341.99	818	31,361
35,000	75.10×10^6	24,713	77	4.53×10^5	31.27	6.81	328.29	532	24,181
25,000	57.30×10^6	17,151	59	3.41×10^5	48.18	6.72	300.44	405	16,746
15,000	38.38×10^6	9,742	41	2.24×10^5	65.94	5.47	257.38	213	9,530
10,000	28.78×10^6	6,058	32	1.63×10^5	75.25	4.97	216.14	177	5,881
5,000	16.70×10^6	2,713	18	0.95×10^5	85.57	0.95	164.58	25	2,688
3,000	11.01×10^6	1,492	12	0.63×10^5	90.45	0.43	132.30	10	1,481

The left-hand maps in Figure 2.6 show the optimal supply chain configuration and associated flows for two budget cases. The red circles indicate the farm locations, the yellow ring indicates that a struvite recovery technology has been installed at that location, and the yellow circle represents the struvite collection point. The blue lines are organic waste flows and the yellow lines are struvite flows. We can see that, for the 55,000 USD/-day budget case, there are manure exchanges across nodes so as to take full advantage of technology capacities. When the budget is reduced to 15,000 USD/day, it is more eco-

nomical to treat all waste on-site and to transport struvite to the collection point. This is an indication that waste transportation costs dominate the budget. This is because the dairy waste has on average 87% water content by weight (MacDonald et al., 2009), while struvite produced in our case-study is water-free. Consequently, by treating the waste locally, the cost associated with transporting the associated water content can be saved.

2.4.2 *P Recovery Analysis (with Geographical Priorities)*

From the tradeoff analysis shown in Table 2.1 we can see that, in order to process all the waste generated by the farms, *we would need an investment of over 100 million USD*. Under a constrained budget, it thus becomes important to prioritize geographical locations. We thus assign priorities to fields based on the existing soil P concentration at that location. In other words, we assign a higher priority to the waste generated at endangered areas. Under the proposed framework, this is done by making the waste supply cost α_i^s inversely proportional to the concentration of P at the corresponding location. In other words, a node with a high P concentration will supply waste at a lower cost and will thus have preference over other waste suppliers. Our objective is thus to maximize struvite demand delivered while minimizing supply waste cost (using the prioritized costs).

The results of this study are summarized in Table 2.2 and on the right-hand maps of Figure 2.1). We observe that, when the budget is 55,000 USD/day, the amount of struvite recovered (6.30 x 10^5 kg/day) is the same for both the cases. However, when the budget is reduced to 15,000 USD/day, the amount of struvite recovered for the case with priorities (1.42 x 10^5 kg/day) is less than that recovered for the case without priorities (2.24 x 10^5 kg/day). This is because, when priorities are included, the supply chain focuses on processing waste at farms with high soil P concentration even if this comes at the expense of transporting the surplus waste from endangered areas over longer distances for treatment (and thus incurring higher costs). This can be visualized by comparing the maps in the right-hand side of Figure 2.6. In particular, under prioritization, there is

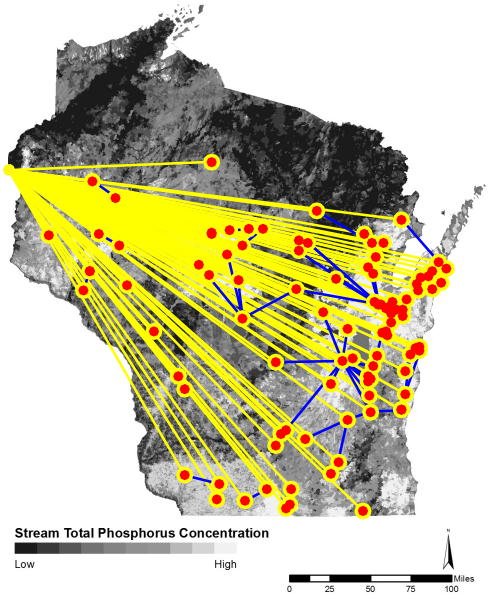

$\texttt{Budget} = 55,000$ USD/*day*

$\phi_{\texttt{str}} = 6.30\text{x}10^5$ kg/day

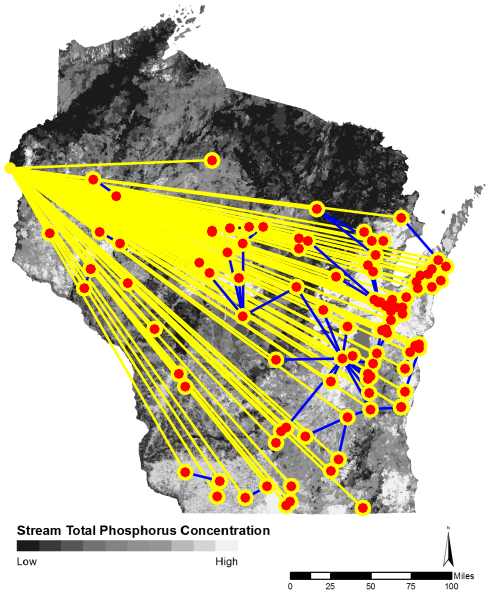

$\texttt{Budget} = 55,000$ USD/*day*

$\phi_{\texttt{str}} = 6.30\text{x}10^5$ kg/day

(Geographical Priorities)

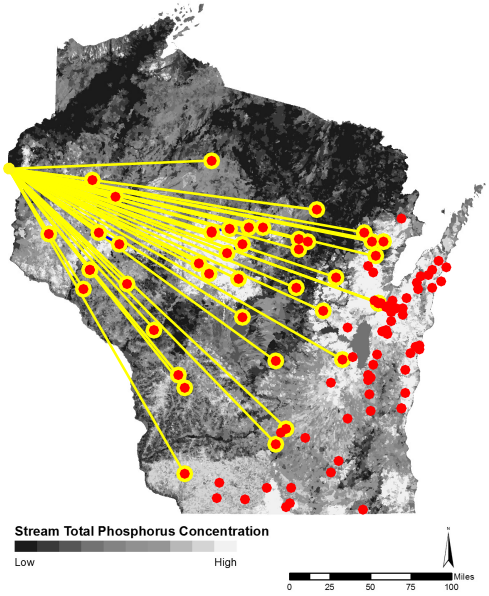

$\texttt{Budget} = 15,000$ USD/*day*

$\phi_{\texttt{str}} = 2.24\text{x}10^5$ kg/day

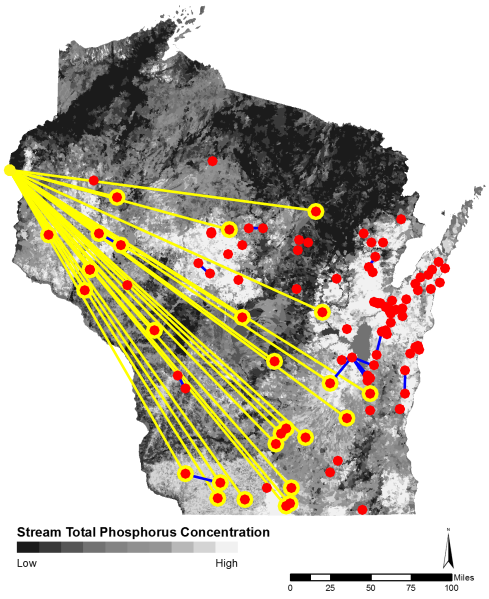

$\texttt{Budget} = 15,000$ USD/*day*

$\phi_{\texttt{str}} = 1.42\text{x}10^5$ kg/day

(Geographical Priorities)

Figure 2.6: Optimal technology locations and product flows under different budgets.

more movement of struvite in the supply chain. By comparing the left-hand and right-hand side maps we also see that, under a constrained budget, the technology locations are different (priorities do influence the supply chain design). On the other hand, under an unconstrained budget, there are no differences.

Table 2.2: Trade-off analysis results for struvite recovery study (with geographical priorities).

Budget (USD/day)	ϕ_I (USD)	ϕ_f (USD/day)	Total Tech. Sited	$\phi_{\texttt{str}}$ (kg/day)	$r_{\texttt{Waste}}$ (%)	$h_{\texttt{Waste}}$ (km/day)	$h_{\texttt{str}}$ (km/day)	$\phi_{f,waste}$ (USD/day)	$\phi_{f,str}$ (USD/day)
500,000	102.60×10^6	485,944	101	6.59×10^5	0.00	33.63	92.97	441,619	41,925
70,000	103.31×10^6	55,848	101	6.59×10^5	0.00	46.58	217.95	18,625	37,223
55,000	101.90×10^6	41,040	100	6.30×10^5	4.51	21.51	346.19	5,420	35,621
45,000	91.54×10^6	32,461	92	5.42×10^5	17.71	11.00	337.77	2,405	30,055
35,000	74.05×10^6	24,856	75	4.26×10^5	35.32	10.81	321.42	2,222	22,634
25,000	52.29×10^6	17,837	55	2.95×10^5	55.17	9.19	303.70	2,805	15,032
15,000	25.96×10^6	11,444	27	1.42×10^5	78.48	11.13	282.45	4,718	6,725
10,000	15.97×10^6	7,813	18	0.88×10^5	86.70	10.26	236.75	4,228	3,585
5,000	4.62×10^6	4,367	5	0.28×10^5	95.79	9.04	133.78	3,623	745
3,000	0.70×10^6	2,904	1	0.04×10^5	99.47	7.98	74.08	2862	42

2.4.3 *P and Biogas Recovery*

We now illustrate how to use the proposed framework to handle conflicting priorities among stakeholders. We consider a case study to locate technologies to recover both struvite and biogas. Stakeholders disagree on what product (struvite or biogas) should be prioritized. This setting can be interpreted as that of conflicting priorities from government officials or communities on using an available budget to address water quality (associated to P runoff) or air quality (associated to methane leaks). We compute compromise solutions for this problem by balancing the dissatisfactions of stakeholders.

We express the total struvite $\phi_{\texttt{str}}$ and biogas $\phi_{\texttt{bio}}$ recovered in terms of the demands served. Here, again, we assume that struvite is delivered at a single point (we consider a case with more collection points later on) and that biogas is delivered at the point of recovery (e.g., to fulfill local demands). Technologies `Str_I`, `Str_II`, and `Str_III` perform struvite recovery; technologies `Bio_I`, `Bio_II` and `Bio_III` perform biogas recovery; and

technologies BioStr_I, BioStr_II and BioStr_III perform simultaneous struvite and biogas recovery. The corresponding data matrices for these technologies are:

$$\begin{bmatrix} \texttt{Technology} & \bar{\xi}_t(\text{kg/day}) & \phi_t^I(\text{USD}) & p(t) \\ \texttt{Str\_I} & 18,144 & 364,000 & \texttt{Waste} \\ \texttt{Str\_II} & 54,431 & 704,000 & \texttt{Waste} \\ \texttt{Str\_III} & 108,862 & 1,070,000 & \texttt{Waste} \\ \texttt{Bio\_I} & 18,144 & 574,509 & \texttt{Waste} \\ \texttt{Bio\_II} & 54,431 & 1,013,795 & \texttt{Waste} \\ \texttt{Bio\_III} & 108,862 & 1,672,723 & \texttt{Waste} \\ \texttt{BioStr\_I} & 18,144 & 938,509 & \texttt{Waste} \\ \texttt{BioStr\_II} & 54,431 & 1,717,795 & \texttt{Waste} \\ \texttt{BioStr\_III} & 108,862 & 2,742,723 & \texttt{Waste} \end{bmatrix}$$

The investment cost for biogas recovery have been calculated using a general cost analysis formula reported by EPA's *AgStar* program (Meyer and Powers, 2011). For simplicity, the combined technology costs have been assumed to be the addition of the investment costs for the individual technologies. The transformation factors for the technologies (on a per mass basis) are given by:

$$\begin{bmatrix} \texttt{Technology} & \texttt{Waste} & \texttt{Struvite} & \texttt{Digestate} & \texttt{Biogas} \\ \texttt{Str\_I} & -1 & 0.0647 & 0.9353 & 0 \\ \texttt{Str\_II} & -1 & 0.0647 & 0.9353 & 0 \\ \texttt{Str\_III} & -1 & 0.0647 & 0.9353 & 0 \\ \texttt{Bio\_I} & -1 & 0 & 0.96 & 0.04 \\ \texttt{Bio\_II} & -1 & 0 & 0.96 & 0.04 \\ \texttt{Bio\_III} & -1 & 0 & 0.96 & 0.04 \\ \texttt{BioStr\_I} & -1 & 0.0621 & 0.8979 & 0.04 \\ \texttt{BioStr\_II} & -1 & 0.0621 & 0.8979 & 0.04 \\ \texttt{BioStr\_III} & -1 & 0.0621 & 0.8979 & 0.04 \end{bmatrix}$$

We consider a set of five different *types of stakeholders* that have different priorities on the product to be recovered. The first type of stakeholder has 100% preference on struvite recovery, the second type of stakeholder has 100% preference on biogas recovery, the third stakeholder is neutral, and the fourth and fifth stakeholders have have biased preferences for struvite and biogas recovery, respectively. We can see that the first two types of stakeholders take extreme positions.

We begin our analysis by first reporting the ideal design for each stakeholder (those obtained by fully satisfying the priorities of each stakeholder). The results are presented in Table 2.3. As can be seen, there are strong trade-offs on the amount of products produced and on the associated investment and transportation costs. The supply chain layouts are shown in Figure 2.7. As can be seen, the design of the first stakeholder type installs only struvite recovery technologies and requires transportation to the collection point (yellow circle). The design of the second stakeholder type only performs biogas recovery (blue rings) and does not require any transportation because biogas is consumed on-site. The third stakeholder type solution (with neutral priorities) is quite interesting and consists of installing struvite recovery facilities on one side of the state (close to the collection point) and biogas recovery facilities on the other side of the state. For this stakeholder, some facilities recover both biogas and struvite (green rings) and these are located in the middle of the state. This result implies that the location of the *collection point of struvite has a strong effect on the optimal configuration of the supply chain*. With such a diverse set of conflicting stakeholder designs, it becomes imperative to identify efficient compromise solutions.

In Table 2.4 we present the costs and dissatisfactions associated to each stakeholder type under different compromise solutions. In particular, we consider varying values of the probability level β and recall that $\beta = 0$ achieves a compromise in which the worst dissatisfaction is minimized and that a value of $\beta = 1$ achieves a compromise in which the average collective dissatisfaction is minimized. In Figure 2.8 we present the optimal configuration for these two cases. As can be seen, the first two types of stakeholders are

the ones with the highest dissatisfactions (this is because they take extreme positions). Moreover, the first type of stakeholder (focusing on struvite) is the most dissatisfied. In particular, under the average compromise solution ($\beta = 1$), the first stakeholder type will be strongly dissatisfied compared to the rest while the worst-case compromise ($\beta = 0$) achieves a more even dissatisfaction among the stakeholders. Interestingly, in all cases the third stakeholder is fully satisfied with the compromise (its dissatisfaction is very small). This indicates that the compromise solutions are close to that of the neutral stakeholder.

We also observe that the worst-case compromise solution requires less investment but more transportation cost while the average compromise solution requires more investment but less transportation cost. This indicates that the worst-case compromise is seeking to satisfy the first stakeholder type by producing more struvite, even if this comes at the expense of more transportation costs to the collection point. On the other hand, the average compromise seeks to satisfy the second stakeholder and installs biogas facilities that use the fuel on-site, thus decreasing transportation cost. Such trade-offs are not perceptible from the configurations shown in Figure 2.8. Here, the most evident difference is that the average compromise installs a few more technologies that perform joint recovery of biogas and struvite. Again, we see that the compromise solutions cluster biogas facilities on the east region of the state and struvite on the west region (close to the collection point). Again, this highlights that the collection point has a strong influence on the nature of the system layout. To reinforce this observation, in Figure 2.9 we present optimal supply chain designs obtained from the stakeholder compromise solution when *multiple struvite collection points* are considered. As can be seen, the nature of the design changes drastically, with the struvite facilities now installed in the southeast and northeast regions of the state. These results indicate that the selection of collection points requires careful deliberations on the final use of struvite. The results also indicate that there exist complex trade-offs between the different types of environmental impact (water against air quality) that can result from deploying sub-optimal layouts. As a result, strong dissatisfactions will exist among stakeholders if facility locations are selected without carefully

trading-off investment and transportation costs as well as geographical and stakeholder priorities.

Table 2.3: Ideal individual solutions for different stakeholder types.

Stakeholder	w_{str} (%)	w_{bio} (%)	ϕ_{str} (kg/day)	ϕ_{bio} (m^3/day)	ϕ^I (USD)	ϕ^f (USD/day)	ϕ^f_{waste} (USD/day)	ϕ^f_{str} (USD/day)
I	100	0	2.24×10^5	0.00	38.07×10^6	9,786	278	9,508
II	0	100	0.00	2.33×10^5	105.48×10^6	550	550	0
III	50	50	1.08×10^5	1.45×10^5	85.12×10^6	3,340	109	3,231
IV	33	67	3.38×10^3	2.30×10^5	104.82×10^6	641	600	41
V	67	33	2.24×10^5	0.00	38.41×10^6	9,739	369	9,370

Table 2.4: Costs and dissatisfactions under multi-stakeholder compromise solutions.

β	ϕ_{str} (kg/day)	ϕ_{bio} (m^3/day)	ϕ^I (USD)	ϕ^f (USD/day)	ϕ^f_{waste} (USD/day)	ϕ^f_{str} (USD/day)	d_I (%)	d_{II} (%)	d_{III} (%)	d_{IV} (%)	d_V (%)
0	1.24×10^5	1.29×10^5	79.47×10^6	4,114	225	3,889	45	45	0	12	12
0.5	1.25×10^5	1.29×10^5	79.23×10^6	4,147	130	4017	46	43	0	11	12
0.7	1.22×10^5	1.32×10^5	80.54×10^6	3,967	109	3,858	47	42	0	11	13
1	1.07×10^5	1.45×10^5	84.41×10^6	3,436	205	3,231	54	35	0	8	15

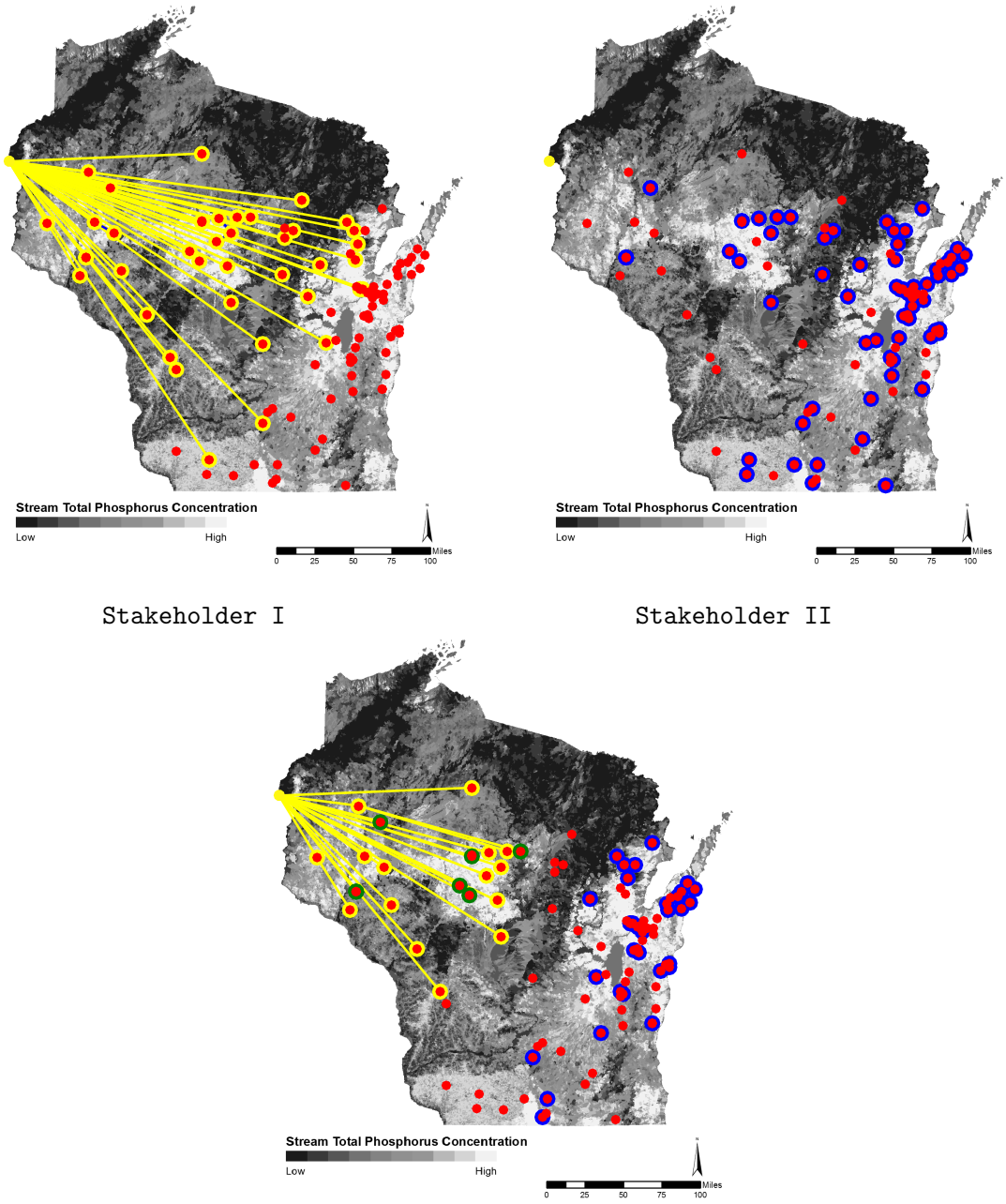

Stakeholder I

Stakeholder II

Stakeholder III

Figure 2.7: Technology locations and flows for ideal stakeholder solutions.

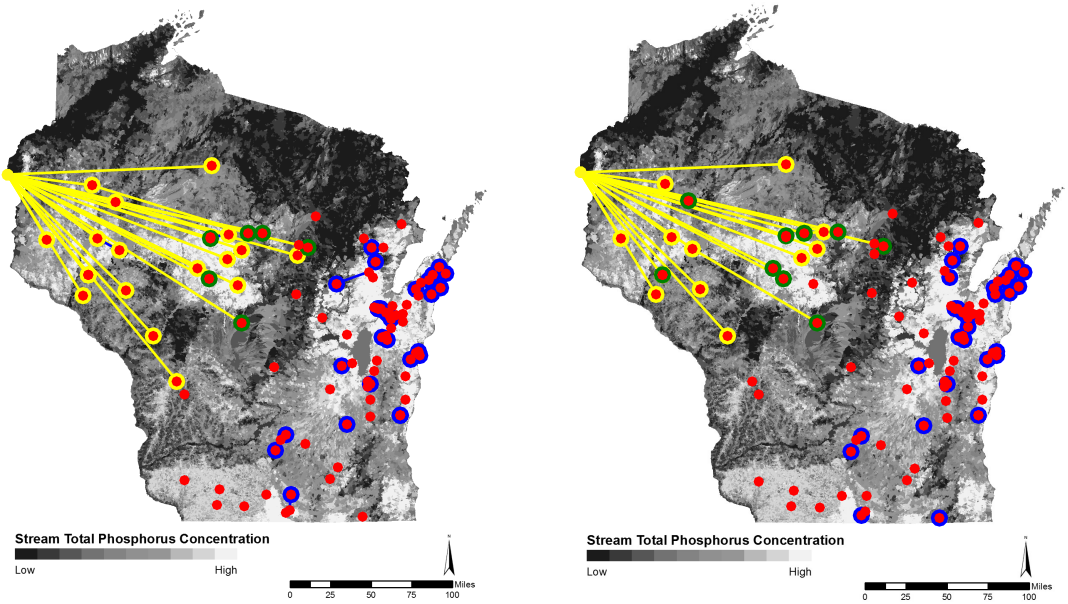

β = 0.0 (Worst-Case) β = 1.0 (Average)

Figure 2.8: Technology locations and flows for multi-stakeholder compromise solutions.

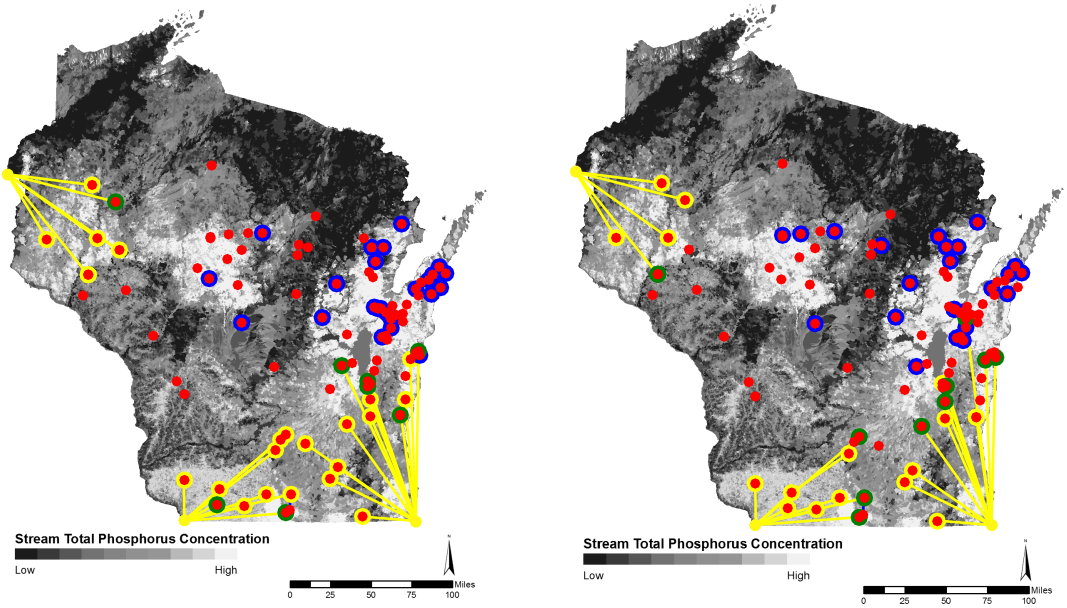

β = 0.0 (Worst-Case) β = 1.0 (Average)

Figure 2.9: Technology locations and flows for multi-stakeholder compromise solutions (for multiple collection sites).

2.4.4 *Computational Requirements*

All the above optimization problems (MILPs) have been implemented in the algebraic modeling language `JuMP` and solved with the mixed-integer linear solver `Gurobi` on a computing server with 32 processor cores (2 sockets and 16 cores each) using Intel(R) Xeon(R) CPU E5-2698 v3 @ 2.30GHz. The problem sizes range are: 300-900 binary variables, 30,000-42,000 continuous variables, 600-800 equality constraints, and 6,000-18,000 inequality constraints. The CPU times range from a few seconds to one hour. The higher CPU times correspond to the instances where the investment budget constraints are tight (because of the increasing difficulty in finding a feasible solution).

2.5 Summary

In this chapter, we have presented a general optimization formulation for multi-product supply chain networks. The formulation uses a general graph representation that considers a set of technologies placed at different spatially-dispersed nodes under which a set of products undergo transformations. Interactions between products are captured using a hierarchical graph that maps product flows at each node using a transformation matrix and that maps network nodes using transportation paths (arcs). The proposed network seeks to generalize a wide range of settings existing in the literature and to capture conflicting priorities. We demonstrate the applicability using a case study in the State of Wisconsin in which we seek to design supply chains to process livestock organic waste to mitigate P and methane emissions. The nature of the optimal layouts obtained indicates that complex trade-offs exist between investment, transportation, and environmental impact.

In Chapter 3, we will demonstrate the application of the multi-product network design formulation through a detailed analysis for P recovery from organic waste. We will present different P recovery technologies and use the proposed network design model to

find an environmentally and economically sustainable waste management strategy.

3

TECHNOLOGIES FOR NUTRIENT RECOVERY

3.1 Introduction

Livestock waste (manure) generated at concentrated animal feeding operations (CAFOs) in the United States (U.S.) is estimated to be 300 million tons per year (Gurian-Sherman, 2008). This is twice the amount of waste produced by the entire U.S. human population (Gurian-Sherman, 2008). Dairy farms are one of the major contributors of this waste. A single dairy cow generates 20 tons of waste per year and there are 9.3 million dairy cows in the U.S. (U.S. Department of Agriculture-National Agricultural Statistics Service, 2014). This translates to 180 million tons of waste generated each year from dairy cows. This waste tends to accumulate in geographical regions where large CAFOs are located. Application of manure as fertilizer in these regions results in phosphorus (P) runoff and eutrophication of ground and surface waters that are used for recreation, sanitation, consumption, and irrigation. There are significant economic and environmental impacts associated with P eutrophication (Pretty et al., 2003; Costanza et al., 1997; Bockstael et al., 2000; Spash and Vatn, 2006; Dodds et al., 2009). In the U.S., it is estimated that eutrophication creates a total economic loss of 2.2 billion USD per year (Dodds et al., 2009). This this due to damaged recreational water usage and waterfront real estate, decline in the

population of threatened and endangered species, and reduced drinking water quality.

Eutrophication can be mitigated by installing nutrient separation (recovery) technologies that mobilize P from rich (high concentration) regions to nutrient-deficient ones. P can also be recovered in the form of valuable concentrated products such as struvite (Doyle and Parsons, 2002), which can be used as a slow-release fertilizer. In addition to help prevent eutrophication, P recovery from livestock waste is a key step in closing the P cycle which helps in achieving more sustainable food production systems (Childers et al., 2011). P runoff from agricultural fields and livestock facilities is the largest source for P loss (Cordell et al., 2009) and thus provides an important opportunity for P recovery.

The majority of P contained in livestock waste is particulate-bound (Gerritse and Vriesema, 1984; Zhang et al., 2010), which means that P is suspended in the form of small, colloidal non-crystalline particles attached to either calcium or magnesium (Chapuis-Lardy et al., 2004; Güngör and Karthikeyan, 2005a,b). The rest of P is present in solubilized form. Consequently, recovering P from livestock waste is technically challenging. Various forms of mechanical and biochemical separation technologies have been considered to achieve this (Ma et al., 2013). Mechanical technologies are easy to install and operate but cannot achieve high efficiency of P separation. The more efficient chemical and biochemical techniques such as struvite crystallization and enhanced biological P recovery technologies are thus becoming increasingly popular. As expected, however, technology costs can drastically increase with efficiency (thus leading to strong trade-offs) (Ma et al., 2013). For instance, a simple mechanical screening operation (with recovery efficiency in the range of 15-25%) has operating and capital costs of USD 5-6/cow/year and USD 32-36/cow, respectively (Ma et al., 2013). A more advanced technology such as struvite crystallization (with recovery efficiency of 75%), on the other hand, has operating and capital costs of USD 90-110/cow/year and USD 100-150/cow, respectively (Ma et al., 2013). These technical trade-offs, coupled with the lack of developed markets of renewable fertilizers and the need to transport and process large amounts of waste and by-products, generate significant uncertainty on the economic potential of P recovery

technologies.

Systems analysis tools can help capture complex techno-economic and logistical trade-offs arising in P recovery. The work presented in Cordell et al. (2011) introduces a systems framework to analyze a wide range of P recovery and reuse options. This framework aids technology selection and investment decisions and can help close the gap between science and policy that would drive widespread installation of P recovery technologies. However, this framework is limited in that it does not capture interactions between technology selection and location, transportation logistics, and interdependencies between products. In this chapter, we use the multi-product supply chain modeling framework presented in (Sampat et al., 2017) to identify optimal technology types and placement for P recovery technologies that capture transportation logistics as well as environmental impacts over wide geographical regions. We present a case study in the State of Wisconsin using detailed techno-economic data of different P recovery technologies (Martín-Hernández et al., 2018) . Our analysis reveals that there exist complex and non-obvious trade-offs between technology selection, transportation, and product values that need to be carefully taken into account. In particular, our analysis reveals that, while manure mobilization and mechanical P recovery are inexpensive options that can mitigate environmental issues, these are not self-sustaining solutions from an economic standpoint because they generate little or no revenue. Deploying technologies for P recovery in the form of struvite appears to be economically sustainable over a wide range of scenarios but it is highly susceptible to yield factors (which remain highly uncertain). Our computational framework is used to analyze the impact of different scenarios for market prices of recovered products, recovery yields, and remediation costs. With this we seek to help policy makers analyze complex trade-offs arising in nutrient recovery and to help experimental researchers identify critical pieces of technology data that need to be refined.

The paper is structured as follows. In Section 3.2 we present a summary of P recovery technologies considered in our study. In Section 3.3 we describe the multi-product supply chain model that is used to guide technology selection and placement. In Section 3.4 we

summarize results and findings on diverse case studies in the State of Wisconsin.

3.2 Phosphorus Separation Technologies

In this section, we provide a brief overview of the technologies that we consider to recover P from process livestock waste. A more detailed description can be found in Martín-Hernández et al. (2018). Our analysis is focused on P recovery, which has been identified as a major surface water pollution issue in the State of Wisconsin (see https://dnr.wi.gov/topic/surfacewater/phosphorus). Water pollution due to other nutrients such as nitrogen is an important topic but it is not considered in this chapter.

3.2.1 *Filtration*

Filtration is a low-cost technology that is appropriate for small facilities, where the amount of P to be removed is not very high. Various types of filter media are suitable for P recovery. The reactive filter media (e.g. Polonite®, Dolomite, Wollastonite, and Filtra P®) are comprised of compounds rich in cations under a basic environment (usually in the form of calcium silicates). When operated at pH values above nine, the cation rich compounds react with P to form an orthophosphate precipitate (Pratt et al., 2012; Gustafsson et al., 2008). Metallurgical slag is another potential filter medium that captures P by adsorption at pH values close to neutral (Pratt et al., 2012).

In previous work we found that metallurgical slag is the optimal filter media for P recovery (Martín-Hernández et al., 2018). This solution was found by solving a mixed-integer nonlinear program (MINLP) which accounts for the cost and product yields of different filters. The filter media can also be combined with with nitrogen filters to simultaneously remove N and P. An advantage of this filter technology is that the cake produced (consisting of a mixture of P, N, and other solid compounds) can be used as a soil fertilizer (Hylander et al., 2006). In this chapter, we focus on filtration systems that use metal slag (Cucarella et al., 2008) as the filter media. We denote the P rich product

produced by these filters as $cake_1$, while $digestate_1$ represents the product containing the residual compounds of the influent waste stream not included in $cake_1$.

3.2.2 *Coagulation-Flocculatioin*

Coagulation-Flocculation is a chemical treatment consisting of multiple processing steps. First, the waste is mixed with coagulation agents. This destabilizes the waste stream by reducing the attractive forces. Flocculating agents are then added to these destabilized colloids to form flocs. This subsequently results in the precipitation of nutrients with other sediment solids. These nutrient rich solids are recovered from the liquid phase by clarification. Both N and P can be recovered from the influent waste stream through coagulation-flocculation. P is recovered primarily in the form of metal hydroxides, which is the dominant process at typical plant pH values (Szabó et al., 2008). N recovery is related to the removal of the colloidal matter (Aguilar et al., 2002). The final step involves the partial drying of the recovered solids using a centrifuge to form a cake consisting of a mixture of P, N, and other solid compounds. We denote this nutrient rich compound as $cake_2$, while $digestate_2$ represents the product containing the residual compounds of the influent waste stream not included in $cake_2$.

In previous work we found that $AlCl_3$ is the best coagulation agent for P recovery compared to $FeCl_3$, $Fe_2(SO_4)_3$, and $Al_2(SO4)_3$ (Martín-Hernández et al., 2018). In this chapter, we consider $AlCl_3$ as the coagulation agent used in coagulation-flocculation technologies. This achieves a P recovery efficiency of up to 99% (Aguilar et al., 2002).

3.2.3 *Centrifugation*

Centrifugation is a simple process, involving a mixing tank that mixes the influent waste stream with precipitation agents. The addition of precipitation agents improves the P and N recovery efficiency significantly. P recovery yield of 95% can be achieved by this process. In our analysis, we consider a mixture of $CaCO_3$ and $FeCl_3$ (Meixner et al., 2015)

as the precipitation agents. The precipitates are cakes that are rich in P, N, and other solids. We denote these nutrient rich compounds as $cake_3$, while $digestate_3$ represents the product containing the residual compounds of the influent waste stream not included in $cake_3$. The operational cost of this technology is high due to electrical power consumption (Martín-Hernández et al., 2018).

3.2.4 *Struvite Production*

P and N from the waste can also be recovered by the formation of struvite ($NH_4MgPO_4 \cdot 6H_2O$), a phosphate mineral. The advantage of this technology is that struvite is a solid with high nutrient density, making it easier to transport. Struvite can also be used as a slow-release fertilizer without any post-processing (Doyle and Parsons, 2002). Struvite crystals are produced by the addition of $MgCl_2$.

$$Mg^{2+} + NH_4^+ + H_nPO_4^{n-3} + 6H_2O \rightarrow MgNH_4PO_4 \cdot 6H_2O + nH^+$$

Struvite is crystallized from solubilized P in the waste stream. Experimental data from the literature reveal that it is possible to directly recover P from undigested dairy manure but recovery yields reported are highly variable (Schuiling and Andrade, 1999; Qureshi et al., 2008; Jin et al., 2009; Zhang et al., 2015). A pre-treatment may be needed to increase the fraction of solubilized P in the undigested manure. In our case, the addition of NaOH to adjust the pH increases the solubilized P fraction in the waste stream (He et al., 2004; Ylivainio and Turtola, 2013). Due to the presence of potassium in the waste stream, a side product called potassium struvite, or K-Struvite is also produced. In this case, the ammonium cation is substituted by the potassium cation (Wilsenach et al., 2007).

$$Mg^{2+} + K^+ + H_nPO_4^{n-3} + 6H_2O \rightarrow KMgPO_4 \cdot 6H_2O + nH^+$$

Since the formation of struvite is favored over the formation of K-Struvite, we have consid-

ered that only 15% of the potassium contained in the waste will react to form K-Struvite (Zeng and Li, 2006).

We evaluate two reactor types for struvite recovery: a fluidized bed reactor (FBR) and a continuous stirred tank reactor (CSTR). The FBR-based system is composed of three elements: a mixing tank with an agitator, the FBR itself, and a hydrocyclone. The operation of FBR technology begins with the addition of $MgCl_2$ to the influent waste stream in the mixing tank. As the concentration of NH_4^+ is high, the only element to be added is Mg^{2+} in the form of $MgCl_2$. Struvite seeds of around 0.8 mm in size are also added to promote the growth of struvite crystals. This stream is then sent to a FBR where solid struvite crystals are formed. The solid struvite is then removed from the reactor through the bottoms. The other stream leaving the reactor contains a mixture of water with an excess of Mg^{2+}, the total solids from the waste, and small amounts of nutrients. This stream is sent to a hydrocyclone to recover struvite fines. We denote the liquid stream leaving the FBR as $digestate_4$. In the case of the CSTR-based system, the system is composed of four elements: the CSTR reactor, a centrifuge, and a dryer with a corresponding heat exchanger. Since the residence time in the CSTR is large, a pre-mixing tank is not required; $MgCl_2$ is added directly to the reactor. Struvite is thus formed in one step in the CSTR. The precipitated struvite is then recovered from the bottoms of the reactor and dried in a two-step process. The first step consists of a centrifuge that recovers struvite with 5% (by weight) water. A drum dryer is next used to remove the residual moisture to reach commercial standards and reduce transportation costs. A disadvantage of the CSTR system is that large crystals can be formed in the reactor, thus causing fouling and mechanical failures. Both struvite recovery systems are assumed to reach nominal P recovery yields of 90% of the solubilized P present in the influent waste stream (Lin et al., 2015; Bhuiyan et al., 2008). In our studies, we also account for uncertainty in these yields due to variability of the waste stream composition. Cost estimation correlations as well as mass and energy balances for both systems can be found in (Martín-Hernández et al., 2018).

3.3 Multi-Product Supply Chain Model

We use the modeling abstraction for network design presented in Section 2.3.2 to guide technology placement and transportation decisions. We formulate the *supply chain design* problem by defining a set of candidate technology types $\mathcal{T}$ (i.e., filtration, centrifugation, coagulation, struvite in FBR, and struvite in CSTR) that can be installed at a set of predefined candidate network nodes (e.g., CAFOs). We use the binary variable $y_t \in \{0, 1\}$ to indicate that technology $t \in \mathcal{T}_n$ is installed at node $n \in \mathcal{N}$.

The total supply, demand, and transportation costs in the network are given by:

$$\phi^s = \sum_{i \in \mathcal{S}} \alpha_i^s s_i \tag{3.3.1a}$$

$$\phi^d = \sum_{j \in \mathcal{D}} \alpha_j^d d_j \tag{3.3.1b}$$

$$\phi^f = \sum_{\ell \in \mathcal{F}} \alpha_\ell^f f_\ell. \tag{3.3.1c}$$

Investment and operational costs are expressed in terms of the binary variables y_t as:

$$\phi^I = \sum_{n \in \mathcal{N}} \sum_{t \in \mathcal{T}_n} \alpha_t^I y_t \tag{3.3.2a}$$

$$\phi^\xi = \sum_{n \in \mathcal{N}} \sum_{t \in \mathcal{T}_n} \alpha_t^\xi y_t. \tag{3.3.2b}$$

The supply chain design problem can thus be cast as the following multi-objective mixed-integer linear program (MILP):

$$\max \quad \{\phi^d, -\phi^I, -\phi^s, -\phi^f, -\phi^\xi\} \tag{3.3.3a}$$

$$\text{s.t.} \quad (2.3.15) - (2.3.19). \tag{3.3.3b}$$

We can compute compromise (Pareto) solutions for this problem by using scalarization or ϵ-constrained methods. For instance, we can seek to identify technology types and

locations that maximize the social welfare ($\phi^d - \phi^s - \phi^f - \phi^{\xi}$) subject to investment budget constraints:

$$\max \quad \phi^d - \phi^s - \phi^f - \phi^{\xi} \tag{3.3.4a}$$

$$\text{s.t.} \quad (2.3.15) - (2.3.19) \tag{3.3.4b}$$

$$\phi^I \leq \epsilon_I. \tag{3.3.4c}$$

The social welfare is the total profit in the entire supply chain, given by the difference of the total revenues collected and the costs associated to supplies, transportation flows, and technology operations. The investment cost can also be added to objective by annualizing it, but the ϵ-constrained formulation is often of interest to identify what is the impact of increasing the investment budget on social welfare. We note that maximizing the social welfare is done in a cooperative manner (as opposed to a competitive manner, as in a game-theoretical approach).

In our model we allow the value of the demands α_j^d to be either positive or negative. When the value is positive, it indicates that there is an economic incentive to satisfy the demand (we thus seek to maximize the demand served d_j to the associated node). In other words, product flows are attracted to the demand node. On the other hand, when the demand value is negative, it indicates that there is an incentive to not satisfy the demand at the associated node (the product flows are pushed away from the demand node). In this case, the demand d_j acts as a slack (residual) variable that we seek to minimize. As we will see in our case studies, negative demand values can be used to model environmental remediation effects, because we can consider the environment as a sink, consumer, or "stakeholder" that demands a product (waste, digestate) at a negative price. This also highlights the fact that, in our framework, products always have a final destination (i.e., for either consumption or for perpetual storage in the environment). We also highlight that the values for supplies and transportation costs are all assumed to be positive. Consequently, maximizing the social welfare minimizes supply, transportation,

and operational costs.

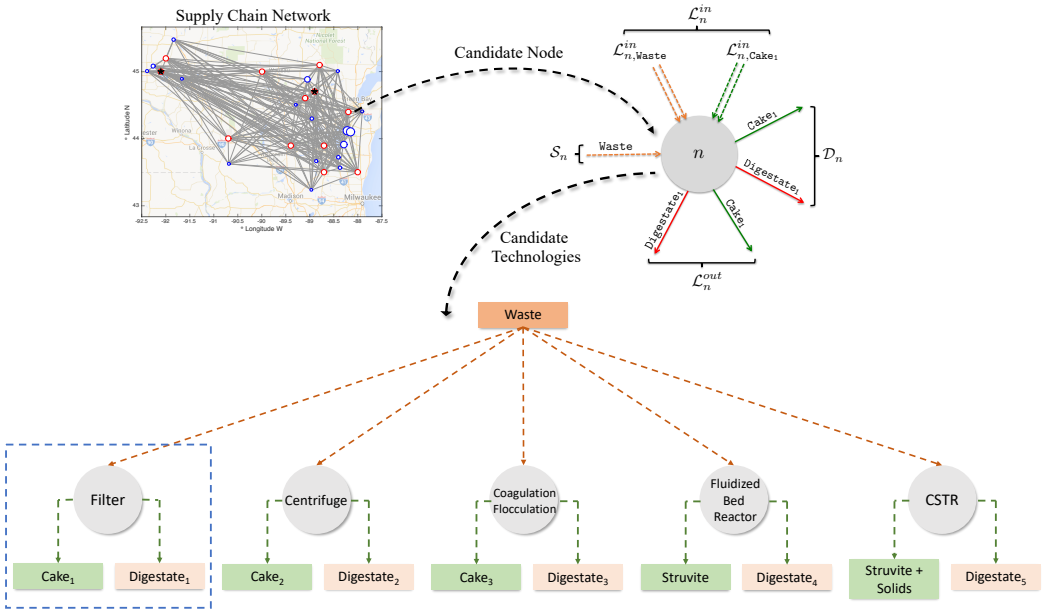

Figure 3.1: Sketch of input and output flow sets into a candidate node $n \in \mathcal{N}$ (in a supply chain) for products $\mathcal{P} = \{\texttt{Waste}, \texttt{Cake}_1, \texttt{Digestate}_1\}$. The multiproduct model selects the technology form a set of candidate technologies ($\mathcal{T}$) illustrated in the graph.

The model notations and node-level interactions are sketched in Figure 3.1. Here, we consider a candidate node (e.g. a dairy farm) in the supply chain, where the waste generated on farm is a part of the source set $\mathcal{S}_n$. Other dairy farms in the supply chain can also transfer their waste to this candidate node for processing. Such waste flows are captured as a part of the incoming flow to the node ($\mathcal{L}_{n,\texttt{Waste}}^{in}$). Similarly, other farms can also transfer cake$_1$ for use at the candidate node. These flows are also captured under the set of incoming flows $\mathcal{L}_n^{in}$. The model selects the optimal technology from an array of candidate technologies available for P recovery. For this illustration, the selected technology is a filter unit that recovers cake$_1$. The products used on-site or sold at this farm are considered under the demand set $\mathcal{D}_n$. The remaining amount of products sent to other nodes in the network are captured through the set of outgoing flow ($\mathcal{L}_n^{out}$).

In summary, the problem statement for the supply chain network design problem is

as follows: given a set of products ($\mathcal{P}$), sources ($\mathcal{S}$), sinks ($\mathcal{D}$), candidate locations ($\mathcal{N}$), and candidate technologies ($\mathcal{T}$) the goal is to determine the optimal locations for siting technologies (y_t), product flows (f_ℓ), and resource allocations (s_i and d_j) in the network that are a Pareto optimal solution of the problem (3.3.3).

3.4 Case Studies

We use our proposed optimization framework to investigate optimal strategies to recover P in the form of nutrient cakes and struvite from waste generated at 100 largest dairy CAFOs (ranked by the number of animal units) in the State of Wisconsin (Wisconsin Department of Natural Resources, 2017). We begin with a base case study where P is not recovered but only mobilized by transportation to mitigate environmental impact in sensitive areas. We then evaluate the impact of installing P recovery technologies with the goal of maximizing net profit from recovered products and analyze how the value of such products affect technology placement decisions. We highlight that data sources available in the literature on market values for recovered products and technology performance are scarce and highly uncertain. Consequently, our framework is not meant to provide definitive answers. Instead, the framework is meant to be used as a tool to analyze the impact of different scenarios for market prices of recovered products, recovery yields, and remediation costs. With this we seek to help policy makers analyze complex trade-offs arising in nutrient recovery and to help experimental researchers identify critical pieces of technology data that need to be refined.

In our studies, we consider the technologies described in Section 3.2 to create the set of candidate technologies $\mathcal{T}$. Two different capacity variants have been considered for each technology. These are quantified in terms of the animal unit (AU) equivalent of the waste they can process. We consider technologies with processing capacities of 500 and 3000 AUs. These processing capacities are selected in order to capture the average sizes of small and large dairy farms in the State of Wisconsin. The 500 and 3000 AU capacities

correspond to an influent waste flow rate of 18 and 108 tons/day (or 19 and 115 m^3/day), respectively. These technologies are assumed to take waste as an input and generate P-concentrated product (cakes or struvite) and digestate as the output products. This gives rise to the set of products $\mathcal{P} := \{\texttt{waste}, \texttt{cake}_1, \texttt{cake}_2, \texttt{cake}_3, \texttt{struvite}, \texttt{struvite} + \texttt{solids}, \texttt{digestate}_1, \texttt{digestate}_2, \texttt{digestate}_3, \texttt{digestate}_4, \texttt{digestate}_5\}$. For simplicity, we use the pseudonyms $p_i, i \in \{1, ..., 11\}$ for these products. A standard non-linear (six-tenths) scaling relationship (Peters et al., 1968) is used between the investment cost with respect to the equipment capacity to capture economies of scale. The data for the technologies is given by the following technology matrix:

Technology	Symbol	$\bar{\xi}_t$(kg/day))	ϕ_t^I(USD)	ϕ_t^ξ(USD/yr)	$p(t)$
Filter_I	t_1	108,862	1,731	15,088	Waste
Centrifuge_I	t_2	108,862	780,005	670,113	Waste
Coagulation_I	t_3	108,862	1,484,612	373,519	Waste
FBR_I	t_4	108,862	420,689	1,511,809	Waste
CSTR_I	t_5	108,862	1,853,453	1,860,919	Waste
Filter_II	t_6	18,143	521	6,779	Waste
Centrifuge_II	t_7	18,143	234,820	301,100	Waste
Coagulation_II	t_8	18,143	446,942	167,832	Waste
FBR_II	t_9	18,143	126,648	679,298	Waste
CSTR_II	t_{10}	18,143	557,982	836,163	Waste

The per-unit transportation cost for products is assumed to be 0.08 USD/km/ton in hauling trucks (Paudel et al., 2009). In our analysis, we also quantify the total amount of emissions generated by transportation. To do so, we use an emission factor $\alpha_\ell^{CO_2}$ of 0.1 grams of CO_2 per kg of product transported per km (Mathers et al., 2014). We define the total emissions resulting from transportation as $\phi_{CO_2} = \sum_{\ell \in \mathcal{L}} \alpha_\ell^{CO_2} f_\ell h_\ell$, where h_ℓ is the distance covered by transportation link ℓ.

The reference product for all technologies is waste ($p(t) = \texttt{waste}$) and the technology yield factors are given by:

Technology	p_1	p_2	p_3	p_4	p_5	p_6	p_7	p_8	p_9	p_{10}	p_{11}
t_1	−1	0.1372	0	0	0	0	0.8628	0	0	0	0
t_2	−1	0	0.2279	0	0	0		0.7721	0	0	0
t_3	−1	0	0	0.3315	0	0	0	0	0.6685	0	0
t_4	−1	0	0	0	0.0652	0	0	0	0	0.9348	0
t_5	−1	0	0	0	0	0.1137	0	0	0	0	0.8863
t_6	−1	0.1372	0	0	0	0	0.8628	0	0	0	0
t_7	−1	0	0.2279	0	0	0	0	0.7721	0	0	0
t_8	−1	0	0	0.3315	0	0	0	0	0.6685	0	0
t_9	−1	0	0	0	0.0652	0	0	0	0	0.9348	0
t_{10}	−1	0	0	0	0	0.1137	0	0	0	0	0.8863

Table 3.1: Market value and remediation costs for different products

Products	Product Name	Phosphorus Concentration (kg P/kg product)	Market Value (USD/kg product)	Remediation Cost (USD/kg product)
p_1	Waste	0.0013	–	0.06
p_2	Cake_1	0.0081	0.36	0.36
p_3	Cake_2	0.0054	0.24	0.24
p_4	Cake_3	0.0039	0.17	0.17
p_5	Struvite	0.0179	0.80	0.79
p_6	Struvite + Solids	0.0103	0.46	0.45
p_7	Digestate_1	0.0002	–	0.01
p_8	Digestate_2	0.0001	–	0.004
p_9	Digestate_3	0.00002	–	0.001
p_{10}	Digestate_4	0.0001	–	0.01
p_{11}	Digestate_5	0.0001	–	0.01

To capture the impact of transportation and technology placement on environmental impact, we define a set of waste demands $\mathcal{D}_r \subseteq \mathcal{D}$ located at different locations in the State that have a *negative value* $\alpha_j^r \in \mathbb{R}_-$. The use of negative demand values is used to reflect remediation costs associated with sending nutrients to a given location. We define the remediation cost as:

$$\phi^r = \sum_{j \in \mathcal{D}_r} \alpha_j^r d_j$$

In our studies, we consider a P recovery cost of USD 20/lb of phosphorus (Minnesota

Pollution Control Agency, 2017) as demand values α_j^r. We scale these remediation costs by a factor $\beta_j \in [0, 1]$ based on the geographical location in order to capture priorities of endangered areas. This helps us classify different regions in the State of Wisconsin based on P concentration and prioritize P removal from high concentration areas. To do so, the factor β_j is defined to be proportional to the current P soil concentration at a given location. We also use this estimate to compute the remediation cost for each recovered product (based on their individual P concentration). This allows us to model the possibility that P might be recovered as a P-rich product to be transported to another location for eventual "storage" in the environment.

For each product we also define demands $d_j \in \mathcal{D}$ with positive market values $\alpha_j^d \in \mathbb{R}_+$. The market value for the different cake products is estimated based on the P content of the product and we use struvite as a reference basis (which has an average market value of USD 800/ton (Dockhorn, 2009)). The product values are summarized in Table 3.1. We also consider a spectrum of cake values to analyze their impact on technology sizing and placement. We assume that the demands of struvite and cakes with positive market value are located at the CAFOs.

In our studies, we keep track of the average distance that waste is transported (defined as $h_{\texttt{waste}}$) and the percentage of waste that is transported (defined as $\zeta_{\texttt{waste}}$). We also keep track of the percentage of waste that is processed $r_{\texttt{waste}}$ by a technology.

3.4.1 *Effect of Transportation*

We first analyze the overall environmental remediation cost if no technologies are installed and if no transportation of waste is permitted. In this case, the remediation cost corresponds to the "do nothing" scenario in which the manure is left untreated at their supply point (the CAFOs). By leaving the waste untreated, nutrients in the unprocessed waste eventually contaminate ground waters or surface waters and these will eventually

need to be remediated to enable consumption. The formulation takes the form:

$$\max \quad \phi^r \tag{3.4.5a}$$

$$\text{s.t.} \quad (2.3.15) - (2.3.19) \tag{3.4.5b}$$

$$y_t = 0, \ t \in \mathcal{T}_n, n \in \mathcal{N}. \tag{3.4.5c}$$

Our supply chain model estimates that the *total remediation cost associated with leaving waste untreated is 101 million USD per year*. As can be seen, the remediation cost is significant and motivates the use of transportation and processing technologies to mitigate it.

We now analyze transportation strategies to reduce the total remediation cost (without using any processing technologies). In other words, the waste is allowed to be re-distributed (mobilized) to geographical areas with lower P soil concentrations. Here, we seek to minimize the remediation cost ϕ^r and we introduce an ϵ-constraint on transportation cost to analyze the impact of increasing transportation budgets (i.e. increasing the mobilization of waste which is implicitly captured by increasing the budget available for transportation expenses). The trade-off can be observed in Figure 3.2 and Table 3.2. In Figure 3.3 we illustrate the transportation flows that are needed to re-distribute the flow in a couple of budget instances. We note that allocating a budget for transportation of 13.8 million USD per year results in a reduction of 78% of the "do nothing" remediation cost. The largest remediation cost is around 100 million USD per year (the "do nothing" scenario previously discussed) and this is reduced to 22.3 million USD. Consequently, in absolute numbers, the reduction in remediation cost is of 77.7 million dollars per year, which is almost four times the budget allocated for transportation. Also, increasing the transportation cost beyond 13.8 million USD per year does not result in a further reduction of the remediation cost (Figure 3.2). This indicates the maximum reduction in remediation cost that can be achieved by transporting waste.

We have also found that that there is a fast (nonlinear) decrease in remediation cost as a function of the transportation budget. This is illustrated in Figure 3.2. This result

highlights that redistribution of waste provides a flexible and valuable option to mitigate environmental costs. However, the transportation option does not fully mitigate the remediation cost and does not generate any economic value and it is thus unsustainable from an economic standpoint. In other words, such a solution would need to be sustained based on government subsidies, which would most likely be covered using taxes applied to CAFOs or to the State population. If the tax is applied to the State population this would be of around 3.15 USD per inhabitant per year (the population of the State of Wisconsin is 5.8 million). Moreover, the transportation option achieves improvement in water quality at the expense of increased CO_2 emissions due to intense truck hauling. In particular, in Table 3.2 we see that manure needs to be transported over an average distance of 33 km (20 miles) in order to achieve the maximum reduction of the remediation cost. Moreover, we see that 74% of the total manure needs to be transported in order achieve such maximum reduction.

We highlight that the transportation solution only provides a short-term solution to prevent contamination in endangered areas because nutrients will accumulate in the newly allocated areas in the long run.

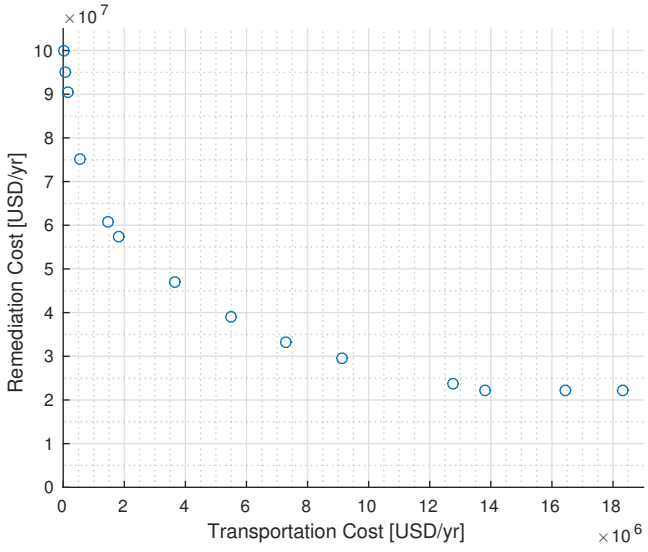

Figure 3.2: Remediation cost as a function of transportation budgets.

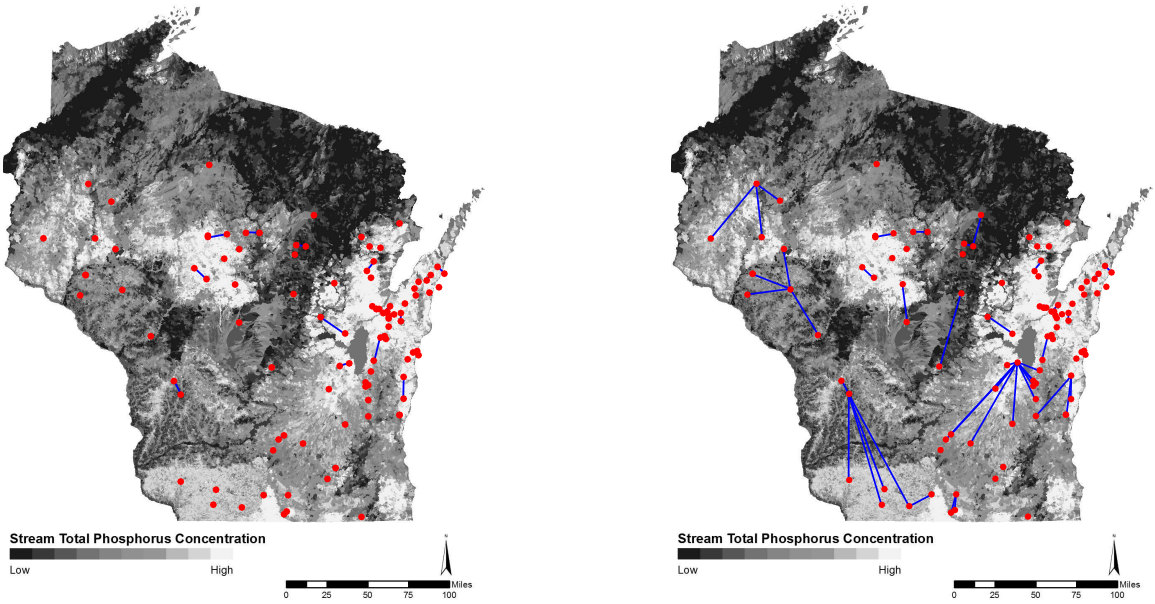

$\phi^f = 1.46 \times 10^6$ USD/yr
$\phi^r = 6.09 \times 10^7$ USD/yr
$\zeta_{\texttt{waste}} = 27\%$

$\phi^f = 9.13 \times 10^6$ USD/yr
$\phi^r = 2.94 \times 10^7$ USD/yr
$\zeta_{\texttt{waste}} = 51\%$

Figure 3.3: Optimal redistribution waste flows under different transportation budgets (Section 3.4.1). The red dots indicate the location of CAFOs and the blue lines indicate the flow of waste between them (base map of the State of Wisconsin adapted from U.S. Environmental Protection Agency (2014)).

Table 3.2: Remediation cost as a function of transportation cost (Section 3.4.1).

ϕ^f (USD/yr)	ϕ^r (USD/yr)	$\zeta_{\texttt{waste}}$ (%)	$h_{\texttt{waste}}$ (km)	ϕ_{CO_2} (tons/yr)
1.83×10^7	2.23×10^7	74	33	11,406
1.38×10^7	2.23×10^7	57	41	8,648
9.13×10^6	2.94×10^7	51	30	5,703
1.46×10^6	6.09×10^7	27	9	913
5.47×10^5	7.52×10^7	18	5	342
1.46×10^5	9.06×10^7	9	3	91
1.83×10^4	9.85×10^7	3	1	11
9.13×10^2	1.00×10^8	2	0.1	1

3.4.2 *Effect of Simultaneous Transportation and Processing (No Product Sales)*

We now analyze the impact of transporting waste and installing technologies to process it and recover different products. We first assume that no revenue is collected from the

recovered products:

$$\max \quad \phi^r - \phi^{\xi} - \phi^f \tag{3.4.6a}$$

$$\text{s.t.} \quad (2.3.15) - (2.3.19) \tag{3.4.6b}$$

Moreover, in this formulation, we do not impose any budget limit in investment. This case seeks to identify the most effective technology installation strategy to convert waste in order to mitigate transportation costs and with this facilitate mobility and mitigate remediation costs. In other words, it is possible to reduce transportation costs by processing the waste before hauling it.

The characteristics of the optimal solution are summarized in Table 3.3. We have found that the optimal solution is to install technology $\mathtt{t}_1$ (large filters) to convert the waste into cake_1 and to store it in this form in the environment (i.e., there is a remediation cost associated to the cake). We also note that the optimal solution only decides to install a small number of units (a total of $\sum_{n\in\mathcal{N}, t\in\mathcal{T}_n} y_t = 31$). As a result, only 25% of the total manure is processed. This indicates that installing too many filters will be suboptimal because this would lead to high operational costs that will offset reductions in environmental remediation costs. This also implies that the remediation costs alone are insufficient to promote the full processing of manure. Consequently, in order to promote the processing of all the manure in the CAFOs, an artificial increase in the remediation cost is required. This can be achieved by regulatory intervention or will occur naturally as ecosystems keep degrading over time.

Table 3.3: Solutions for simultaneous transportation and processing case study (Section 3.4.2)

ϕ^I (USD)	ϕ^f (USD/yr)	ϕ_{CO_2} (tons/yr)	ϕ^{ξ} (USD/yr)	Technology Installed	Total Tech. Sited	Cake_1 Recovered (kg/yr)	$r_{\mathtt{waste}}$ (%)	ϕ^r (USD/yr)	$\zeta_{\mathtt{waste}}$ (%)	$\mathrm{h}_{\mathtt{waste}}$ (km)	Total Profit (USD/yr)
5.34×10^4	4.31×10^6	2,686	4.68×10^5	$\mathtt{t}_1$	31	4.68×10^5	25	2.64×10^7	31	14	-3.11×10^7

3.4.3 *Effect of Simultaneous Transportation and Processing (with Product Sales)*

We now consider the impact of transporting waste and installing technologies to process waste while recovering income from the sale of different products. The objective is to maximize the revenue obtained from the recovered products while minimizing the remediation costs and operational costs. In other words, we maximize the social welfare (which in this case is equivalent to maximize total profit). We introduce an ϵ-constraint on the investment cost to explore how the investment budget ϵ_I affects the total profit and to identify the break-even level of investment:

$$\max \quad \phi^d + \phi^r - \phi^\xi - \phi^f \tag{3.4.7a}$$

$$\text{s.t.} \quad (2.3.15) - (2.3.19) \tag{3.4.7b}$$

$$\phi^I \leq \epsilon_I. \tag{3.4.7c}$$

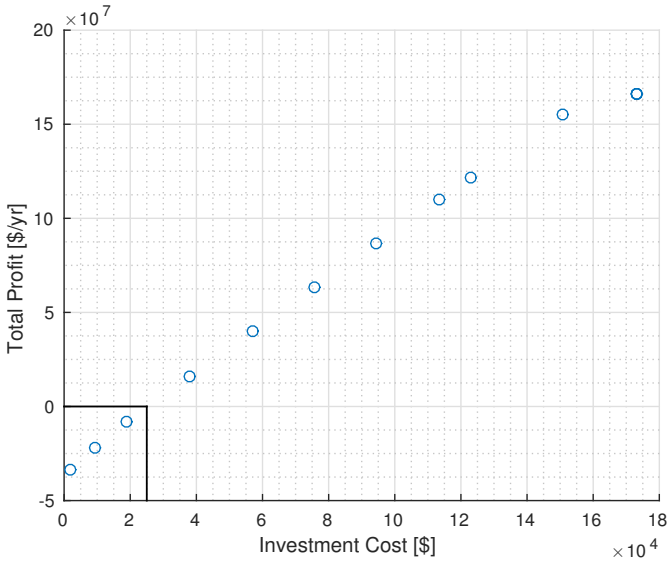

Figure 3.4: Effect of investment cost on total profit.

The results of this case study are summarized in Table 3.4 and in Figure 3.4 we show the behavior of the total profit as a function of investment budget. From Figure 3.4 we

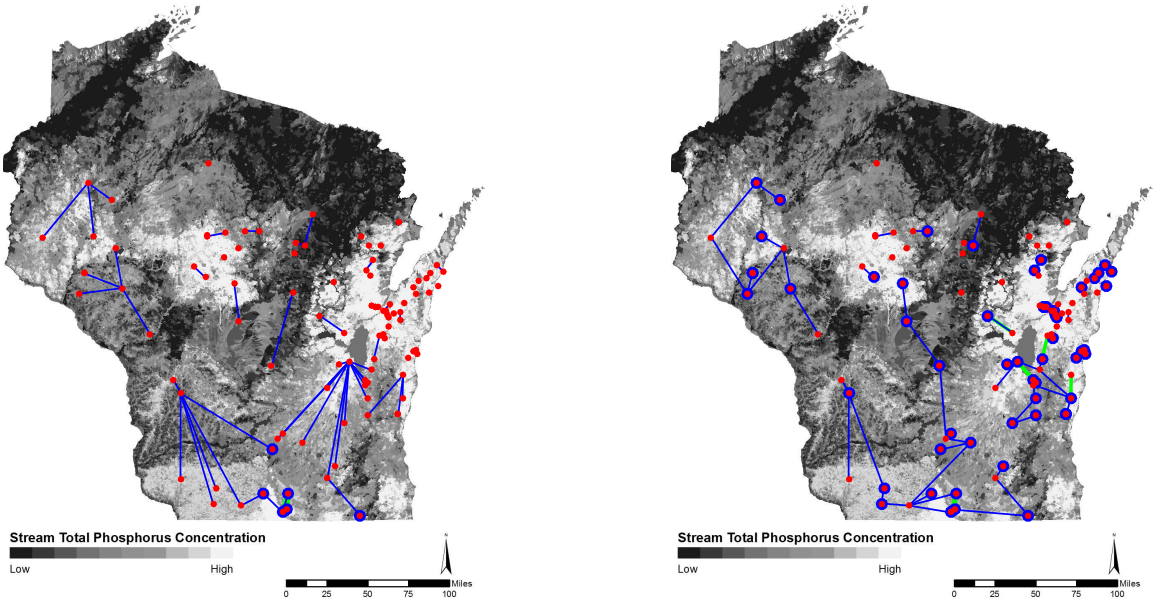

$\phi^I = 9.18 \times 10^3$ USD
$\phi^r = 2.21 \times 10^7$ USD/yr
$\zeta_{\texttt{waste}} = 52\%$

$\phi^I = 9.45 \times 10^4$ USD
$\phi^r = 1.50 \times 10^7$ USD/yr
$\zeta_{\texttt{waste}} = 24\%$

Figure 3.5: Optimal waste flows under different investment budgets (Section 3.4.3). The red dots indicate the location of CAFOs and the blue and green lines indicate the flow of waste and digestate$_1$ repectively. Rings denote locations of nutrient cake recovery technologies.

can see that the break-even point (at zero profit) occurs at an investment budget of about 25,000 USD. The total profit reaches a maximum of 1.66×10^8 USD per year with an investment of 173,133 USD and one can observe diminishing returns as the investment budget is increased. The low investment costs are attributed to the fact that the selected technologies are always filters ($\texttt{t}_1$ and $\texttt{t}_6$). These technologies are selected because of their low investment and operational cost relative to the rest of the technologies. Moreover, in this study, we use product values for cakes based on their P content relative to struvite. This results in a relatively high value of the recovered product (i.e. 0.36, 0.24, and 0.17 USD/kg for $\texttt{cake}_1$, $\texttt{cake}_2$, and $\texttt{cake}_3$ respectively).

From Table 3.4 we see that installation of large filters ($\texttt{t}_1$) is favored over small ones ($\texttt{t}_6$). This highlights that economies of scale dominate transportation costs. We also see

Table 3.4: Solutions as a function of investment budget for simultaneous transportation and processing case study (Section 3.4.3).

ϕ^I (USD)	ϕ^f (USD/yr)	ϕ_{CO_2} (tons/yr)	ϕ^s (USD/yr)	Technology Installed	**Total Tech. Sited**	$Cake_1$ Recovered (kg/yr)	ϕ^r (USD/yr)	r_{waste} (%)	$Cake_1$ Revenue (USD/yr)	ζ_{waste} (%)	h_{waste} (km)	Total Profit (USD/yr)
1.73×10^5	7.51×10^6	4,694	1.51×10^6	t_1	100	5.10×10^8	8.06×10^6	100	1.84×10^8	18	49	1.66×10^8
1.51×10^5	5.26×10^6	3,287	1.31×10^6	t_1	87	4.74×10^8	8.65×10^6	93	1.71×10^8	21	27	1.55×10^8
9.45×10^4	4.10×10^6	2,562	8.28×10^5	t_1, t_6	54, 2	2.96×10^8	1.50×10^7	58	1.07×10^8	24	21	8.69×10^7
7.55×10^4	4.11×10^6	2,566	6.62×10^5	t_1, t_6	43, 2	2.36×10^8	1.72×10^7	46	8.50×10^7	24	21	6.31×10^7
5.70×10^4	3.53×10^6	2,205	5.03×10^5	t_1, t_6	32, 3	1.77×10^8	2.00×10^7	35	6.38×10^7	28	15	3.98×10^7
1.89×10^4	6.77×10^6	4,229	1.71×10^5	t_1, t_6	10, 3	5.72×10^7	2.21×10^7	11	2.06×10^7	47	24	-8.43×10^6
9.18×10^3	9.75×10^6	6,092	8.22×10^4	t_1, t_6	5, 1	2.82×10^7	2.21×10^7	6	1.01×10^7	52	31	-2.18×10^7
1.73×10^3	1.29×10^7	8,084	1.51×10^4	t_1	1	5.45×10^6	2.23×10^7	1	2.04×10^6	53	41	-3.33×10^7

that, under this option, the remediation cost is reduced to 8 million USD per year (compared to the 22 million USD obtained in the transportation only case study of Section 3.4.1). We can also see that there are complex trade-offs between technology investment and transportation costs. In other words, logistic management of waste offsets a lack of processing capacity. In particular, we can see that at large investment budgets, the best strategy to maximize profit is to process manure on-site (only 18% of the manure is transported); while at low budgets it is necessary to mobilize manure to maximize profit (53% of the manure is mobilized). This result is highlighted in Figure 3.5, where we see that decreasing the investment budget results in fewer technologies installed and in more mobility. Figure 3.5 also illustrates how the supply chain model prioritizes geographical regions for technology installations that are counter-intuitive (that do not necessarily match areas of high P concentration). This highlights that complex interactions between technology performance, logistics, and environmental performance exist.

3.4.4 *Effect of Product Market Prices*

We now analyze the effect of different market prices for cake, which is often a significant uncertainty in P recovery systems. With this, we also seek to analyze under what conditions is struvite recovery a competitive technology. In this case study, we seek to maximize the total profit and we factor the investment cost directly in the profit (the investment cost is annualized using a project life of T=20 years). This gives the optimization

problem:

$$\max \quad \phi^d + \phi^r - \phi^\xi - \phi^f - \phi^I \tag{3.4.8a}$$

$$\text{s.t.} \quad (2.3.15) - (2.3.19) \tag{3.4.8b}$$

The results of Section 3.4.3 are obtained using values of cake products that are proportional to their P content. In this section we scale these values down and we summarize results in Tables 3.5 and 3.6. Under the prices used in Section 3.4.3 (labeled in the Tables 3.5 and 3.6 as Case 1), the model installs $\texttt{cake}_1$ and $\texttt{cake}_3$ recovery technologies (i.e., filter units and centrifugation units) and no struvite technologies are installed in this case. This indicates that the cake values are beneficial (and too optimistic). Reducing the cake values by a 50% (labelled as Case 2) results in installation of only $\texttt{cake}_1$ recovery technologies. One reason for this is the higher value for $\texttt{cake}_1$ than $\texttt{cake}_3$ because of its higher P concentration, and the relatively lower investment and operating cost associated with the $\texttt{cake}_1$ recovery technology (filter units). Reducing the cake prices further (Case 3) starts promoting the installation of struvite recovery technologies. We note, however, that the total revenue ϕ^d collected from product sales remains fairly constant in all cases and in all cases we obtain a positive total profit.

The last row of Table 3.5 (Case 7) shows the optimal solution using cake values reported in Hernández et al. (2017) and we observe that these prices also favor struvite recovery. We note that such product values are remarkably low compared to the values computed using the P content of the products. We also observe, however, that the revenue at these low values is quite high, reaching levels of 189 million USD per year and the total profit under these prices is positive (reaches 34 million USD/yr), despite the fact that the remediation cost is 8.6 million USD (Table 3.6). The fact that the remediation cost is not fully eliminated (even after processing almost all the waste) is due to the fact that the digestate generated after processing all the waste still contains nutrients (albeit at a smaller concentration compared to waste). Consequently, digestate has associated remediation

cost because it ultimately must be disposed of in the environment. This highlights the fact that nutrients persist in the environment and thus always induce a certain level of remediation cost. In the proposed model, digestate is allowed to be redistributed in order to reduce the overall remediation cost (digestate flows are shown as green lines in Figure 3.6).

The large difference observed between the revenue and the total profit is due to the high investment and operational costs of struvite recovery systems. In particular, investment costs in these cases reach 38 million USD while operational costs reach 138 million USD per year. Despite this, the results indicate that the production of struvite provides an economically sustainable option to mitigate environmental impacts in both water quality and emissions. In addition, we note that only 22% of the waste needs to be transported, thus decreasing CO_2 emissions (emissions are on the order of 4,000 tons per year, compared to the 11,000 tons per year of the transportation-only case study of Section 3.4.1). We also note that fluidized bed reactors (FBR) are the preferred technology to recover struvite (t_4), due to their lower investment costs relative to CSTR systems. Despite the high uncertainty in the final values of the recovered products, we highlight that concentrating nutrients provides a flexible approach to redistribute them and prevent accumulation in geographical regions.

Table 3.5: Optimal solution for varying prices of cakes (Section 3.4.4).

Case	$Cake_1$ Price (USD/tonne)	$Cake_2$ Price (USD/tonne)	$Cake_3$ Price (USD/tonne)	Technology Installed	**Total Tech. Sited**	$Cake_1$ recovered (kg/yr)	$Cake_3$ recovered (kg/yr)	Struvite Recovered (kg/yr)	r_{waste} (%)	Total Product Revenue (USD/yr)
1	360	240	170	t_1, t_3	74, 25	3.74×10^8	3.29×10^8	0	100	1.90×10^8
2	180	120	85	t_1	100	5.04×10^8	0	0	99	9.06×10^7
3	72	48	34	t_1, t_4, t_6	3, 90, 2	8.08×10^6	0	2.33×10^8	98	1.87×10^8
4	36	24	17	t_4	92	0	0	2.38×10^8	98	1.91×10^8
5	7.2	4.8	3.4	t_4	91	0	0	2.36×10^8	97	1.89×10^8
6	3.6	2.4	1.7	t_4	91	0	0	2.36×10^8	97	1.89×10^8
7	9.32	7.65	8.48	t_4	91	0	0	2.36×10^8	97	1.89×10^8

Table 3.6: Optimal solution for varying cake prices (Section 3.4.4).

Case	ϕ^I (USD)	ϕ^f (USD/yr)	ϕ_{CO_2} (tons/yr)	ϕ^s (USD/yr)	ζ_{waste} (%)	h_{waste} (km)	$Cake_1$ Revenue (USD/yr)	$Cake_3$ Revenue (USD/yr)	Struvite Revenue (USD/yr)	ϕ^r (USD/yr)	Total profit (USD/yr)
1	3.72×10^7	7.51×10^6	4,692	1.05×10^7	20	49	1.34×10^8	5.60×10^7	0	3.45×10^6	1.67×10^8
2	1.73×10^5	6.10×10^6	3,811	1.51×10^6	17	39	9.06×10^7	0	0	8.25×10^6	7.48×10^7
3	3.79×10^7	6.33×10^6	3,955	1.36×10^8	21	33	5.82×10^5	0	1.87×10^8	8.71×10^6	3.41×10^7
4	3.87×10^7	7.27×10^6	4,545	1.39×10^8	23	38	0	0	1.91×10^8	8.46×10^6	3.40×10^7
5	3.83×10^7	6.48×10^6	4,047	1.38×10^8	22	33	0	0	1.89×10^8	8.66×10^6	3.41×10^7
6	3.83×10^7	6.44×10^6	4,022	1.38×10^8	22	33	0	0	1.89×10^8	8.66×10^6	3.41×10^7
7	3.83×10^7	6.58×10^6	4,111	1.38×10^8	22	34	0	0	1.89×10^8	8.66×10^6	3.40×10^7

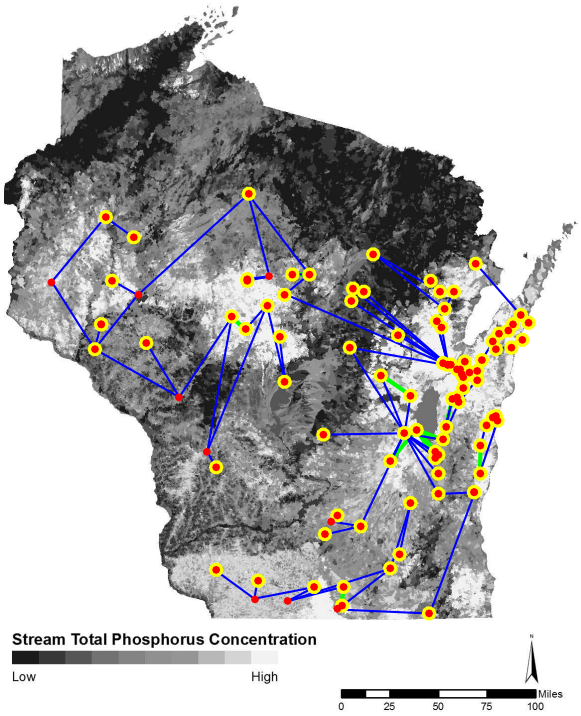

$$\phi^I = 3.83 \times 10^7 \text{ USD}$$
$$\phi^r = 8.66 \times 10^6 \text{ USD/yr}$$
$$\zeta_{\texttt{waste}} = 22\%$$

Figure 3.6: Optimal system layouts for Case 7 (Section 3.4.4). The red dots indicate the location of CAFOs and the blue and green lines indicate the flow of waste and digestate$_4$ respectively. Rings denote locations of struvite recovery technologies.

3.4.5 *Effect of Struvite Yields*

Struvite recovery from livestock waste is a relatively new technology. As a result, there is a large uncertainty associated with technology performance. In order to account for the effect of these uncertainties on the supply chain design, we consider different yield factors for struvite recovery from livestock waste (Table 3.7). We gradually decrease the yield factors for struvite recovery technologies. With this we seek to identify the range of

yields under which struvite recovery remains an economically attractive option. In this analysis, we consider the market prices of cake_1, cake_2, and cake_3 to be 9.32, 7.65, and 8.45 USD/tonne, respectively (Hernández et al., 2017) (same prices as those used in Case 7 of Section 3.4.4). The market price of struvite (produced using FBR) and struvite + solids (produced using CSTR) is considered to be 800 and 460 USD/tonne, respectively (same prices as those used in Sections 3.4.3 and 3.4.4). Using these values, we seek to maximize the total profit where we factor the investment cost directly in the profit (similar to our analysis in Section 3.4.4, the investment cost is annualized using a project life of 20 years). The optimization problem is:

$$\max \quad \phi^d + \phi^r - \phi^\xi - \phi^f - \phi^I \tag{3.4.9a}$$

$$\text{s.t.} \quad (2.3.15) - (2.3.19) \tag{3.4.9b}$$

Table 3.7: Optimal solution for varying yields of struvite recovery (Section 3.4.4).

Case	New $\gamma_{t,p}$ / Old $\gamma_{t,p}$	Struvite Yield (kg/kg waste)	Struvite + Solids Yield (kg/kg waste)	Technology Installed	**Total Tech. Sited**	Cake 1 recovered (kg/yr)	Struvite Recovered (kg/yr)	r_{waste} (%)	Total Product Revenue (USD/yr)
1 (base case)	1	0.0652	0.1137	t_4	91	0	2.36×10^8	97	1.89×10^8
2	0.9	0.0587	0.1023	t_4	89	0	2.08×10^8	95	1.66×10^8
3	0.8	0.0522	0.0910	t_1, t_4, t_6	98	2.96×10^7	1.72×10^8	95	1.38×10^8
4	0.7	0.0456	0.0796	t_1	99	4.70×10^8	0	92	4.38×10^6
5	0.5	0.0326	0.0569	t_1	99	4.71×10^8	0	92	4.38×10^6
6	0.1	0.0065	0.0114	t_1	99	4.71×10^8	0	92	4.38×10^6

Table 3.8: Optimal solution for varying yields of struvite recovery (Section 3.4.4).

Case	ϕ^I (USD)	ϕ^f (USD/yr)	ϕ_{CO_2} (tons/yr)	ϕ^ξ (USD/yr)	ζ_{waste} (%)	h_{waste} (km)	Cake_1 Revenue (USD/yr)	Struvite Revenue (USD/yr)	ϕ^r (USD/yr)	Total profit (USD/yr)
1 (base case)	3.83×10^7	6.58×10^6	4,111	1.38×10^8	22	34	0	1.89×10^8	8.66×10^6	4.02×10^7
2	3.74×10^7	5.46×10^6	3,415	1.35×10^8	21	26	0	1.66×10^8	8.75×10^6	1.55×10^7
3	3.49×10^7	4.47×10^6	2,796	1.26×10^8	20	20	2.76×10^5	1.38×10^8	8.93×10^6	-2.84×10^6
4	1.70×10^5	2.96×10^6	1,851	1.49×10^6	15	14	4.38×10^6	0	9.09×10^6	-9.17×10^6
5	1.70×10^5	3.03×10^6	1,896	1.49×10^6	15	15	4.38×10^6	0	9.03×10^6	-9.18×10^6
6	1.70×10^5	2.96×10^6	1,851	1.49×10^6	15	14	4.38×10^6	0	9.09×10^6	-9.17×10^6

The results in this case study are summarized in Tables 3.7 and 3.8. The model finds it economically beneficial to recover struvite using FBRs (t_4) when the base case yield factors are reduced to 90% of their original value. The total profit reduces to 1.55×10^7 USD/yr (39% of the base case value). This reveals a non-linear relationship between technology performance and total profit. Reducing yield factors further to 80% of the

original value, the model solution transitions towards recovering cake_1 along with recovering struvite by installing filter units (t_4 and t_6) and FBRs (t_1), respectively. In this case, the reduced product revenue and increased remediation cost make the overall profit negative. Further reductions in the yield factors leads to solutions in which recovery of cake_1 is the best option. This indicates that, for struvite recovery technologies to be economically competitive, the yield should be higher than 80% of the base case values.

3.5 Computational Requirements

All the optimization problems are MILPs that have been implemented in the algebraic modeling language `JuMP` and solved with the solver `Gurobi` on a computing server with 32 processor cores (2 sockets and 16 cores each) using Intel(R) Xeon(R) CPU E5-2698 v3 @ 2.30GHz. The problems contain around 1000 binary variables, 130,500 continuous variables, 8,000 equality constraints, and 48,000 inequality constraints. The CPU times range from a few seconds to one hour, depending on the complexity of the formulation. The higher CPU times correspond to instances where the investment or transportation budget constraints are relaxed (because of the larger feasible space).

3.6 Summary

In this chapter, we have applied the supply chain design framework presented in Chapter 2 to analyze the interplays between technology selection and placement, transportation logistics, and environmental impact associated with phosphorus (P) recovery from livestock waste. We use these computational capabilities to analyze strategies to manage waste generated at large CAFOs in the State of Wisconsin. We found that transportation of waste alone (without any processing for P recovery) can achieve significant reductions in environmental impact due to waste mobilization. We also found that struvite crystallization in fluidized beds can be an economically sustainable option to process

waste and mitigate environmental impacts. We have also found that mechanical separation (filtering) technologies that recover P in the form of nutrient cakes can achieve high environmental benefits and reduced transportation costs but are only economically self-sustaining at high cake prices. Our analysis indicates that the value of recovered products and assumed remediation costs have a strong influence on the nature of the optimal waste management strategies. This is important because markets for many of these products are immature and highly volatile.

In Chapter 4, we will investigate the effect of different policy strategies to promote the installation of P recovery technologies and to co-locate them with anaerobic digesters that produce biogas. We will also analyze the impact of policy and government incentives on the economic prospects of the analyzed technologies and recovered products.

4

POLICY DESIGN: ENVIRONMENTAL REGULATIONS AND INCENTIVES

4.1 Introduction

Livestock waste (manure) generates significant air and water quality issues in the form of methane and pathogens emissions as well as nutrient runoff to water bodies, which ultimately leads to eutrophication, algal blooms, and hypoxia (Burkholder et al., 2007; Aguirre-Villegas and Larson, 2017). Nutrient pollution is one of the leading causes of water quality impairment in the United States (U.S. Environmental Protection Agency, 2015). Lake Erie, for example, faces persistent algal bloom issues due to phosphorus runoff. In the summer of 2014 the city of Toledo, Ohio issued a two-day drinking water ban due to the formation of harmful algal blooms. This resulted in about 500,000 people losing access to drinking water (Fitzsimmons, 3rd August 2014). One strategy to contain nutrient runoff consists of processing the livestock waste to recover excess nutrients and with this balance nutrient budgets in endangered areas (Ashley et al., 2011). The nutrient-rich products (e.g. struvite which is a phosphorus-rich product) can then be sold to the market as a fertilizer (Maaß et al., 2014) or can be transported to less endangered areas. Methane can also be recovered in gaseous or liquid form and can be used as a

transportation fuel or to generate heat and electricity (Kennedy et al., 2015).

Despite the significant environmental benefits associated to waste processing, the recovery of value-added products from livestock waste is not commonplace at present due to high investment costs and to low market values being offered for the recovered products. In the case of electricity, for instance, utility companies purchase electricity at an average value of 0.04 USD/kWh (Dynamic Concepts, LLC, 2016). For electricity recovered from livestock waste this value is insufficient to offset investment and operation costs of the processing units (particularly in small to medium farms). In addition, the difficulty to attribute an economic value to the environmental benefits resulting from waste treatment is another cause for the lack in deployment of technologies. Federal and state incentives such as the Renewable Energy Credits (RECs) and Renewable Identification Numbers (RINs) can help offset high production costs and promote investment. These incentives can also help capture the environmental benefits of organic materials treatment in a systematic way. However, selecting suitable recovery pathways is a complicated task because of the multiple products and technology options that need to be evaluated and because of complex transportation (logistical) issues.

Existing research studies have not addressed the problem of livestock waste management from a holistic (systems-wide) standpoint. Decisions are often based on techno-economic feasibility studies for individual technologies (Galinato et al., 2016; Astill and Shumway, 2016; Coppedge et al., 2012; Krich et al., 2005; U.S. Department of Agriculture, U.S. Environmental Protection Agency, U.S. Department of Energy , 2014; Beddoes et al., 2007). These techno-economic studies consider the costs associated with the installation and operation of a variety of technologies such as anaerobic digestion in combination with nutrient recovery and biogas upgrading. They also consider the potential economic returns that can be obtained from product sales and objectives. These studies are site-specific and often assume a processing capacity that is equal to the waste generation capacity of the farm. Due to economies of scale, however, production cost fluctuates significantly with farm sizes. This can make waste processing in smaller farms economically

infeasible. A better option for such farms could be to transport the raw or preprocessed waste to larger centralized facilities to conduct final processing. Such possibilities can be explored under a systems-wide approach that simultaneously determines technologies types and sizes as well as product transportation strategies.

Facility location studies in livestock waste processing reported in the literature explore the use of hub and spoke (semi-centralized) layouts (Dynamic Concepts, LLC, 2016) and centralized layouts (Prasodjo et al., 2013). The study in Dynamic Concepts, LLC (2016), for instance, proposes a hub and spoke processing configuration for dairy farms in the Kewaunee County in the State of Wisconsin (WI). The study proposes to recover nutrients and renewable natural gas that is cleaned and injected in a transmission pipeline. The location of the hubs (or the processing units) is determined by assigning the larger concentrated animal feeding operations (CAFOs) as hubs and the smaller farms as the spokes which transfer their dairy waste to the hubs. The spokes for a hub are selected by drawing a five-mile radius around the hub and refining the boundaries until a desired number of hubs are obtained. This approach presents a simple strategy for building a supply chain network. Another approach is to use a geographic information systems (GIS) based framework to determine the location of the processing facilities (Ma et al., 2005). In such analysis, the location is determined by considering different factors such as distance of farms to transmission lines, natural gas pipelines, power plants, and roads. Economic and environmental aspects are also considered in these types of studies but they often assume a single technology option (due to inherent complexity associated to technology selection and sizing). The benefits of centralized biogas processing facilities have also been studied in the literature (Prasodjo et al., 2013). For swine manure management in North Carolina, for instance, it has been found that the most cost-effective solution is to design a supply chain with a single centralized directed biogas facility (Prasodjo et al., 2013). The selection of a suitable supply chain configuration is a complex decision-making process that is highly dependent on the spatial location of the dairy farms, the final destination of products, geographical prioritization, and on local economic (market) and policy conditions.

In this chapter, we use a multiproduct supply chain framework (Sampat et al., 2017) to simultaneously conduct technology selection, sizing, and placement. The model captures transportation flows and conversion of multiple products across spatially dispersed CAFOs. We show that this framework can easily accommodate diverse types of material management incentives obtained at federal and state levels (including pilot initiatives such as the Agriculture Environmental Stewardship Act of 2017 (115th Congress (2017-2018)) and Trading and Offsets in the Chesapeake Bay Watershed (Virginia's Legislative Information System)). Such analyses help us to implicitly place a monetary value on the environmental benefits (impact reduction) of processing organic waste. These capabilities allow us to conduct systematic studies on the effect of incentives on economic and environmental viability of different technology types for the recovery of a diverse set of energy and nutrient products. Our analysis reveals that the optimal strategy to manage livestock waste from dairy farms in the State of Wisconsin is to perform nutrient recovery as well as biogas recovery and upgrading *simultaneously* (in the form of coupled hybrid technologies). This synergistic strategy generates a high return on investment and helps target both air and water quality issues.

4.2 Current Incentives for Environmental Impact Reduction

The electricity generated from any renewable source (e.g., wind, solar, biomass, and biogas) is currently incentivized in the U.S. by using RECs (U.S. Environmental Protection Agency, 2017b). Under this system, every unit (MWh) of renewable electricity generated receives an REC. The producer of renewable energy can then sell the RECs either in a compliance market or in a voluntary market (Figure 4.1). Compliance markets are generated when an individual state introduces a Renewable Portfolio Standard (RPS) that mandates the utility companies generate a portion of their total energy from renewable sources. For example, the State of California established an RPS in 2002 to achieve 50% of its total energy generation from renewable sources by 2050 (California Energy Commission -

Tracking Progress, 2017). To achieve this goal, California has mandated a gradual increase in energy generation from renewable sources (requiring 33% by 2020; 40% by 2024; 45% by 2027; 50% by 2030) (Durkay, 2017). Utility companies that cannot achieve this goal have an option to buy the RECs from renewable energy producers. This results in the formation of a compliance market for RECs where the value of an REC varies with supply and demand. The value of one REC in a compliance market has historically fluctuated between 0.50 USD/MWh to 60 USD/MWh (O'Shaughnessy et al., 2015). State regulations play an important role in driving demand values and thus influencing the price of RECs. For example, the State of New Jersey has a subprogram in place to support electricity production from solar energy and it has set a goal to achieve 4.1% of energy generation from solar energy by the year 2027-2028 (Database of State Incentives for Renewables & Efficiency (DSIRE)). The RECs corresponding to solar energy are termed SRECs and can have a market value as high as 600 USD/MWh (O'Shaughnessy et al., 2015). Voluntary markets arise when customers volunteer to purchase RECs to support the generation of energy from renewable sources. In a voluntary market, the value of one REC has varied between 0.50 USD/MWh and 2.00 USD/MWh (O'Shaughnessy et al., 2015).

Another strategy for incentivizing renewable energy generation is through RINs for transportation fuels. As per the Renewable Fuel Standard (RFS) created under the Energy Policy Act of 2005, the producers of non-renewable fuels are required to blend a certain amount of renewable fuels in their final products. Consequently, when a non-renewable fuel is produced, a Renewable Volume Obligation (RVO) is generated, which needs to be fulfilled by purchasing RINs. Similar to RVOs, RINs are generated when a renewable fuel is produced. The concepts of RVO and RIN are also based on supply and demand. RVO is the demand value required to be fulfilled on the generation of a non-renewable fuel, while RIN is the supply value that can satisfy this demand. One RIN corresponds to one gallon of renewable fuel. The RFS categorizes RINs into four classes of fuels: biomass-based diesel, cellulosic biofuel, advanced biofuel, and total renewable fuel (Figure 4.1). Each of these classes has an associated RIN. The RVO includes requirements for these

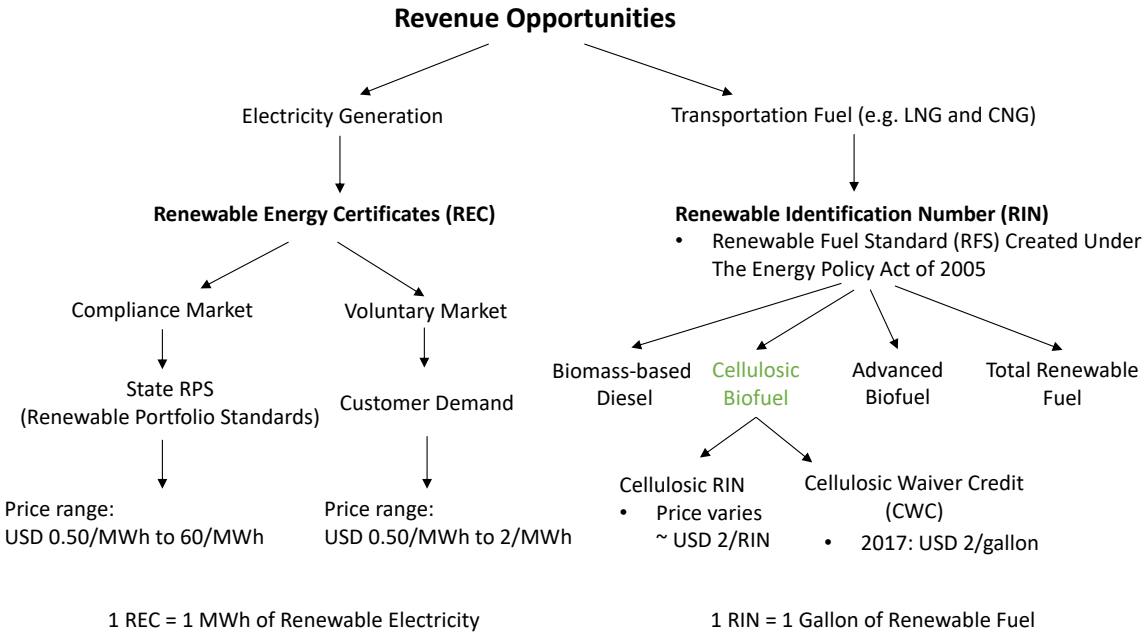

Figure 4.1: Economic incentives associated with renewable energy and fuel recovery from livestock waste

different RINs. In the context presented in this chapter, the fuels produced from livestock waste fall under the category of cellulosic biofuels (Tomich and Mintz, 2017). There are limited sources of cellulosic biofuels (i.e., the demand for cellulosic biofuels is higher than supply) and thus have a high value of around 2.00 USD/RIN. In cases where the non-renewable fuel generators cannot find cellulosic RINs to meet their requirement, they have an option to buy Cellulosic Waiver Credit (CWC). The CWCs are made available by the U.S. Environmental Protection Agency (U.S. EPA) when the projected volume of cellulosic biofuel production is less than the applicable volume of cellulosic biofuel set forth in the Clean Air Act. The U.S. EPA determines the price of CWCs using a formula specified in the Clean Air Act (U.S. Environmental Protection Agency, 2017a). For the year 2017, the value of a single CWC is 2.00 USD (U.S. Environmental Protection Agency, 2016).

Renewable electricity production tax credits (PTC) have been used in the past in the U.S. to help the development of energy from renewable sources such as wind, geother-

mal, and biomass (Sherlock, 2014). Until 2015, a full PTC credit of 2.3 cents/kWh (0.023 USD/kWh) was given to electricity generated from sources such as wind, closed-loop biomass (any organic material from the plant which is planted exclusively for energy generation), and geothermal. A half credit of 1.2 cents/kWh (0.012 USD/kWh) was given to technologies such as open-loop biomass (e.g. agricultural livestock waste), municipal solid waste, and hydropower.

In April 2017, the Agriculture Environmental Stewardship Act of 2017 was introduced in the U.S. Senate. This program proposed to introduce energy tax credits through 2021 for qualified biogas facilities and qualified manure resource recovery facilities (115th Congress (2017-2018)). Qualified biogas facilities include anaerobic digesters that convert biomass to a gas with at least 52% methane. Manure resource recovery includes technologies that recover phosphorus and nitrogen by separating at least 50% of the mass of phosphorus and nitrogen.

Incentives for nutrient recovery provide a mechanism to mitigate water quality issues. The State of Virginia, for instance, runs a nutrient trading program in the Chesapeake Bay watershed where Phosphorus credits (P credits) have a value of 10.10 USD/lb P (22.04 USD/kg P) (Virginia's Legislative Information System). Nutrient trading can also allow one source to meet its regulatory obligations by using pollutant reductions created by another source with lower pollution controls (U.S. Environmental Protection Agency).

4.3 Multi-Product Supply Chain Model

We use the modeling abstraction for network design presented in Section 2.3.2 to guide technology sizing and placement and transportation decisions. We will use this framework to analyze the impact of using different policy incentive mechanisms on the economic and environmental viability of technologies. The model used for our case studies is summarized as:

$$\max \quad \{\phi^d, -\phi^I, -\phi^s, -\phi^f, -\phi^\xi\} \tag{4.3.1a}$$

$$\text{s.t.} \quad (2.3.15) - (2.3.19) \tag{4.3.1b}$$

The objective function is the total profit in the supply chain network, given by the difference of the total revenues collected in the supply chain ϕ^d and the costs associated to supplies, transportation flows, and technology operations.

In the proposed model, we allow the value of the demands α_j^d to be either positive or negative. When the value is positive, it indicates that there is an economic incentive to satisfy the demand (we thus seek to maximize the demand served d_j to the associated node). In other words, product flows are attracted to the demand node. On the other hand, when the demand value is negative, it indicates that there is an incentive to not satisfy the demand at the associated node (the product flows are pushed away from the demand node). In this case, the demand d_j acts as a slack (residual) variable that we seek to minimize. Negative demand values can be used to model environmental remediation effects because we can consider the environment as a sink, consumer, or "stakeholder" that demands a product (waste, digestate) at a negative price. This also highlights the fact that, in our framework, products always have a final destination (i.e., for either consumption or for storage in the environment). We also highlight that the values for supplies and transportation costs are all assumed to be positive. Consequently, maximizing the objective function minimizes supply, transportation, and operational costs.

The model notation and node-level interactions are sketched in Figure 4.2. Here, we consider a candidate node (e.g. a dairy farm) in the supply chain network, where the `waste` generated on-farm is processed to recover electricity and cake_1 (a nutrient rich product). The `waste` generated on-farm is a part of the source set $\mathcal{S}_n$. Other dairy farms in the supply chain network can also transfer their `waste` to this candidate node for processing. Such `waste` flows are captured as a part of the incoming flow to the node

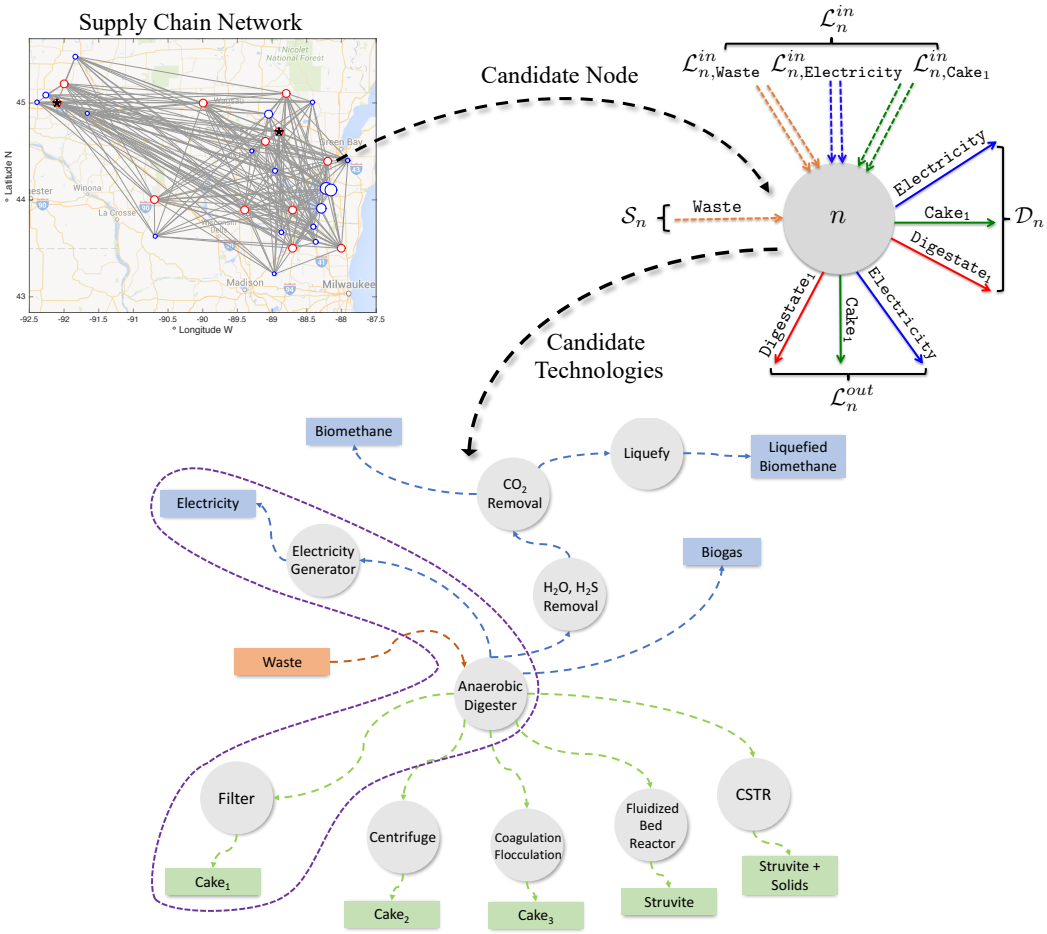

Figure 4.2: Sketch of input and output flow sets into a candidate node $n \in \mathcal{N}$ (in a supply chain network) for products $\mathcal{P}$={Waste, Electricity, Cake$_1$, Digestate$_1$}. The multiproduct model selects the technology from a set of candidate technologies ($\mathcal{T}$) illustrated in the graph.

($\mathcal{L}_{n,\texttt{waste}}^{in}$). Similarly, other farms can also transfer electricity and cake$_1$ for use at the candidate node. These flows are also captured under the set of incoming flows $\mathcal{L}_n^{in}$. The multiproduct model selects the optimal technology from a wide array of candidate technologies available for waste treatment. For this illustration, the selected technology consists of an anaerobic digester followed by an electricity generator for the production of electricity. The digestate obtained from anaerobic digestion is processed through a filter to recover cake$_1$. The products used on-site or sold at this farm are considered under the

demand set $\mathcal{D}_n$. The remaining amount of products sent to other nodes in the network are captured through the set of outgoing flow ($\mathcal{L}_n^{out}$).

In summary, the problem statement for the network design problem is as follows: Given a set of products ($\mathcal{P}$), sources ($\mathcal{S}$), sinks ($\mathcal{D}$), candidate locations ($\mathcal{N}$), and candidate technologies ($\mathcal{T}$) the goal is to determine the optimal locations for siting technologies ($y_{t,n}$), product flows (f_ℓ), and resource allocations (s_i and d_j) in the network that are a Pareto optimal solution of problem (4.3.1).

4.4 Case Studies

We use the proposed framework to investigate optimal technology deployment strategies to recover value-added products from waste generated at the 100 largest dairy CAFOs in the State of Wisconsin (Wisconsin Department of Natural Resources, 2017). We begin with a purely economic analysis that does not factor in incentives. We perform this analysis for each product independently and determine the market value at which it becomes economically feasible to recover such product. We then formulate a problem in which we include a wide range of product recovery technologies to identify optimal technology combinations. Finally, we incorporate incentives associated with the recovery of renewable energy and fuels (e.g. RECs, RINs) and nutrient credits to understand how such incentives alter the optimal technology landscape to achieve water and air quality improvements. The supply chain model was implemented in the mathematical modeling package `JuMP` and solved with `Gurobi`. All scripts and data needed to reproduce the results are available at `https://github.com/zavalab/JuliaBox/tree/master/WasteIncentives`.

We consider different nutrient recovery and biogas upgrading technologies. A key observation is that all these routes require anaerobic digestion (AD). Anaerobic digestion takes dairy waste as the input and produces `biogas` and $\texttt{digestate}_{\texttt{AD}}$. The produced `biogas` can be upgraded to recover value-added products such as electricity and transportation fuels. The $\texttt{digestate}_{\texttt{AD}}$ can be treated to recover nutrients such as phosphorus

(P) and nitrogen (N). Figure 4.3 illustrates the technology options considered. To illustrate the conversion efficiencies (yields) for various technologies, we begin with a base value of 100 kg of dairy waste. This dairy waste is assumed to include wash-water used at dairy farms along with the excreted manure. The total solids content of this dairy waste is considered to be 7%. The composition of the excreted manure is calculated by considering a herd consisting of 72% lactating cows, 4.5% dry cows, 23.3% heifers, and 0.2% calves and using the corresponding N, P, TS (total solids), and VS (volatile solids) values reported in Lorimor et al. (Lorimor et al., 2004). The water content of excreted manure is 88% (i.e. a TS of 12%). We consider a mass dilution to 93% water content due to the addition of wash-water, resulting in the final composition of dairy waste (reported in Table 4.1).

Table 4.1: Waste composition (100 kg of excreted manure after dilution with wash water)

Component	**kg**	**%**
Water	159.43	93.00
Phosphorus (P)	0.13	0.08
Nitrogen (N)	0.32	0.19
Potassium (K)	0.32	0.32
Carbon (C)	6.26	3.65
Miscellaneous	4.67	2.72
Total	171	100

Anaerobic digestion of 100 kg of the dairy waste produces 1.24 standard cubic meter (scm) of `biogas` and 98.83 kg of $\texttt{digestate}_{\texttt{AD}}$. This amount of biogas produced is estimated by considering that one kg of VS results in 0.22 scm of biogas (Ileleji et al., 2010). The dairy manure has a VS content of 80% of TS (Ileleji et al., 2010). Consequently, 100 kg of `waste` contains 5.61 kg of VS, which results in the production of 1.24 scm of `biogas`. This `biogas` (containing 60% CH_4 and 39 % CO_2 on a volume basis) is assumed to have a density of 1.15 kg/m^3 (Jørgensen, 2009). The amount of $\texttt{digestate}_{\texttt{AD}}$ produced is then estimated by a mass balance analysis.

The `biogas` can either be used for heating purposes or for electricity generation. The amount of electricity generated is based on the CH_4 content of the biogas. CH_4 has a heating value of 1000 BTU/ft^3 (37.3 MJ/m^3). The produced `biogas` has 60% CH_4 on a

volume basis. Assuming a thermal efficiency of 28%, one kWh of electricity generation corresponds to 12 ft^3 (0.345 scm) of CH_4. We thus estimate that 2.18 kWh of electricity can be generated from 100 kg of dairy waste.

An alternative to generating electricity is the recovery of either biomethane or transportation fuels from the biogas. Both of these products require further cleaning of raw `biogas` to remove impurities such as H_2O, H_2S, and CO_2. The H_2O can be removed by condensation, while the H_2S is removed using an iron sponge technology (Krich et al., 2005). The clean biogas can be further upgraded to remove CO_2 by using a scrubbing technology to produce pipeline quality biomethane (0.74 scm/100 kg `waste`) (Krich et al., 2005). The amount of biomethane produced is estimated by considering a yield factor of 0.596 scm of biomethane per scm of biogas (Carnevale and Lombardi, 2015). The produced `biomethane` can be injected directly into the natural gas pipeline infrastructure. Yet another alternative is to liquefy the `biomethane` to produce `liquefied biomethane` (LBM). This results in 0.31 gal (1.17 liters) LBM. The yield of LBM is based on the assumption that 84 ft^3 of `biomethane` correspond to one gal of LBM (Krich et al., 2005).

For nutrient recovery, we consider five technology variants that take $\texttt{digestate}_{\texttt{AD}}$ as the input and produce P-concentrated products (cakes or struvite) and `digestate` as the output products. The conversion efficiencies and associated investment and operational costs have been estimated by using the models reported in Martín-Hernández et al. (2018). The first technology considered is based on reactive filtration where a metal slag is used as the filter medium. This technology produces 12.22 kg of $\texttt{cake}_1$ containing 0.57% P. The second technology is centrifugation with pretreatment, where a mixture of $CaCO_3$ and $FeCl_3$ is added to enhance the separation efficiency of P. A total of 37.73 kg of a nutrient-rich cake ($\texttt{cake}_2$) is produced containing 0.21% P. The next technology considered is coagulation flocculation, where first the $\texttt{digestate}_{\texttt{AD}}$ in the form of suspension is destabilized by reducing attractive forces. A flocculation process is then carried out to form flocs from the previously destabilized colloids, and this results in their subsequent precipitation resulting in 15.23 kg of $\texttt{cake}_3$ which has a P content of 0.52%. The next tech-

nology is a fluidized bed reactor (FBR) where struvite ($NH_4MgPO_4.6H_2O$) is precipitated by the addition of $MgCl_2$. The advantage of this technology is that struvite is a solid with high nutrient density (which makes it more convenient to transport compared to transporting `waste`) and can be used as a slow-release fertilizer without any post-processing (Doyle and Parsons, 2002). FBR produces 0.62 kg of `struvite` (containing 12.57% P) per 98.83 kg of input $\texttt{digestate}_{\texttt{AD}}$. The final nutrient recovery technology that we consider is a continuous stirred tank reactor (CSTR), where the final product also contains struvite but with a P content of 1.22%. Because the residence time in the CSTR is long, it is not necessary to use a pre-mixing tank (as in the case of FBR) and $MgCl_2$ is added directly to the reactor. Consequently, 5.86 kg of `struvite` + `solids` is formed in one step in the CSTR. The amount of `digestate` produced from the above-listed nutrient recovery technologies is estimated via mass balance analysis.

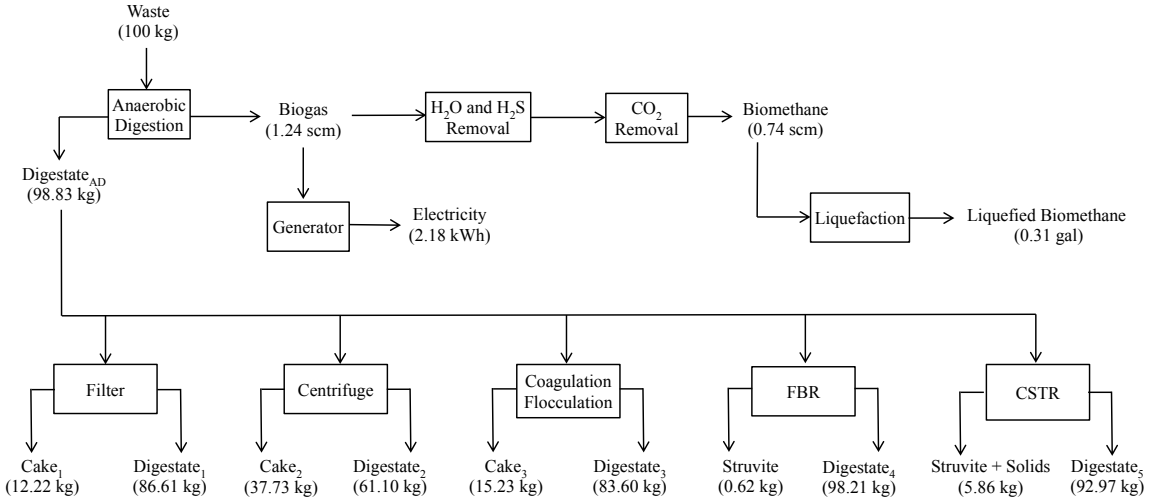

Figure 4.3: Product slate with corresponding product yields for an input of 100 kg of waste

4.4.1 *Pure Economic Analysis*

We first investigate the waste treatment problem from a purely economic perspective. The objective is to find a technology deployment strategy that maximizes the economic

returns without including any incentives. Penalties associated with nutrient emissions are also not imposed in this analysis. We assign a market value to all the products (Table 4.2). We assume that utility companies buy electricity at an average price of 0.04 USD/kWh (Dynamic Concepts, LLC, 2016). When biogas is used for heating purposes, the associated cost is calculated based on its heating value. In our analysis, the untreated biogas after AD has a CH_4 content of 60% on a volume basis. Thus one standard cubic meter (scm) of biogas has a heating value of 21,333 BTU or 0.021 MMBTU. Based on the average market value of natural gas at 2.25USD/MMBTU (U.S. Energy Information Administration), we estimate the value of biogas to be 0.048 USD/scm.

`Biomethane` is obtained after the biogas is upgraded to remove H_2O, H_2S, and CO_2 to achieve the purity of pipeline quality natural gas. This `biomethane` can then be injected into the natural gas pipeline infrastructure. The value of biomethane is assumed to be the same of natural gas (0.15 USD/scm). Liquefied biomethane is obtained by the liquefaction of `biomethane`. Its value is assumed to be the same as that of liquefied natural gas (LNG) at 1.0 USD/gal (Krich et al., 2005). The value for nutrient-rich cakes (i.e. $cake_1$, $cake_2$, and $cake_3$) are estimated to be 15 USD/ton, 4.9 USD/ton, and 12.5 USD/ton, respectively, based on the analysis provided in Hernández et al. (2017). The average market value of struvite is considered to be 800 USD/ton (Dockhorn, 2009). The corresponding market value for struvite plus solids is estimated to be 77.3 USD/ton based on its relative P concentration of 1.22% with respect to P concentration of struvite of 12.57%. The livestock waste has been assigned a market value of zero. Similarly, the effluent streams $digestate_{AD}$, $digestate_1$, $digestate_2$, $digestate_3$, $digestate_4$, and $digestate_5$ have been assigned a market value of zero in this case. This is equivalent to assuming that the untreated livestock waste and the effluent streams are spread on the field and there is no disposal cost associated with this practice.

We also report the carbon efficiencies corresponding to each final product recovered as described in Table 4.2. Carbon efficiency is a green chemistry indicator that represents the percentage of carbon in the reactants that remain in the final product (Constable

et al., 2002). The majority of carbon from the `waste` is captured in nutrient-rich products (85%) while the remaining carbon is recovered in biogas or related products (10% - 15%). These values are computed by a simple mass balance analysis. Nutrient recovery is thus a major source of carbon capture compared to biogas recovery. The input `waste` has a carbon content of 3.65% (Table 4.1). The biogas generated after anaerobic digestion has majority carbon in the form of CH_4 and CO_2 corresponding to 15% of the total carbon in the input `waste`. Further processing of biogas to produce biomethane and liquefied biomethane involves removal of CO_2, thus resulting in a reduced carbon efficiency (10%) for these products. The remaining carbon of the input `waste` is considered to remain in the $\text{digestate}_{\text{AD}}$ after anaerobic digestion. The models reported in Martín-Hernández et al. (2018) consider that carbon present in $\text{digestate}_{\text{AD}}$ is recovered with the nutrient-rich products. Table 4.2 also reports the P content of the input `waste` and the various nutrient-rich products based on the models reported in Martín-Hernández et al. (2018). We also report the phosphorus (P) efficiency associated with each product. This is similar to the concept of carbon efficiency. P efficiency is the percentage of phosphorus in the reactants that remains in the final product. It is interesting to note that even though struvite has a high P content (12.57%), its P efficiency (90%) is lower than that of cake_2 (95%) and cake_3 (99%) because the amount of struvite produced per unit mass of `waste` is less compared to the yield factors associated with that of cake_2 and cake_3, thus reducing the total P recovered in the process.

In our studies, we consider the technologies identified in Table 4.3 to create the set of candidate technologies $\mathcal{T}$. Two different capacity variants have been considered for each technology. These are quantified in terms of the animal unit (AU) equivalent of the waste they can process. The AU is a standard unit used for calculating the relative grazing impact of different kinds and classes of livestock. It is defined as an animal equivalent of 1000 pounds live weight. To provide a reference, a single lactating dairy cow weighs about 1,400 pounds or 1.4 AUs. We consider technologies with processing capacities of 5,000 and 10,000 AUs. The data for investment and operation costs were obtained from

Table 4.2: Market value for different products with the associated phosphorus content, phosphorus efficiency, and carbon efficiency

Products	Product Name	Market Value	Units	Phosphorus Content (% wt)	Phosphorus Efficiency (%)	Carbon Efficiency (%)
$p1$	Waste	0	USD/ton	0.08	-	-
$p2$	Electricity	0.04	USD/kWh	0	0	0
$p3$	Biogas	0.048	USD/scm	0	0	15
$p4$	Biomethane	0.15	USD/scm	0	0	10
$p5$	Liq. Biomethane	1	USD/gal	0	0	10
$p6$	Cake1	15	USD/ton	0.57	86	85
$p7$	Cake2	4.9	USD/ton	0.21	95	85
$p8$	Cake3	12.5	USD/ton	0.52	99	85
$p9$	Struvite	800	USD/ton	12.57	90	85
$p10$	Struvite + Solids	77.3	USD/ton	1.22	90	85
$p11$	DigestateAD	0	USD/ton	0.08	-	-
$p12$	Digestate1	0	USD/ton	0.012	-	-
$p13$	Digestate2	0	USD/ton	0.002	-	-
$p14$	Digestate3	0	USD/ton	0.001	-	-
$p15$	Digestate4	0	USD/ton	0.002	-	-
$p16$	Digestate5	0	USD/ton	0.01	-	-

a variety of sources. For the case of anaerobic digestion, we estimate the investment cost based on the cost projection formula given in Meyer and Powers (Meyer and Powers, 2011).

The operating cost for an anaerobic digester is assumed to be 2.4% of the investment cost (Beddoes et al., 2007). The cost of technologies (t_2 and t_{26}) for biogas production, followed by electricity generation is estimated from the prices reported for a dairy farm in Indiana (Agstar, February 2014). The capital cost is reported to be 12 million USD (Agstar, February 2014) for a two-stage mixed plug flow digester (capacity corresponding to 9000 cows) with engine and generator (Tomich and Mintz, 2017). The operating costs are reported to be 600,000 USD per year. We scale these costs using the six-tenths-factor rule (Peters et al., 1968) to estimate the cost associated with technologies t_2 and t_{26} having capacity corresponding to 5,000 and 10,000 AU respectively. We also scale the operating costs using the six-tenths-factor rule because the detailed process data are not reported for these technologies. In addition, because the operating cost is usually 10% of the capital cost (i.e. proportional to the capital cost), we assume that it follows a similar scaling relationship as that of the capital cost. Similarly, the cost of biogas cleaning and

upgrading to pipeline quality biogas (biomethane) or liquefaction to liquefied biomethane is estimated using the six-tenths rule from the costs reported in Krich et al. (2005). Krich et al. (2005) estimate the technology cost for dairy farms in California based on the data collected from biogas upgrading plants in Sweden. For the case of nutrient recovery technologies (filtration, centrifugation, coagulation flocculation, FBR, and CSTR), the cost data were based on models reported in Martín-Hernández et al. (2018).

Table 4.3: List of candidate technologies with corresponding investment and operation costs

		Capacity = 3.75×10^5 (kg/day) (5,000 AU)			Capacity = 7.49×10^5 (kg/day) (10,000 AU)		
Sr. No.	**Technology**	**Tech. No.**	**Investment Cost (USD)**	**Operation Cost (USD/yr)**	**Tech. No.**	**Investment Cost (USD)**	**Operation Cost (USD/yr)**
1	AD	t_1	2.69×10^6	6.45×10^4	t_{25}	5.01×10^6	1.20×10^5
2	AD + Generator	t_2	6.46×10^6	3.23×10^5	t_{26}	1.02×10^7	5.10×10^5
3	AD + Cleaning	t_3	4.51×10^6	2.12×10^5	t_{27}	7.89×10^6	3.53×10^5
4	AD + Cleaning + Liquefaction	t_4	9.05×10^6	2.79×10^5	t_{28}	1.51×10^7	4.59×10^5
5	AD + Filter	t_5	2.70×10^6	1.34×10^6	t_{29}	5.04×10^6	2.14×10^6
6	AD + Centrifuge	t_6	4.09×10^6	2.04×10^6	t_{30}	7.24×10^6	3.26×10^6
7	AD + Coag. Floc.	t_7	6.46×10^6	1.74×10^6	t_{31}	1.10×10^7	2.79×10^6
8	AD + FBR	t_8	5.33×10^6	3.06×10^6	t_{32}	9.21×10^6	4.87×10^6
9	AD + CSTR	t_9	5.90×10^6	3.26×10^6	t_{33}	1.01×10^7	5.20×10^6
10	AD + Filter + Generator	t_{10}	6.47×10^6	1.59×10^6	t_{34}	1.02×10^7	2.53×10^6
11	AD + Filter + Cleaning	t_{11}	4.52×10^6	1.48×10^6	t_{35}	7.91×10^6	2.37×10^6
12	AD + Filter + Cleaning + Liquefaction	t_{12}	9.06×10^6	1.55×10^6	t_{36}	1.51×10^7	2.48×10^6
13	AD + Centrifuge + Generator	t_{13}	7.86×10^6	2.30×10^6	t_{37}	1.24×10^7	3.65×10^6
14	AD + Centrifuge + Cleaning	t_{14}	5.91×10^6	2.19×10^6	t_{38}	1.01×10^7	3.49×10^6
15	AD + Centrifuge + Cleaning + Liquefaction	t_{15}	1.05×10^7	2.25×10^6	t_{39}	1.73×10^7	3.59×10^6
16	AD + Coag. Floc. + Generator	t_{16}	1.02×10^7	2.00×10^6	t_{40}	1.62×10^7	3.18×10^6
17	AD + Coag. Floc. + Cleaning	t_{17}	8.28×10^6	1.89×10^6	t_{41}	1.39×10^7	3.02×10^6
18	AD + Coag. Floc. + Cleaning + Liquefaction	t_{18}	1.28×10^7	1.96×10^6	t_{42}	2.10×10^7	3.12×10^6
19	AD + FBR + Generator	t_{19}	9.10×10^6	3.31×10^6	t_{43}	1.44×10^7	5.26×10^6
20	AD + FBR + Cleaning	t_{20}	7.15×10^6	3.20×10^6	t_{44}	1.21×10^7	5.10×10^6
21	AD + FBR + Cleaning + Liquefaction	t_{21}	1.17×10^7	3.27×10^6	t_{45}	1.93×10^7	5.21×10^6
22	AD + CSTR + Generator	t_{22}	9.68×10^6	3.52×10^6	t_{46}	1.53×10^7	5.59×10^6
23	AD + CSTR + Cleaning	t_{23}	7.73×10^6	3.41×10^6	t_{47}	1.30×10^7	5.43×10^6
24	AD + CSTR + Cleaning + Liquefaction	t_{24}	1.23×10^7	3.48×10^6	t_{48}	2.02×10^7	5.54×10^6

A common limiting factor for the economic viability of waste treatment technologies is the competition from non-renewable sources that usually offer the same product at a much lower price. We analyze how production costs for recovered products from dairy waste compare with current market prices by performing an economic analysis. First, we calculate the total production cost per unit product by accounting for the investment and operating cost data (Table 4.4). Because of economies of scale, the per-unit cost associated with a high capacity technology like 10,000 AU is less than the cost associated with a lower capacity technology like 5,000 AU. For example, the electricity production cost for a technology with a capacity of 10,000 AU is 0.11 USD/kWh while for a capacity of

5,000 AU the cost is 0.22 USD/kWh. These production costs do not account for transportation logistics. In order to include the cost associated with transportation, we run the supply chain model (Sampat et al., 2017) for each product recovery technology. We execute this analysis by limiting the list of candidate technologies to those that recover the particular product being analyzed. For example, when analyzing electricity generation, the candidate technologies that are considered are $\mathtt{t}_2$ and $\mathtt{t}_{26}$. The objective function in this analysis is to maximize the total profit, which includes the total revenues (ϕ^d) obtained from sales of an individual product while minimizing the associated investment (ϕ^I), operational (ϕ^ξ), and transportation cost (ϕ^f)):

$$\max \quad \phi^d - \phi^I - \phi^\xi - \phi^f \tag{4.4.2a}$$

$$\text{s.t.} \quad (2.3.15) - (2.3.19) \tag{4.4.2b}$$

The costs are expressed on an annualized basis and we assume an equipment life of 20 years. Our results show that, for most of the products being considered, the current market values are too low to justify waste processing. Consequently, the optimal solution (from an economic perspective) is to do nothing and to leave the waste untreated. We thus gradually increase the value of the product to estimate the price at which the model finds it economically feasible to recover the product (profit becomes positive). In other words, this analysis determines the optimal break-even cost that accounts for transportation costs and economies of scale associated to technology sizing. From Table 4.4 we can see that the break-even value associated with electricity recovery is 0.18 USD/kWh (while the utility companies currently offer 0.04 USD/kWh to purchase electricity). This reveals that it is generally not economically advantageous for dairy farmers in the U.S. to recover electricity from manure. The estimated break-even electricity cost also explains why electricity recovery from manure has been economically feasible in Spain, Germany, and Denmark, where the average value of electricity is 0.30, 0.35, and 0.40 USD/kWh, respectively (OVO Energy).

Table 4.4: Product value analysis. (Note that the break-even values reported here are for each product considered in isolation.)

Product	Market Value (from Literature)	$\phi^I + \phi^\xi$ (5,000 AU, from data)	$\phi^I + \phi^\xi$ (10,000 AU, from data)	Break-even value (from model)	Units
Electricity	0.04	0.22	0.11	0.18	USD/kWh
Biogas	0.048	0.12	0.11	0.15	USD/scm
Biomethane	0.15	0.24	0.22	0.40	USD/scm
Liq. Biomethane	1.00	1.26	0.86	1.5	USD/gal
Cake1	15.0	64	60	70	USD/ton
Cake2	4.9	36	31	35	USD/ton
Cake3	12.5	80	71	78	USD/ton
Struvite	800	3457	2930	3300	USD/ton
Struvite + Solids	77.3	395	333	350	USD/ton

The break-even values listed above assume single product recovery. We now expand our analysis to consider all product recovery options simultaneously and allow the model to make a decision about which sets of products should be recovered and on which technologies. In our study, we allow for some technologies to be combined to recover multiple products simultaneously. Specifically, biogas upgrading can be combined with nutrient recovery to recover energy and nutrient-rich products. Because anaerobic digestion is the common first step in both biogas upgrading and nutrient recovery, the overall production costs for the final products can be brought down by synergizing these technologies. For this case study, we expand the list of candidate technologies to allow for the combination of such technologies. The candidate technologies listed in Table 4.3 consider all combinations possible for biogas upgrading and nutrient recovery. We note that this list also includes the single product recovery options to allow the model to select between synergizing technologies or recovering single products. The model uses the same objective function and constraints in Eq. 4.4.2 and uses the expanded list of candidate technologies as shown in Table 4.3. As with the single product case, this case finds that leaving the waste unprocessed (do-nothing) is the best strategy from an economic perspective. This is because the market values for all the value-added products are lower than their respective production costs (Table 4.4). Moreover, we conclude that synergizing technologies is not sufficient to achieve economic viability.

4.4.2 *Effect of Incentives*

In this section, we analyze the effect of current incentives such as the RECs, RINs, and P credits on the economic viability of waste processing technologies.

Renewable Energy Credits (REC) Analysis

We use the proposed model to estimate the value of the REC incentive required to make electricity recovery an economically attractive option. This analysis is different from our analysis on market values as we now consider all 48 candidate technologies listed in Table 4.3. Thus, for the model to select electricity recovery technologies, the profits obtained from electricity generation not only need to be economically viable, but also should also achieve the highest economic returns compared to other product recovery options. The objective is to maximize the annualized profit including the revenue obtained from REC credits (ϕ^{REC}) :

$$\max \quad \phi^{d} + \phi^{REC} - \phi^{I} - \phi^{\xi} - \phi^{f} \tag{4.4.3a}$$

$$\text{s.t.} \quad (2.3.15) - (2.3.19) \tag{4.4.3b}$$

In our studies, we gradually increase incentives for electricity generation, as shown in Table 4.5. We begin by introducing REC incentives for every MWh of electricity generated. As shown in Table 4.5, the optimal supply chain does not recover electricity until the REC value is increased to 200 USD/MWh (0.2 USD/kWh). This is about 400% higher than the purchase price of electricity by utility companies (0.04 USD/kWh). Clearly, this is a high value and, even with such a high value, the return on investment (ROI) is low (1.92%). To obtain an acceptable investment and a shorter payback period, the REC value needs to be further increased (see Table 4.5). Such a heavy incentive strategy is not economically sustainable since it makes the entire waste processing infrastructure heavily dependent on external incentives.

Table 4.5: Economic performance of supply chains under REC analysis

REC Value (USD/MWh)	Electricity Recovered (MWh/yr)	WI Electricity Share (%)	Total Tech. Sited	$r_{\texttt{Waste}}$ (%)	ϕ^I (USD)	ϕ^{ξ} (USD/yr)	ϕ_t (USD/yr)	$\phi^d_{\texttt{electricity}}$ (USD/yr)	ϕ^{REC} (USD/yr)	ROI (%)	Payback Period (yrs)
$\leq$ 100	0	0	0	0	0	0	0	0	0	0	N/A
200	8.35×10^4	0.13	17	49.9	1.51×10^8	7.55×10^6	2.04×10^6	3.34×10^6	1.67×10^7	1.92	52
500	1.65×10^5	0.25	43	98.5	3.38×10^8	1.69×10^7	9.69×10^6	6.59×10^6	8.24×10^7	13.48	7
800	1.67×10^5	0.25	43	99.8	3.45×10^8	1.73×10^7	1.03×10^7	6.68×10^6	1.34×10^8	27.64	4
1000	1.67×10^5	0.25	44	100	3.48×10^8	1.74×10^7	1.06×10^7	6.69×10^6	1.67×10^8	36.96	3

Another interesting result found is that increasing the REC incentive above 500 USD/MWh does not significantly increase the amount of electricity recovered. The largest possible amount of electricity that can be generated by processing all the waste (i.e., $r_{\texttt{waste}}$ = 100%) is 1.67×10^5 MWh/yr. This value corresponds to 0.25% of the total electricity demand by the State of Wisconsin. From the point of view of the Renewable Fuel Standard (RFS) for the state, this percentage is negligible. According to the RFS established in 1998, the State of Wisconsin had set a goal to reach 10% of the total energy generation be from renewable sources by the year 2015. Clearly, electricity generation from dairy waste does not contribute significantly to such goals.

Renewable Identification Number (RIN) Analysis

We now analyze the effect of introducing incentives associated with the production of renewable transportation fuel in the form of RINs. As described previously, liquefied biomethane generated from dairy waste is incentivized under the Cellulosic RINs category. In years when the projected supply for the cellulosic RINs is less than the projected demand value, CWC values are declared by the U.S. EPA. The CWC for the year 2017 is 2 USD/gal of liquefied biomethane produced. We perform our analysis around this nominal value of 2 USD/gal and evaluate the return on investment (ROI) for the project as a function of RIN. The objective is to maximize the annualized profit including the revenue obtained from RIN credits (ϕ_{RIN}) :

$$\max \quad \phi^d + \phi^{RIN} - \phi^I - \phi^{\xi} - \phi^f \tag{4.4.4a}$$

$$\text{s.t.} \quad (2.3.15) - (2.3.19) \tag{4.4.4b}$$

With a RIN value of 2 USD/gal, the recovery of LBM is economically viable (Table 4.6). The ROI, however, is rather low for this case (5.24%), resulting in a payback period of 19 years. For a lower RIN value of 0.5 USD/gal, it is also economically viable to recover LBM but the payback period is larger than the assumed project life of 20 years. Increasing the RIN value helps bring down the payback period to about 10 years. The results in Table 4.6 also reflect the stable nature of the solution (i.e. increasing the RIN value results in a gradual increase in the ROI). We see, however, that the revenue collected from RINs is of the same order of magnitude as the revenue obtained from product sales, indicating that the supply chain will be heavily reliant on incentives. We also highlight that the revenue collected from RINs by technology provides and producers is in fact money invested by federal and local governments to incentivize technologies. Interestingly, we see that the investment needed to incentivize technologies via RECs or RINs (to achieve a similar ROI of 10%) are quite similar (on the order of 60-70 MUSD/yr).

Table 4.6: Economics of Renewable Identification Number (RIN) analysis

RIN Value (USD/gal)	LBM Recovered (gal/yr)	Total Tech. Sited	$r_{\texttt{Waste}}$ (%)	ϕ^{I} (USD)	ϕ^{ξ} (USD/yr)	ϕ^{f} (USD/yr)	$\phi^{d}_{\texttt{LBM}}$ (USD/yr)	ϕ^{RIN} (USD/yr)	ROI (%)	Payback Period (yrs)
0.5	2.54×10^{6}	3	10.69	4.53×10^{7}	1.38×10^{6}	1.99×10^{4}	2.54×10^{6}	1.27×10^{6}	0.34	296
1	1.31×10^{7}	20	55.25	2.48×10^{8}	7.56×10^{6}	2.34×10^{6}	1.31×10^{7}	1.31×10^{7}	1.62	62
1.5	1.86×10^{7}	29	78.41	3.53×10^{8}	1.08×10^{7}	5.88×10^{6}	1.86×10^{7}	2.80×10^{7}	3.48	29
2	2.17×10^{7}	37	91.32	4.26×10^{8}	1.30×10^{7}	8.55×10^{6}	2.17×10^{7}	4.34×10^{7}	5.24	19
2.5	4.50×10^{8}	39	96.22	4.50×10^{8}	1.38×10^{7}	1.04×10^{7}	2.29×10^{7}	5.72×10^{7}	7.45	13
3	2.30×10^{7}	39	96.69	4.50×10^{8}	1.38×10^{7}	1.09×10^{7}	2.30×10^{7}	6.90×10^{7}	9.98	10

One drawback associated to the recovery of LBM is that it cannot be stored over an extended period of time (Krich et al., 2005). In particular, evaporation losses make it economically infeasible to store LBM for more than a week. LBM storage pressure varies with the size of the storage tank: large tanks have a very low pressure of less than 5 psig [0.3 barg], while smaller tanks (70,000 gallons and less), can have pressure between 5 psig [0.3 barg] to over 250 psig [16 barg]. LBM must be maintained at low temperatures (at least below -177 F [-83 C]) to remain a liquid, independent of pressure (CH-IV International). Thus, for LBM recovery to be viable, there should be a stable customer base that can utilize the LBM soon after production. One possibility to achieve this would be to use LBM as a fuel for manure hauling trucks.

4.4.3 *Phosphorus Credits Analysis*

In our analysis, we consider the reduction in the P discharge brought by the recovery of nutrient-rich products to generate P credits at a dairy farm. A standardized quality specification of the recovered P is needed in order to regulate such product recovery based nutrient trading program. For this analysis, we consider that all the nutrient-rich products ($\texttt{cake}_1$, $\texttt{cake}_2$, $\texttt{cake}_3$, `struvite`, and `struvite + solids`) are eligible to claim P credits.

Since different nutrient recovery products ($\texttt{cake}_1$, $\texttt{cake}_2$, $\texttt{cake}_3$, `struvite`, and `struvite + solids`) have different P concentrations (0.57%, 0.21%, 0.52%, 12.57%, and 1.22%, respectively), their recovery will generate different P credits. We use the optimization model to decide which nutrient recovery option will generate highest profit given the associated production and logistical costs. No other incentives (such as RECs and RINs) are included in this analysis. The goal is to study the impact of nutrient credits on the overall project economics. As shown in Table 4.7 we test different values of P credits. The objective function for this case study is to maximize the annualized profit including the revenue generated from P credits (ϕ_P):

$$\max \quad \phi^d + \phi^P - \phi^I - \phi^\xi - \phi^f \tag{4.4.5a}$$

$$\text{s.t.} \quad (2.3.15) - (2.3.19) \tag{4.4.5b}$$

For a P credit of less than 2 USD/lb P, the optimization model does not find it profitable to process waste and recover products (Table 4.7 and Table 4.8). When the credit increases to 20 USD/lb P, the model finds it more profitable to process all waste and recover nutrient cakes. Even though the nutrient cakes have a lower P concentration and a lower product value (compared to struvite), the associated production costs are also lower. Also, cake recovery technologies (filter and coagulation-flocculation) are much simpler to deploy than the struvite recovery technologies.

Table 4.7: Products recovered for varying phosphorus credits

Sr. No.	P Credit (USD/lb P)	$\texttt{Cake}_1$ Recovered (tonne/yr)	$\texttt{Cake}_3$ Recovered (tonne/yr)	Biogas Recovered (million scm/yr)	Waste Processed (%)
1	≤ 2	0	0	0	0
2	5	4.02×10^5	0	40.69	43
3	10	9.20×10^5	0	93.25	98
4	15	8.61×10^5	8.33×10^4	94.27	99
5	20	1.84×10^5	9.38×10^6	94.94	100

Table 4.8: Economics of phosphorus credits

Sr. No.	Total Tech. Sited	ϕ^I (USD)	ϕ^ξ (USD/yr)	ϕ^f (USD/yr)	ϕ^d (USD/yr)	ϕ^P (USD/yr)	ROI (%)	Payback Period (yrs)
1	0	0	0	0	0	0	0	N/A
2	12	6.05×10^7	2.57×10^7	2.31×10^6	7.96×10^6	2.52×10^7	3.5	28.4
3	33	1.41×10^8	6.18×10^7	1.46×10^7	1.82×10^7	1.15×10^8	35.7	2.8
4	32	1.54×10^8	6.34×10^7	1.62×10^7	1.85×10^7	1.77×10^8	69.9	1.4
5	33	2.78×10^8	7.73×10^7	1.77×10^7	1.90×10^7	2.61×10^8	61.6	1.6

A P credit of 5 USD/lb P produces profit but a low ROI of 3.5%. Increasing the P credit to 10 USD/kg P increases the ROI by an order of magnitude (to 35.7%), bringing down the payback period to less than 3 yrs. This sudden jump in ROI reveals that there exists a highly non-linear relationship between the P credit and the ROI. Further increasing the P credit to 15 USD/lb P and 20 USD/lb P brings down the payback period to less than 2 years. The ROI for 15 USD/lb P, however, is higher than the ROI for 20 USD/lb P because our objective function is to maximize the profit, which is higher in the case of 20 USD/lb P while associated production costs are higher for 20 USD/lb P, thus reducing the corresponding ROI.

4.4.4 *Combining Incentives from RECs, RINs, and P Credits*

We now introduce incentives from electricity recovery (RECs), transportation fuel production (RINs), and nutrient recovery (P credits) simultaneously. We analyze the incentive values offered at present. A REC value of 2 USD/MWh,RIN value of 2 USD/gal, and P credit of 10.10 USD/lb P (i.e. 22.04 USD/kg P) are considered. The objective for this

analysis is to maximize the overall profit including the revenues from all the incentives:

$$\max \quad \phi^d + \phi^{REC} + \phi^{RIN} + \phi^P - \phi^I - \phi^\xi - \phi^f \tag{4.4.6a}$$

$$\text{s.t.} \quad (2.3.15) - (2.3.19) \tag{4.4.6b}$$

In Table 4.9, we present the recovered products when all incentives are realized and the overall profit is maximized. We observe that the best strategy is to combine biogas upgrading and nutrient recovery. In particular, the model finds that the optimal strategy is to recover cake_1, cake_3, and liquefied biomethane using technologies $\mathtt{t}_{12}$, $\mathtt{t}_{18}$, and $\mathtt{t}_{36}$. The technologies $\mathtt{t}_{12}$ and $\mathtt{t}_{36}$ are the same, just differing in production scales. These technologies recover cake_1 and liquefied biomethane. Technology $\mathtt{t}_{18}$ recovers cake_3 and liquefied biomethane.

Table 4.9: Products recovered when all incentives are realized and the overall profit is maximized

REC (USD/MWh)	RIN (USD/gal)	P Credit (USD/lb P)	$\phi^d_{\text{cake}_1}$ (tons/yr)	$\phi^d_{\text{cake}_3}$ (tons/yr)	ϕ^d_{LBM} (tons/yr)	r_{Waste} (%)
2	2	10	9.20×10^5	2.08×10^4	23.74	100

The supply chain model decides to install a total of 31 technologies. Notably, all of the selected technologies produce liquefied biomethane and recover nutrient-rich cakes. This helps realize RIN and P credits simultaneously. Also, because AD is the common processing step for biogas upgrading and nutrient recovery, the production cost for LBM and nutrient cakes is reduced as the cost of AD is split between the two products. The ROI for this solution is 20.9%, resulting in a payback period of less than 5 years (Table 4.10). We highlight that these favorable results are obtained with *current* policy incentives.

Table 4.10: Economics for analysis with simultaneous incentives

Total Tech. Sited	ϕ^I (USD)	ϕ^ξ (USD/yr)	ϕ^f (USD/yr)	ϕ^d (USD/yr)	ϕ^{REC} (USD/yr)	ϕ^{RIN} (USD/yr)	ϕ^P (USD/yr)	ROI (%)	Payback Period (yrs)
31	4.36×10^8	7.17×10^7	1.84×10^7	3.78×10^7	0	4.75×10^7	1.18×10^8	20.9	4.8

The left diagrams in Figure 4.4 showcase the technologies selected by the model and

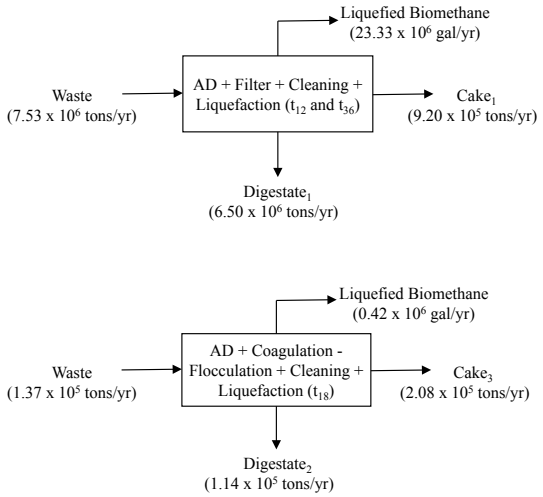

$\phi^I = 436 \times 10^6$ USD

$\phi^d = 37.8 \times 10^6$ USD/yr

(a)

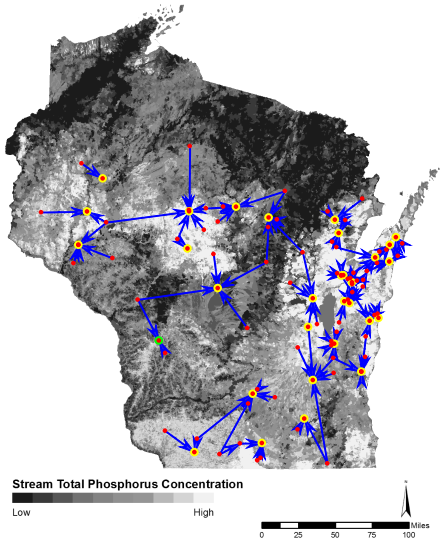

$\phi^f = 18.48 \times 10^6$ USD/yr

$\zeta_{\texttt{waste}} = 59\%$

(b)

Figure 4.4: Optimal solution when all incentives are realized simultaneously. **(a)** Block diagram representing the technologies sited. **(b)** Optimal system layouts. The red dots indicate the location of CAFOs and the blue lines indicate the flow of `waste`. Yellow rings denote the locations of technologies $\texttt{t}_{12}$ and $\texttt{t}_{36}$. Green ring indicates the siting of technology $\texttt{t}_{18}$. (The map of the State of Wisconsin has been adapted from (U.S. Environmental Protection Agency, 2014))

the amount of products recovered annually. The diagram on the right indicates the locations where these technologies are installed and the optimal transportation routes between them. 59% of the total waste generated in the system is moved across the state ($\zeta_{\texttt{waste}}$). The yellow rings indicate the siting of cake$_1$ and LBM recovery technologies ($\texttt{t}_{12}$ and $\texttt{t}_{36}$), while the green ring indicates the siting of cake$_3$ and LBM recovery technology ($\texttt{t}_{18}$). The blue arrows indicate the flow of manure between dairy farms.

4.5 Summary

We applied the supply chain framework presented in Chapter 2 to analyze different technology deployment and incentive strategies for the conversion of post-livestock organic material to value-added products. The management of dairy waste in the State of Wisconsin was employed as the case study. We have found that sustainable waste management would not be an economically viable option unless incentives are provided. It was found that, with current RIN incentives, the deployment of liquefied biomethane production facilities is an economically viable option but the payback period is low (19 yrs). Nutrient credits can make the recovery of nutrient-rich products profitable with an attractive payback period (3 yrs), but this result is based on the consideration that the value of nutrient credits for the recovered nutrient-rich products will be the same as that being currently offered for the avoided P discharge to the water bodies. In the case of RECs, current incentives do not make electricity recovery economically viable. When all incentives are simultaneously considered, it is found that combined technologies to produce liquefied biomethane and nutrient cakes can achieve payback periods of less than 5 years. These conclusions are based on data available in the literature for the treatment of dairy waste which can fluctuate significantly.

In Chapter 5, we will develop a market modeling framework to derive prices for products. We will explore the pricing properties resulting from the proposed network representation. In particular, the dual variables for the product balances can be interpreted as locational marginal prices for different products. We will use this framework to tackle more sophisticated case studies with time-dependent effects, more interdependent products and transportation alternatives, and different study areas.

5

COORDINATED MANAGEMENT AND INHERENT VALUE OF PRODUCTS

5.1 Introduction

Coordinated management systems enable efficient exchange of products in complex decision-making environments that involve large numbers of stakeholders, that rely on shared and constrained infrastructures, and that are driven by complex spatio-temporal physical phenomena and externalities (e.g., weather). Such systems are common place in industry. Symbiotic relationship between industrial plants contributes to a more environmentally and economically sustainable system (Boix et al., 2015). Optimization based approaches have been used to design eco-industrial parks or industrial symbioses where the participating industries share resources and achieve higher water (Lovelady and El-Halwagi, 2009; Rubio-Castro et al., 2011) and energy (Chae et al., 2010; Taskhiri et al., 2015) usage efficiencies. Advanced coordinated systems are also used to manage complex infrastructures such as the power grid (Blumstein et al., 2002; Nygren et al., 2010). Power grid management systems are operated as coordinated (but competitive) markets, in which suppliers and consumers of power and of transmission capacity offer services. Power and transmission capacities and prices are allocated among the stakeholders by solving

a central dispatch optimization problem that seeks to maximize the social welfare. The solution of this problem ensures physical feasibility of allocations and generates prices that properly remunerate the stakeholders. This aspect of coordination is key, as early decentralized management of the power grid driven by individual transactions between utilities lead to significant inefficiencies (e.g., shortages in supply) and market manipulation practices that hindered competition. Our work is motivated by the observation that the historical evolution of coordinated management of power networks provides important lessons and significant empirical evidence that can be leveraged to justify the need and guide the design of coordinated systems for organic waste management. A detailed perspective on coordinated management of power grids and on the status of organic waste management systems is provided in Section A.1 of Appendix A.

In this chapter, we propose a coordinated management system for organic waste. In this system, bids are submitted by suppliers and consumers for waste and derived products as well as by transportation and technology providers for their services. An independent system operator (ISO) uses this bid information to run a dispatch system that finds optimal transportation and transformation pathways that balance supply and demands in a given geographical region. This approach captures system-wide interdependencies and constraints that arise from transportation and bio-physico-chemical transformations of waste into diverse products. The system operates as a coordinated market, generating prices for each waste type and derived product and at each geographical location. With this, bids and prices can be updated with a certain temporal frequency to capture variations in demand and supply (e.g., due to changing environmental conditions, resource availability, and other externalities). We show that allocations and prices obtained with the system satisfy a number of fundamental economic and efficiency properties that are expected from competitive markets. As with coordinated power grids, the proposed system is driven by a fundamental social service: to provide waste management services in the most efficient and reliable manner possible. These services are provided by finding optimal strategies to transport, process, and dispose of waste and products that maximize

the social welfare. We show that the proposed market provides a systematic framework to monetize environmental and health impacts, and benefits associated with waste management. Moreover, prices reveal the true value of waste streams and derived products, and can be used to create incentives for investment and development of new technologies. Prices also capture spatial and temporal variations that help prioritize endangered locations/times and that reveal the need for investment in transportation, facility relocation, or seasonal waste storage. The framework can also be used by government agencies to understand and predict the effect of different regulation and incentive mechanisms. The proposed framework is scalable in that it provides open access that fosters transactions and interactions between large numbers of small and large market players in urban and rural areas and in that it enables coordination with other infrastructures such as power grid and natural gas, water, and food distribution networks. Our work aims to provide a stepping stone towards a coordinated market that better captures interdependencies between products exchanged in different infrastructures and their environmental impacts. Such a framework will become increasingly necessary to provide reliable services as the human population grows and mobilizes and as resource availability becomes less predictable and more constrained. The proposed framework can potentially also be used to manage other complex supply chain networks.

5.2 Coordination Framework

We extend the modeling abstraction presented in Chapter 2 to capture the coordination framework. We consider a system that comprises a set of geographical locations (nodes) $\mathcal{N}$, products $\mathcal{P}$, suppliers $\mathcal{S}$, consumers $\mathcal{D}$, transportation providers $\mathcal{L}$, and transformation (technology) providers $\mathcal{T}$. Products comprise different waste stream types and derived products, transportation providers offer alternatives (e.g., hauling, railway, pipelines) to move products between locations, and technology providers offer alternatives to process products to produce other higher value products.

Associated with each supplier $i \in \mathcal{S}$ there is a supply flow $s_i \in \mathbb{R}_+$, product type $p(i) \in \mathcal{P}$, maximum offered capacity $\bar{s}_i \in \mathbb{R}_+$, location $n(i) \in \mathcal{N}$, and bidding cost $\alpha_i^s \in \mathbb{R}_+$. Associated with each consumer $j \in \mathcal{D}$ there is a demand flow $d_j \in \mathbb{R}_+$, product type $p(j) \in \mathcal{P}$, maximum requested capacity $\bar{d}_j \in \mathbb{R}_+$, location $n(j) \in \mathcal{N}$, and bidding cost $\alpha_j^d \in \mathbb{R}_+$. We use attributes to define the nested sets $\mathcal{S}_{n,p} \subseteq \mathcal{S}_n \subset \mathcal{S}$ with $\mathcal{S}_n := \{i \mid n(i) = n\}$ (i.e., all suppliers attached to node n) and $\mathcal{S}_{n,p} := \{i \mid n(i) = n, p(i) = p\}$ (i.e., all suppliers of product p attached to node n). We follow a similar reasoning to define the nested sets $\mathcal{D}_{n,p} \subseteq \mathcal{D}_n \subset \mathcal{D}$.

Associated with each transportation provider $\ell \in \mathcal{L}$ there is a flow $f_\ell \in \mathbb{R}_+$, product type transported $p(\ell) \in \mathcal{P}$, maximum capacity $\bar{f}_\ell \in \mathbb{R}_+$, bidding cost $\alpha_\ell^f \in \mathbb{R}_+$, sending (source) node $n_s(\ell) \in \mathcal{N}$, and receiving (destination) node $n_r(\ell) \in \mathcal{N}$. The bidding cost captures operational costs associated with the movement of a unit of flow from the source to the destination node. The set $\mathcal{L}_n^{in} := \{\ell \mid n_r(\ell) = n\}$ is the set of all flows entering node $n \in \mathcal{N}$, the set $\mathcal{L}_n^{out} := \{\ell \mid n_s(\ell) = n\}$ is the set of all flows leaving node $n \in \mathcal{N}$. We also define the nested subsets for entering flows $\mathcal{L}_{n,p}^{in} \subseteq \mathcal{L}_n^{in} \subseteq \mathcal{L}$ where $\mathcal{L}_{n,p}^{in} := \{\ell \mid n_r(\ell) = n, p(\ell) = p\}$ is the set of flows entering node n and carrying product p and we note that $\cup_{p \in \mathcal{P}} \mathcal{L}_{n,p}^{in} = \mathcal{L}_n^{in}$. We use similar definitions to construct subsets $\mathcal{L}_{n,p}^{out} \subseteq \mathcal{L}$.

Associated with each transformation provider $t \in \mathcal{T}$ there are transformation (yield) factors $\gamma_{t,p} \in \mathbb{R}$, a reference product $p(t) \in \mathcal{P}$, processing capacity $\bar{\xi}_t \in \mathbb{R}_+$, processing (operating) cost $\alpha_t^\xi \in \mathbb{R}_+$, and location $n(t) \in \mathcal{N}$. Transformation factors represent units of product p consumed/generated per unit of reference product $p(t)$ consumed/generated in the transformation technology. We use the convention that $\gamma_{t,p} > 0$ if product p is generated in the technology t, $\gamma_{t,p} < 0$ if product p is consumed in the technology, and $\gamma_{t,p} = 0$ if product p is neither produced nor consumed in technology. Moreover, we use the convention that $\gamma_{t,p(t)} = -1$ (i.e., one unit of reference product is consumed to produce/consume other products). For each technology we also define an extent of transformation $\xi_t \in \mathbb{R}_+$, which is the total amount of $p(t)$ processed.

The management system proposed is operated by an ISO that collects *bidding informa-*

tion from all participants (costs, capacities, and transformation factors) to obtain optimal allocations of product supply, demand, transportation, and transformation services. The ISO determines these allocations by solving a *dispatch problem* that finds optimal transportation and transformation pathways for waste and derived products that maximize the social welfare and that balance supply and demand for all products across a geographical region. For reasons that will become apparent, this dispatch problem can be seen as a market clearing problem. We use the short-hand notation (s, d, f, ξ) to denote the dispatched allocations. If the allocation of a given player is non-zero we say that the player has been cleared (otherwise we say that the player is not cleared and does not participate). We use $\mathcal{S}^* \subseteq \mathcal{S}$ to denote the set of *cleared* suppliers (i.e., those with $s_i > 0,\ i \in \mathcal{S}^*$). Similarly, we define the set of cleared consumers $\mathcal{D}^* \subseteq \mathcal{D}$, transportation providers $\mathcal{L}^* \subseteq \mathcal{L}$, and technology providers $\mathcal{T}^* \subseteq \mathcal{T}$. The cleared transportation providers create a transportation network that connects nodes in the system that perform exchange of products. An efficient management system is expected to clear suppliers and providers that offer services at low costs and will give preference to consumers with higher bidding costs. The clearing problem also aims to find *prices* that are used to properly remunerate suppliers and providers to cover their service costs and to charge consumers for the service provided. These *price incentives* must take into consideration complex geographical and product interdependencies and physical constraints that arise from transportation and transformation. We now proceed to describe the design elements of a clearing mechanism that achieves all these goals.

5.2.1 *Dispatch Formulation*

Given the bidding information $(\alpha^s, \alpha^d, \alpha^f, \alpha^\xi)$ and $(\bar{s}, \bar{d}, \bar{f}, \bar{\xi})$, the ISO solves the clearing problem (5.2.1) to find allocations (s, d, f, ξ) (as illustrated in Figure 5.1). These allocations maximize the social welfare (5.2.1a) and satisfy the physical conservation laws (5.2.1b), and capacity constraints (5.2.1c)-(5.2.1f). Maximizing the social welfare function

maximizes the demand served and minimizes the costs of supply, transportation, and transformation. The conservation laws are also known as the balancing constraints or market clearing constraints. The first term in parenthesis is the total input flow for product p into node n (given by supply flows and transportation flows entering the node). The second term in parenthesis is the total output flow of product p from node n (given by the demand flows and transportation flows leaving the node). The third term is the generation/consumption rate of product p in all technologies located at node n.

$$\max_{(s,d,f,\xi)} \sum_{j\in\mathcal{D}} \alpha_j^d d_j - \sum_{i\in\mathcal{S}} \alpha_i^s s_i - \sum_{\ell\in\mathcal{L}} \alpha_\ell^f f_\ell - \sum_{t\in\mathcal{T}} \alpha_t^\xi \xi_t \tag{5.2.1a}$$

$$\text{s.t.} \left(\sum_{i\in\mathcal{S}_{n,p}} s_i + \sum_{\ell\in\mathcal{L}^{in}_{n,p}} f_\ell \right) - \left(\sum_{j\in\mathcal{D}_{n,p}} d_j + \sum_{\ell\in\mathcal{L}^{out}_{n,p}} f_\ell \right) + \sum_{t\in\mathcal{T}_n} \gamma_{t,p}\, \xi_t = 0,\ (n,p)\in\mathcal{N}\times\mathcal{P},\ (\pi_{n,p}) \tag{5.2.1b}$$

$$0 \le s_i \le \bar{s}_i,\ i\in\mathcal{S} \tag{5.2.1c}$$

$$0 \le d_j \le \bar{d}_j,\ j\in\mathcal{D} \tag{5.2.1d}$$

$$0 \le f_\ell \le \bar{f}_\ell,\ \ell\in\mathcal{L} \tag{5.2.1e}$$

$$0 \le \xi_t \le \bar{\xi}_t,\ t\in\mathcal{T}. \tag{5.2.1f}$$

We define the set of feasible allocations $\mathcal{C}$ as the set of all possible allocations (s,d,f,ξ) satisfying the capacity constraints (5.2.1c)-(5.2.1f). The trivial allocation $(s,d,f,\xi) = (0,0,0,0)$ is feasible and satisfies the conservation laws. This trivial allocation corresponds to a *dry market* (in which no player is cleared). The dual variables $\pi_{n,p}$, $(n,p)\in\mathcal{N}\times\mathcal{P}$ of the conservation laws (5.2.1b) act as *market clearing prices* that set values for products at different geographical locations. Because of this, we refer to $\pi_{n,p}$ as the *nodal prices* or *locational marginal prices*. We use the short-hand notation π to denote all dual variables.

Allocations and prices derived from the clearing formulation play a fundamental role in establishing economic properties. Specifically, allocations and prices are used to re-

munerate providers and charge consumers. Moreover, prices are used as incentives that promote coordination between stakeholders. Because of this, clearing prices are also known as *coordination prices*. To explain how this takes place, we use the compact notation $\pi_i := \pi_{n(i),p(i)}$, $i \in \mathcal{S}$ and $\pi_j := \pi_{n(j),p(j)}$, $j \in \mathcal{D}$. The revenue collected by supplier $i \in \mathcal{S}$ from the coordination system is $\pi_i s_i$ while $\alpha_i^s s_i$ is its operating cost. For consumers, $\alpha_j^d d_j$ is the value of the allocated demand and $\pi_i d_j$ is the payment made to the coordination system. To see how transportation providers are remunerated, we define $\pi_\ell := \pi_{n_r(\ell),p(\ell)} - \pi_{n_s(\ell),p(\ell)}$, $\ell \in \mathcal{L}$ and call these the *transportation prices*. For reasons that will become apparent, the quantity $\pi_\ell f_\ell$ is paid by the system to the transportation provider and $\alpha_\ell^f f_\ell$ is the transportation cost. We define $\pi_t := \sum_{p\in\mathcal{P}} \pi_{n(t),p}\gamma_{t,p}$, $t \in \mathcal{T}$ and we call these the *transformation prices*. The technology provider is paid $\pi_t \xi_t$ by the system and $\alpha_t^\xi \xi_t$ is its operating cost. The quantity $\pi_t \xi_t = \sum_{p\in\mathcal{P}} \pi_{n(t),p}\gamma_{t,p}\xi_t$ represents the net revenue of provider t. This quantity captures the fact that, if a technology t produces a certain product p (i.e., $\gamma_{t,p} > 0$), the corresponding revenue associated with such product $\pi_{n(t),p}\gamma_{t,p}\xi_t$ will be non-negative ($\pi_{n(t),p} \geq 0$). Similarly, when a technology consumes p (i.e., $\gamma_{t,p} < 0$), the corresponding revenue $\pi_{n(t),p}\gamma_{t,p}\xi_t$ will be non-positive and thus this represents a cost. The *player profits* are a function of payments, charges, and costs:

$$\phi_i^s(\pi_i, \alpha_i^s, s_i) := (\pi_i - \alpha_i^s)s_i,\ i \in \mathcal{S} \tag{5.2.2a}$$

$$\phi_j^d(\pi_j, \alpha_j^d, d_j) := (\alpha_j^d - \pi_j)d_j,\ j \in \mathcal{D} \tag{5.2.2b}$$

$$\phi_\ell^f(\pi_\ell, \alpha_\ell^f, f_\ell) := (\pi_\ell - \alpha_\ell^f)f_\ell,\ \ell \in \mathcal{L} \tag{5.2.2c}$$

$$\phi_t^\xi(\pi_t, \alpha_t^\xi, \xi_t) := (\pi_t - \alpha_t^\xi)\xi_t, t \in \mathcal{T}. \tag{5.2.2d}$$

We use the notation $\phi := (\phi_s, \phi_d, \phi_f, \phi_\xi)$ to denote the profits of all stakeholders that result from the clearing process.

The partial Lagrange function of the clearing problem is given by:

$$\mathcal{L}(s, d, f, \xi, \pi) = \sum_{i\in\mathcal{S}} \alpha_i^s s_i - \sum_{j\in\mathcal{D}} \alpha_j^d d_j + \sum_{\ell\in\mathcal{L}} \alpha_\ell^f f_\ell + \sum_{t\in\mathcal{T}} \alpha_t^\xi \xi_t$$

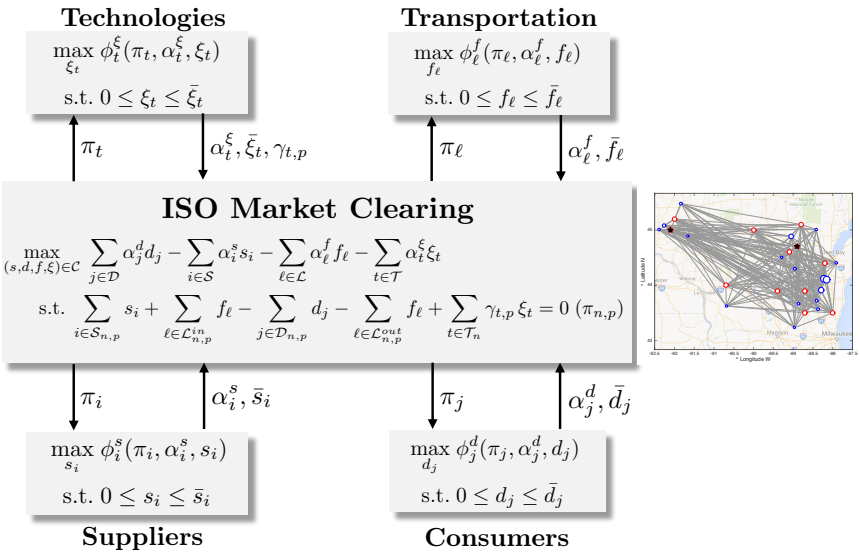

Figure 5.1: Coordination system. Suppliers, consumers, and service providers submit bidding information to the ISO. This information is used by the ISO to obtain prices and allocations that clear the market. The market is cleared by solving an optimization problem that finds optimal transportation and transformation pathways that maximize the social welfare and that balance supply and demand across a given region. Under the proposed design, solving the clearing problem is equivalent to maximizing the collective profit of the market players.

$$- \sum_{n \in \mathcal{N}} \sum_{p \in \mathcal{P}} \pi_{n,p} \left(\sum_{i \in \mathcal{S}_{n,p}} s_i + \sum_{\ell \in \mathcal{L}^{in}_{n,p}} f_\ell - \sum_{j \in \mathcal{D}_{n,p}} d_j - \sum_{\ell \in \mathcal{L}^{out}_{n,p}} f_\ell + \sum_{t \in \mathcal{T}_n} \gamma_{t,p}\, \xi_t \right). \tag{5.2.3}$$

Assuming that strong duality holds, an optimal solution of the clearing problem can also be found by solving the Lagrangian dual problem:

$$\max_{\pi} \min_{(s,d,f,\xi) \in \mathcal{C}} \mathcal{L}(s, d, f, \xi, \pi) \tag{5.2.4}$$

Since the clearing problem is a linear program, strong duality holds under standard constraint qualifications (Boţ et al., 2005). The Lagrangian dual representation is essential to establish fundamental economic and efficiency properties of the coordination framework. The following basic observations will become useful in establishing such properties. First note that the following relationship holds:

$$\begin{aligned} &\sum_{n \in \mathcal{N}} \sum_{p \in \mathcal{P}} \pi_{n,p} \left(\sum_{i \in \mathcal{S}_{n,p}} s_i + \sum_{\ell \in \mathcal{L}^{in}_{n,p}} f_\ell - \sum_{j \in \mathcal{D}_{n,p}} d_j - \sum_{\ell \in \mathcal{L}^{out}_{n,p}} f_\ell + \sum_{t \in \mathcal{T}_n} \gamma_{t,p}\, \xi_t \right) \\ &\quad = \sum_{i \in \mathcal{S}} \pi_i s_i + \sum_{\ell \in \mathcal{L}} \pi_\ell f_\ell + \sum_{t \in \mathcal{T}} \pi_t \xi_t - \sum_{j \in \mathcal{D}} \pi_j d_j. \end{aligned} \tag{5.2.5}$$

This follows from the following identities:

$$\begin{aligned} \sum_{n \in \mathcal{N}} \sum_{p \in \mathcal{P}} \pi_{n,p} \sum_{i \in \mathcal{S}_{n,p}} s_i &= \sum_{i \in \mathcal{S}} \pi_{n(i),p(i)} s_i \\ \sum_{n \in \mathcal{N}} \sum_{p \in \mathcal{P}} \pi_{n,p} \sum_{j \in \mathcal{D}_{n,p}} d_j &= \sum_{j \in \mathcal{D}} \pi_{n(j),p(j)} d_j \\ \sum_{n \in \mathcal{N}} \sum_{p \in \mathcal{P}} \pi_{n,p} \left(\sum_{\ell \in \mathcal{L}^{in}_{n,p}} f_\ell - \sum_{\ell \in \mathcal{L}^{out}_{n,p}} f_\ell \right) &= \sum_{\ell \in \mathcal{L}} (\pi_{n_r(\ell),p(\ell)} - \pi_{n_s(\ell),p(\ell)}) f_\ell, \end{aligned} \tag{5.2.6}$$

where the last expression can also be written as $\sum_{\ell \in \mathcal{L}} \pi_\ell f_\ell$. Moreover, we have that:

$$\sum_{n \in \mathcal{N}} \sum_{p \in \mathcal{P}} \pi_{n,p} \sum_{t \in \mathcal{T}_n} \gamma_{t,p} \xi_t = \sum_{p \in \mathcal{P}} \sum_{n \in \mathcal{N}} \sum_{t \in \mathcal{T}_n} \pi_{n(t),p} \gamma_{t,p} \xi_t$$

$$= \sum_{p \in \mathcal{P}} \sum_{t \in \mathcal{T}} \pi_{n(t),p} \gamma_{t,p} \xi_t, \tag{5.2.7}$$

where the last expression can also be written as $\sum_{t \in \mathcal{T}} \pi_t \xi_t$. From these properties we also have that the partial Lagrange function can be expressed as:

$$\begin{aligned}
\mathcal{L}(s, d, f, \xi, \pi) &= \sum_{i \in \mathcal{S}} \alpha_i^s s_i - \sum_{j \in \mathcal{D}} \alpha_j^d d_j + \sum_{\ell \in \mathcal{L}} \alpha_\ell^f f_\ell + \sum_{t \in \mathcal{T}} \alpha_t^\xi \xi_t - \sum_{i \in \mathcal{S}} \pi_i s_i + \sum_{j \in \mathcal{D}} \pi_j d_j - \sum_{\ell \in \mathcal{L}} \pi_\ell f_\ell - \sum_{t \in \mathcal{T}} \pi_t \xi_t \\
&= \sum_{i \in \mathcal{S}} (\alpha_i^s - \pi_i) s_i + \sum_{j \in \mathcal{D}} (\pi_j - \alpha_j^d) d_j + \sum_{\ell \in \mathcal{L}} \left(\alpha_\ell^f - \pi_\ell \right) f_\ell + \sum_{t \in \mathcal{T}} (\alpha_t^\xi - \pi_t) \xi_t \\
&= - \sum_{i \in \mathcal{S}} \phi_i^s(\pi_i, s_i) - \sum_{j \in \mathcal{D}} \phi_j^d(\pi_j, d_j) - \sum_{\ell \in \mathcal{L}} \phi_\ell^f(\pi_\ell, f_\ell) - \sum_{t \in \mathcal{T}} \phi_t^\xi(\pi_t, \xi_t).
\end{aligned} \tag{5.2.8}$$

5.2.2 *System Properties*

We now establish fundamental properties of the coordination framework that proves that the system operates as a competitive market and that it generates efficient allocations. Some of these properties have been widely studied in the context of electricity markets (Bohn et al., 1984; Hogan et al., 1996; Zavala et al., 2017; Pritchard et al., 2010). Our results extend these results to a multi-product setting that exhibits product interdependencies that arise from transportation and transformation.

Theorem 1. *The coordination system delivers prices π and allocations (s, d, f, ξ) that maximize the collective profits $(\phi_s, \phi_d, \phi_f, \phi_\xi)$ and the profits are all non-negative.*

Proof: Consider an arbitrary (and fixed) set of prices π. At such π, the trivial allocation $(s, d, f, \xi) = (0, 0, 0, 0)$ yields zero profits $\phi_i^s(\pi_i, s_i) = 0$, $\phi_j^d(\pi_j, d_j) = 0$, $\phi_\ell^f(\pi_\ell, f_\ell) = 0$, and $\phi_t^\xi(\pi_t, \xi_t) = 0$. From (5.2.8) we have that the Lagrange function is the summation of the profits and thus $\mathcal{L}(0, 0, 0, 0, \pi) = 0$. For fixed π, the Lagrangian dual problem finds an allocation (s, d, f, ξ) that minimizes the Lagrange function and thus $\mathcal{L}(s, d, f, \xi, \pi) \leq 0$. Moreover, because minimizing the Lagrangian at fixed π is equivalent to maximizing the players profits individually and thus we can always find an allocation that is at least as good as the trivial allocation for each player. We thus have that $\phi_i^s(\pi_i, s_i) \geq 0$,

$\phi_j^d(\pi_j, d_j) \geq 0$, $\phi_\ell^f(\pi_\ell, f_\ell) \geq 0$, and $\phi_t^\xi(\pi_t, \xi_t) \geq 0$. Since π is an arbitrary set of prices then the profits are non-negative at the optimal clearing prices and corresponding allocation. □

The theorem reveals that, under the proposed remuneration scheme, the stakeholders either make a profit or they are not cleared (but they do not incur a financial loss). Moreover, it reveals that the clearing procedure assumes that the all the players seek to maximize their profit (as expected).

Theorem 2. *The coordination system delivers prices π and allocations (s, d, f, ξ) that represent a competitive economic equilibrium.*

Proof: For any set of prices π, the minimization of the Lagrange function with respect to the allocations (s, d, f, ξ) is equivalent to finding individual allocations that maximize the individual stakeholder profits. Moreover, because strong duality holds, the solution of the Lagrangian dual problem also solves the clearing problem and thus the optimal allocation satisfies the clearing constraints. □

This theorem is also known as the *first welfare theorem* and indicates that ISO coordination does not interfere with the competitive nature of the system. In other words, coordination is only used as a mechanism to find a feasible allocation that satisfies transportation and technology constraints.

Theorem 3. *The coordination system delivers prices π and allocations (s, d, f, ξ) that lead to revenue adequacy:*

$$\sum_{j \in \mathcal{D}} \pi_j d_j = \sum_{i \in \mathcal{S}} \pi_i s_i + \sum_{\ell \in \mathcal{L}} \pi_\ell f_\ell + \sum_{t \in \mathcal{T}} \pi_t \xi_t.$$

Proof: The clearing constraints hold at any optimal allocation of the clearing problem. Consequently, we have that:

$$\left(\sum_{i \in \mathcal{S}_{n,p}} s_i + \sum_{\ell \in \mathcal{L}_{n,p}^{in}} f_\ell - \sum_{j \in \mathcal{D}_{n,p}} d_j - \sum_{\ell \in \mathcal{L}_{n,p}^{out}} f_\ell + \sum_{t \in \mathcal{T}_n} \gamma_{t,p}\, \xi_t \right) = 0 \tag{5.2.9}$$

From (5.2.5) we thus have that $\sum_{i\in\mathcal{S}} \pi_i s_i + \sum_{\ell\in\mathcal{L}} \pi_\ell f_\ell + \sum_{t\in\mathcal{T}} \pi_t \xi_t - \sum_{j\in\mathcal{D}} \pi_j d_j = 0$. Consequently, the revenue collected from the consumers covers the payments made to suppliers and service providers. □

Revenue adequacy means that the revenue collected from the consumers covers the total payments made to the suppliers and providers for their services (there is no money lost in the transactions).

Theorem 4. *The coordination prices satisfy the bounds: $\pi_i \geq \alpha_i^s$ for all $i \in \mathcal{S}^*$, $\pi_j \leq \alpha_j^d$ for all $j \in \mathcal{D}^*$, $\pi_t \geq \alpha_t^\xi$ for all $t \in \mathcal{T}^*$, and $\pi_\ell \geq \alpha_\ell^f$ for all $\ell \in \mathcal{L}^*$.*

Proof: From Theorem 1 we have that the profits $(\phi_s, \phi_d, \phi_f, \phi_\xi)$ are all non-negative. Moreover, the allocations of all the cleared players are positive and thus we must have that $(\pi_i - \alpha_i^s) \geq 0$ for all $i \in \mathcal{S}^*$, $(\alpha_j^d - \pi_j) \geq 0$ for all $j \in \mathcal{D}^*$, $(\pi_\ell - \alpha_\ell^f) \geq 0$ for all $\ell \in \mathcal{L}^*$, and $(\pi_t - \alpha_t^\xi) \geq 0$ for all $t \in \mathcal{T}^*$. □

This theorem provides general price bounding properties based on the bidding costs of the cleared stakeholders (those that are not cleared do not affect the prices because their allocations are zero). The supply bidding costs act as lower bounds for the prices at nodes at which the suppliers are connected to. Consequently, when the supply bidding costs are positive, the prices at such nodes will be positive. Note, however, that at nodes in which there is no supplier connected to (or cleared), the price can become negative. The consumer bidding costs act as upper bounds for the prices at nodes at which they are connected to. This is important, because demands often drive the system. If there are multiple suppliers and consumers at the given location, we have that prices will be bounded by the bidding costs of all the players connected to that node. For instance, if there is a supplier $i \in \mathcal{S}^*$ and a consumer $j \in \mathcal{D}^*$ at a given node $n = n(i) = n(j)$, the price at this location must satisfy $\alpha_i^s \leq \pi_n \leq \alpha_j^d$. This basic bounding property can be used to derive more general pricing results. For instance, it can be verified that $\max_{i\in\mathcal{S}_n^*}\{\alpha_i^s\} \leq \pi_n \leq \min_{j\in\mathcal{D}_n^*}\{\alpha_j^d\}$ holds, indicating that the price at a given node n will be bounded by the highest supplier bid cleared and the lowest consumer bid cleared.

For transportation prices we observe that $\pi_\ell \geq 0$ for all $\ell \in \mathcal{L}^*$ with $\alpha_\ell^f \geq 0$ and

that this implies that $\pi_{n_r(\ell),p(\ell)} \geq \pi_{n_s(\ell),p(\ell)}$ for all $\ell \in \mathcal{L}^*$. This indicates that there is an incentive (economic driving force) to transport a product if this is more valuable at the destination node than at the origin node, thus leading to a positive profit for the transportation provider. The magnitude of the driving force is lower bounded by the bidding cost α_ℓ^f. On other hand, if there is no price difference between nodes we have that $\pi_\ell = 0$ then there is no incentive to move the product to a different location and thus the transportation profit for the associated provider will be zero. Consequently, transportation prices implicitly capture global (system-wide) geographical interdependencies between nodes i.e. the prices embed information on the topology of the transportation network that results from the clearing procedure.

For the transformation/technology prices we have that, when $\pi_t > 0$, the technology providers have an incentive (economic driving force) to transform products to make a profit. Moreover, the prices $\pi_t = \sum_{p \in \mathcal{P}} \pi_{n(t),p} \gamma_{t,p}$ are a mix of prices of raw materials and products entering and leaving the technology (weighted by the transformation factors $\gamma_{t,p}$). Consequently, $\pi_t > 0$ indicates that the derived products have more value than the input products. From this we can also see that the transformation prices π_t can be interpreted as a driving force to transfer a set of products from a given bio-physico-chemical state into another state of higher value. Moreover, the technology prices capture economic interdependencies between products. We also highlight that the coordination system does not permit negative profits for technology providers and thus avoids inefficient routes to process and transform products. Together with the transportation prices, the technology prices embed complex topological information of geographical and bio-physico-chemical interdependencies between products.

The following result establishes an important transportation efficiency result.

Theorem 5. *If the transportation bidding costs α^f are all positive, no cleared allocation f contains transportation cycles.*

Proof: We prove this result by contradiction. Assume that the system is cleared for an arbitrary given product p with a transportation cycle that contains c nodes of the form

$n_1 \rightarrow n_2 \rightarrow \ldots \rightarrow n_{c-1} \rightarrow n_c \rightarrow n_1$. From Theorem 2 we have that $\pi_\ell \geq \alpha_\ell^f > 0$ for all cleared providers $\ell \in \mathcal{L}^*$ that connect the nodes in the cycle. This implies that $\pi_{n_c,p} > \pi_{n_{c-1},p} > \cdots > \pi_{n_2,p} > \pi_{n_1,p} > \pi_{n_c,p}$, but this is a contradiction. □

This result highlights that coordinated clearing captures system-wide geographical interactions between suppliers, consumers, and providers and that this helps avoid inefficient routes. Such system-wide interactions are difficult to capture in uncoordinated management systems, which are driven by transactions between individual consumers and suppliers, and thus can lead to inefficiencies. The ability to capture system-wide interactions and constraints is key to find efficient transportation and transformation pathways, to enable coordinated responses to externalities such as extreme weather events or shortages of resources, and to achieve complex societal goals such as geographical nutrient balancing. Examples that illustrate the theoretical properties are presented in Section 3 of the Supporting information, respectively.

5.2.3 *Special Settings - Disposal, Storage, and Remediation Costs*

The proposed framework can accommodate suppliers and consumers that *offer negative bid costs*. *Waste storage/disposal facilities* or the *environment* can act as consumers with negative bidding costs because such participants are often willing to take a certain product but only if they are paid for doing so (the bidding cost can thus be interpreted as a disposal, storage, or remediation cost). The contribution of this type of consumer to the Lagrange function is $-\alpha_j^d d_j$ and, since this term is minimized and $\alpha_j^d < 0$, we have that the clearing problem seeks to minimize d_j. Consequently, the demand allocation d_j acts as a slack variable and α_j^d acts as a penalty cost. As a result, the larger α_j^d, the less product the consumer is willing to take (i.e., the more expensive it is to dispose of at the given location). The negative bidding cost can also be interpreted as a force that tends to repel the product away from the associated node.

When negative bidding costs are allowed in the system, the results from Theorem 1 state that the profits are still guaranteed to be non-negative but the prices might need to become negative in order to enable this. For instance, for a consumer with negative bidding costs we have that the profit is $\phi_j^d(\pi_j, d_j) = (\alpha_j^d - \pi_j)d_j$. Consequently, for the profit to be positive it is required that $\pi_j < \alpha_j^d < 0$ (the clearing price has to be negative at node $n(j)$). The observation is also reinforced from price bounds established in Theorem 4. The competitive equilibrium result of Theorem 2, the revenue adequacy result of Theorem 3, and the transportation adequacy result of Theorem 5 remain unchanged under negative consumer bidding costs.

Suppliers with negative bid prices can be accommodated in a similar way to capture situations in which a given player is willing to pay the system to take away a given product (e.g., keeping waste at a given location might incur a cost). This situation will introduce negative clearing prices that can incentivize the consumption of waste products by transformation providers to generate valuable products. The properties on player profits, competitive equilibrium, revenue adequacy, price bounds, and transportation adequacy remain unchanged under negative supplier bidding costs.

5.2.4 *Significance and Uses of the Coordination System*

In electricity systems, demand bidding costs for inflexible consumers (such as urban areas) are usually set to a large value known as the “value of lost load" (VOLL), which quantifies the lost economic opportunity that arises from the power grid not being able to provide a service to society. The magnitude of VOLL is often estimated by performing detailed studies on the potential value of critical functions enabled by the provision of electricity. High VOLL values exert socio-economic pressure to markets (it activates the markets). In the absence of this external pressure, suppliers might not have a natural incentive to serve electricity demands at certain times and/or locations. In the context of organic waste, a similar socio-economic pressure exists but manifests as the need

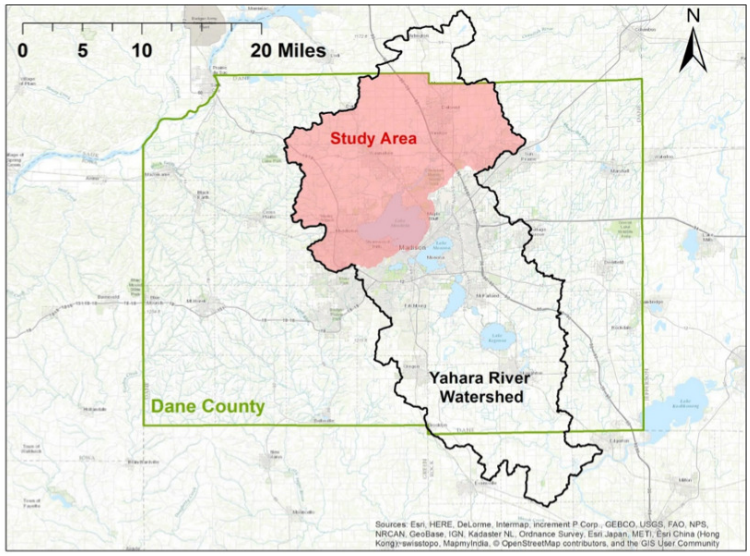

(a)

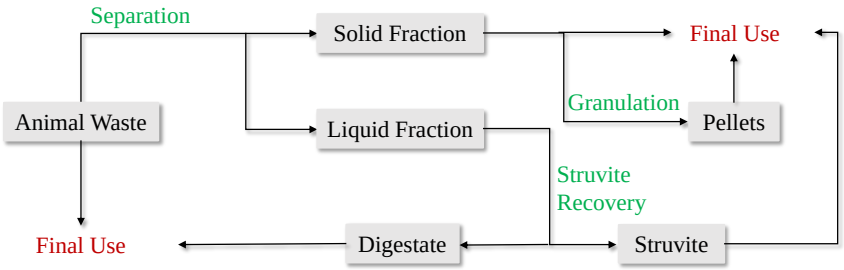

(b)

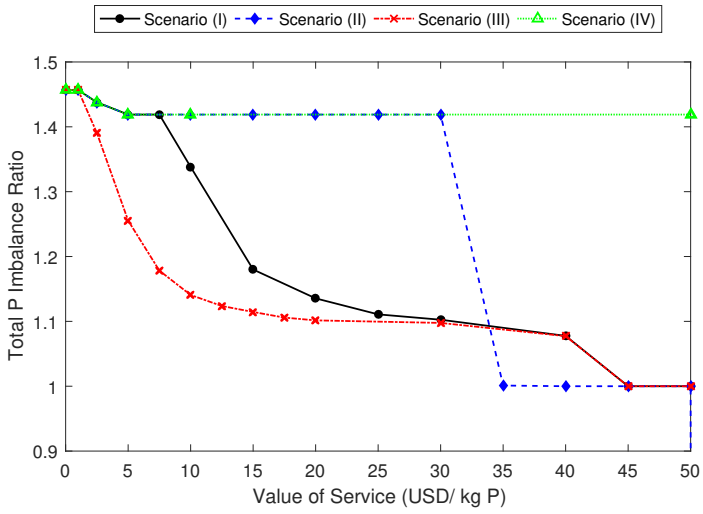

(c)

Figure 5.2: Geographical nutrient balancing using coordinated system in Upper Yahara region. (a) Study area in Yahara watershed in Dane County, WI. (b) Processing technology pathway options for livestock waste. (c) Total P imbalance ratio in the region as a function of value of service (VOS).

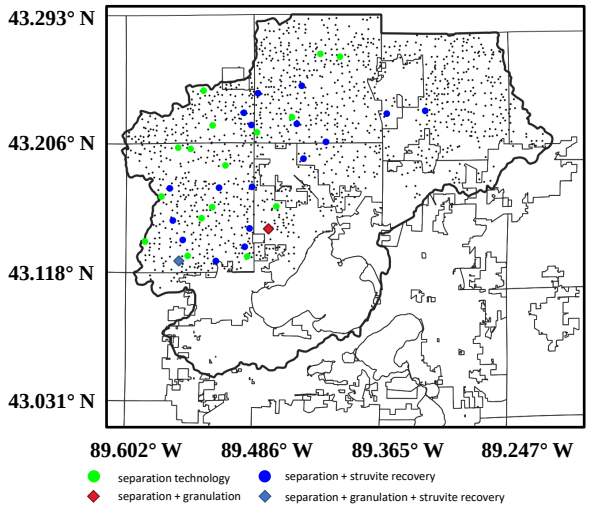

Figure 5.3: Locations for farms, agricultural lands, and waste processing technologies in the Upper Yahara region. Small dots indicate location of farms and agricultural lands.

to process waste to mitigate environmental impacts. This pressure can be captured in our framework in the form of consumers (the environment) with negative bidding costs. Analogous to the case of VOLL, negative bidding costs for the environment can represent *value of service* (VOS) and can be estimated by determining environmental remediation and human health costs associated with leaving waste untreated. The need to determine suitable magnitudes for VOS at different geographical locations will create an incentive for government agencies to properly quantify local socio-economic, health, and environmental impacts associated with waste disposal. Negative consumer bidding costs will activate the market because they force clearing prices to be negative, creating an incentive for transformation providers to purchase waste (and getting paid for it) to produce valuable products. This basic principle drives the existence of infrastructures for wastewater treatment facilities (which transform wastewater into higher quality/value water). A negative bidding cost will also create an incentive for waste disposal providers, which is the basic principle driving landfill operations. Consequently, the proposed market can help determine suitable gate/tipping fees.

Prices generated under the proposed coordination framework can help justify invest-

ment in infrastructure and technology innovation. For instance, WWTPs and local governments need to justify investment in new technologies to their stakeholders. In particular, one could use market prices for biosolids with high and low P concentrations to justify the need for investment in a P recovery technology. Developing a mature market with more predictable prices is also essential in minimizing investment risk. A coordinated framework can also help set best practices to characterize and price complex organic waste streams and derived products and with this standardize waste exchange practices. Electricity markets, for instance, use a standardized framework to report bidding values. Moreover, competition induced by markets fosters disclosure of true values for products and technology operating costs.

Prices obtained from the proposed framework can also help inform and foster transactions between diverse market players in urban, rural, and industrial sectors. For instance, a coordinated market can help promote food waste separation and composting practices. One can also envision deploying coordinated markets in a hierarchical manner (as is done in electricity markets). For instance, one could create a coordinated market per county and have the county markets coordinate in a regional/state market. States market could then be coordinated in a national market. This hierarchical organization arrangement can enable management of a large number of market players and facilitate cross-regional transactions. This can be exploited, for instance, to identify nutrient-deficient regions in which excess manure fertilizer and associated nutrients can be more valuable. In other words, coordinated markets can help balance (homogenize) nutrient budgets across counties and regions more effectively as well as identify processing options needed that facilitate long-distance transportation e.g., pelletization (Hadas et al., 1990; Meers et al., 2006).

A coordinated framework enables fast system-wide adaptations of allocations and prices to respond to spatiotemporal externalities. Specifically, the allocations and prices generated by the clearing procedure implicitly capture geographical priorities and transportation constraints. For instance, negative demand bidding costs with large magnitudes

can be used to capture endangered areas e.g., regions with high nutrient concentration in the soil and water bodies. This will naturally create *price regions* that reflect how valuable or undesirable a particular waste stream is. Because the system will be cleared on a rolling basis (i.e., say daily), market players can adjust their bids to capture natural fluctuations of weather and other externalities. For instance, bidding costs can be adjusted during the raining season to prevent the application of manure in a certain area, which can lead to in-excess run-off, nutrient pollution, and harmful algal blooms which pose severe toxicity risk for communities, livestock, and wildlife. In this case, waste prices will implicitly capture the fact that an area will be endangered during a particular season compared to others when it is safer for manure to be applied. The market framework will thus provide a more natural and economically sound mechanism to prevent application of manure at certain times (as opposed to simply forbid application). A coordinated framework also provides a systematic approach to enable concerted and effective responses to externalities that might threaten urban and rural activities such as droughts and extreme weather events. *Resilience* provided by coordination is in fact one of the main drivers behind coordinated electricity markets. Along these lines, a coordinated system can help identify new pathways to produce and use electricity. As a result, coordination of waste and electricity markets can potentially achieve mutual benefits. For instance, current electricity rates provided by utility companies to biogas-based electricity producers in the US are too low to justify investment in anaerobic digestion and associated infrastructure. Coordination of electricity and waste markets can thus help provide a more systematic approach to uncover the true value of electricity generated from waste.

Prices obtained with the proposed framework can also help create incentives and justify the installation of livestock manure storage facilities to prevent application at certain times. In particular, under the proposed framework, prices provide a reflection of the time value of waste and of the associated environmental damages that storage and relocation can help overcome. Currently, small dairy farms are consolidating into increasingly larger operations to exploit economies of scale and reduce production costs.

Consolidation, however, has the effect of concentrating livestock waste and associated environmental impacts in smaller areas. Moreover, the human population is increasingly being concentrated in urban areas and this creates a wider separation in the food and waste supply chain. Prices obtained under the proposed framework will provide a reflection of the costs associated with consolidation that urban planners and farmers can use to identify suitable degrees of consolidation and/or to identify optimal locations for operations. A coordinated market framework can also help predict the effect of incentives such as RECs, RINs, and nutrient discharge and emission constraints on social welfare and prices. In addition, this framework can inform stakeholders to optimize the investment of funds for incentives associated with organic waste management and to minimize the impacts of regulations on the economy and business.

The framework can also be used to explore potential impacts of fundamental changes in infrastructure options to process organic waste. For instance, in Sweden, households are designed to separate urine from other biosolids, which can be processed separately to recover P (Mihelcic et al., 2011). Fundamental changes in infrastructure are expensive and can involve complicated debates regarding public perception on health hazards. Coordination can facilitate such discussions by providing information on how infrastructure changes can impact environmental remediation and product prices and how changes can create new economic opportunities for stakeholders involved (e.g., householders and livestock producers).

The proposed framework can also be synergized with other environmental policy initiatives. For instance, on February 2019, a legislation (LRB-1244) was introduced in the State of Wisconsin's senate to create a clearinghouse for reducing nutrient pollution in the waterbodies. The clearing house will facilitate trading of water pollution reduction credits between point-source polluters (e.g. wastewater treatment plants and factories) and the non-point sources (e.g. farms and residential areas). The proposed coordinated markets framework can guide in determining the prices for these credits, clearing the market, and determining the incentives required to facilitate transactions.

5.3 Geographical Nutrient Balancing in Upper Yahara Watershed

We analyzed the potential use of the coordinated management framework to conduct *geographical nutrient balancing*. Specifically, we focus on phosphorus (P) balancing for the Upper Yahara watershed region in the State of Wisconsin (Figure 5.2a). Excessive amounts of P have accumulated in this area, primarily due to livestock manure and the heavy use of agricultural fertilizers. Rain and snow melt often wash these nutrients into waterways, which lead to the blue-green algae blooms in the Yahara lakes (University of Wisconsin-Center for Limnology, 2018). We use ρ to denote the total P imbalance ratio in the region, which is given by the ratio of total P applied to land in the region (primarily in the form of livestock manure) and the total P that can be absorbed by crops. Perfect balancing in the region indicates that $\rho = 1$. P surplus indicates that $\rho > 1$ and there could be a risk of water deterioration; while P deficiency indicates that $\rho < 1$ and this is not sustainable in the long-term. The total imbalance ratio in the watershed was estimated to be 1.95 in 2012 and 1.35 in 2013 (Larson et al., 2016), and we estimate that it was 1.46 in 2017 based on the crop types in agriculture lands, the nutrient removal amounts for different crops, the animal units in each farm, and the nutrient from animal excretions. Exact values of such imbalance are difficult to ascertain due to inherent uncertainty in crop yield values and manure composition. Total P balancing has improved over the years due to changes in crop production but some locations remain highly imbalanced and endangered. For instance, specific locations reach imbalance ratios of 300 (Figure 5.4). Balancing total and localized (point) P imbalances is a key societal goal because such imbalances threaten the quality of large and small water bodies.

The study comprises 1,372 nodes, 351 waste suppliers, and 20 different products. We consider 203 farms in the region (55 beef farms and 148 dairy farms). These farms represent over 99% of the P generation associated with livestock waste and are considered suppliers in the system. Waste is categorized as beef, dairy cow, and heifer manure and was originally assumed to be offered for free. Dairy cow manure has a higher P con-

centration (Nennich et al., 2005; usd, 1992). Derived products from manure are struvite, granulated compressed pellets, digestate, and the manure solid fraction. The consumers in this system are: agricultural lands inside the region that demand raw manure, solid fraction of manure, and digested manure; external players (outside the region) accepting waste surplus; external players that buy struvite, pellets, and the solid fraction of manure. We considered 1,167 agricultural land nodes that can be used for waste application. The external players are located in Madison, WI or Sauk County, WI (outside the region). We consider a demand bidding costs for struvite of 800 USD/tonne, for pelleted waste of 100 USD/tonne, for the solid waste fraction of 0.05 USD/tonne, for the liquid waste fraction of 0.002 USD/tonne, and for the digestate of 0 USD/tonne (Sharara et al., 2018; Sampat et al., 2018). Location and capacity data for supply and demand nodes are obtained from (Sharara et al., 2017, 2018; Sampat et al., 2018). We considered transportation bidding cost at each arc as the product of the length of the arc and 0.3 USD/tonne-km for manure and digestate (this value is 0.15 USD/tonne-km for struvite and pellets because solids that are easier to transport). For simplicity, we assume that transportation paths between nodes are linear and we assume that transportation bids exist to move product between all nodes in the system. This gives rise to hundreds of thousands of possible paths. To give an idea of the logistical complexity involved, the clearing problem is a linear programming problem containing over 30 million decision variables and 0.5 million constraints. This problem can be solved in 15 mins using modern solution tools such as Gurobi 7.5.2 (Gurobi Optimization, LLC, 2018). All scripts needed to reproduce the results are available at `https://github.com/zavalab/JuliaBox/tree/master/CoordMarket`.

We considered the possibility of processing the three types of waste using three different technology pathways of increasing complexity (Figure 5.2b). The first pathway separates the manure into its solid and liquid fractions, the second pathway performs an additional granulation step of the solid fraction to recover P in the form of pellets, the third pathway recovers P in the form of struvite from the liquid fraction. Struvite recovery also generates digestate as byproduct with traces of P. The processing costs for the

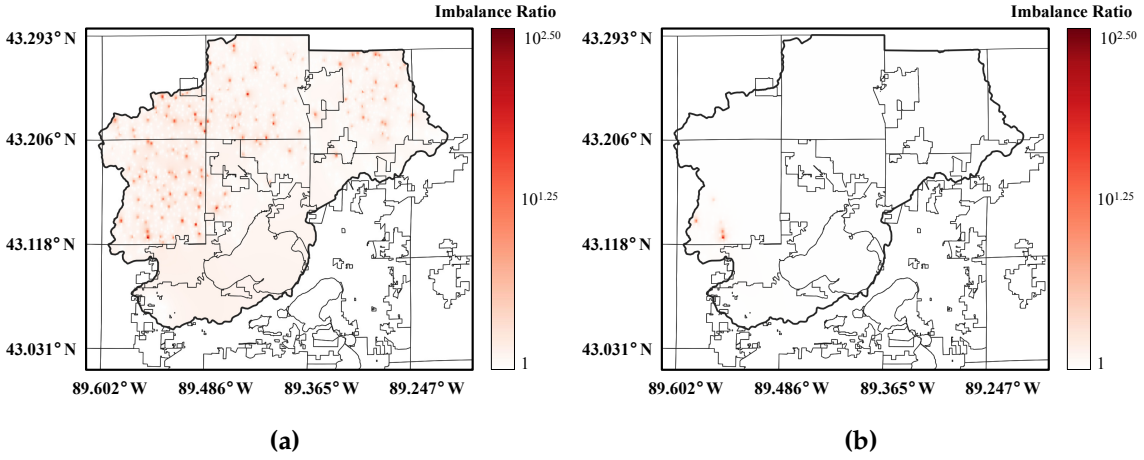

Figure 5.4: Phosphorus (P) imbalance maps in Upper Yahara region as a function of value of service (VOS). Imbalance ratio shown in logarithmic scale. (a) VOS of 0 USD/kg P and (b) VOS of 30 USD/kg P. Perfect balancing in all locations is achieved for a VOS of 45 USD/kg P.

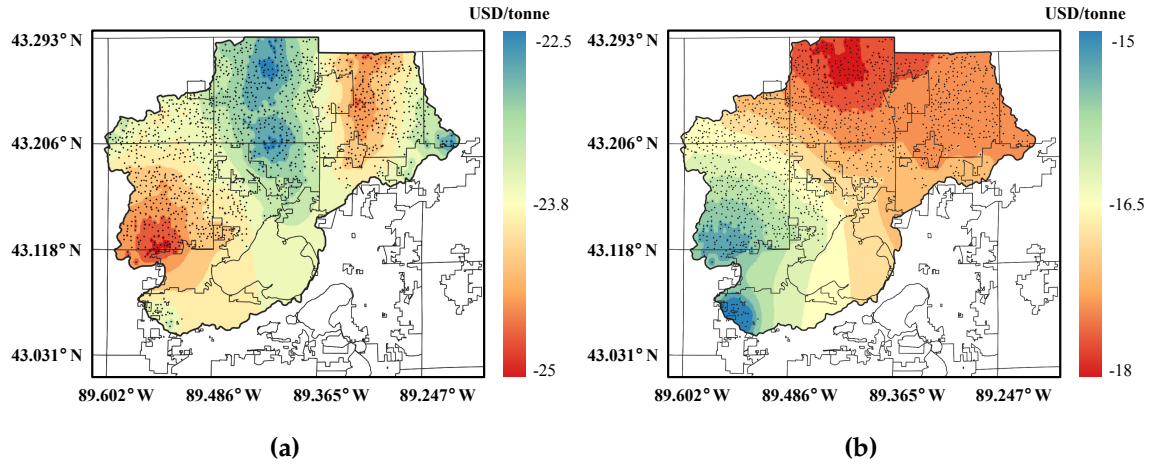

Figure 5.5: Clearing prices in the Upper Yahara region for different waste and derived products. (a) prices for lactating cow manure and (b) prices for manure solids. Results obtained for scenario I and for a VOS of 45 USD/kg P.

technologies are 0.23 USD per tonne of raw manure for separation, 4.00 USD per tonne of raw manure for granulation, and 38.10 USD per tonne of liquid feed for stuvite recovery (Sharara et al., 2018; Sampat et al., 2018). Recovering struvite is a more expensive option because it involves a more sophisticated technology. However, struvite is a more valuable and concentrated product than pellets; while pellets is a more valuable and concentrated product than the manure solid fraction (higher concentration facilitates transportation and geographical nutrient balancing). We considered 126 hypothetical technology installations only in large farms which have more than 500 animal units (61 for separation, 3 for granulation, and 62 for struvite recovery). The installation locations are shown in Figure 5.3. We analyze the system behavior under four scenarios in which different combinations of technologies are assumed to be available in the system. The scenarios were used to analyze the degree of technology complexity needed to achieve balancing. In scenario I, we consider that all technologies (separation, granulation, and struvite recovery) can be used by the system. In scenario II, we consider that only separation and struvite recovery are available. In these two cases we also consider that a small demand for the solid waste fraction exists so that the system is constrained on what can be done with this product. In scenario III, we consider that all technologies are available and that a large demand for solid fraction exists outside the region (in Madison, WI). In scenario IV, we consider that separation is the only technology available and that there is a small demand for the solid fraction of manure. For all scenarios, we evaluate the impact of VOS on the total regional and point P imbalance ratios.

Direct application of the coordination framework with the considered bidding costs revealed that the cleared market is dry i.e. no waste is transported or processed and no transactions take place. Consequently, P within the study region remains imbalanced. This result indicates that the added value of derived products is insufficient to overcome transportation and processing costs to transport excess P outside the study area. In order to ensure that suppliers participate in the system, we found it necessary to supply waste at negative bidding costs. Even with negative bidding costs, however, the system did

not achieve the desired P balancing (the optimal allocation consisted of short-distance transactions between suppliers and consumers inside the region). This indicates that, in order to balance P, it is necessary to use an economic driver that pushes excess P outside the region in a cost-effective manner. To do so, we considered the case in which surplus P at agricultural land locations incurs a cost and we note that this corresponds to having consumers with negative bidding costs (consumers that are willing to take P at a given location but only if paid for it). Such consumers can represent local governments or communities that seek to control environmental impact such as preventing harmful algae blooms at specific locations. In other words, nutrient balancing acts as an economic force that drives the system and negative bidding costs can be interpreted as environmental disposal/remediation costs that we call value of service (VOS).

Figure 5.2c shows the impact of VOS on the total regional imbalance. The imbalance does not decrease unless VOS is considered. This again indicates that the value of derived products alone cannot promote balancing. In Figure 5.2c we see that, as we increase VOS, the system provides incentives for service providers to process waste and transport excess P outside the region and the total imbalance decays. In scenario I we observe that a perfect imbalance ratio of one is achieved for a VOS of around 45 USD/kg P and saturates beyond that value (further incentives do not have an impact). Figure 5.4 shows how an increasing value of VOS progressively eliminates point imbalances (perfect balancing at all locations is achieved for a VOS of 45 USD/kg P). This illustrates how policy makers can use coordinated system to identify suitable incentive mechanisms. As VOS is increased, manure separation is the first technology to be cleared because it is a low-cost option and because it is also a necessary processing step for both struvite recovery and granulation. The second technology to be cleared is granulation and the third is struvite recovery. This order is consistent with the processing costs. We have also found that combinations of technologies are needed to balance the region. Specifically, in scenario IV we observe that separation alone cannot balance the region. In contrast, in scenario II we see that the imbalance remains fairly large and constant up to a VOS value

of around 35 USD/kg P; at this point, there is a sufficiently strong economic incentive for directly driving raw manure outside and P balance can be achieved; however, to activate the struvite recovery technology, a higher VOS is necessary and an upper bound on external demand of raw manure should be placed. From the trend of scenario III we observe that having a larger demand for the solid fraction of manure provides flexibility to the system and thus a perfect balance can be achieved for a small VOS of around 3 USD/kg P. This highlights how the entry of additional consumers into the system can help decrease VOS. In other words, as the market matures and more players participate, the need for external incentives decreases. In scenario III we see that increasing VOS further leads to a lower imbalance ratio. In our results we selected a common value of VOS for the entire region in order to simplify the analysis. However, different values based on diverse impacts can be selected to prioritize areas. This illustrates that VOS can be used to drive the system and adaptively control geographical nutrient balancing. This can be of interest to the government, which currently has limited tools to systematically control nutrient pollution (Wisconsin Department of Natural Resources, 2018b).

Figure 5.5 shows locational marginal prices for lactating cow manure and solids. We see that waste prices are all negative and they are smaller in certain areas. This is because these areas contain more dairy farms which results in higher density of P per unit area (Sharara et al., 2017). We can also see that manure solid prices are all negative but show a different distribution over the study region. This highlights that non-obvious geographical dependencies exist due to transportation, transformation, and external customers. Clearing prices and transportation flows for different products are presented in Figs. 5.6 and 5.7. From the transportation paths we see that the optimal strategy to balance P in the region is to transport raw lactating cow manure, manure pellets, and the solid fraction of manure outside the region. We also see that within the study region, manure is transported over short distances to homogenize imbalances and to be processed into pellets and solid/liquid fractions to facilitate longer-distance transportation.

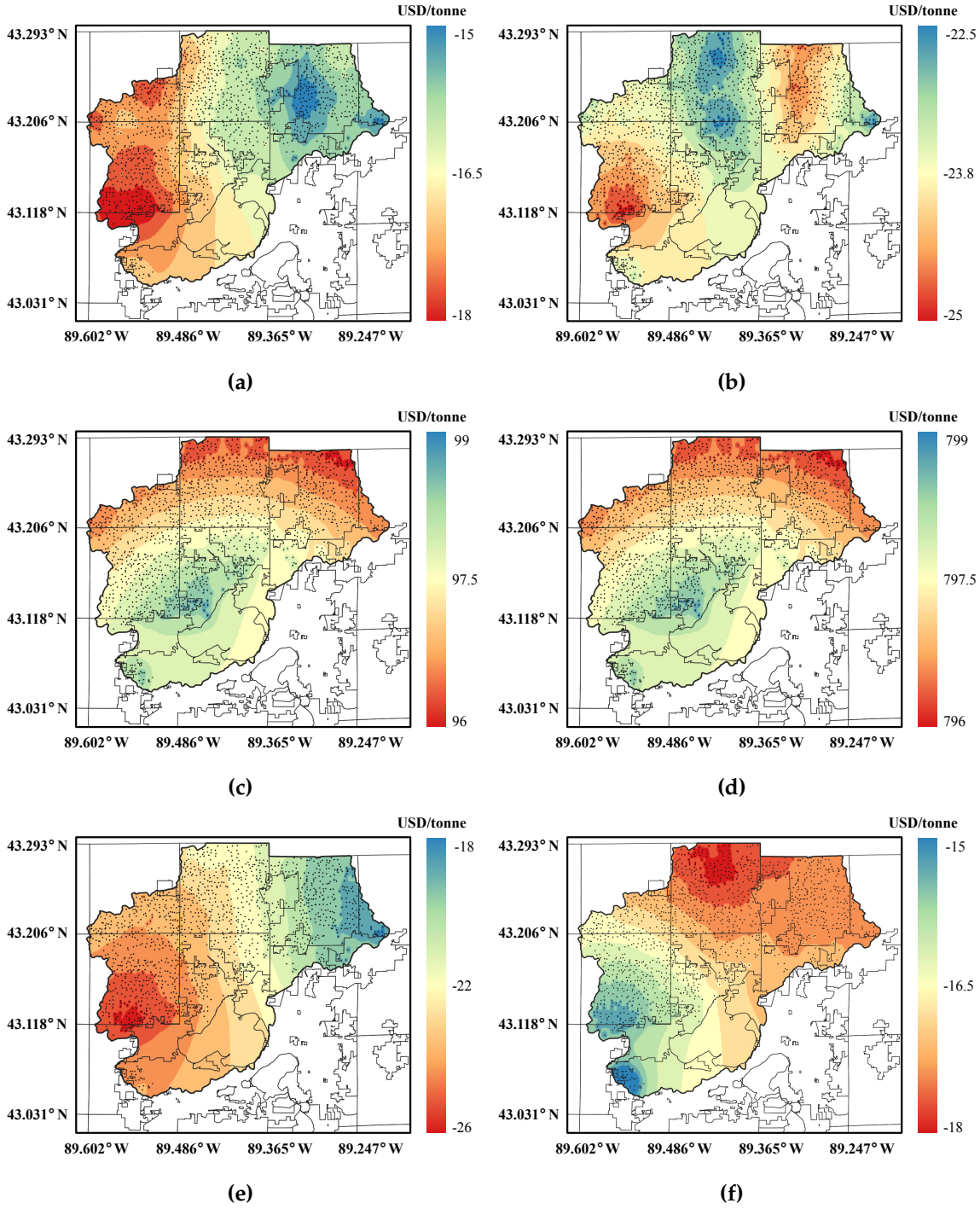

Figure 5.6: Clearing prices in the Upper Yahara region for different waste types and derived products. (a) Beef manure, (b) Dairy cow manure, (c) Beef manure pellets, (d) Struvite, (e) Liquid fraction of dairy cow manure, and (f) Solid fraction of dairy cow manure.

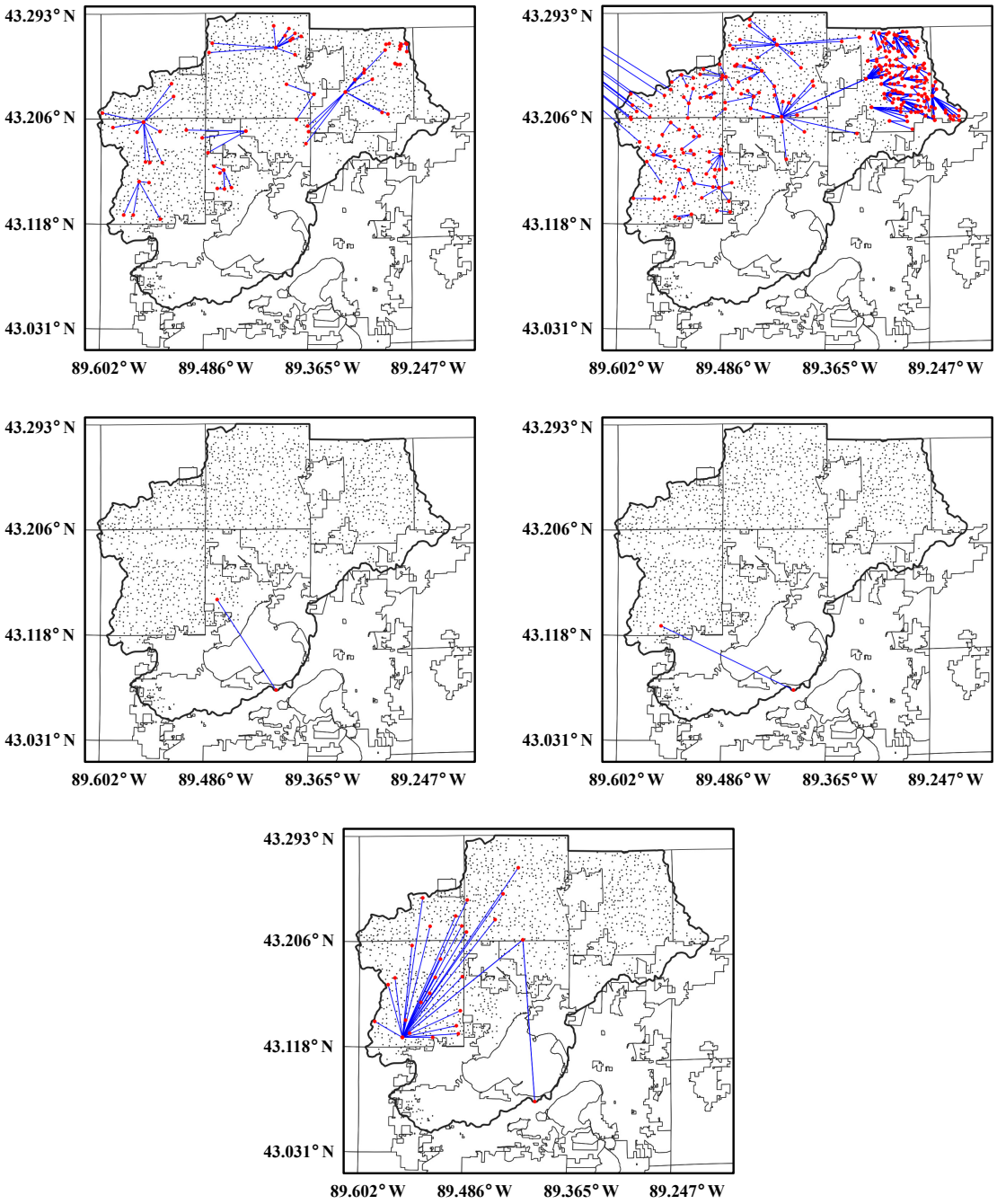

Figure 5.7: Cleared transportation flows in the Upper Yahara for different waste and derived products. (a) Beef manure, (b) Dairy cow manure, (c) Beef manure pellets, (d) Dairy cow manure pellets, and (e) Solid fraction of dairy cow manure. The external destination in (b) is Sauk County, WI; and the southmost point in (c), (d), and (e) is Madison, WI (point outside study region).

5.4 Summary

We presented a coordination framework to facilitate the management of organic waste in a scalable manner by performing coordinated exchange, transportation, and transformation into value-added products. The framework operates as a coordinated market under which suppliers and consumers of waste as well as transportation and technology provides offer services to an independent system operator. Prices for waste and derived products at different geographical locations are obtained by solving a dispatch problem that maximizes the social welfare and that balances products across the region. Coordination enables handling of complex interdependencies between products and locations as well as physical constraints. We prove that the system delivers prices and allocations that satisfy fundamental economic and efficiency properties that are expected from a competitive market. We also show that the proposed system provides a systematic framework to monetize environmental and health impacts and benefits of remediation. Moreover, prices reveal the true value of waste streams and capture spatiotemporal variations that help prioritize endangered areas/times and that reveal the need for investment in processing technologies, transportation, facility relocation, and seasonal storage. The framework can also be used by the government to analyze and predict the effect of different regulations and incentive mechanisms. The proposed framework is scalable in that it can provide open access that fosters geographical transactions between large numbers of small and large players in urban and rural areas and in that it enables coordination with other infrastructures. A coordinated framework will become increasingly necessary as the human population grows and mobilizes, and as resource availability becomes more uncertain.

In Chapter 6 we will combine the coordination framework with a gate-to-gate approach that quantifies the environmental impacts of nutrient pollution. This approach will provide insights into activating the market for organic waste processing by quantifying the economic impacts of releasing excess nutrients to the environment.

6

QUANTIFYING ECONOMIC IMPACTS OF PHOSPHORUS RUNOFF

6.1 Introduction

Agricultural non-point nutrient pollution is the leading source of water quality impairments to rivers, the third largest source for lakes, the second largest for wetlands, and is a major contributor to the contamination of groundwater (U.S. Environmental Protection Agency, 2019). When excess nutrients (in the form of chemical fertilizers or manure) are applied to croplands having legacy phosphorus in soils and there is either rain or snowmelt following the application, the nutrients runoff to the waterbodies resulting in ecosystem responses such as excess growth of algae. The rapid growth of algae is known as harmful algae blooms (HABs) and toxins released during HABs can be detrimental to both aquatic life and human health. HAB events can cause closure of beaches (CNN news, 2019a) and shellfish beds (CNN news, 2019b), massive fish kills (Woods Hole Oceanographic Institution), death of marine mammals and sea birds (Sea-Bird Scientific), coral reefs (Bauman et al., 2010), and alter marine habitats (Stumpf and Tomlinson, 2005). This hurts commercial and recreational fishing, tourism, and valued habitats, which are important to local economies (National Oceanic and Atmospheric Administration (NOOA), 2019). In July 2019, all 21 beaches in the State of Mississippi were closed due to HABs

(CNN news, 2019a). Dodds et al. (2009) estimate an average annual loss of 770 million USD in recreational activities due to eutrophication of U.S. freshwaters. In the State of Florida, HABs have resulted in a monthly loss of 2.8 and 3.7 million USD corresponding to restaurant and lodging revenue, respectively (Larkin and Adams, 2007). Frequent occurrence of HABs also lowers property values of lakefront properties. The loss in property values are the largest impact bearers of eutrophication with an estimated average economic loss of 1.6 billion USD annually (Dodds et al., 2009).

Estimating the scale of economic losses associated to HABs provides valuable information to determine appropriate counter measures to prevent or mitigate the loses (Hoagland and Scatasta, 2006). Unfortunately, not many studies have been conducted to quantify the economic impacts of HABs. Most of the reported studies are driven by impacts of toxins in commercial fisheries (Sanseverino et al., 2016; Pretty et al., 2003; Jin et al., 2008). Hoagland et al. (2002) first estimated an expenditure of 20 million USD annually in public health due to seafood poisoning caused by HABs in the United States. HABs can also cause respiratory illness such as pneumonia, bronchitis, and asthma. In the gulf coast of Florida, wind causes toxins released by HABs to form aerosols and causes damage to the respiratory system (Fleming et al., 2005). For the Saratosa County in the State of Florida alone, the cost of respiratory illnesses associated with HABs is estimated to be 0.5 to 4 million USD annually (Hoagland et al., 2009). Phaneuf et al. (2013) developed a tool that estimates the monetary impact on recreational use of freshwater lakes in the southeast for a change in water quality. As an input, the tool requires the current and desired concentrations of phosphorus, nitrogen, and chlorophyll a. It also requires an estimate on the number of trips to the lake. It then outputs the total economic impact of improving the water quality from a recreational use perspective. As it will become evident later, our work can provide an extension to this tool by providing a methodology to estimate the impact on the number of trips to the lake as a function of water clarity, estimating the impact on lakefront property values, and quantifying the clean up expenses. Quantifying the impacts of nutrient pollution can also drive the decision-making for re-

covery processes. Sena et al. (2020) observe that recovering struvite from a waste water treatment plant in Madison, WI is economically viable if we consider the avoided cost of nutrient pollution.

A number of the economic analyses available in literature rely on survey data for estimating the economic impact of algae blooms (Dodds et al., 2009; Fleming et al., 2005). Dodds et al. (2009) use data on total phosphorus and nitrogen concentrations in different ecoregions to estimate economic damages of eutrophication in U.S. freshwaters. Fleming et al. (2005) estimate health impacts of red tides in the Saratosa county in Florida through a statistical model that correlates the HABs outbreak with the cost of emergency visits to the Saratosa Memorial Hospital for respiratory illnesses. Such methodologies are difficult to scale to different geographical areas facing similar HABs related issues. A model based on easily measurable quantities (e.g., water clarity) can help extend the model to different geographical locations and provide a preliminary estimate towards quantifying the economic impacts of HABs. Vesterinen et al. (2010) propose a hurdle model to quantify the change in demand for recreational activities as a function of water clarity. The hurdle model is proposed for Finland, but it can be useful in estimating the economic impacts in other locations by modifying the parameter values specific to the study area. Dodds et al. (2009) propose a linear relationship between water clarity and the loss in property value. The advantage of such methodologies is that water clarity can be easily linked to the total phosphorus (TP) concentration in the waterbody (Lillie et al., 1993) (thus providing a direct way to quantify the economic impacts of HABs).

In this chapter, we provide a computational framework to utilize models that link the change in water clarity (caused by increase in TP concentration) with a socio-economic impact. We demonstrate the importance of estimating these economic impacts through a case study for the coordinated management of livestock waste in the upper Yahara watershed region. We observe that incorporating an economic cost for excess P in the affected watershed region can provide a driving force for waste processing, help in balancing P in the region, and achieve nutrient pollution reduction targets in an environmentally and

economically sustainable manner.

6.2 Hidden Economic Impacts of Algae Blooms

The U.S. Environmental Protection Agency (U.S. Environmental Protection Agency, 2015) identifies seven major economic categories that are impacted by the eutrophication of waterbodies. Amongst these categories, the largest economic losses in U.S. freshwater are attributed to property values and recreational use (Dodds et al., 2009). For the scope of this chapter, we quantify the impacts associated with property values, recreational costs, and cleanup expenses. Impacts on commercial fishing and human health are location specific and are difficult to generalize through mathematical modeling. Also, for our study area (Upper Yahara watershed region), the impacts in these categories are negligible (Wisconsin Department of Natural Resources, 2012).

6.2.1 *Property Values*

The value of lakefront properties depends strongly on water clarity. Dodds et al. (2009) estimate that the property value decreases by 15.6% for every meter decrease in water clarity (measured by Secchi depth). The Secchi depth (SD) is a metric used for water clarity that is calculated by inserting a black and white colored disc in the water and by measuring the maximum depth until which the disc is visible. Algae blooms have a direct impact on water clarity; specifically, a high total phosphorus (TP) concentration during an algae bloom turns the water turbid, reducing the Secchi depth. The relationship between the Secchi depth and total phosphorus concentration is given by (Lillie et al., 1993):

$$\ln(\text{SD}) = a + b \ln(\text{TP}) \tag{6.2.1}$$

where SD is the Secchi depth in meters and TP is the total phosphorus concentration in $\mu g/L$. Parameters a and b depend on the lake type. For stratified natural lakes (e.g. Lake

Mendota, WI), $a = 2.10$ and $b = -0.44$ (Lillie et al., 1993).

6.2.2 *Recreational Costs*

A decrease in water clarity also reduces the demand for recreation activities such as swimming and fishing (Wisconsin Department of Natural Resources, 2012). Vesterinen et al. (2010) propose a hurdle model to quantify the change in demand for recreational activities as a function of water quality. This hurdle model is proposed for the waterbodies in Finland. Currently, no other relevant studies exist that quantify the impact of water quality on recreational activities. Also, we can apply this model for the State of Wisconsin based on the observation that both Finland and Wisconsin have similar population sizes and similar median household income, and both face problems of eutrophication of water bodies (Wisconsin Department of Natural Resources, 2012). In fact, this model is used by the Wisconsin Department of Natural Resources.

The hurdle model is a two stage model: a logit (or logistic regression) model to estimate the probability of participation in a recreational activity, and a negative binomial model to estimate the frequency of participation. The logit model has the general form:

$$y = \ln(O) = \ln(\frac{p}{1-p}) = \beta_0 + \beta^T X \tag{6.2.2}$$

here, p is the probability of participation and y is the logarithm of the odds $O = (\frac{p}{1-p})$. $\beta_0 \in \mathbb{R}$ and $\beta \in \mathbb{R}^n$ are logit coefficients. $X \in \mathbb{R}^n$ is is vector of n characteristics (e.g. water clarity, number of summer days, etc.) that affect the odds of participation in the recreational activity. The logit coefficients for different recreational activities (β_1^A) reported by Vesterinen et al. (2010) with respect to change in water clarity are listed in Table 6.1. Here A represents the activity from the set {swimming, fishing}. Vesterinen et al. (2010) estimate that a decrease in Secchi depth does not have a significant effect on the odds of participation in swimming ($\beta_1^S = -0.006$), but the frequency of participation (days spent swimming) decreases ($\gamma_1^S = 0.059$). For boating, they find water clarify has no direct effect

either in probability or frequency of participation. For fishing, both the probability and frequency of participation decreases with a reduction in Secchi depth.

As per the logit model, the odds of participation in a recreational activity $A \in$ {swimming, fishing} are:

$$O^A = \exp(y^A) \tag{6.2.3}$$

$$= \exp(\beta_0^A + (\beta^A)^T X) \tag{6.2.4}$$

For a change in the Secchi depth, the odds ratio (OR^A) of an activity is given by:

$$OR^A = \frac{O_2^A}{O_1^A} = \exp(\beta_1^A \Delta X_1) \tag{6.2.5}$$

where ΔX_1 is the change in Secchi depth (in meters) and β_1^A is the corresponding logit coefficient. O_1^A and O_2^A are the odds of participation in an activity (A) before and after the Secchi depth decreases respectively.

Table 6.1: Logit and negative binomial coefficients for water recreational activities with respect to water clarity (based on the hurdle model by Vesterinen et al. (2010))

Independent Variable	Swimming		Fishing	
	Logit (β_1^S)	Negbin (γ_1^S)	Logit (β_1^F)	Negbin (γ_1^F)
Water Clarity	-0.006	0.059	0.107	0.097

Next, we quantify the change in frequency of participation in recreational activities using the negative binomial model and the associated coefficients (Table 6.1) reported in ref (Vesterinen et al., 2010). The ratio of the frequency of participation in an activity A is given by the "Incidence rate ratio" (IRR^A):

$$IRR^A = \frac{\mu_2^A}{\mu_1^A} = \exp(\gamma_1^A \Delta X_1) \tag{6.2.6}$$

here μ_1^A and μ_2^A are the rates (or frequencies) of participation and γ_1^A is the negative binomial coefficient for an activity with respect to change in Secchi depth.

Once the impacts on the probability and frequency of participation are calculated, we estimate the annual loss in recreation trips (Ω^A) for an activity A, given population size N:

$$\Omega^A = N \times (O_1^A - O_2^A) \times (\mu_1^A - \mu_2^A) \tag{6.2.7}$$

Using this information, we estimate the loss in recreational activities by using the cost per trip data (δ^A):

$$\text{Loss in Revenue} = \sum_{a \in \mathcal{A}} \Omega^a \times \delta^a \tag{6.2.8}$$

In case of fishing and swimming, Kaval and Loomis (2003) estimate the value of δ^A to be on average 63.27 USD/trip and 57.27 USD/trip respectively (converted to 2018 USD).

6.2.3 *Cleanup Expenses*

In cases when excess nutrients are already introduced in the waterbodies, mitigation and restoration technologies are required to prevent the manifestation of nutrient problems and algae blooms. Common treatment technologies include aeration systems, alum treatment, biomanipulation, dredging, herbicide treatment, and hypolimnetic treatment. More details on these technologies and corresponding cost estimates can be found in ref (U.S. Environmental Protection Agency, 2015). In areas where the affected waterbody is a source for drinking water, clean up procedures such as alum treatment are required to make the water potable. The alum treatment costs are based on acres of the water surface treated. Wisconsin Department of Natural Resources (Wisconsin Department of Natural Resources, 2012) reports the alum treatment cost to range between 344 and 861 USD/acres plus a fixed cost of 25,000 USD. We note that in some instances the clean up expenses may be higher than it would be worth to the affected community to live with the degraded waterbody. Our methodology to estimate the economic impacts of nutrient runoff provides a systematic way to compare these two expenses.

6.2.4 *Human and Pet Health*

Direct contact with waterbodies that are affected by HABs, either by swimming or other recreational activities, can cause illness in humans and animals. Common symptoms include dermal rashes, respiratory irritation, gastrointestinal distress, and cold/flu-like illness symptoms. Many of the health related costs of HABs are realized in the U.S. coastal states. Hoagland et al. (2009) estimate that the annual cost of respiratory illnesses associated with the red tides in Saratosa County, Florida ranges from 0.02 to 0.13 million USD annually. The authors use a statistical exposure-response model that is based on number of hospital emergency department visits for respiratory illness and the occurrence of algae blooms. For our case study, the HABs related health care costs in the State of Wisconsin are minor (Wisconsin Department of Natural Resources, 2012). Thus, the associated costs are not included in our analysis.

6.2.5 *Waste Processing*

One strategy to prevent phosphorus runoff (and HABs in turn) is by processing livestock waste and recovering phosphorus. We consider three technology variations in our case study (Figure 6.1). These technologies capture the different levels of complexity (ranging from simple mechanical separation to the more advanced chemical treatment) commonly employed for waste processing. The first pathway uses a screw press to separate the livestock waste into solid and liquid fractions. The solid fraction can be used as a crop fertilizer (Aguirre-Villegas et al., 2019). The second pathway performs an additional granulation step of the solid fraction to recover P in the form of pellets (Sharara et al., 2018). The third pathway recovers P in the form of struvite from the liquid fraction. The economic viability of these waste processing routes depends strongly on economies of scale, transportation costs, and the composition of waste streams (which is highly variable). Also, the logistical issues associated with waste collection and transportation hinder the large scale deployment of waste treatment technologies. Diverse government regulations

and incentives to promote waste treatment have not been able to overcome these techno-economic and logistical issues. As a result, the waste management infrastructure remains limited and fragmented, presenting a significant obstacle to mitigate the deterioration of water, land, and air resources as well as to enable sustainable growth of urban, agricultural, and food sectors.

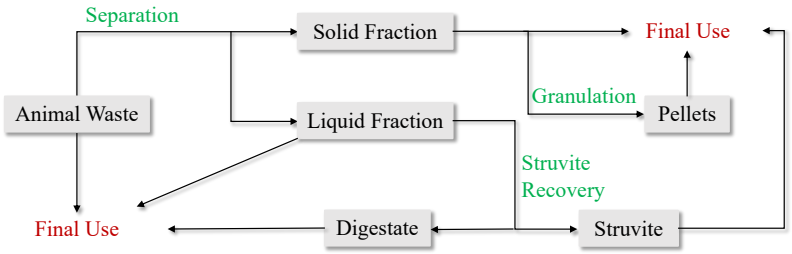

Figure 6.1: Processing technology pathway options for livestock waste

A coordinated management framework (Sampat et al., 2019) can enable efficient exchange of products in such complex decision-making environments that involve large numbers of stakeholders, that rely on shared and constrained infrastructures, and that are driven by complex spatio-temporal physical phenomena and externalities (e.g., weather). In this system, bids are submitted by suppliers and consumers for waste and derived products as well as by transportation and technology providers for their services. An independent system operator (ISO) uses this bid information to run a dispatch system that finds optimal transportation and transformation pathways that balance supply and demands in a given geographical region (Figure 6.3). This approach captures system-wide interdependencies and constraints that arise from transportation and bio-physico-chemical transformations of waste into diverse products. The management system operates as a *coordinated market* that generates prices for each waste type and derived product at each geographical location. This framework helps us determine how economics impacts of HABs can incentivize waste transportation and processing technologies. We provide a brief overview of this coordination markets model in the next section. More details about this framework and the economic properties satisfied by the cleared prices

can be found in Sampat et al. (2019).

6.2.6 *Coordinated Market Model*

In this section, we use the coordination framework presented in Section 5.2.1 to capture the economic impact of HABs resulting from excess P in the region (denoted by θ_j). We define the environment as one of the market players (represented by set $\mathcal{D}' \subset \mathcal{D}$). The idea being that, if there is excess P in the region, it can be released to the environment but at a cost (λ). This cost can be seeing as a tipping cost or a *value of service* (VOS) that the environment charges society. The VOS captures the economic impacts of nutrient pollution (and HABs), which include both external costs borne by local economies and communities impacted by environmental and human effects. The VOS for this case study, based on the analysis presented in the earlier section, is set to 74.5 USD/kg excess P. As it will become clear later, this VOS value acts as an incentive that exerts sufficient socio-economic pressure to activate a waste management market. The model can be summarized as:

$$\max_{(s,d,f,\xi)} \sum_{j\in\mathcal{D}} \alpha_j^d d_j - \sum_{i\in\mathcal{S}} \alpha_i^s s_i - \sum_{\ell\in\mathcal{L}} \alpha_\ell^f f_\ell - \sum_{t\in\mathcal{T}} \alpha_t^\xi \xi_t - \lambda \sum_{j\in\mathcal{D}', p(j)=P} \theta_j \tag{6.2.9a}$$

$$\text{s.t.} \left(\sum_{i\in\mathcal{S}_{n,p}} s_i + \sum_{\ell\in\mathcal{L}^{in}_{n,p}} f_\ell \right) - \left(\sum_{j\in\mathcal{D}_{n,p}} d_j + \sum_{\ell\in\mathcal{L}^{out}_{n,p}} f_\ell \right) + \sum_{t\in\mathcal{T}_n} \gamma_{t,p}\, \xi_t = 0,\ (n,p) \in \mathcal{N}\times\mathcal{P},\ (\pi_{n,p}) \tag{6.2.9b}$$

$$\theta_j \geq d_j - \bar{d}_j,\ j \in \mathcal{D}', p(j) = P \tag{6.2.9c}$$

$$\theta_j \geq 0,\ j \in \mathcal{D}', p(j) = P \tag{6.2.9d}$$

$$0 \leq s_i \leq \bar{s}_i,\ i \in \mathcal{S} \tag{6.2.9e}$$

$$0 \leq d_j \leq \bar{d}_j,\ j \in \mathcal{D} \tag{6.2.9f}$$

$$0 \leq f_\ell \leq \bar{f}_\ell,\ \ell \in \mathcal{L} \tag{6.2.9g}$$

$$0 \leq \xi_t \leq \bar{\xi}_t,\ t \in \mathcal{T}. \tag{6.2.9h}$$

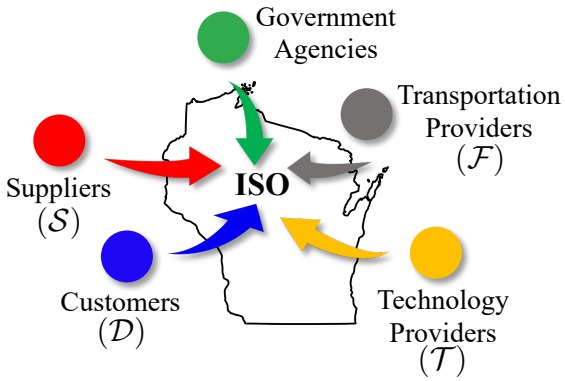

Figure 6.2: Market players and the corresponding mathematical set notations indicated in parenthesis. The market players submit bid prices and capacity limits for their services to the ISO.

6.3 Case Study

We consider the upper Yahara watershed region in the State of Wisconsin (Figure 6.4) to reduce the occurrence of harmful algae blooms in Lake Mendota. Excessive amounts of phosphorus have accumulated in this area, primarily due to livestock manure and the heavy use of agricultural fertilizers. Rain and snow melt often wash these nutrients into waterways, which lead to the blue-green algae blooms in Lake Mendota (University of Wisconsin-Center for Limnology, 2018). In this chapter, we quantify the economic impacts associated with algae blooms in Lake Mendota.

We consider 203 farms in the region (55 beef farms and 148 dairy farms). These farms represent over 99% of the P generation associated with livestock waste. Here, we consider that all the farms within the study area spread the waste on the associated croplands. This corresponds to spreading of 1.34 million tons of waste annually, resulting in a P release rate of 917.83 tons/yr. The croplands in our study area have a total P uptake capacity of 629.74 tons/yr (Sampat et al., 2019). There is thus a surplus of 288.09 tons/yr of P. We consider that 10% of this excess P runs off to Lake Mendota. To keep the calculations on a conservative side, we have assumed that 10% of excess P runs off to the lake instead of the 10% of applied P (which is the number used in state-of-the-art LCA methods like ReCiPe

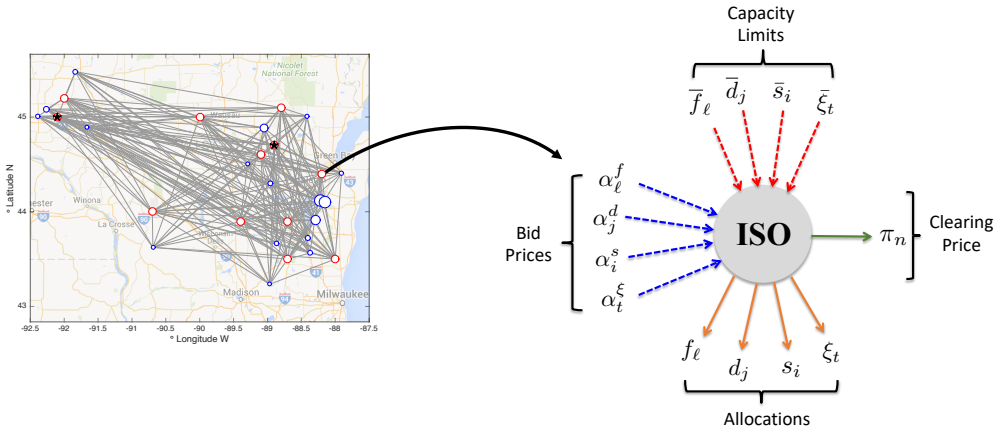

Figure 6.3: For every node in the supply chain network, the ISO (independent system operator) accepts bid prices and capacity limits from the market players (e.g. farmers, fertilizer consumers, federal and state agencies etc.). The ISO then solves the market clearing problem (Equations 6.2.9) to find the clearing prices of the services and the corresponding service allocations.

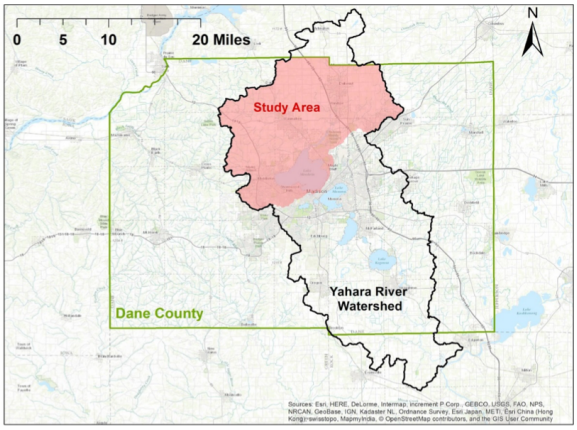

Figure 6.4: Lake Mendota in the Upper Yahara watershed region in Dane County, WI is the study area for quantifying the hidden economic impacts of nutrient runoff.

(Huijbregts et al., 2016) for mid-point and end-point environmental impact categories). The initial TP concentration of Lake Mendota is considered to be 53 $\mu g/L$ (based on the average TP concentration for the years 2014 - 2017) (Wisconsin Department of Natural Resources, 2018a). Due to the P runoff from the overapplication of waste, we estimate (by mass balance calculations) the TP concentration of Lake Mendota increases to 110 $\mu g/L$ (considering the lake volume to be 505 million m^3 (Lathrop and Carpenter, 2011)). This increase in TP concentration acts as a basis for our calculations for quantifying the hidden economic impacts associated with algae blooms.

6.3.1 *Economic Impacts of Algae Blooms in the Upper Yahara Watershed Region*

Property Values

When the initial TP concentration in Lake Mendota is 53 $\mu g/L$, the Secchi depth is 0.97 m (by Equation 6.2.1). After P runoff, when the TP concentration of the lake increases to 110 $\mu g/L$, the Secchi depth decreases to 0.64 m. This 0.34 m decrease in Secchi depth corresponds to an estimated 5.3% reduction in all property values on the Lake Mendota shoreline (according to Dodds et al. (2009) 1 m reduction in Secchi depth reduces property values by 15.3%). Lake Mendota has a shoreline length of 33.8 km (North Temperate Lakes, 2018). Assuming an average lot length of 54.64 m (Wisconsin Department of Natural Resources, 2012), there are 619 lots on the lakeshore. We consider 85% (Wisconsin Department of Natural Resources, 2012) of these lots are private properties, and have a median property value of 269,100 USD (Zillow.com, 2018). The reduction in Secchi depth results in a total loss of 7.46 million USD/yr. This is equivalent to 25.9 USD/kg excess P released.

Recreational Cost

In our case study for the Upper Yahara watershed region, the Secchi depth decreases by 0.34 m. The impact of a reduction in Secchi depth on the frequency of participation in

fishing and swimming is summarized in Table 6.2. For the current odds of participation, a survey by the Wisconsin Department of Natural Resources (2011) reports that 37.4% of residents participate in freshwater fishing and 41.7% swim in lakes. The current odds for fishing and swimming are thus 0.60 and 0.72, respectively. Using the Equation 6.2.5 and the logit coefficients from Table 6.1, the new odds for fishing and swimming are 0.58 and 0.72 respectively. This corresponds to a new participation of 36.6% and 41.7% in fishing and swimming respectively. In case of fishing, the participation reduces by 0.8% while there is no change observed in case of swimming. There is no impact on the participation probability in swimming because the logit coefficient (β_1^S) estimated by Vesterinen et al. (2010) is close to zero (Table 6.1).

Table 6.2: Impact of reduction in Secchi depth (of 0.34 m) on the probability of participation in fishing and swimming in Lake Mendota.

Activity	**Fishing**	**Swimming**
Current Participation	37.4%	41.7%
Current Odds (O_1^A)	0.60	0.72
New Odds (O_2^A)	0.58	0.72
New Participation	36.6%	41.7%
Loss in Participation	0.8%	0%

Wisconsin anglers participate in 17.3 days (U.S. Fish and Wildlife Service, 2008) of fishing annually, while the frequency of swimming trips (by Wisconsin residents) is considered to be 5 days (Wisconsin Department of Natural Resources, 2012). Using these frequencies of participation and the negative binomial coefficients listed in Table 6.1, we estimate that a decrease in Secchi Depth of 0.34 m reduces the frequency of participation in fishing and swimming to 16.8 and 4.9 days respectively (by Equation 6.2.6). These results are summarized in Table 6.3.

Table 6.3: Impact of reduction in Secchi depth (of 0.34 m) on the frequency of participation in fishing and swimming in the Upper Yahara watershed region.

Activity	**Fishing** (days/yr)	**Swimming** (days/yr)
Current Frequency (μ_2^A)	17.3	5
New Frequency (μ_1^A)	16.8	4.9

After quantifying the impacts on the probabilities and the frequencies of participation, we estimate the corresponding loss in revenue (summarized in Table 6.4). Kaval and Loomis (2003) estimate the value of a day spent fishing and swimming to be on average of 63.27 USD and 57.27 USD, respectively (converted to 2018 USD). For our study area, we consider that the participants are from the Dane County, WI, which has a population of 536,416 (U.S. Census Bureau). We have not considered participation from non-resident anglers or swimmers in our calculations. For our study area, we estimate a total loss of 11.8 million USD/yr and 1.19 million USD/yr in fishing and swimming respectively (by Equations 6.2.7 and 6.2.8). This translates to a loss in revenue (from recreational activities) of 45.4 USD/kg excess P.

Table 6.4: Loss in revenue from recreational activities due to a decrease in Secchi depth of 0.34 m in Lake Mendota

Activity	**Fishing**	**Swimming**
Loss in Trips (trips/yr)	1.9×10^5	2.1×10^4
Average Trip Cost (USD/trip)	63.3	57.3
Loss in Revenue (USD/yr)	11.9×10^6	1.2×10^6

Clean-up Expenses

Lake Mendota is not a source of drinking water and thus alum treatment is not performed. However, the excessive amount of phosphorus runoff in the Yahara river waterbodies over the years has resulted in high phosphorus deposition in the bed of the streams that feed into the lake. Thus, even if all the agricultural runoff was successfully prevented from entering the Yahara river waterbodies, Lake Mendota would still be prone to algae blooms for decades to come (Dane County Land and Water Resources Department). The Dane County is implementing a project called Suck the Muck (Wisconsin State Journal, 2018) to pump out phosphorus-laden sludge from the bottom of creeks and streams to combat the toxic algae blooms. The estimated cost of this project is 12 million USD for removing 870,000 pounds of phosphorus (or 30.2 USD/kg P removed) from the streams leading to the Yahara lakes. For our case study, where the excess P is 288 tons/yr and 10% of this

excess P is assumed to runoff, the annual cost of lake cleanup translates to 3.0 USD/kg excess P.

Summary of Economic Impacts

We summarize the economic estimates for the hidden impacts due to harmful algae blooms in Lake Mendota in Table 6.5. From our analysis, the impact on the recreational activities is the highest (45.4 USD/kg excess P) followed by the impact on the property values (25.9 USD/kg excess P). Overall, every excess kg of P results in an economic loss of 74.5 USD. As we demonstrate in the next section, this economic impact can be useful in designing and activating a market that facilitates the coordinated management of organic waste.

Table 6.5: Summary of economic impacts of excess phosphorus (resulting in HABs) in the Upper Yahara watershed region.

Impacted Category	**Economic Loss** (USD/kg excess P)
Property Value	25.9
Recreational Activities	45.4
Lake Cleanup	3.0
Human and Pet Health	-
Total Monetized Loss	**74.5**

6.3.2 *Upper Yahara Coordinated Market*

For our case study in the Upper Yahara watershed region, we consider the 203 livestock farms as the suppliers of waste. We categorize waste as beef, dairy cow, and heifer manure and originally assume to be offered for free. Dairy cow manure has a higher P concentration (Nennich et al., 2005; usd, 1992). As described in the Waste Processing section, derived products from manure are struvite, granulated compressed pellets, digestate, and the manure solid fraction. In this coordinated market, the consumers ($\mathcal{D}$): agricultural lands inside the region that demand raw manure, solid fraction of manure,

and digested manure; external players (outside the region) accepting waste surplus; external players (outside the region) that buy struvite, pellets, and the solid fraction of manure. We consider 1,167 agricultural land nodes that can be used for waste application (as a fertilizer to fulfill nutrient demands). The external players are located in Madison, WI or Sauk County, WI (outside the region). We consider a demand bidding costs for struvite of 800 USD/tonne, for pelleted waste of 100 USD/tonne, for the solid waste fraction of 0.05 USD/tonne, for the liquid waste fraction of 0.002 USD/tonne, and for the digestate of 0 USD/tonne (Sharara et al., 2018; Sampat et al., 2018). Location and capacity data for supply and demand nodes are obtained from (Sharara et al., 2017, 2018; Sampat et al., 2018). The supply capacity of waste for dairy farms are based on the number of cows present at the farm and the demand capacity for croplands is based on the land area and the type of crop grown. We consider transportation bidding cost at each arc (route) as the product of the length of the arc and 0.3 USD/tonne-km for manure and digestate (this value is 0.15 USD/tonne-km for struvite and pellets because solids that are easier to transport). For simplicity, we assume that transportation paths between nodes are linear and we assume that transportation bids exist to move product between all nodes in the market. This gives rise to hundreds of thousands of possible paths. To give an idea of the logistical complexity involved, the market clearing problem is a linear programming problem containing over 30 million decision variables and 0.5 million constraints. This problem can be solved in 15 mins using modern solution tools such as `Gurobi` (version 7.5.2) (Gurobi Optimization, LLC, 2018). All the scripts required to reproduce the results are available at `https://github.com/zavalab/JuliaBox/tree/master/EconomicImpacts`.

As described earlier in the Waste Processing section, we consider the possibility of processing the three types of waste using three different technology pathways of increasing complexity (Figure 6.1). The processing costs for the technologies are 0.23 USD per tonne of raw manure for separation, 4.00 USD per tonne of raw manure for granulation, and 38.1 USD per tonne of liquid feed for stuvite recovery (Sharara et al., 2018; Sampat et al., 2018). Recovering struvite is a more expensive option because it involves a more

sophisticated technology. However, struvite is a more valuable and concentrated product than pellets; while pellets is a more valuable and concentrated product than the manure solid fraction (higher concentration facilitates transportation and geographical nutrient balancing). We considered 126 hypothetical technology installations only in large farms which have more than 500 animal units (61 for separation, 3 for granulation, and 62 for struvite recovery). Only CAFOs (concentrated animal feeding operations) with over 1000 animal units were considered for the installation of granulation technology. The installation locations are randomly selected and shown in Figure 6.5.

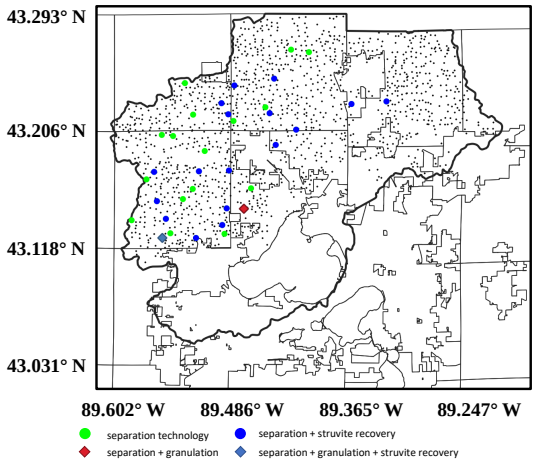

Figure 6.5: Locations for farms, agricultural lands, and waste processing technologies in the Upper Yahara region. Small dots indicate location of farms and agricultural lands.

Under this setting of market players for livestock waste management in the Upper Yahara, we apply the coordination framework (described in the Coordinated Market Model section). Attributing an economic impact (value of service VOS or λ) of 74.5 USD to every kg excess P provides an external driving force to process waste and balance the P in the study area (Table 6.6). This VOS can be provided by federal or state agencies to the dairy farmers as a part of incentives for processing waste and avoiding nutrient pollution. Under this scheme, the optimal strategy is to use separation and granulation technologies to process waste and transport the excess P (in the form of pellets) out of the watershed

region to areas that are deficient in soil P concentration. As a result, the market model predicts that there is no excess P in this scenario.

Since there is uncertainty around the exact value of VOS, we perform a sensitivity analysis to study its impact on the overall P distribution. We observe that, in absence of an external driving force (VOS = 0 USD/kg excess P), no waste is processed and there is 45.6% excess P (Figure 6.6). If the VOS value is reduced to 19 USD/kg excess P (25% of the estimated value), there would still be 14.3% excess P in the study area. This VOS value would only be able to activate the use of separation technologies, leaving some waste in the study area untreated. Whereas, when the VOS is 149 USD/kg excess P (twice the estimated value), the external driving force is high enough to balance P in the region by using separation and granulation technologies. A VOS value of 45 USD/kg excess P is the break-even value that completely balances excess P in the upper Yahara watershed region. We note that, in none of these scenarios, struvite recovery technology was selected. Even though struvite has a higher market value, the high processing cost associated to this product prevents it from being economically competitive to separation and granulation technologies.

Table 6.6: Sensitivity analysis for different values of economic impact (or VOS).

Hidden Economic Impact (USD/kg P)	**Excess P** (%)	**Technology Selected**
0	45.6%	-
19	14.3%	Separation
45 (break-even value)	0%	Separation + Granulation
74.5 (estimated value)	0%	Separation + Granulation
149	0%	Separation + Granulation

For an economic impact of 74.5 USD/kg excess P, the clearing prices for beef and dairy cow manure are summarized in Figure 6.7. Here, the clearing prices are negative, indicating that the farmers need to pay a monetary amount in order to get rid of their waste. In case of beef and dairy cow manure, the farmers need to pay on average 16.6

USD/tonne and 23.5 USD/tonne respectively. The clearing price of dairy cow manure is higher since it has more P concentration (Nennich et al., 2005; usd, 1992) compared to the beef cow manure. Moreover, the clearing prices capture the geographical distribution of P in the study area. For the areas with higher concentration of P, the clearing prices are more negative. These values also act as a price signal that can drive more investment in the areas with more negative clearing prices. One strategy to fund these payments can be through federal and state incentives that promote waste management practices in areas where phosphorus loading is high. This allocation of environmental cost amongst stakeholders will be analyzed in detail in our future work.

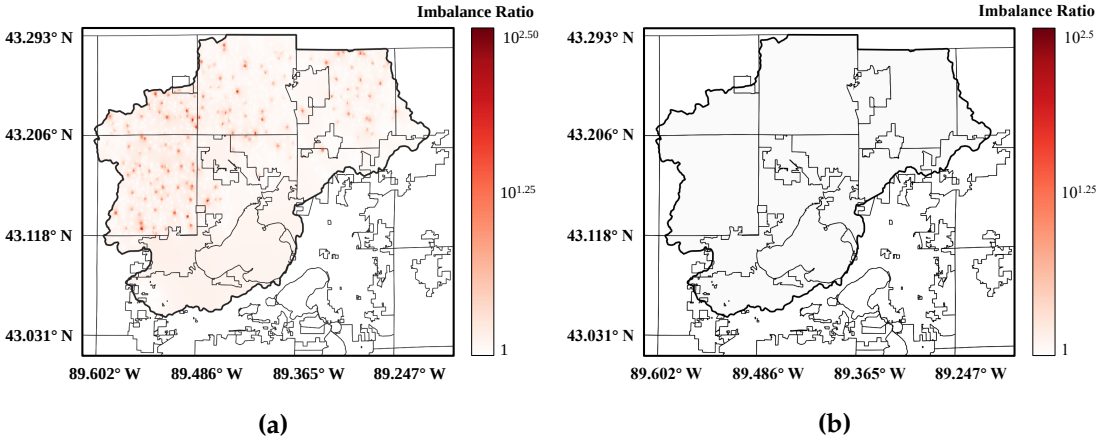

Figure 6.6: Phosphorus (P) imbalance maps in Upper Yahara watershed region as a function of value of service (VOS). Imbalance ratio shown in logarithmic scale. (a) VOS of 0 USD/kg excess P (b) VOS of 74.5 USD/kg excess P. Perfect balancing in all locations is achieved for a VOS greater than 45 USD/kg excess P.

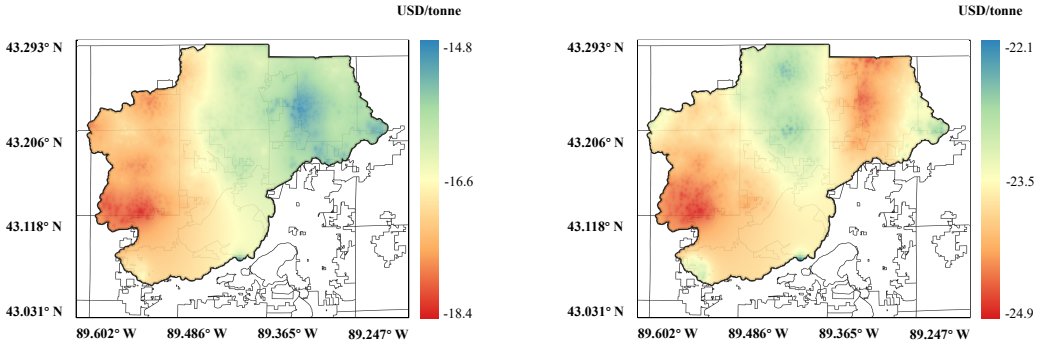

(a) **(b)**

Figure 6.7: Clearing prices in the Upper Yahara region for waste (for VOS = 74.5 USD/kg excess P). (a) prices for beef cow manure and (b) prices for dairy cow manure.

6.4 Summary

We have presented a computational framework to estimate the economic impacts of nutrient pollution from livestock waste. It is difficult to distinguish the economic impact of nutrient pollution from that of HABs. Nonetheless an order of magnitude estimate of this impact can guide federal and state agencies to design policies and tools that reduce nutrient pollution (U.S. Environmental Protection Agency, 2015) which in turn causes HABs. Moreover, our methodology can capture the geographical features of nutrient pollution through the environmental cost (or VOS) and clearing prices (Figure 6.7). Our analysis reveals that every excess kilogram of phosphorus in the Upper Yahara watershed region results in an economic loss of 74.5 USD. In addition, we observe that for this case study the environmental cost is higher than the break-even cost to drive processing of livestock waste. Thus justifying the investment in waste processing technologies. This analysis is based on a steady state analysis and does not account the temporal system variations.

In Chapter 7, we will present a fundamental perspective on allocating resources amongst multiple stakeholders. This analysis will provide mathematical formulations for addressing the question of who should pay for the environmental costs i.e. which

stakeholder should pay for the economic loss in order to drive waste processing.

7

FAIRNESS MEASURES FOR DECISION-MAKING AND CONFLICT RESOLUTION

7.1 Introduction

A common measure used in determining utility allocations among stakeholders (representing sub-organizations, subsystems, individuals) that comprise a community (reperesenting enterprises, systems, markets) is the *total utility* (the sum of individual utilities). This allocation paradigm, often known as the classical utilitarian approach or as the *social welfare* approach, is intuitive but might yield allocations that are not fair. The lack of fairness is the result of inherent solution degeneracies (multiple allocations can yield the same total utility) and to the extreme sensitivity of this approach to subsystem scales. For example, in the case of wholesale electricity markets, the market is cleared by solving a maximum total utility allocation problem that determines demand and supply allocations to various stakeholders (utility companies and power producers) (Zavala et al., 2017). Here, allocations tend to favor large stakeholders over small ones and multiplicity of solutions are often encountered when many market participants are present (due to large numbers of degrees of freedom).

In the field of game theory, the utility allocation problem has been viewed as a bar-

gaining game between stakeholders. Nash (Nash Jr, 1950) first provided an axiomatic approach to obtain solutions to the bargaining problem. These axioms include Pareto optimality, symmetry, affine invariance, and independence of irrelevant alternatives. Nash also proved that there exists a utility allocation scheme that satisfies these axioms (what is now known as the Nash solution). A generalization of Nash's scheme is the proportional fairness scheme, which has been widely used to allocate bandwidth in telecommunication networks (Zukerman et al., 2005). Fairness measures have also been widely used to quantify income inequality (Venkatasubramanian, 2017). For instance, the Gini coefficient is often used to rank nations according to prevalent income inequality and to quantify the impacts of various economic policies to reshape the income distribution (Pessino and Fenochietto, 2010). Other inequality measures include the Jain's index and the Shannon entropy.

An important observation is that the ultimate goal of a fairness measure is to *shape an allocation distribution* in a desirable way. As such, the utility allocation problem can also be interpreted as a stochastic programming (SP) problem in which one seeks to find allocations that shape a distribution of outcomes (in SP the outcome distribution is shaped by using a risk measure) (Dowling et al., 2016; Hu and Mehrotra, 2012). As in the case of fairness measures, axioms have been proposed in the SP literature to study the selection of suitable risk measures (Artzner et al., 1999). These properties have been recently exploited to identify compromise solutions that maximize the collective satisfaction of multiple stakeholders (Dowling et al., 2016).

In this chapter, we analyze the axiomatic properties of different fairness measures and associated solutions. Our goal is to establish fundamental connections that can help guide the selection of suitable measures to allocate utility in complex decision-making environments. Our work also seeks to highlight important caveats of the social welfare approach, which is the standard approach used in the engineering literature.

The paper is structured as follows: Section 7.2 describes the nomenclature and notation used in our analysis. Section 7.3 provides an axiomatic analysis of different measures.

Section 7.4 provides case studies to demonstrate the properties of different measures.

7.2 Fundamental Axioms of a Fair Allocations

We consider a decision-making setting consisting of a set of stakeholders $\mathcal{N} := \{1, \dots, n\}$. Let $X \subseteq \mathbb{R}^{n_x}$ be the set of possible decisions that can be used to manipulate the utility functions $f_j : X \to \mathbb{R}_+$ of the stakeholders $j \in \mathcal{N}$. We define the set of all achievable (feasible) utility allocations as:

$$\mathcal{U} := \{u \in \mathbb{R}^n_+ \mid \exists\, x \in X : f_j(x) = u_j, \quad j \in \mathcal{N}\}. \tag{7.2.1}$$

The fundamental problem arising in this setting is to find a utility allocation $u^* \in \mathcal{U}$ that satisfies some desirable properties (Moulin, 1991). An allocation *scheme* chooses a vector $u^* = \varphi(\mathcal{U})$ by means of a choice function $\varphi : \mathcal{U} \to \mathbb{R}^n$. In what follows, the utility set $\mathcal{U}$ is assumed to be convex and compact (e.g., the functions $f_j(\cdot)$ are convex). Convexity will be necessary to establish certain axiomatic properties. Compactness is required to ensure that the utility functions have bounded (finite) values.

We define the *ideal* utility vector $\overline{u} \in \mathcal{U}$ as the allocation achieved by maximizing the individual utility of each stakeholder. The ideal utility vector satisfies $\bar{u}_j \geq u_j$, $j \in \mathcal{N}$ for all $u \in \mathcal{U}$. This ideal solution is often unattainable and is thus referred to as the *utopia* point. We also define the *status quo* allocation $\underline{u} \in \mathcal{U}$ that represents the utility under a reference (e.g., worst-case) condition. The status-quo vector satisfies $\underline{u}_j \leq u_j$, $j \in \mathcal{N}$ for all $u \in \mathcal{U}$.

In seminal work, Nash (Nash Jr, 1950) proposed a set of axioms that a solution to a two-stakeholder utility allocation problem should satisfy. Nash proved that there exists a unique solution satisfying such axioms, that is now known as the Nash solution. These results have been extended to n-stakeholder settings in (Roth, 1979b). The fundamental axioms that a fair allocation must satisfy are described next.

Axiom 1. *Pareto Optimality: An allocation scheme $\varphi(\mathcal{U})$ is Pareto optimal if there does not exist a utility allocation $u \in \mathcal{U}$ that dominates $\varphi(\mathcal{U})$.*

We recall that an allocation u is said to dominate u^* (written as $u \succeq u^*$) if $u_j \geq u_j^*$ for all $j \in \mathcal{N}$ and $u_j > u_j^*$ for at least one j. Pareto optimality is an efficiency requirement that ensures that no utility is wasted. The following property provides some guidance as to how to construct an allocation scheme that delivers a Pareto optimal allocation.

Property 1. *The allocation $\varphi(\mathcal{U}) = \arg\max_{u \in \mathcal{U}} h(u)$ is Pareto optimal if $h : \mathbb{R}^n \to \mathbb{R}$ is a strictly monotonically increasing function.*

Proof. We prove the result by contradiction. Consider that $u^* = \varphi(\mathcal{U})$ is not Pareto optimal; thus, there exists an alternative $u \in \mathcal{U}$ such that $u \succeq u^*$. Since $h(u)$ is a strictly monotonically increasing function, we have $h(u) > h(u^*)$. This is a contradiction because u^* maximizes $h(\cdot)$. □

To establish the next axiom, we define a permutation operator $\sigma : \mathbb{R}_+^n \to \mathbb{R}_+^n$. The operator applied to a utility vector $\sigma(u)$ permutes its entries. Consequently, the operator applied to the utility set is given by $\sigma(\mathcal{U}) = \{\sigma(u) \in \mathbb{R}_+^n \mid \exists\, x \in X : f_j(x) = u_j,\ j \in \mathcal{N}\}$.

Axiom 2. *Symmetry (Anonymity): An allocation scheme $\varphi(\mathcal{U})$ is symmetric if it satisfies $\sigma(\varphi(\mathcal{U})) = \varphi(\sigma(\mathcal{U}))$.*

Symmetry indicates that a fair allocation under permuted identities is equal to the permutation of the fair allocation under the original identities. This ensures that there is no discrimination (voluntary or involuntary) among stakeholders (Roth, 1979a). In the results that follow, we will see that this fundamental axiom can be easily violated when the allocation provided by a given scheme is non-unique.

To establish the next axiom, we consider an affine operator $A : \mathbb{R}^n \to \mathbb{R}^n$. The operator applied to the utility vector gives $A(u) = (A_1(u_1), A_2(u_2), \ldots A_n(u_n))$ with $A_j(u) = c_j u_j$ and $c_j \in \mathbb{R}_+$. The operator applied to the utility set gives $A(\mathcal{U}) = \{u \in \mathbb{R}_+^n \mid \exists\, x \in X : f_j(x) = A_j(u_j),\ j \in \mathcal{N}\}$.

Axiom 3. *Affine Invariance (AI): An allocation scheme $\varphi(\mathcal{U})$ is affine invariant if it satisfies $A(\varphi(\mathcal{U})) = \varphi(A(\mathcal{U}))$.*

Affine invariance indicates that an allocation under scaling of the utilities is equal to the affine transformation of the allocation obtained under the original system. This ensures that the allocation is *scale-invariant*.

A *weak* version of affine invariance (that we call weak AI) corresponds to the special case in which the affine operator is of the form $A_j(u) = cu_j$ with $c \in \mathbb{R}_+$. In other words, scaling is *uniform* across stakeholders. In the results that follow it will become evident that most allocation schemes are only weak affine invariant. Notably, however, certain schemes are affine invariant.

To establish the next axiom, we consider utility sets $\mathcal{U}$ and $\mathcal{U}'$ satisfying $\mathcal{U} \subset \mathcal{U}'$ and a choice function satisfying $\varphi(\mathcal{U}') \in \mathcal{U}$ (the choice in the largest set also exists in the smallest set).

Axiom 4. *Independence of Irrelevant Alternatives (IIA): An allocation scheme $\varphi(\mathcal{U})$ is independent of irrelevant alternatives if it satisfies $\varphi(\mathcal{U}) = \varphi(\mathcal{U}')$.*

This axiom implies that the choice of a utility allocation over another is not affected by irrelevant utilities in the set.

In the following axiom, we consider utility sets $\mathcal{U}$ and $\mathcal{U}'$ that satisfy $\mathcal{U} \subset \mathcal{U}'$.

Axiom 5. *Restricted Monotonicity: An allocation scheme satisfies restricted monotonicity if it satisfies $\varphi(\mathcal{U}') \succeq \varphi(\mathcal{U})$.*

Restricted monotonicity states that, if the feasible utility set is expanded, then the allocation under the expanded set should dominate that in the original set. This condition can be difficult to satisfy as it can prevent trading-off even a small portion of an allocation in exchange for a major allocation gain for another stakeholder.

We now proceed to analyze the axiomatic properties of different utility allocation schemes. In doing so, it is important to note that no utility allocation scheme can satisfy all of the above axioms. This is stated in the following fundamental result.

Theorem 6. *For $n \geq 3$ stakeholders, no allocation scheme can simultaneously satisfy all Axioms 1-5.*

The proof of this result can be found in (Roth, 1979b).

7.3 Utility Allocation Schemes

7.3.1 *Social Welfare Scheme*

The social welfare scheme is the most widely used approach to allocate utility among stakeholders. This scheme allocates utility by maximizing the total utility function $h_{SW}(u) := \sum_{j \in \mathcal{N}} u_j - \underline{u}_j$:

$$\varphi_{SW}(\mathcal{U}) := \arg\max_{u \in \mathcal{U}} h_{SW}(u).$$

A key observation is that the total utility function $h_{SW}(\cdot)$ is an affine function and thus the allocation $\varphi_{SW}(\mathcal{U})$ is often *non-unique* (i.e., multiple allocations can lead to the same maximum value for the total utility). In other words, the allocation problem is often degenerate (ill-posed). This poses problems from an implementation perspective because in general it is difficult to compute all solutions of the social welfare allocation problem. Moreover, even if the entire solution set is available, an *additional criterion would be needed* to select a suitable allocation (thus introducing *ambiguity*). We also note that the total utility function is n times the arithmetic mean of the utility allocations (this observation will become relevant when interpreting allocation schemes from a statistical stand-point). In other words, the social welfare scheme maximizes the mean utility.

The axiomatic properties of the social welfare allocation scheme are:

- **Pareto Optimality:** Satisfied. This holds because the total utility function $h_{SW}(\cdot)$ is strictly monotonically increasing (i.e., $u \succeq u^*$ implies $h_{SW}(u) > h_{SW}(u^*)$).
- **Symmetry:** Not Satisfied. Since the social welfare function $h_{SW}(\cdot)$ is affine, there is degeneracy present in the solution. Consequently, it is possible to find $\sigma(\varphi_{SW}(\mathcal{U})) \neq \varphi_{SW}(\sigma(\mathcal{U}))$.
- **Affine Invariance:** Satisfied under weak AI. Under weak affine invariance we have:

$$\begin{aligned}\varphi_{SW}(A(u)) &= \arg\max_{u\in\mathcal{U}} \sum_{j\in\mathcal{N}} c(u_j - \underline{u}_j) \\ &= c\varphi_{SW}(u).\end{aligned}$$

  We note that the solution under a uniform affine transformation is in the solution set of the original problem. Since the solution might be non-unique, there is no guarantee that the allocation for the transformed system is the same as that in the original system.

- **Independent of Irrelevant Alternatives:** Satisfied. If $\mathcal{U} \subset \mathcal{U}'$ and u^* maximizes $h_{SW}(\cdot)$ over $\mathcal{U}'$ and $u^* \in \mathcal{U}$, then u^* also maximizes $h_{SW}(\cdot)$ over $\mathcal{U}$.
- **Restricted Monotonicity:** Not Satisfied (see Example I).

EXAMPLE I. To illustrate the concept of restricted monotonicity, we will be using the following example. Consider an allocation problem with $n = 3$ stakeholders. The utility set is $\mathcal{U} = \{u, v, w, z\}$ with $u = \{1, 1, 0\}$, $v = \{1, 0, 1\}$, $w = \{0, 1, 1\}$, and $z = \{1/2, 1/2, 1\}$. Under the social welfare scheme, all elements of $\mathcal{U}$ maximize the social welfare ($h_{SW}(u) = h_{SW}(v) = h_{SW}(w) = h_{SW}(z) = 2$). Now, we expand the utility set $\mathcal{U}$ to set $\mathcal{U}'$ by adding another allocation vector given by $y = \{2/3, 2/3, 2/3\}$. The new allocation also maximizes the social welfare ($h_{SW}(y) = 2$). Now select allocations $z \in \mathcal{U}$ and $y \in \mathcal{U}'$. The utility of the third stakeholder reduces when expanding the utility set ($y_3 < z_3$) and thus the

solution does not satisfy restricted monotonicity. This counterexample will be used to show that allocation schemes (with their corresponding utility functions $h(\cdot)$) in general cannot satisfy restricted monotonicity.

7.3.2 *Nash Scheme*

We explore the axiomatic properties of the Nash scheme, which allocates utility by solving:

$$\varphi_{NS}(\mathcal{U}) := \arg\max_{u \in \mathcal{U}} h_{NS}(u). \tag{7.3.2}$$

Here, the Nash utility function is given by $h_{NS}(u) := \prod_{j \in \mathcal{N}} (u_j - \underline{u}_j)$. Note that this function is related to the geometric mean of the utility allocations as $(h_{NS}(u))^{1/n} = (\prod_{j \in \mathcal{N}} (u_j - \underline{u}_j))^{1/n}$. The Nash allocation $\varphi_{NS}(\mathcal{U})$ can also be obtained by maximizing the geometric mean. This can be easily shown by using a logarithmic transformation and by using the fact that the log function is strictly concave. As we prove next, the geometric mean is a strictly concave function and thus has a *unique* optimal solution (i.e., there are no alternative allocations that yield the same optimal value for the Nash utility function). This avoidance of degeneracy is a key benefit over the social welfare solution that has several axiomatic implications.

Property 2. *The geometric mean function* $(h_{NS}(\cdot))^{1/n}$ *is strictly concave.*

Proof. Without loss of generality, we use the transformation $u \leftarrow u - \underline{u}$. The Hessian of the geometric mean is given by $H = \frac{h_{NS}(u)}{n^2} M$, with:

$$M_{i,j} = \begin{cases} (1-n)u_i^{-2} & \text{for} \quad i = j \\ u_i^{-1} u_j^{-1} & \text{for} \quad i \neq j \end{cases}$$

For every non-zero vector v we have that:

$$v^T H v = \left(\sum_{j \in \mathcal{N}} u_j^{-1} v_j \right)^2 - n \sum_{j \in \mathcal{N}} u_j^{-2} v_j^2 < 0$$

where the upper bound follows from Cauchy–Schwarz inequality. The Hessian is thus negative definite and the function is strictly concave. □

We now explore the axiomatic properties of the Nash scheme. Details on these results can be found in Roth (Roth, 1979a).

- **Pareto Optimality:** Satisfied. This follows because $h_{NS}(\cdot)$ is strictly monotonically increasing (i.e., $u \succeq u^*$ implies $h_{NS}(u) > h_{NS}(u^*)$).
- **Symmetry:** Satisfied. Since the maximum is obtained at a unique point in $\mathcal{U}$, we have that $\varphi_{NS}(\sigma(\mathcal{U})) = \sigma(\varphi_{NS}(\mathcal{U}))$.
- **Affine Invariance:** Satisfied. This follows from:

$$\begin{aligned} \varphi_{NS}(A(u)) &= \arg\max_{u \in \mathcal{U}} \prod_{j \in \mathcal{N}} c_j \cdot (u_j - \underline{u}_j) \\ &= \arg\max_{u \in \mathcal{U}} \left(\prod_{j \in \mathcal{N}} c_j \right) \cdot \left(\prod_{j \in \mathcal{N}} (u_j - \underline{u}_j) \right) \\ &= \arg\max_{u \in \mathcal{U}} \prod_{j \in \mathcal{N}} (u_j - \underline{u}_j). \end{aligned}$$

- **Independence of Irrelevant Alternatives:** Satisfied. If $\mathcal{U} \subset \mathcal{U}'$ and $\varphi_{NS}(\mathcal{U}') \in \mathcal{U}$ (it maximizes $h_{NS}(\cdot)$ over $\mathcal{U}'$ and it is also contained in $\mathcal{U}$) then $\varphi_{NS}(\mathcal{U}')$ also maximizes $h_{NS}(\cdot)$ over $\mathcal{U}$.
- **Restricted Monotonicity:** Not Satisfied. See Example I (expanding the utility set increases $h_{NS}(\cdot)$ but the utility of one of the stakeholders decreases).

7.3.3 *Kalai-Smorodinsky Solution*

The Nash allocation often faces criticism because it is independent of the utopia point. Raiffa (Raiffa, 1953) proposed a two-stakeholder ($n = 2$) allocation scheme that takes into account this utopia point and Kalai and Smorodinsky analyzed the axiomatic properties of this allocation (Kalai and Smorodinsky, 1975). This allocation is often referred to the Kalai-Smorodinsky (KS) solution and is defined as a Pareto optimal point satisfying:

$$\frac{u_1 - \underline{u}_1}{\overline{u}_1 - \underline{u}_1} = \frac{u_2 - \underline{u}_2}{\overline{u}_2 - \underline{u}_2}.$$

The KS solution selects the maximal point on the line joining $\underline{u}$ to $\overline{u}$, thus ensuring that the allocation is proportional with the players maximal potential gain. The two-stakeholder KS allocation satisfies Axioms 1,2,3, and 5 (Kalai and Smorodinsky, 1975). Unlike the Nash allocation, however, the KS allocation cannot be easily extended to a n-stakeholder problem. Moreover, this allocation scheme does not satisfy Axiom 4.

7.3.4 *Proportional Fairness Scheme*

Proportional fairness is a generalization of the Nash scheme that has been widely studied in the area of telecommunications (Bertsimas et al., 2011). A proportionally fair allocation (denoted by $u^* = \varphi_{PF}(\mathcal{U})$) satisfies the property that: (Kelly et al., 1998):

$$\sum_{j \in \mathcal{N}} \frac{u_j - u_j^*}{u_j^*} \leq 0, \quad u \in \mathcal{U} \tag{7.3.3}$$

In other words, the sum of proportional changes is non-positive for all alternative utility allocations. As shown by Bertsimas et al. (Bertsimas et al., 2011), when the utility set $\mathcal{U}$ is convex, a proportional fair allocation can be obtained by solving the problem:

$$\varphi_{PF}(\mathcal{U}) = \arg\max_{u \in \mathcal{U}} h_{PF}(u). \tag{7.3.4}$$

The objective function $h_{PF}(u) := \sum_{i \in \mathcal{N}} \log(u_i - \underline{u}_i)$ (that we call the proportional fairness function) is a logarithmic transformation of the Nash utility function. Since the logarithm is a concave function, we have that the proportional fairness function is strictly concave and thus has a unique maximum.

Property 3. *The proportional fairness function $h_{PF}(\cdot)$ is strictly concave.*

Proof. The Hessian of the function has entries:

$$H_{i,j} = \begin{cases} \frac{-1}{(u_i - \underline{u}_i)^2} & \text{for } \ i = j \\ 0 & \text{otherwise} \end{cases}$$

For every non-zero vector v we have that:

$$v^T H v = \sum_{j=1}^{n} \frac{-v_j^2}{(u_j - \underline{u}_j)^2} < 0.$$

□

The proportional fairness allocation can also be obtained by maximizing the product of the utilities (i.e., it is equivalent to the Nash scheme). As such, the proportional fairness solution satisfies Axioms 1-4 but does not satisfy Axiom 5.

7.3.5 *Max-Min Scheme*

The max-min allocation scheme is a generalization of Rawlsian justice allocation scheme. The Rawlsian justice (Rawls, 2009) proposes that priority should be given to stakeholders that have the least utility (i.e., the allocation should be such that the smallest allocation is as high as possible). The allocation under this scheme can be obtained by solving the problem:

$$\varphi_{MM}(\mathcal{U}) = \arg\max_{u \in \mathcal{U}} \ h_{MM}(u)$$

where $h_{MM}(u) := \min_{j\in\mathcal{N}}(u_j - \underline{u}_j)$ is the worst utility function. The problem can be reformulated as:

$$\begin{aligned}\varphi_{MM}(\mathcal{U}) = \underset{u\in\mathcal{U},t}{\arg\max}\ & t \\ \text{s.t.}\quad & u_j - \underline{u}_j \geq t, \quad j \in \mathcal{N}.\end{aligned}$$

As with the social welfare, the allocation is often non-unique (different stakeholders can have the same worst allocation). The axiomatic properties of the max-min scheme are:

- **Pareto Optimality:** Not Satisfied. This follows because the worst utility function is not strictly monotonically increasing (i.e., $u \succeq u^*$ does not imply $h_{MM}(u) > h_{MM}(u^*)$).
- **Symmetry:** Not satisfied. This follows from the non-uniqueness of the solution. Consequently, it is possible to find $\sigma(\varphi_{MM}(\mathcal{U})) \neq \varphi_{MM}(\sigma(\mathcal{U}))$.
- **Affine Invariance:** Satisfied under weak AI. As with the social welfare, the solution under a uniform affine transformation is in the solution set of the original problem. Since the solution might be non-unique, however, there is no guarantee that the allocations obtained are the same.
- **Independent of Irrelevant Alternatives:** Satisfied. If $\mathcal{U} \subset \mathcal{U}'$ and $\varphi_{MM}(\mathcal{U}') \in \mathcal{U}$ (it maximizes $h_{MM}(\cdot)$ over $\mathcal{U}'$ and it is also contained in $\mathcal{U}$) then $\varphi_{MM}(\mathcal{U}')$ also maximizes $h_{MM}(\cdot)$ over $\mathcal{U}$.
- **Restricted Monotonicity:** Not Satisfied. See Example I with $h_{MM}(\cdot)$.

7.3.6 *α-Fair Scheme*

This is a family of utility allocation schemes of the form:

$$\varphi_\alpha(\mathcal{U}) := \underset{u\in\mathcal{U}}{\arg\max}\, h_\alpha(u) \tag{7.3.5}$$

where $h_\alpha(\cdot)$ is a function parameterized in $\alpha \in [0, \infty)$ (the α-fairness function) and given by:

$$h_\alpha(u) := \begin{cases} \sum_{j \in \mathcal{N}} \frac{(u_j - \underline{u}_j)^{1-\alpha}}{1-\alpha}, & \text{for } \alpha \geq 0, \alpha \neq 1 \\ \sum_{j \in \mathcal{N}} \log(u_j - \underline{u}_j), & \text{for } \alpha = 1. \end{cases} \tag{7.3.6}$$

Notably, this scheme reduces to the social welfare, proportional fairness (and thus Nash), and max-min fairness when $\alpha = 0$, $\alpha = 1$, and $\alpha \to \infty$, respectively (Lan et al., 2010).

For $\alpha = 0, 1, \infty$, the scheme satisfies the Axioms of the corresponding equivalent schemes. For $\alpha \in (2, \infty)$, the allocation obtained with α-fairness is unique. This is seen from the following property:

Property 4. *The α-fairness function $h_\alpha(\cdot)$ is concave for $\alpha = 2$ and strictly concave for $\alpha > 2$:*

Proof. For convenience, we prove that $-h_\alpha(\cdot)$ is convex for $\alpha = 2$ and strictly convex for $\alpha > 2$. The Hessian of $-h_{\alpha \in [2,\infty)}(u)$ is:

$$H_{i,j} = \begin{cases} \frac{(\alpha-2)}{(u_i - \underline{u}_i)^{\alpha-3}} & \text{for } i = j \\ 0 & \text{otherwise} \end{cases}$$

For every non-zero vector v we have that:

$$v^T H v = \sum_{j=1}^{n} \frac{v_j^2(\alpha - 2)}{(u_j - \underline{u}_j)^{\alpha-3}}$$

The Hessian is positive semi-definite for $\alpha = 2$ and positive definite for $\alpha > 2$. □

The axiomatic properties of the α-fair scheme for $\alpha \in (2, \infty)$ are:

- **Pareto Optimality:** Satisfied. The α-fairness function is strictly monotonically increasing.
- **Symmetry:** Satisfied. This follows from uniqueness of the solution for $\alpha \in (2, \infty)$.

- **Affine Invariance:** Satisfied under weak AI. This follows from:

$$\begin{aligned}\varphi_{\alpha\in(2,\infty)}(A(\mathcal{U})) &= \arg\max_{u\in\mathcal{U}} \quad \frac{1}{1-\alpha}\sum_{j\in\mathcal{N}}(cu_j - c\underline{u}_j)^{1-\alpha} \\ &= c^{1-\alpha}\arg\max_{u\in\mathcal{U}} \quad \frac{1}{1-\alpha}\sum_{j\in\mathcal{N}}(u_j - \underline{u}_j)^{1-\alpha} \\ &= \arg\max_{u\in\mathcal{U}} \quad \frac{1}{1-\alpha}\sum_{j\in\mathcal{N}}(u_j - \underline{u}_j)^{1-\alpha}.\end{aligned}$$

- **Independent of irrelevant alternatives:** Satisfied. If $\mathcal{U} \subset \mathcal{U}'$ and $\varphi_{\alpha\in(2,\infty)}(\mathcal{U}') \in \mathcal{U}$ (it maximizes $h_{MM}(\cdot)$ over $\mathcal{U}'$ and it is contained in $\mathcal{U}$) then $\varphi_{\alpha\in(2,\infty)}(\mathcal{U}')$ also maximizes $\varphi_{\alpha\in(2,\infty)}(\cdot)$ over $\mathcal{U}$.

- **Restricted Monotonicity:** Not Satisfied. See Example I with $h_{\alpha\in(2,\infty)}(\cdot)$.

7.3.7 *Shannon Entropy Solution*

The Shannon entropy (usually called just *entropy*) is used in the area of information theory to quantify the diversity or randomness of a system. The concept of entropy provides a bridge between economic theory and statistics (Venkatasubramanian and Luo, 2018). In particular, a system achieves maximum diversity (randomness) when the entropy is maximized. The Shannon entropy function is given by:

$$h_S(p) := -\sum_{j\in\mathcal{N}} p_j \log p_j$$

with the implicit restriction that $\sum_{j\in\mathcal{N}} p_j = 1$. The entropy function can be used to compute a utility allocation by solving the optimization problem:

$$\varphi_S(\mathcal{U}) := \arg\max_{u\in\mathcal{U}} \quad h_S(p(u)) \tag{7.3.7}$$

where $h_S(p(u)) = -\sum_{j=1}^{n} p_j(u) \log p_j(u)$ and

$$p_j(u) = \left(\frac{(u_j - \underline{u}_j)}{\sum_{j=1}^{n}(u_j - \underline{u}_j)} \right), \; j \in \mathcal{N}. \tag{7.3.8}$$

For simplicity, we denote the entropy function as $h_S(u)$. Entropy in a utility allocation context is also known as the Theil index.

Under the assumption that the total utility $\sum_{j\in\mathcal{N}}(u_j - \underline{u}_j)$ is fixed (constant), Venkatasubramanian and Luo (Venkatasubramanian and Luo, 2018) proved that maximizing entropy achieves an allocation that satisfies:

$$\frac{u_1 - u_1^0}{\sum_{j\in\mathcal{N}}(u_j - \underline{u}_j)} = \frac{u_2 - u_2^0}{\sum_{j\in\mathcal{N}}(u_j - \underline{u}_j)} \cdots = \frac{u_n - u_n^0}{\sum_{j\in\mathcal{N}}(u_j - \underline{u}_j)} \tag{7.3.9}$$

This condition indicates that the relative utility gains are equal for all the stakeholders. This result is formally established below.

Property 5. *Assume that the total utility $\sum_{j\in\mathcal{N}}(u_j - \underline{u}_j)$ is constant. The entropy function $h_S(\cdot)$ achieves a maximum value when all the utility gains $(u_j - \underline{u}_j)$, $j \in \mathcal{N}$ are equal.*

Proof. Assuming $\sum_{j\in\mathcal{N}}(u_j - \underline{u}_j) = U$, the entries of the gradient of the entropy function are given by:

$$g_j(u) = -1 - \log\left(\frac{u_j - \underline{u}_j}{U} \right), \quad j \in \mathcal{N}$$

The maximum is achieved at $g_j(u) = 0$, $j \in \mathcal{N}$, which implies:

$$\log\left(\frac{u_j - \underline{u}_j}{U} \right) = -1, \quad j \in \mathcal{N}.$$

Since the log function is strictly concave, this implies that $(u_1 - \underline{u}_1) = (u_2 - \underline{u}_2) \cdots = (u_n - \underline{u}_n)$ and (7.3.9). □

We now prove that the entropy function $h_S(\cdot)$ is strictly concave. Consequently, the allocation obtained by maximizing entropy is unique.

Property 6. *Assume that the total utility $\sum_{j\in\mathcal{N}}(u_j - \underline{u}_j)$ is constant. The entropy function $h_S(\cdot)$ is strictly concave.*

Proof. Assuming $\sum_{j\in\mathcal{N}}(u_j - \underline{u}_j) = U$, the Hessian of the entropy function is given by:

$$H_{i,j} = \begin{cases} \frac{-1}{(u_i - \underline{u}_i)U} & \text{for } \; i = j \\ 0 & \text{otherwise} \end{cases}$$

For every non-zero vector v we have that:

$$v^T H v = \sum_{j\in\mathcal{N}} \frac{-v_j^2}{(u_j - \underline{u}_j)U} < 0.$$

The Hessian is thus negative definite. □

We now analyze the axiomatic properties of the entropy allocation scheme. We only consider the case when the total utility gain is constant.

- **Pareto Optimality:** Satisfied. The entropy function is strictly monotonically increasing.
- **Symmetry:** Satisfied. Entropy maximization is equivalent to enforcing (7.3.9). This condition ensures that the solution is symmetric (permutations do not affect the allocation).
- **Affine Invariance:** Satisfied under weak AI. This follows from:

$$\begin{aligned} \varphi_S(A(u)) &= \arg\max_{u\in\mathcal{U}} \; -\sum_{j\in\mathcal{N}} \left(\frac{c(u_j - \underline{u}_j)}{\sum_{i\in\mathcal{N}} c(u_i - \underline{u}_i)}\right) \log\left(\frac{c(u_j - \underline{u}_j)}{\sum_{i\in\mathcal{N}} c(u_i - \underline{u}_i)}\right) \\ &= \arg\max_{u\in\mathcal{U}} \; -\sum_{j\in\mathcal{N}} \left(\frac{(u_j - \underline{u}_j)}{\sum_{i\in\mathcal{N}} (u_i - \underline{u}_i)}\right) \log\left(\frac{(u_j - \underline{u}_j)}{\sum_{i\in\mathcal{N}} (u_i - \underline{u}_i)}\right). \end{aligned}$$

- **Independent of Irrelevant Alternatives:** Satisfied. If $\mathcal{U} \subset \mathcal{U}'$ and $\varphi_S(\mathcal{U}') \in \mathcal{U}$ (it maximizes $h_S(\cdot)$ over $\mathcal{U}'$ and it is also contained in $\mathcal{U}$) then $\varphi_S(\mathcal{U}')$ also maximizes $\varphi_S(\cdot)$ over $\mathcal{U}$.

- **Restricted Monotonicity:** Not satisfied. See Example I with $h_S(\cdot)$.

7.3.8 *Superquantile Scheme*

The superquantile (Rockafellar et al., 2000) has been routinely used as a risk measure in finance and economics. Recently, Dowling et al. (2016) proposed using the superquantile to shape distributions of allocations among stakeholders. This can be done by solving the allocation problem:

$$\varphi_{Q_\alpha}(u) := \arg\min_{u \in \mathcal{U}} \; h_{Q_\alpha}(u). \tag{7.3.10}$$

where

$$h_{Q_\alpha}(u) := \min_{t \in \mathbb{R}} \; t + \frac{1}{1-\alpha} \sum_{j \in \mathcal{N}} [d_j(u) - t]_+ \tag{7.3.11}$$

is the superquantile function, $\alpha \in (0,1)$ is a probability level, and $d_j(u) = \underline{u}_j - u_j$ is the *disutility* of stakeholder $j \in \mathcal{N}$. Computing the superquantile of the disutility vector is equivalent to arranging the disutilities in increasing order (utilities in decreasing order), and taking the arithmetic mean of the the largest $(1-\alpha)$ faction of disutilities (Dowling et al., 2016). The superquantile allocation thus converges to the social welfare allocation as $\alpha \to 0$ (Pavlikov and Uryasev, 2014) and it converges to the max-min allocation as $\alpha \to 1$. We note that a superquantile scheme can also be constructed by using a disutility of the form $d_j(u) = \overline{u}_j - u_j$ (the utopia utility is used as reference). Here, we prefer to use the status quo utility as reference in order to establish connections with the rest of the schemes.

In this setting, the disutilities $d_j(u)$ are interpreted as outcomes (of equal probability $1/n$) of a discrete random variable $d(u)$. Consequently, we can also express the problem

in terms of the expectation operator:

$$\varphi_{Q_\alpha}(\mathcal{U}) := \arg\min_{u\in\mathcal{U}} \min_{t\in\mathbb{R}} \; t + \frac{1}{1-\alpha}\mathbb{E}[d(u)-t]_+.$$

The axiomatic properties of the superquantile allocation are:

- **Pareto Optimality:** Satisfied only for $\alpha = 0$. The superquantile function is not a strictly monotonic function for all the utility values u_j (it ignores the smaller disutilities) when $\alpha > 0$. For the case when $\alpha = 0$, the superquantile solution considers all utilities (it is the social welfare and thus it is Pareto optimal). In (Dowling et al., 2016) it is shown that the superquantile allocation is only *weak* Pareto optimal.

- **Symmetry:** Not Satisfied. The superquantile allocation ignores the smallest disutilities and thus there is no guarantee that the solution is unique. Consequently, it is possible to find $\sigma(\varphi_{Q_\alpha}(\mathcal{U})) \neq \varphi_{Q_\alpha}(\sigma(\mathcal{U}))$.

- **Affine Invariance:** Satisfied under weak AI. The disutility under a uniform affine transformation yields:

$$\begin{aligned}
\varphi_{Q_\alpha}(A(u)) &= \arg\min_{t\in\mathbb{R}} \quad t + \frac{1}{n(1-\alpha)} \sum_{i\in\mathcal{N}} [cd_i(u) - t]_+ \\
&= \arg\min_{t\in\mathbb{R}} \quad t + \frac{1}{n(1-\alpha)} c \sum_{i\in\mathcal{N}} [d_i(u) - t/c]_+ \\
&= c \arg\min_{t\in\mathbb{R}} \quad t' + \frac{1}{n(1-\alpha)} \sum_{i\in\mathcal{N}} [d_i(u) - t']_+.
\end{aligned}$$

  where $t' = t/c$ can be redefined as $t' \leftarrow t/c$.

- **Independence of Irrelevant Alternatives:** Satisfied. If $\mathcal{U} \subset \mathcal{U}'$ and $\varphi_{Q_\alpha}(\mathcal{U}') \in \mathcal{U}$ (it maximizes $h_{Q_\alpha}(\cdot)$ over $\mathcal{U}'$ and it is also contained in $\mathcal{U}$) then $\varphi_{Q_\alpha}(\mathcal{U}')$ also maximizes $\varphi_{Q_\alpha}(\cdot)$ over $\mathcal{U}$.

- **Restricted Monotonicity:** Not satisfied. See Example I with $h_{Q_\alpha}(\cdot)$.

7.3.9 *Generalized Entropy Scheme*

The generalized entropy (GE) scheme uses a parametric function to determine allocations. This parametric function (called the generalized entropy) includes the Theil index, the log-mean deviation, and the squared coefficient of variation as special cases (Cowell and Kuga, 1981). As with the entropy and superquantile schemes, this approach interprets utilities as outcomes of a discrete random variable.

In this scheme, the utility allocation is chosen by solving the problem:

$$\varphi_{GE_\beta}(\mathcal{U}) := \operatorname*{arg\,min}_{u \in \mathcal{U}} \quad h_{GE_\beta}(u)$$

where $h_{GE_\beta}(\cdot)$ is the GE function:

$$h_{GE_\beta}(u) := \frac{1}{n\beta(\beta-1)} \sum_{j \in \mathcal{N}} \left[\left(\frac{u_j - \underline{u}_j}{u_m - \underline{u}_m} \right)^\beta - 1 \right]. \tag{7.3.12}$$

and $\beta \in (-\infty, \infty)$ is a parameter and $u_m := (1/n)\sum_{j \in \mathcal{N}} u_j$ and $\underline{u}_m := (1/n)\sum_{j \in \mathcal{N}} \underline{u}_j$ are the means of the utilities and status quo utilities, respectively. For some special cases, the GE function takes the following form:

$$h_{GE_\beta}(u) = \begin{cases} \dfrac{1}{n} \displaystyle\sum_{j \in \mathcal{N}} \frac{u_j - \underline{u}_j}{u_m - \underline{u}_m} \log \frac{u_j - \underline{u}_j}{u_m - \underline{u}_m}, & \beta = 1 \\ \\ -\dfrac{1}{n} \displaystyle\sum_{j \in \mathcal{N}} \log \frac{u_j - \underline{u}_j}{u_m - \underline{u}_m}, & \beta = 0 \end{cases} \tag{7.3.13}$$

The *Theil index* corresponds to $h_{GE_{\beta=1}}(\cdot)$ and the mean log deviation corresponds to $h_{GE_{\beta=0}}(\cdot)$.

For an allocation problem with *fixed total utility* (which implies a fixed mean), the GE allocation with $\beta = 0$ is the Nash allocation (i.e., $\varphi_{GE_{\beta=0}}(\mathcal{U}) = \varphi_{NS}(\mathcal{U})$). This can be

established as follows:

$$\begin{aligned}\varphi_{GE_{\beta=0}}(\mathcal{U}) &= \arg\min_{u\in\mathcal{U}} \quad -\frac{1}{n}\sum_{j\in\mathcal{N}} \log\frac{u_j-\underline{u}_j}{u_m-\underline{u}_m} \\ &= \arg\min_{u\in\mathcal{U}} \quad -\frac{1}{n}\sum_{j\in\mathcal{N}} \log\left(u_j-\underline{u}_j\right) \\ &= \varphi_{NS}(\mathcal{U}) \end{aligned} \tag{7.3.14}$$

We thus have that $\varphi_{GE_{\beta=0}}(\mathcal{U})$ satisfies the same Axioms as those of the Nash scheme.

The GE allocation with $\beta = 1$ is the Shannon entropy allocation. This follows from:

$$\begin{aligned}\varphi_{GE_{\beta=1}}(\mathcal{U}) &= \arg\min_{u\in\mathcal{U}} \quad \frac{1}{n}\sum_{i\in\mathcal{N}} \frac{u_i-\underline{u}_i}{u_m-\underline{u}_m}\log\frac{u_i-\underline{u}_i}{u_m-\underline{u}_m} \\ &= \frac{1}{n}\arg\min_{u\in\mathcal{U}} \quad \sum_{i\in\mathcal{N}} \frac{(u_i-\underline{u}_i)}{\frac{\sum_{j\in\mathcal{N}}(u_j-\underline{u}_j)}{n}}\log\frac{(u_i-\underline{u}_i)}{\frac{\sum_{j\in\mathcal{N}}(u_j-\underline{u}_j)}{n}} \\ &= \arg\min_{u\in\mathcal{U}} \quad \sum_{i\in\mathcal{N}} \frac{(u_i-\underline{u}_i)}{\sum_{j\in\mathcal{N}}(u_j-\underline{u}_j)}\log\frac{(u_i-\underline{u}_i)}{\sum_{j\in\mathcal{N}}(u_j-\underline{u}_j)} + \sum_{i\in\mathcal{N}} \frac{(u_i-\underline{u}_i)}{\sum_{j\in\mathcal{N}}(u_j-\underline{u}_j)}\log n \\ &= \arg\min_{u\in\mathcal{U}} \quad \sum_{i\in\mathcal{N}} \frac{(u_i-\underline{u}_i)}{\sum_{j\in\mathcal{N}}(u_j-\underline{u}_j)}\log\frac{(u_i-\underline{u}_i)}{\sum_{j\in\mathcal{N}}(u_j-\underline{u}_j)} \\ &= \varphi_S(\mathcal{U}). \end{aligned} \tag{7.3.15}$$

Here, we used the property that $\sum_{i\in\mathcal{N}} \frac{(u_i-\underline{u}_i)}{\sum_{j\in\mathcal{N}}(u_j-\underline{u}_j)} = 1$. Thus, $\varphi_{GE_{\beta=1}}(\mathcal{U})$ satisfies the same Axioms as those of the Shannon entropy scheme.

For $\beta \in [2,\infty)$ can express the GE allocation as:

$$\begin{aligned}\varphi_{GE_{\beta\in[2,\infty)}}(\mathcal{U}) &= \arg\min_{u\in\mathcal{U}} \quad \frac{1}{n\beta(\beta-1)}\sum_{j\in\mathcal{N}}\left[\left(\frac{u_j-\underline{u}_j}{u_m-\underline{u}_m}\right)^{\beta}-1\right] \\ &= \arg\min_{u\in\mathcal{U}} \quad \sum_{j\in\mathcal{N}}\left(\frac{u_j-\underline{u}_j}{u_m-\underline{u}_m}\right)^{\beta}. \end{aligned} \tag{7.3.16}$$

Moreover, for fixed total utility, we have:

$$\varphi_{GE_{\beta\in[2,\infty)}}(\mathcal{U}) = \arg\min_{u\in\mathcal{U}} \quad \sum_{i\in\mathcal{N}}\left(u_i-\underline{u}_i\right)^{\beta}.$$

We now prove that the GE allocation for $\beta \in [2, \infty)$ and fixed total utility is unique.

Property 7. *The GE function $h_{GE_{\beta\in[2,\infty)}}(\cdot)$ under fixed total utility is strictly convex.*

Proof. The entries of the gradient of the GE function are given by:

$$g_j(u) = \frac{1}{n(\beta-1)} \left[\left(\frac{u_i - \underline{u}_i}{u_m - \underline{u}_m} \right)^{\beta-1} \right], \quad j \in \mathcal{N}$$

and the Hessian has entries:

$$H_{i,j}(u) = \begin{cases} \frac{1}{n} \left[\left(\frac{u_i - \underline{u}_i}{u_m - \underline{u}_m} \right)^{\beta-2} \right] & \text{for } \; i = j \\ 0 & \text{otherwise.} \end{cases}$$

For every non-zero vector v, we have that:

$$v^T H(u) v = \frac{1}{n} \sum_{i=j}^{n} v_j^2 \left[\left(\frac{u_j - \underline{u}_j}{u_m - \underline{u}_m} \right)^{\beta-2} \right] > 0$$

The Hessian is thus positive definite. □

We now analyze the properties of the GE scheme for $\beta \in [2, \infty)$ and under fixed total utility.

- **Pareto Optimality:** Satisfied. The GE function is strictly monotonically increasing.
- **Symmetry:** Satisfied. Due to the strict convexity of the GE function, the solution is unique and thus invariant under permutations.
- **Affine Invariance:** Satisfied under weak AI. This follows from:

  $$\varphi_{GE_{\beta\in[2,\infty)}}(A(u)) = \arg\min_{u\in\mathcal{U}} \frac{1}{n\beta(\beta-1)} \sum_{j\in\mathcal{N}} \left[\left(\frac{c(u_j - \underline{u}_j)}{v_m - \underline{v}_m} \right)^{\beta} - 1 \right]$$

  where v_m is the arithmetic mean of the transformed utilities ($v_j = cu_j$). We have $v_m - \underline{v}_m = c(u_m - \underline{u}_m)$ and the result follows.

- **Independent of Irrelevant Alternatives:** Satisfied. If $\mathcal{U} \subset \mathcal{U}'$ and $\varphi_{GE_{\beta\in[2,\infty)}}(\mathcal{U}') \in \mathcal{U}$ (it maximizes $h_{GE_{\beta\in[2,\infty)}}(\cdot)$ over $\mathcal{U}'$ and it is also contained in $\mathcal{U}$) then $\varphi_{GE_{\beta\in[2,\infty)}}(\mathcal{U}')$ also maximizes $\varphi_{GE_{\beta\in[2,\infty)}}(\cdot)$ over $\mathcal{U}$.

- **Restricted Monotonicity:** Not satisfied. See Example I.

Interestingly, the GE function can be expressed as a *moment expansion* of the form:

$$h_{GE_{\beta\in[2,\infty)}}(u) = \frac{1}{2!}\frac{\mu_2}{\mu_1^2} + \frac{(\beta-2)}{3!}\frac{\mu_3}{\mu_1^3} + \frac{(\beta-2)(\beta-3)}{4!}\frac{\mu_4}{\mu_1^4} + \cdots + \frac{(\beta-2)\ldots(\beta-(n+1))}{n!}\frac{\mu_n}{\mu_1^n} + \mathcal{O}(\mu_n). \tag{7.3.17}$$

where $\mu_k := \mathbb{E}[(d - \mathbb{E}[d])^k]$, $k = 2, 3, ...$, is the k-th central moment of the discrete random variable v with outcomes $u_j - \underline{u}_j$ of equal probability $1/n$ and $\mu_1 := \mathbb{E}[v] = (1/n)\sum_{j\in\mathcal{N}}(u_j - \underline{u}_j) = u_m - \underline{u}_m$. To see how the expansion is obtained, we note that the generalized entropy can be expressed as (Cowell, 2000):

$$h_{GE_\beta}(u) := \frac{1}{\beta(\beta-1)}\,\mathbb{E}\left[\left(\frac{v}{\mu_1}\right)^\beta - 1\right]. \tag{7.3.18}$$

Now consider the Taylor series expansion $h_{GE_\beta}(\cdot)$ around $\mu_1 = \mathbb{E}[v]$:

$$\begin{aligned}
&h_{GE_\beta}(u)\\
&= \frac{1}{\beta(\beta-1)}\frac{1}{\mu_1^\beta}\,\mathbb{E}\left[\mu_1^\beta + \frac{\beta\mu_1^{\beta-1}}{1!}((u-\underline{u})-\mu_1) + \cdots + \frac{\beta(\beta-1)\ldots(\beta-(n-1))\mu_1^{\beta-n}}{n!}((u-\underline{u})-\mu_1)^n + \mathcal{O}(u)^{n+1} - \mu_1^\beta\right]\\
&= \frac{1}{\beta(\beta-1)}\,\mathbb{E}\left[\frac{\beta\mu_1^{-1}}{1!}((u-\underline{u})-\mu_1) + \frac{\beta(\beta-1)\mu_1^{-2}}{2!}((u-\underline{u})-\mu_1)^2 + \ldots\right.\\
&\qquad\left. + \frac{\beta(\beta-1)(\beta-2)\ldots(\beta-(n-1))\mu_1^{-n}}{n!}((u-\underline{u})-\mu_1)^n + \mathcal{O}(u^{n+1})\right]\\
&= \mathbb{E}\left[\frac{\mu_1^{-1}}{\beta-1}((u-\underline{u})-\mu_1) + \frac{\mu_1^{-2}}{2}((u-\underline{u})-\mu_1)^2 + \frac{\mu_1^{-3}(\beta-2)}{3!}((u-\underline{u})-\mu_1)^3 + \ldots\right.\\
&\qquad\left. + \frac{(\beta-2)\ldots(\beta-(n-1))\mu_1^{-n}}{n!}((u-\underline{u})-\mu_1)^n + \mathcal{O}(u^{n+1})\right]\\
&= \mathbb{E}\left[\frac{\mu_1^{-2}}{2!}((u-\underline{u})-\mu_1)^2 + \frac{\mu_1^{-3}(\beta-2)}{3!}((u-\underline{u})-\mu_1)^3 + \cdots + \frac{(\beta-2)\ldots(\beta-(n-1))\mu_1^{-n}}{n!}((u-\underline{u})-\mu_1)^n + \mathcal{O}(u^{n+1})\right]
\end{aligned}$$

$$= \frac{1}{2!}\frac{\mu_2}{\mu_1^2} + \frac{(\beta-2)}{3!}\frac{\mu_3}{\mu_1^3} + \frac{(\beta-2)(\beta-3)}{4!}\frac{\mu_4}{\mu_1^4} + \cdots + \frac{(\beta-2)\ldots(\beta-(n-1))}{n!}\frac{\mu_n}{\mu_1^n} + \mathcal{O}(\mu_{n+1}).$$

The moment expansion representation allows us to establish the following properties.

Property 8. *For fixed total utility, the Nash allocation is the solution of the problem:*

$$\arg\min_{u\in\mathcal{U}} \frac{1}{2}\frac{\mu_2}{\mu_1^2} - \frac{1}{3}\frac{\mu_3}{\mu_1^3} + \frac{1}{4}\frac{\mu_4}{\mu_1^4} + \cdots + \frac{(-1)^n}{n}\frac{\mu_n}{\mu_1^n} + \mathcal{O}(\mu_{n+1}). \tag{7.3.19}$$

Proof. We recall that, for fixed total utility, the Nash allocation is the GE allocation for $\beta = 0$. The result thus follows by substituting $\beta = 0$ in the moment expansion (7.3.17) and noticing that we obtain (7.3.19). □

Property 9. *The Shannon entropy allocation is the solution of the problem:*

$$\arg\min_{u\in\mathcal{U}} \frac{1}{2}\frac{\mu_2}{\mu_1^2} - \frac{1}{6}\frac{\mu_3}{\mu_1^3} + \frac{1}{12}\frac{\mu_4}{\mu_1^4} + \cdots + \frac{(-1)^n}{n(n-1)}\frac{\mu_n}{\mu_1^n} + \mathcal{O}(\mu_{n+1}). \tag{7.3.20}$$

Proof. We recall that, for a fixed total allocation, the entropy allocation is the GE solution for $\beta = 1$. The result follows by substituting $\beta = 1$ in the moment expansion (7.3.17) and noticing that we obtain (7.3.20). □

From the moment expansion we see that the first term is one-half the *squared coefficient of variation*:

$$\frac{1}{2}\frac{\mu_2}{\mu_1^2} = \frac{1}{2}\frac{\mathbb{E}[(v-\mathbb{E}[v])^2]}{\mathbb{E}[v]^2}. \tag{7.3.21}$$

This reveals the role of the *utility variance* μ_2, which is a natural measure of dispersion. In particular, one would expect that minimizing the variance of the utilities results in a fair allocation. We see, however, that in the GE allocation scheme the variance of the utilities is minimized but the mean utility is maximized (simultaneously). It is not difficult to see that minimizing variance alone would not result in a satisfactory fairness scheme, since it

violates important axioms (particularly Pareto optimality and symmetry).

7.3.10 *Summary of Axiomatic Properties*

The axiomatic properties of different utility allocation schemes is summarized in Table 7.1. We recall that no scheme can satisfy Axioms 1-5 simultaneously. In particular, of all the schemes analyzed, only the two-stakeholder KS scheme satisfies restricted monotonicity. We also see that the Nash, Shannon entropy, and generalized entropy schemes satisfy the most axioms (four out of five) but Nash satisfies AI (while entropy approaches only satisfy weak AI). We also note that the Nash scheme does not assume a fixed total utility (and therefore it is a more flexible approach than entropy approaches). Notably, the social welfare scheme only satisfies three out of five axioms (and only satisfies weak AI). Connections between the utility allocation schemes are shown in Figure 7.1. We observe that the generalized entropy and the α-fair allocation schemes are linked to majority of the allocation schemes. These connections explain the similar axiomatic properties of the α-fair and entropy solutions. We also note that the Kalai-Smorodinsky solution is not linked to any allocation scheme and is the only scheme satisfying restricted monotonicity.

Table 7.1: Summary of axiomatic properties of utility allocation schemes.

Scheme	Pareto	Symmetry	AI	Weak AI	IIA	Monotonicity	Fixed Total Utility	Unique Solution
Social Welfare	✓	✗	✗	✓	✓	✗	N	N
Nash	✓	✓	✓	✓	✓	✗	N	Y
KS with $n = 2$	✓	✓	✓	✓	✗	✓	N	Y
Max-Min	✗	✗	✗	✓	✓	✗	N	N
α-Fair with $\alpha \in (2, \infty)$	✓	✓	✗	✓	✓	✗	N	Y
Entropy	✓	✓	✗	✓	✓	✗	Y	Y
Superquantile with $\alpha \in (0, 1)$	✗	✗	✗	✓	✓	✗	N	N
GE with $\beta \in [2, \infty)$	✓	✓	✗	✓	✓	✗	Y	Y

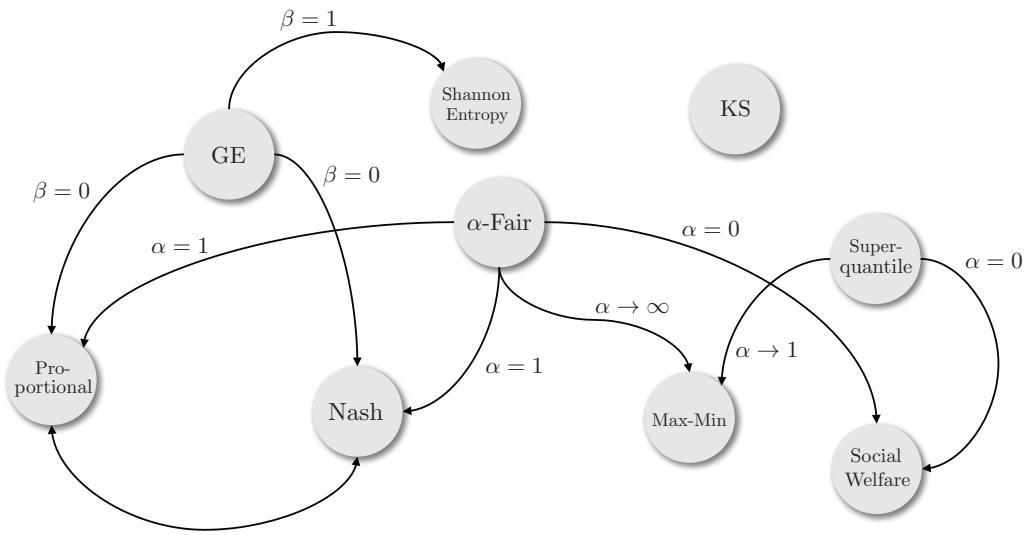

Figure 7.1: Connections between utility allocation schemes

7.4 Case Studies

We illustrate the properties of the different utility allocation schemes for a simple power allocation problem and for a sophisticated problem arising in environmental management. The case studies presented in this section were implemented in the mathematical modeling package JuMP. All the scripts and data needed to reproduce the results are available at: https://github.com/zavalab/JuliaBox/tree/master/FairnessMeasures.

7.4.1 *Power Allocation*

Consider the problem of electrical load allocation to two consumers u_1 and u_2. A total of 800 kW of electricity is generated by a power plant. The transmission line capacity between the power plant and the first consumer is 200 kW while the transmission line capacity between the power plant and the second consumer is 1,000 kW. We consider the utilities of the consumers to be equivalent to the demand served (we want to maximize

the demand served). The utility set is given by:

$$\mathcal{U} = \{u_1, u_2 \,|\, 0 \leq u_1 \leq 200,\ 0 \leq u_2 \leq 1000,\ u_1 + u_2 = 800\}$$

The status quo point here is considered to be zero kW (no demand served) while the utopia point is 200 kW for the first consumer and 800 kW for the second consumer (they obtain all the power that they can possibly accommodate). We refer to this allocation problem as Case I. The utility allocations under the different schemes studied are shown in Table 7.2. We observe that the Nash, max-min, α-fair, entropy, and generalized entropy allocations are the same. These schemes allocate $u_1 = 200$ kW and $u_2 = 600$ kW. The Kalai-Smorodinsky solution favors the second consumer and allocates u_1 =133.33 kW and u_2 =666.67 kW. This is because the utopia point for the second consumer is five times larger than that of the first consumer. The social welfare and the superquantile (with $\alpha = 0$) are equivalent and thus allocate all utility to the second consumer, thereby starving the first consumer. We note that that the allocations under these schemes is non-unique. In particular, the allocations under every scheme give the same total utility (800 kW). This illustrates the inherent degeneracy of the social welfare scheme.

Table 7.2: Allocations for Case I

Scheme	u_1 (kW)	u_2 (kW)
Nash	200	600
KS	133.33	666.67
Social Welfare	0	800
Max-Min	200	600
α-Fair ($\alpha \geq 2$)	200	600
Entropy	200	600
Superquantile ($\alpha = 0$)	0	800
GE ($\beta \geq 0$)	200	600

We now modify the problem such that both the consumers have the same transmission

line capacity of 1,000 kW (Case II). The utility set is now given by:

$$\mathcal{U} = \{u_1, u_2 \,|\, 0 \leq u_1 \leq 1000,\ 0 \leq u_2 \leq 1000,\ u_1 + u_2 = 800\}.$$

Note that this change corresponds to an expansion of the utility set (relative to Case I). The allocations under this case are reported in Table 7.3. Here, we observe that all schemes allocate load evenly (except the social welfare). We also note that the superquantile solution differs from that of the social welfare (but the total utility is the same).

Table 7.3: Allocations for Case II

Scheme	u_1 (kW)	u_2 (kW)
Nash	400	400
KS	400	400
Social Welfare	800	0
Max-Min	400	400
α-Fair ($\alpha \geq 2$)	400	400
Entropy	400	400
Superquantile ($\alpha = 0$)	400	400
GE ($\beta \geq 0$)	400	400

7.4.2 *Geographical Nutrient Balancing*

In this case study, we consider the problem of balancing soil phosphorus (P) concentration in the upper Yahara watershed region (Figure 7.2) in the State of Wisconsin. Excessive amounts of P have accumulated in this area, primarily due to livestock manure and the heavy use of agricultural fertilizers. Rain and snow melt often wash excess P into waterways, ultimately leading to blue-green algae blooms and eutrophication (Sampat et al., 2019).

We consider 50 dairy farms that produce waste (containing P) and 50 croplands where the waste can be applied to supply P needs. The croplands are stakeholders that can take waste. Each of these croplands has a different P uptake capacity $\bar{P}_j$. We consider that spreading of waste on the cropland releases 0.76 kg P/tonne of waste applied. The total

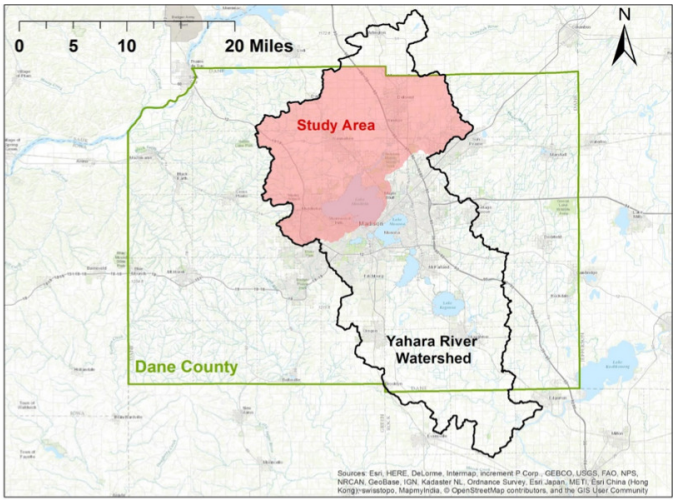

Figure 7.2: Study area in the Yahara watershed in Dane County, WI considered for the phosphorus balancing.

livestock waste generated annually in our study area is 0.16 million tonnes. This waste supply is equivalent to a P mass of 122 tonnes per year. The total P uptake capacity in the study area was set to 150 tonnes per year. The goal is to distribute the P from dairy farms to the croplands without saturating croplands.

The cropland utilities u_j are defined as the difference between the P limit and the P spread:

$$u_j = \overline{P}_j - P_j, \quad j \in \mathcal{N}$$

The status quo point in this case is set to zero indicating that the cropland is already saturated with P. The goal is to maximize the cropland utilities which is equivalent to minimizing P applied to the croplands (to avoid oversaturation). We analyze different allocation schemes: social welfare, Nash, α-fairness ($\alpha = 2, 3$), generalized entropy ($\beta = 2$), max-min, and entropy. The results are summarized in Figure 7.3.

In Figure 7.3a we observe that the allocation under social welfare gives rise to multiple areas with disproportionate amounts of P. Specifically, a red region indicates that the cropland is saturated with P while the blue regions indicate the cropland can still accept

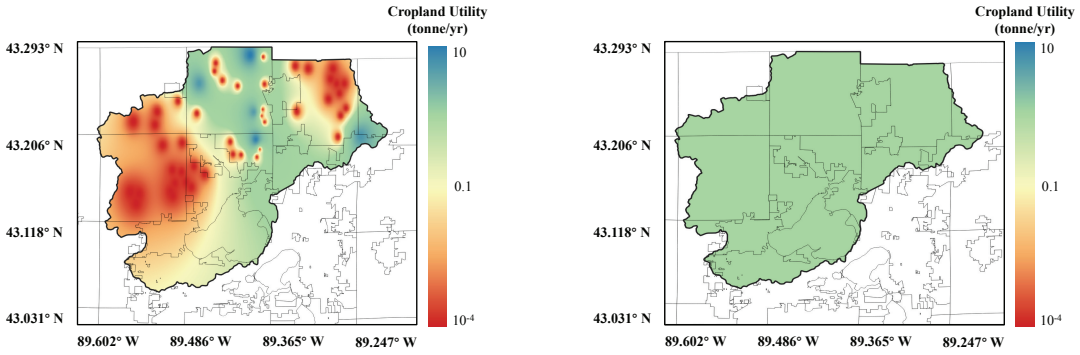

(a) **(b)**

Figure 7.3: Cropland utility maps in the Upper Yahara watershed region using different utility allocations chemes (a) Social welfare (b) Nash, α-fair ($\alpha = 2, 3$), entropy, max-min, and generalized entropy ($\beta = 2$).

P. The maximum social welfare achieved was 28.54 tonne/yr. In Figure 7.3b we also see that the rest of the allocation schemes result in a fully uniform distribution of P, with a cropland utility value of 0.57 tonne/yr. Interestingly, such uniform distribution is achievable *while maintaining a social welfare value of 28.54 tonne/yr*. This again, highlights the degenerate nature of the social welfare solutions, which tends to be exacerbated in applications with many stakeholders (as in this case).

7.5 Summary

We presented an axiomatic analysis of various utility allocation schemes and derived fundamental connections between them. Such an analysis can guide decision-makers in selecting a suitable measure to allocate utilities among multiple stakeholders. Moreover, our theoretical and case study analysis highlights that solution degeneracy can lead to allocations that are not fair.

As a part of the future work, we are interested in applying the proposed fairness schemes to diverse problems arising in engineering. For instance, it would be interesting to apply the schemes in a coordinated market framework. The market clearing prices in

such markets are obtained by computing the dual variables of an optimization problem, where the objective is to maximize the social welfare. Since the social welfare is not a fair allocation scheme, the profit distribution is also not fair. Using a fair allocation scheme such as the Nash solution, our goal would be to derive market clearing prices that ensure fair profit allocations. This is needed in order to properly balance profits of large and small generators.

8

CONCLUSIONS AND FUTURE DIRECTIONS

8.1 Contributions

The key research contribution of this work is the development of multi-product network models that aid decision-making. When multiple stakeholders are involved, the final solution is often derived by qualitative discussions. This work provides quantitative tools to drive those decisions and achieve an optimal compromise solution. From a modeling perspective, this work has developed mathematical frameworks to:

1. Model Supply Chains in a Coherent Manner. In Chapter 2, we presented a general optimization formulation for multi-product supply chain networks. The formulation uses a general graph representation that considers a set of technologies placed at different spatially-dispersed nodes under which a set of products undergo transformations. Interactions between products are captured using a hierarchical graph that maps product flows at each node using a transformation matrix and that maps network nodes using transportation paths (arcs). We demonstrate this formulation in Chapter 3, where we analyze the interplays between technology selection and placement, transportation logistics, and environmental impact associated with phosphorus recovery from livestock waste at

large CAFOs in the State of Wisconsin. Our analysis indicates that the value of recovered products and assumed remediation costs have a strong influence on the nature of the optimal waste management strategies. This is important because markets for many of these products are immature and highly volatile. In Chapter 4, we use the modeling abstraction to drive policy design decisions. We observe that sustainable waste management would not be an economically viable option unless incentives are provided. When REC, RIN, and P credit incentives of 2 USD/MWh, 2 USD/gal, and 10 USD/lb P respectively are simultaneously considered, it is found that combined technologies to produce liquefied biomethane and nutrient cakes can achieve payback periods of less than 5 years. The modeling framework provides the ability to capture complex system-wide interdependencies and quantify the impact of different policy designs.

2. Derive Economic Interpretations of Supply Chains. In Chapter 5, we presented a coordination framework that enables handling of complex interdependencies between products and locations as well as physical constraints. We prove that the system reveals the inherent value of products through the clearing prices and delivers allocations that satisfy fundamental economic and efficiency properties that are expected from a competitive market. We also show that the proposed system provides a systematic framework to monetize environmental and health impacts and benefits of remediation. Moreover, prices reveal the true value of waste streams and capture spatiotemporal variations that help prioritize endangered areas/times and that reveal the need for investment in processing technologies, transportation, facility relocation, and seasonal storage. The framework can also be used by the government to analyze and predict the effect of different regulations and incentive mechanisms. The proposed framework is scalable in that it can provide open access that fosters geographical transactions between large numbers of small and large players in urban and rural areas and in that it enables coordination with other infrastructures. In Chapter 6, we combine the coordination framework with a gate-to-gate approach that quantifies the environmental impacts of nutrient pollution. Our analysis

reveals that every excess kilogram of phosphorus in the Upper Yahara watershed region results in an economic loss of 74.5 USD. This environmental cost is sufficient to activate the market for organic waste processing.

3. **Allocate Resources Amongst Multiple Stakeholders in a Fair Manner**. In Chapter 7, we presented a fundamental perspective on allocating resources amongst multiple stakeholders. For the problem of waste management, this framework sets the foundation for answering the question of how to distribute the environmental cost amongst stakeholders. In this chapter, we provide an axiomatic analysis of various utility allocation schemes and derived fundamental connections between them. Such an analysis can guide decision-makers in selecting a suitable measure to allocate utilities among multiple stakeholders. Moreover, our theoretical and case study analysis highlights that solution degeneracy can lead to allocations that are not fair.

We note that in demonstrating the applicability of the above modeling frameworks, we have also contributed to the area of organic waste management. Specifically for the upper Yahara watershed region in the state of Wisconsin, we have conducted extensive studies that capture the complex spatiotemporal dependencies involved in mitigating phosphorus runoff from organic waste.

8.2 Future Research Directions

The directions for future work are motivated by the goal to drive investment in organic waste management and mitigate nutrient pollution. The future work will seek to develop mathematical frameworks that provide strategies for sustainable implementation of waste management policies. Achieving this goal will also drive innovations in the modeling of multi-product supply chain networks.

8.2.1 *Multiscale Network Coordination*

The work in this dissertation has considered supply chain systems with local or state boundaries. However, multi-product networks are also influenced by the interactions with sectors and couplings at multiple spatial scales. For instance, Wisconsin could become a major exporter of struvite, which can be used in states with P-deficient soils. It is necessary to explore how to enable multi-scale geographical coordination by capturing these interactions. Capturing local, regional, national, and global scale interactions will help to identify critical decisions made at state scales that affect national-level performance. Hierarchical network aggregation schemes can be used to navigate scales. The hierarchical spatial network approach, combined with the market coordination framework presented in Chapter 5, can also provide key insights into how products should be priced according to excess/scarcity at particular location. This strategy can be used by state and federal regulatory agencies to monitor transfer of resources between national, regional, and local scales.

Another interesting direction is to explore how spatial relocation of waste producers (e.g., consolidation into larger dairy farms) can impact social welfare, prices, and the environment. This type of analysis requires of more advanced formulations for facility location and also of game-theoretic approaches that capture infrastructure investment strategies (such as recently developed anchor-tenant models) (Topolski et al., 2018; Sampat et al., 2017).

8.2.2 *Integrate Life Cycle Analysis in Product Pricing*

The market value of a product does not reflect the resource efficiency corresponding to its generation. In order to achieve the goal of environmental sustainability, we need to re-prioritize the federal and state incentives to promote resource efficient products. Life cycle analysis (LCA) can help in quantifying the mid and end-point impacts of products recovered from organic waste. LCA analysis, when combined with the coordination

framework of Chapter 5, can reveal the inherent value of products that also accounts for resource efficiency. Extending the idea of the environment as a market player, as presented in Chapter 6, we can develop mathematical frameworks that reveal the inherent economic and environmental value of products. This research direction will help in designing an economically and environmentally sustainable strategy for organic waste management.

8.2.3 *Designing Fair Markets for Coordinated Systems*

This future direction will ensure fair allocation of profits amongst the stakeholders in a market clearing setting e.g. balancing profits between small and large players. The clearing prices in such markets are obtained by computing the dual variables of an optimization problem, where the objective is to maximize the social welfare (as presented in Chapter 5). The social welfare function results in degenerate solutions i.e. multiple solutions can have the same objective value. To ensure the most fair allocation is selected amongst these solutions, we can use the Nash objective introduced in Chapter 7. These frameworks can be integrated by introducing the Nash objective as a regularization term in the social welfare function. Since the system is no longer linear now, it will be imperative to analyze how the economic properties of the prices derived from this framework depend on the regularization coefficient. Our hypothesis is that for very low values of the regularization coefficient, the pricing properties would still hold. This work will also benefit the operation of other coordinated systems such as the wholesale electricity markets.

8.2.4 *Mixed-Integer Formulations for Fair Classification*

This direction will extend the resource allocation framework presented in Chapter 7to classification models used in machine-learning applications. Classification models are typically used to separate datasets based on a set of descriptors; however, such models

can also be used to make decisions (e.g., make go/no-go decisions in a project). In this context, fairness becomes a major issue because such decisions tend to affect multiple stakeholders and because descriptors might inadvertently introduce biases (Gölz et al., 2019; Hardt et al., 2016; Wattenberg et al., 2016). A recent application of fair classification models include allocation of financial loans (e.g., descriptor is credit score). Fair classification models can also be used to tackle problems of interest to the chemical engineering community. For instance, in a manufacturing facility, access to experimental lab equipment is simultaneously requested by different stakeholders to test a variety of products. The decision here is whether a sample should be tested or not (or when) given the importance of the sample (captured by descriptors) and given that there is limited lab equipment and budgets. Such decisions are often based on minimizing a loss function, which is an aggregate of the cost associated with false positives and false negatives. The model output is a threshold value (based on a linear combination of sample features) that activates the binary decision. The inherent degeneracy of such models can lead to decisions that prioritize testing in an unfair manner (as seen in Chapter 7).

State of the art research in fairness in machine learning focuses on developing algorithms that do not violate state or federal anti-discrimination laws. This is achieved by adding either post-processing steps or additional constraints to the mathematical model to achieve properties such as demographic parity, equalized odds, and equal opportunity (Gölz et al., 2019; Hardt et al., 2016). These conditions can be mutually exclusive and often lack a theoretical basis that connects them to the axiomatic view of fairness. In this work, we will develop mixed-integer formulations that address the problem of fair classification from an axiomatic perspective Moulin (1991). We will showcase how the Nash solution inherently captures the tradeoff between efficiency and fairness, and selects the optimal solution based on the axiomatic properties.

A

APPENDIX A COORDINATED MANAGEMENT AND INHERENT VALUE OF PRODUCTS

a.1 Perspective on Coordinated Systems

Coordinated management systems provide a framework to enable exchange of products in complex decision-making environments that involve large numbers of stakeholders, that rely on shared infrastructures, and that are driven and constrained by complex spatio-temporal physical phenomena and externalities (e.g., extreme weather). Highly advanced coordinated management systems are currently used throughout the world to manage and provide access to infrastructures such as electrical power and computer networks (Blumstein et al., 2002; Nygren et al., 2010). Coordinated systems for the U.S. power grid, in particular, have reached a high level of maturity over the last 30 years and operate as coordinated markets that actively foster technology innovation and competition. Our work is motivated by the observation that the evolution of power grid provides important lessons and significant empirical evidence that can be leveraged to justify the need and guide the design of scalable management systems for organic waste and associated infrastructure. Here we motivate our work by providing a high-level perspective of coordinated electricity markets in the U.S.

Coordinated *wholesale* electricity markets are used in the U.S. to exchange electrical power across wide geographical regions. The stakeholders in the market (the market players) comprise suppliers (companies that own power generation technologies), consumers (industrial consumers or utility companies that distribute power within urban areas), and transportation providers (companies that own the transmission network infrastructure). Power transactions over the geographical region are coordinated in real-time by a non-profit organization known as an independent system operator (ISO). In the U.S., there are currently six ISOs (Califonia, PJM, Midcontinent, ERCOT, New York, and New England). ISOs provide an open-access system and receive bids in real-time from all suppliers and consumers connected to the network. The bidding information is used to run a highly sophisticated power coordination system (also known as power scheduling, dispatch, or market clearing system) that captures physical laws and constraints that govern generation and transmission infrastructure. Specifically, generators are physically constrained in their ability to dynamically ramp up and ramp down their power output, power flows along paths of least resistance in the transmission network, and the network is limited by line capacities and by its topology (connectivity). Capturing these physical laws and constraints in transactions is a critical need and distinctive feature of power grid markets compared to other commodity markets. The existence of the power grid infrastructure and of associated markets is driven by a fundamental social service: the need to provide efficient and reliable supply of electricity to a vast population of consumers (which is essential to perform socio-economic activities). Efficiency ensures that only the most cost-efficient resources and assets are used which drives technological innovation (e.g., new generation and transportation technologies). Reliability ensures that supply can be maintained under diverse externalities that impact the power grid such as heat waves, cold fronts, storms, earthquakes, manmade attacks, and equipment degradation and failures. To give a perspective on the economic impact of reliability, ISOs currently estimate the value of lost power (also known as the value of lost load) to be up to 30,000 USD/MWh (while the average electricity price in the U.S. is 20 USD/MWh) (Hogan,

2016). This value is estimated based on the socio-economic impact of lost electrical supply service (De Nooij et al., 2007; Willis and Garrod, 1997). The need to coordinate power transactions in space and time is thus essential to ensure that the infrastructure provides adequate service to society. PJM currently operates the largest market, which serves 65 million customers across 14 states and manages 1,376 generation sources, 82,000 miles of transmission lines, and 6,038 transmission substations. The PJM day-ahead market updates price signals every hour for 10,000 different locations. Achieving high reliability for systems of this magnitude (which also face constant changes in the number and locations of consumers and generation technologies) would be challenging and risky under an uncoordinated market.

The design of coordinated markets currently operated by ISOs has involved a careful consideration of economics and physics (Hogan et al., 1996). Specifically, current clearing procedures are designed to determine power allocations that are physically realizable and price signals that properly incentivize generation, transport, and consumption. Specifically, prices are generated in a way that they cover the operating costs of generators. Moreover, spatial price differences are designed to remunerate transportation providers through mechanisms such as financial transmission rights (RosellÃşn and Kristiansen, 2013). Allocations and price signals are generated by solving an optimization problem that seeks to maximize the social welfare (service value minus supply cost across the region) subject to the physical laws and constraints governing the infrastructure. Price signals encode effects of physical, temporal, and spatial constraints (which impose market friction). Specifically, shortage of power at a given point in space and time (e.g., due to transmission network congestion or lack of ramping up capacity) will manifest as a large price. On the other hand, excess of power at a given point in space and time (e.g., created by the inability to ramp down generation) will manifest as a small (or even negative) price. Price signals and allocations generated by the clearing system also have the key property that they are the outcome of a competitive market equilibrium. This is key, because it implies that the ISO does not interfere with transactions between suppliers and

consumers (it only ensures that physical compatibility is achieved in the transactions).

Price signals serve as natural catalysts that drive and justify infrastructure investment and technology innovation. For instance, large spatial price differences indicate that opportunities exist to invest in new transmission lines and large temporal price differences indicate that opportunities exist to develop fast power generation and storage units (Fang and Hill, 2003; Sioshansi et al., 2012). Electricity prices are also a key factor that influences location of industrial facilities (e.g., manufacturing and data centers) (Kim et al., 2017). Another important benefit of coordinated markets is that they provide a systematic framework to monetize environmental impacts of power grid infrastructure and to predict the effect of government incentives and regulations. For instance, understanding impacts of water usage and emission constraints on the flexibility of power plants and on prices is essential in developing environmental regulations and policies (Gollop and Roberts, 1983; Stillwell et al., 2011). The coordination scope of power grid markets is currently being expanded to capture physical constraints of the natural gas infrastructure (Zlotnik et al., 2017). This is driven by the increasing dependence of power plants on natural gas and by the fact that the natural gas infrastructure exhibits drastically different spatiotemporal physical constraints (e.g., gas networks exhibit significant delays and have sparser topologies) (Chiang and Zavala, 2016). The need to coordinate with other infrastructures and markets will likely persist, due to the increasing interdependence between the power grid with transportation, water, communication, and computing infrastructures (Rinaldi et al., 2001; Kim et al., 2017).

Uncoordinated and semi-coordinated organic waste markets are currently in operation across the world. The Office of Fair Trading in the United Kingdom conducted an organic waste market study in 2011 that focused on sewage sludge (oft, 2011). The study found that competition and communication in the sewage sludge market is limited and that sludge transactions between WWTPs is rare and negotiations are ad hoc. Nunan (Nunan, 2000) documented the development of urban organic waste markets using a case study of Hubli-Dharwad, India. Before 1997, the Hubli-Dharwad Municipal Corporation

sold waste to farmers by auction activities where the seller and farmer reached an agreement on the prices. After 1997, no auctions have been held, and farmers buy municipal solid waste by contacting the Hubli-Dharwad Municipal Corporation directly. The Hubli-Dharwad Municipal Corporation has also asked private sector companies to tender bids for the provision of solid waste processing. In the U.S., impacts of waste on water quality have been addressed by using carbon and nutrient credit trading initiatives guided by the U.S. Environment Protection Agency and the U.S. Department of Agriculture (Lal et al., 2008). In the nutrient credit market, suppliers generate nutrient credits through conservation activities, and customers buy credits to meet regulatory requirements. However, in the three pilot programs in Wisconsin, the nutrient trading is not considered an active way to manage water quality (Breetz et al., 2004).

Semi-coordinated markets act as brokers that connect suppliers with consumers. In Europe, for example, the European Energy Exchange (EEX) group facilitates trade of energy, environmental credits, and agricultural products (eex, 2017). Semi-coordinated markets certainly facilitate transactions but do not capture system-wide interdependencies and physical constraints associated with transportation and transformation. As demonstrated by coordinated electricity markets, capturing these system-wide effects is essential to achieve high efficiency and scalability. Recent studies have advocated for the need of coordinated organic waste markets that can enable a free movement of waste in order to facilitate processing and recycling as well as to provide incentives for waste generators (e.g., livestock producers) to manage animal waste and associated environmental impacts (Page, 2014; eur, 2014; RÃűmgens and Kruizinga, 2013). Such recommendations are also justified by research studies that develop economic models to capture system-wide geographical, physical, and logistical issues. For instance, Corrales et al. (Corrales et al., 2014) developed a GIS-based watershed assessment model integrated with an economic model to compare nutrient trading scenarios in an agricultural sub-basin of the Lake Okeechobee watershed in Florida. The results show that a coordinated nutrient trading market leads to cost savings. Innes (Innes, 2000) developed a spatial model of regional

livestock production that captures environmental impacts associated with spills from animal waste storage, nutrient runoff due to the application of manure to croplands, and direct ambient pollution. The model was used to analyze the impact from policy effects including scare regulations, fertilizer taxes, and waste handling standards affecting storage and transport. This model provides a number of intriguing and counter-intuitive insights that highlight the complex interdependencies that exist in organic waste management. For instance, it was found that fertilizer taxes in fact increase the welfare of livestock producers. Capturing interdependencies that arise from product transport, processing, and spatial layouts of sources and demands is essential to design and predict the effect of policies.

a.2 Illustrative Case Studies

In this section, we provide simple case studies that illustrate the concepts and capabilities of the proposed market framework.

a.2.1 *System with No Transformation*

We consider a simple market setting (labeled as A) consisting of one supplier (connected to node n_1), two consumers (connected to nodes n_2 and n_3, respectively), and two transportation providers that can connect players along paths $n_1 \rightarrow n_2$ and $n_1 \rightarrow n_3$. There is no transformation of waste in this setting. The supplier offers waste with a capacity of $\bar{s}_1$ = 10,000 tonne and it provides a bidding cost α_1^s. The consumers offer to buy up to $\bar{d}_1$ = 3,000 tonne and $\bar{d}_2$ = 5,000 tonne, respectively, and provide bidding costs α_1^d and α_2^d. The transportation providers offer to move product along path $n_1 \rightarrow n_2$ at cost α_1^f and along path $n_1 \rightarrow n_3$ at cost α_2^f.

We solve the market clearing problem for this setting under different scenarios that capture different bidding values (see Table A.1). We make the following observations:

- In scenario I, a maximum social welfare of 7,000 USD is achieved and we can see that all players have a non-negative profit values (in agreement with Theorem 1). The supplier and the transportation providers have a profit value of zero. This is because the nodal price at node n_1 is same as the bid made by the supplier and the difference in the prices at nodes n_1 and n_2 is the same as the bid of the transportation provider over link $n_1 \rightarrow n_2$ (the same behavior is observed along path $n_1 \rightarrow n_3$). The profit made by the transportation provider is thus zero. The profit of the consumers is positive, indicating that the cleared prices are lower than their bids. It can be easily verified that all the clearing prices satisfy the bounds of Theorem 4. We also highlight that the clearing prices for waste are different in all nodes (the prices are balanced by clearing to ensure that all players have a non-negative profit).

- In scenario II, the bid made by the second consumer is reduced. In this case, we obtain similar results to those of the previous setting but we note that no waste is allocated to the second consumer. This is because there is no economic incentive to transport the waste between node n_1 and n_3. In particular, the difference in the clearing prices between n_1 and n_3 is lower than the bid of the transportation provider along that path. From this setting it is easy to verify that revenue adequacy holds (Theorem 3). In particular, the consumer (connected to node n_2) pays $3.5 \times 3{,}000 = 10{,}500$ USD for the waste provided, the supplier (connected to node n_1) gets paid $1.5 \times 3{,}000 = 4{,}500$ USD, and the transportation provider (for the link $n_1 \rightarrow n_2$) gets paid $(3.5 - 1.5) \times 3{,}000 = 6{,}000$ USD. Consequently, there is no money lost in the system.

- In scenario III, the supplier bid is increased. In this case, no player is cleared (the market is dry and thus the social welfare is zero). The difference in the bidding costs between nodes n_1 and n_2 and between n_1 and n_3 are lower than the bids of the transportation providers along the corresponding paths. These results illustrate how spatial interdependencies between waste values and transportation costs are

captured by the market framework.

a.2.2 *System with Negative Bidding Costs*

We now consider a market setting (labeled as B) that involves negative bidding costs. This setting consists of one waste supplier located in node n_1 (e.g., a WWTP generating sludge waste) with supply capacity $\bar{s}_1$ = 5,000 tonne and bidding cost α_1^s. The sludge can be used for land application and is requested by a consumer (e.g., a farmer) located at node n_2 with bidding cost α_1^d. A transportation provider offers service along path $n_1 \rightarrow n_2$ with bidding cost α_1^f. In this setting, the bidding supply and demand costs are allowed to be negative. A negative supply bid indicates that the WWTP is willing to pay the consumer to dispose of the sludge. Similarly, the negative demand bidding cost represents that the customer requests to be paid in order to accept the waste and apply it to its land. The results obtained under different bidding values are shown in Table A.2. In scenario I we note that, the supplier makes a profit since it ends up paying less to the market (than it's bid value) to get the waste processed. Moreover, we see that neither the consumer nor the transportation provider make a profit. In scenario II we note that, when the consumer submits a negative bid, the supplier still makes a profit (but this is cut in half compared to scenario I). This captures the fact that now a payment needs to be made to the consumer for it to take the waste (so that revenue adequacy holds). This is also reflected by the fact that the price at node n_2 is negative (and thus can be interpreted as a tipping fee). We also note that, the payment made to the consumer makes its profit zero (the consumer is not affected by taking the waste). Consequently, the supplier has an incentive to provide its waste (even when paying for it) and the consumer is not affected by this. This non-intuitive behavior is the result of having a coordinated clearing mechanism that maximizes the social welfare and adjusts the prices in order to ensure that all players benefit from the market. In scenario III we note that, when the consumer increases the magnitude of its negative bid, no player is cleared (the market

is dry). This is because the difference in the supply and demand bids is lower than the bidding cost of the transportation provider (there is no incentive to transport waste).

a.2.3 *System with Transformation*

We now consider a market setting (labeled as C) with waste transformation. This setting is sketched in Fig. A.1. The system comprises a supplier providing a waste product p_1 at node n_1 with a maximum capacity $\bar{s}_{1,p_1}$ = 10,000 tonne and bidding cost α_1^s. The transformation provider is located at node n_2 has a maximum processing capacity of $\bar{\xi}_1$ = 8,000 tonne of waste p_1 and a bidding operating cost α_1^ξ. This transformation provider converts one unit of product p_1 to 0.01 units of a high-value product p_2 and 0.99 units of a low-value product p_3. A bid is put into the market for product p_2 at node n_3 by a consumer with capacity $\bar{d}_1$ and bidding cost α_1^d. A bid is put into the market for product p_3 at node n_4 by a consumer with capacity $\bar{d}_2$ and bidding cost α_2^d.

The results of this market setting are summarized in Table A.3. In scenario I, we can see that there exists an incentive for the transformation provider to create product p_2 from product p_1 and this results in a large profit. This is manifested in a positive transformation price π_1^ξ, which is given by $3{,}495 \times 0.01 - 7 \times 1 - 4 \times 0.99 = 23.99$ USD. We also note that this transformation price is higher than the processing bid cost of 20 USD (consequently, the profit is positive). Interestingly, none of the other market players make a profit in this setting (they are simply not affected by the transaction). In scenario II, the demand bid for p_2 from the first consumer decreases and the market becomes dry (this is because the transformation price is now 19.99 USD (which is lower than the bid). These results illustrate how interdependencies between waste and product values and transformation costs are captured by the market framework.

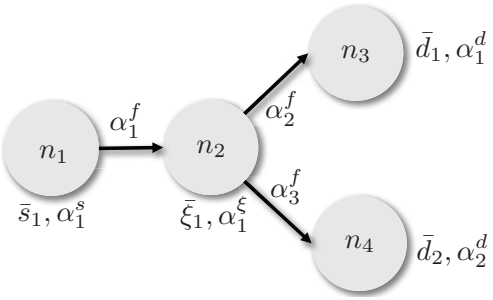

Figure A.1: Sketch of market setting C

Table A.1: Clearing results for market setting A

Scenario	Bids (USD/tonne)					Welfare (USD)	Profits (USD)				Prices (USD/tonne)
	α_1^s	α_1^d	α_2^d	α_1^f	α_2^f	φ	ϕ_1^s	ϕ_1^d	ϕ_2^d	ϕ^f	$[\pi_{n_1}, \pi_{n_2}, \pi_{n_3}]$
I	1.5	5	6	2	4	7,000	0	4,500	2,500	0	$1.5, 3.5, 5.5$
II	1.5	5	5	2	4	4,500	0	4,500	0	0	$1.5, 3.5, 5.0$
III	3.5	5	5	2	4	0	0	0	0	0	$3.5, 5.0, 5.0$

Table A.2: Clearing results for market setting B

Scenario	Bids (USD/tonne)			Welfare (USD)	Profits (USD)			Prices (USD/tonne)
	α_1^s	α_1^d	α_1^f	φ	ϕ_1^s	ϕ_1^d	ϕ_1^f	$[\pi_{n_1}, \pi_{n_2}]$
I	-6	$+0.0$	5	5,000	5,000	0	0	$-5.0, +0.0$
II	-6	-0.5	5	2,500	2,500	0	0	$-5.5, -0.5$
III	-6	-1.5	5	0	0	0	0	$-6.5, -1.5$

Table A.3: Clearing results for market setting C

Scen.	Bids (USD/tonne)	Welfare (USD)	Profits (USD)	Prices (USD/tonne)
	$[\alpha_1^s, \alpha_1^d, \alpha_2^d, \alpha_1^\xi]$	φ	$[\phi_1^s, \phi_1^d, \phi_2^d, \phi^\xi]$	$[\pi_{n_1,p_1}, \pi_{n_3,p_2}, \pi_{n_4,p_3}, \pi_{n_2,p_1}, \pi_{n_2,p_2}, \pi_{n_2,p_3}]$
I	$[2, 3500, 1, 20]$	31,920	$[0, 0, 0, 31920]$	$[2, 3500, 1, 7, 3495, -4]$
II	$[2, 3000, 1, 20]$	0	$[0, 0, 0, 0]$	$[1, 3000, 1, 6, 2995, -4]$

BIBLIOGRAPHY

Agricultural waste management field handbook. *USDA National Resources Conservation Services (NRCS)*, 1992.

Organic waste: An OFT market study. Technical report, Marketing, Office of Fair Trading, UK, 2011.

The efficient functioning of waste markets in the European Union: Legislative and policy options. Technical report, European Commission, 2014.

EEX annual report 2016 - visions for sustainable growth. *European Energy Exchange Group*, 2017.

115th Congress (2017-2018). S.988 - Agriculture Environmental Stewardship Act of 2017 available at https://www.congress.gov/bill/115th-congress/senate-bill/988. [Online; accessed 06-December-2017].

Agstar. Fair Oaks Dairy Digester: Fair Oaks, Indiana. Technical report, U.S. Environmental Protection Agency, February 2014.

Aguilar, M., Saez, J., Llorens, M., Soler, A., and Ortuno, J. Nutrient removal and sludge production in the coagulation–flocculation process. *Water Research*, 36(11):2910–2919, 2002.

Aguirre-Villegas, H. A. and Larson, R. A. Evaluating greenhouse gas emissions from dairy manure management practices using survey data and lifecycle tools. *J. Cleaner Prod.*, 143:169–179, 2017.

Aguirre-Villegas, H. A., Larson, R. A., and Sharara, M. A. Anaerobic digestion, solid-liquid separation, and drying of dairy manure: Measuring constituents and modeling emission. *Science of The Total Environment*, 696:134059, 2019.

Akgul, O., Shah, N., and Papageorgiou, L. G. Economic optimisation of a UK advanced biofuel supply chain. *Biomass and Bioenergy*, 41:57–72, 2012.

Akgul, O., Zamboni, A., Bezzo, F., Shah, N., & Papageorgiou, L. G. Optimization based approaches for bioethanol supply chains. *Industrial & Engineering Chemistry Research*, pages 4927–4938, 2010.

Alex Marvin, W., Schmidt, L. D., Benjaafar, S., Tiffany, D. G., and Daoutidis, P. Economic Optimization of a Lignocellulosic Biomass-to-Ethanol Supply Chain. *Chemical Engineering Science*, 67(1):68–79, 2012.

An, H., Wilhelm, W. E., and Searcy, S. W. A mathematical model to design a lignocellulosic biofuel supply chain system with a case study based on a region in Central Texas. *Bioresource Technology*, 102(17):7860–7870, 2011.

Artzner, P., Delbaen, F., Eber, J.-M., and Heath, D. Coherent measures of risk. *Mathematical finance*, 9(3):203–228, 1999.

Ashley, K., Cordell, D., and Mavinic, D. A brief history of phosphorus: from the philosopher's stone to nutrient recovery and reuse. *Chemosphere*, 84(6):737–746, 2011.

Astill, G. M. and Shumway, C. R. Profits from pollutants: Economic feasibility of integrated anaerobic digester and nutrient management systems. *J. Environ. Manage.*, 184: 353–362, 2016.

Avami, A. A model for biodiesel supply chain: A case study in Iran. *Renewable and Sustainable Energy Reviews*, 16(6):4196–4203, 2012.

Balaman, Ş. Y. and Selim, H. A network design model for biomass to energy supply chains with anaerobic digestion systems. *Applied Energy*, 130:289–304, 2014.

Bauman, A. G., Burt, J. A., Feary, D. A., Marquis, E., and Usseglio, P. Tropical harmful algal blooms: An emerging threat to coral reef communities? *Marine Pollution Bulletin*, 60(11):2117–2122, 2010.

Beddoes, J. C., Bracmort, K. S., Burns, R. T., and Lazarus, W. F. An analysis of energy production costs from anaerobic digestion systems on U.S. livestock production facilities. *USDA NRCS Technical Note*, (1), 2007.

Belsky, A. J., Matzke, A., and Uselman, S. Survey of livestock influences on stream and riparian ecosystems in the western United States. *Journal of Soil and water Conservation*, 54(1):419–431, 1999.

Bertsimas, D., Farias, V. F., and Trichakis, N. The price of fairness. *Operations research*, 59 (1):17–31, 2011.

Bhuiyan, M., Mavinic, D., and Koch, F. Phosphorus recovery from wastewater through struvite formation in fluidized bed reactors: a sustainable approach. *Water Science and Technology*, 57(2):175–181, 2008.

Bloemhof-Ruwaard, J., Van Wassenhove, L., Gabel, H., and Weaver, P. An environmental life cycle optimization model for the European pulp and paper industry. *Omega*, 24(6): 615–629, 1996.

Blumstein, C., Friedman, L. S., and Green, R. The history of electricity restructuring in California. *Journal of Industry, Competition and Trade*, 2(1-2):9–38, 2002.

Bockstael, N. E., Freeman, A. M., Kopp, R. J., Portney, P. R., and Smith, V. K. On measuring economic values for nature. *Environmental Science and Technology*, 34(8):1384–1389, 2000.

Bohn, R. E., Caramanis, M. C., and Schweppe, F. C. Optimal pricing in electrical networks over space and time. *The Rand Journal of Economics*, pages 360–376, 1984.

Boix, M., Montastruc, L., Azzaro-Pantel, C., and Domenech, S. Optimization methods

applied to the design of eco-industrial parks: a literature review. *Journal of Cleaner Production*, 87:303–317, 2015.

Boţ, R., Kassay, G., and Wanka, G. Strong duality for generalized convex optimization problems. *Journal of Optimization Theory and Applications*, 127(1):45–70, 2005.

Bowling, I. M., Ponce-Ortega, J. M., and El-Halwagi, M. M. Facility Location and Supply Chain Optimization for a Biorefinery. *Industrial & Engineering Chemistry Research*, 50 (10):6276–6286, 2011.

Breetz, H. L., Fisher-Vanden, K., Garzon, L., Jacobs, H., Kroetz, K., and Terry, R. Water quality trading and offset initiatives in the U.S.: A comprehensive survey. *Dartmouth College and the Rockefeller Center for the U.S. Environmental Protection Agency*, 2004.

Bundy, L. and Sturgul, S. A phosphorus budget for Wisconsin cropland. *Journal of Soil and Water Conservation*, 56(3):243–249, 2001.

Burak Aksoy, Harry Cullinan, David Webster, Kevin Gue, Sujith Sukumaran, Mario Eden and Jr., N. S. Woody Biomass and Mill Waste Utilization Opportunities in Alabama: Transportation Cost Minimization, Optimum Facility Location, Economic Feasibility, and Impact. *Environmental Progress & Sustainable Energy (Vol.30,*, 30(4):720–732, 2011.

Burkholder, J., Libra, B., Weyer, P., Heathcote, S., Kolpin, D., Thorne, P. S., and Wichman, M. Impacts of waste from concentrated animal feeding operations on water quality. *Environ. Health Perspect.*, 115(2):308, 2007.

California Energy Commission - Tracking Progress. Renewable energy - overview. Technical report, 2017.

Carnevale, E. and Lombardi, L. Comparison of different possibilities for biogas use by life cycle assessment. *Energy Procedia*, 81:215–226, 2015.

CH-IV International. All about LNG available at http://www.ch-iv.com/all-about-lng/. [Online; accessed 07-December-2017].

Chae, S. H., Kim, S. H., Yoon, S.-G., and Park, S. Optimization of a waste heat utilization network in an eco-industrial park. *Applied Energy*, 87(6):1978–1988, 2010.

Chapuis-Lardy, L., Fiorini, J., Toth, J., and Dou, Z. Phosphorus concentration and solubility in dairy feces: Variability and affecting factors. *Journal of dairy science*, 87(12): 4334–4341, 2004.

Chen, C. W. and Fan, Y. Bioethanol supply chain system planning under supply and demand uncertainties. *Transportation Research Part E: Logistics and Transportation Review*, 48(1):150–164, 2012.

Chen, X. An Economic Analysis of the Future U . S . Biofuel Industry , Facility Location , and Supply Chain Network. (February 2015), 2014.

Chiang, N.-Y. and Zavala, V. M. Large-scale optimal control of interconnected natural gas and electrical transmission systems. *Applied Energy*, 168:226–235, 2016.

Childers, D. L., Corman, J., Edwards, M., and Elser, J. J. Sustainability challenges of phosphorus and food: solutions from closing the human phosphorus cycle. *Bioscience*, 61(2):117–124, 2011.

CNN news. All 21 of Mississippi's beaches are closed because of toxic algae available at https://www.cnn.com/2019/07/07/us/mississippi-beaches-algae-closure-trnd/index.html. 2019a. [Online; accessed 15-August-2019].

CNN news. Red tide halts shellfish harvesting all along eastern Massachusetts available at http://thelocalne.ws/2019/07/02/red-tide-halts-shellfish-harvesting-all-along-eastern-mass/. 2019b. [Online; accessed 06-January-2020].

Constable, D. J., Curzons, A. D., and Cunningham, V. L. Metrics to 'green' chemistry - which are the best? *Green Chem.*, 4(6):521–527, 2002.

Copado-Méndez, P. J., Guillén-Gosálbez, G., and Jiménez, L. Milp-based decomposition algorithm for dimensionality reduction in multi-objective optimization: Application to environmental and systems biology problems. *Computers & Chemical Engineering*, 67: 137–147, 2014.

Coppedge, B., Coppedge, G., Evans, D., Jensen, J., Kanoa, E., Scanlan, K., Scanlan, B., Weisberg, P., and Frear, C. Renewable natural gas and nutrient recovery feasibility for deruyter dairy: An anaeroblic digester case study for alternative outtake markets and remediation of nutrient loading concerns within the region. Technical report, Washington State University, 2012.

Cordell, D., Rosemarin, A., Schröder, J., and Smit, A. Towards global phosphorus security: A systems framework for phosphorus recovery and reuse options. *Chemosphere*, 84(6): 747–758, 2011.

Cordell, D., Drangert, J.-O., and White, S. The story of phosphorus: global food security and food for thought. *Global Environmental Change*, 19(2):292–305, 2009.

Corrales, J., Naja, G. M., Bhat, M. G., and Miralles-Wilhelm, F. Modeling a phosphorus credit trading program in an agricultural watershed. *Journal of environmental management*, 143:162–172, 2014.

Corsano, G., Vecchietti, A. R., and Montagna, J. M. Optimal design for sustainable bioethanol supply chain considering detailed plant performance model. *Computers and Chemical Engineering*, 35(8):1384–1398, 2011.

Costanza, R., d'Arge, R., De Groot, R., Farber, S., Grasso, M., Hannon, B., Limburg, K., Naeem, S., O'neill, R. V., Paruelo, J., et al. The value of the world's ecosystem services and natural capital. *Nature*, 387(6630):253–260, 1997.

Cowell, F. A. Measurement of inequality. *Handbook of income distribution*, 1:87–166, 2000.

Cowell, F. A. and Kuga, K. Additivity and the entropy concept: an axiomatic approach to inequality measurement. *Journal of Economic Theory*, 25(1):131–143, 1981.

Cucarella, V., Zaleski, T., Mazurek, R., and Renman, G. Effect of reactive substrates used for the removal of phosphorus from wastewater on the fertility of acid soils. *Bioresource technology*, 99(10):4308–4314, 2008.

Čuček, L., Lam, H. L., Klemeš, J. J., Varbanov, P. S., and Kravanja, Z. Synthesis of regional networks for the supply of energy and bioproducts. *Clean Technologies and Environmental Policy*, 12(6):635–645, 2010.

Čuček, L., Varbanov, P. S., Klemeš, J. J., and Kravanja, Z. Total footprints-based multi-criteria optimisation of regional biomass energy supply chains. *Energy*, 44(1):135–145, 2012.

Čuček, L., Martín, M., Grossmann, I. E., and Kravanja, Z. Multi-period synthesis of optimally integrated biomass and bioenergy supply network. *Computers & Chemical Engineering*, 66:57–70, 2014.

Cuéllar, A. D. and Webber, M. E. Wasted food, wasted energy: the embedded energy in food waste in the United States. *Environmental science & technology*, 44(16):6464–6469, 2010.

Cusick, R. D., Ullery, M. L., Dempsey, B. A., and Logan, B. E. Electrochemical struvite precipitation from digestate with a fluidized bed cathode microbial electrolysis cell. *water research*, 54:297–306, 2014.

Dal-Mas, M., Giarola, S., Zamboni, A., and Bezzo, F. Strategic design and investment capacity planning of the ethanol supply chain under price uncertainty. *Biomass and Bioenergy*, 35(5):2059–2071, 2011.

Dane County Land and Water Resources Department. Legacy Sediment Removal Project

available at https://lwrd.countyofdane.com/Legacy-Sediment-Project. [Online; accessed 20-April-2019].

Database of State Incentives for Renewables & Efficiency (DSIRE). Renewable Portfolio Standard available at http://programs.dsireusa.org/system/program/detail/564. [Online; accessed 06-December-2017].

Dawoud, B., Amer, E., and Gross, D. Experimental investigation of an adsorptive thermal energy storage. *International journal of energy research*, 31(August 2007):135–147, 2007.

De Nooij, M., Koopmans, C., and Bijvoet, C. The value of supply security: The costs of power interruptions: Economic input for damage reduction and investment in networks. *Energy Economics*, 29(2):277–295, 2007.

Dockhorn, T. About the economy of phosphorus recovery. In *International conference on nutrient recovery from wastewater systems*, pages 145–158. IWA Publishing Vancouver, Canada, 2009.

Dodds, W. K., Bouska, W. W., Eitzmann, J. L., Pilger, T. J., Pitts, K. L., Riley, A. J., Schloesser, J. T., and Thornbrugh, D. J. Eutrophication of U.S. freshwaters: Analysis of potential economic damages. *Environmental Science & Technology*, 43(1):12–19, 2009.

Dowling, A. W., Ruiz-Mercado, G., and Zavala, V. M. A framework for multi-stakeholder decision-making and conflict resolution. *Computers & Chemical Engineering*, 90:136–150, 2016.

Doyle, J. D. and Parsons, S. A. Struvite formation, control and recovery. *Water research*, 36 (16):3925–3940, 2002.

Dunnett, A., Adjiman, C., and Shah, N. Biomass to heat supply chains applications of process optimization. *Process Safety and Environmental Protection*, 85(5 B):419–429, 2007.

Durkay, J. State Renewable Portfolio Standards and Goals available at http://www.ncsl.

org/research/energy/renewable-portfolio-standards.aspx#ca. *National Conference of State Legislatures*, 2017. [Online; accessed 05-December-2017].

Dynamic Concepts, LLC. Project Phoenix - Feasibility Study. Technical report, 2016.

Ekşioğlu, S. D., Acharya, A., Leightley, L. E., and Arora, S. Analyzing the design and management of biomass-to-biorefinery supply chain. *Computers & Industrial Engineering*, 57 (4):1342–1352, 2009.

Elia, J. A., Baliban, R. C., Xiao, X., and Floudas, C. A. Optimal energy supply network determination and life cycle analysis for hybrid coal, biomass, and natural gas to liquid (CBGTL) plants using carbon-based hydrogen production. *Computers and Chemical Engineering*, 35(8):1399–1430, 2011.

Fang, R. and Hill, D. J. A new strategy for transmission expansion in competitive electricity markets. *IEEE Transactions on power systems*, 18(1):374–380, 2003.

Fitzsimmons, E. G. Tap water ban for toledo residents. *The New York Times*, 3rd August 2014.

Fleming, L. E., Kirkpatrick, B., Backer, L. C., Bean, J. A., Wanner, A., Dalpra, D., Tamer, R., Zaias, J., Cheng, Y. S., Pierce, R., Naar, J., Abraham, W., Clark, R., Zhou, Y., Henry, M. S., Johnson, D., Van De Bogart, G., Bossart, G. D., Harrington, M., and Baden, D. G. Initial evaluation of the effects of aerosolized florida red tide toxins (brevetoxins) in persons with asthma. *Environmental Health Perspectives*, 113(5):650–657, 2005.

Galinato, S. P., Kruger, C. E., and Frear, C. Economic feasibility of anaerobic digester systems with nutrient recovery technologies. Technical report, Washington State University Extension, 2016.

Garcia, D. J. and You, F. Supply chain design and optimization: Challenges and opportunities. *Computers & Chemical Engineering*, 81:153–170, 2015.

Garcia, D. J. and You, F. The water-energy-food nexus and process systems engineering: a new focus. *Computers & Chemical Engineering*, 91:49–67, 2016.

Gerritse, R. and Vriesema, R. Phosphate distribution in animal waste slurries. *The Journal of Agricultural Science*, 102(1):159–161, 1984.

Giarola, S., Zamboni, A., and Bezzo, F. Spatially explicit multi-objective optimisation for design and planning of hybrid first and second generation biorefineries. *Computers and Chemical Engineering*, 35(9):1782–1797, 2011.

Gollop, F. M. and Roberts, M. J. Environmental regulations and productivity growth: The case of fossil-fueled electric power generation. *Journal of political Economy*, 91(4): 654–674, 1983.

Gölz, P., Kahng, A., and Procaccia, A. D. Paradoxes in fair machine learning. In *Advances in Neural Information Processing Systems*, pages 8340–8350, 2019.

Grossmann, I. E. Challenges in the new millennium: Product discovery and design, enterprise and supply chain optimization, global life cycle assessment. *Computers and Chemical Engineering*, 29(1):29–39, 2004.

Guillén-Gosálbez, G. and Grossmann, I. E. Optimal design and planning of sustainable chemical supply chains under uncertainty. *AIChE Journal*, 55(1):99–121, 2009.

Güngör, K. and Karthikeyan, K. Influence of anaerobic digestion on dairy manure phosphorus extractability. *Transactions of the ASAE*, 48(4):1497–1507, 2005a.

Güngör, K. and Karthikeyan, K. Probable phosphorus solid phases and their stability in anaerobically digested dairy manure. *Transactions of the ASAE*, 48(4):1509–1520, 2005b.

Gurian-Sherman, D. CAFOs uncovered: The untold costs of confined animal feeding operations. *Union of Concerned Scientists*, 2008.

Gurobi Optimization, LLC. Gurobi optimizer reference manual. 2018.

Gustafsson, J. P., Renman, A., Renman, G., and Poll, K. Phosphate removal by mineral-based sorbents used in filters for small-scale wastewater treatment. *Water research*, 42 (1):189–197, 2008.

Hadas, A., Bar Yosef, B., and Portnoy, R. Extractability of phosphorus in manure pellets enriched with fertilizer phosphorus. *Soil Science Society of America Journal*, 54(2):443–448, 1990.

Hardt, M., Price, E., and Srebro, N. Equality of opportunity in supervised learning. In *Advances in neural information processing systems*, pages 3315–3323, 2016.

He, Z., Griffin, T. S., and Honeycutt, C. W. Phosphorus distribution in dairy manures. *Journal of environmental quality*, 33(4):1528–1534, 2004.

Hernández, B., León, E., and Martín, M. Bio-waste selection and blending for the optimal production of power and fuels via anaerobic digestion. *Chemical Engineering Research and Design*, 121:163–172, 2017.

Hoagland, P., Anderson, D. M., Kaoru, Y., and White, A. The economic effects of harmful algal blooms in the United States: estimates, assessment issues, and information needs. *Estuaries*, 25(4):819–837, 2002.

Hoagland, P. and Scatasta, S. The economic effects of harmful algal blooms. In *Ecology of harmful algae*, pages 391–402. Springer, 2006.

Hoagland, P., Jin, D., Polansky, L. Y., Kirkpatrick, B., Kirkpatrick, G., Fleming, L. E., Reich, A., Watkins, S. M., Ullmann, S. G., and Backer, L. C. The costs of respiratory illnesses arising from florida gulf coast karenia brevis blooms. *Environmental Health Perspectives*, 117(8):1239–1243, 2009.

Hogan, W. W. Electricity Market Design available at http://www.ncsl.org/Portals/1/Documents/energy/Energy_Hogan_William_present.pdf. *National Conference of State Legislatures*, 2016. [Online; accessed 28-June-2018].

Hogan, W. W., Read, E. G., and Ring, B. J. Using mathematical programming for electricity spot pricing. *International Transactions in Operational Research*, 3(3-4):209–221, 1996.

Hu, J. and Mehrotra, S. Robust and stochastically weighted multiobjective optimization models and reformulations. *Operations research*, 60(4):936–953, 2012.

Hu, T. C. Multi-commodity network flows. *Operations research*, 11(3):344–360, 1963.

Huang, Y., Chen, C. W., and Fan, Y. Multistage optimization of the supply chains of biofuels. *Transportation Research Part E: Logistics and Transportation Review*, 46(6):820–830, 2010.

Hugo, A. and Pistikopoulos, E. N. Environmentally conscious long-range planning and design of supply chain networks. In *Journal of Cleaner Production*, 2005.

Huijbregts, M., Steinmann, Z., Elshout, P., Stam, G., Verones, F., Vieira, M., Hollander, A., Zijp, M., and Van Zelm, R. ReCiPe 2016: A harmonized life cycle impact assessment method at midpoint and endpoint level report i: Characterization. 2016.

Hylander, L. D., Kietlińska, A., Renman, G., and Simán, G. Phosphorus retention in filter materials for wastewater treatment and its subsequent suitability for plant production. *Bioresource technology*, 97(7):914–921, 2006.

Ileleji, K. E., Martin, C., and Jones, D. Basics of energy production through anaerobic digestion of livestock manure. Technical report, Purdue University Extension, 2010.

Innes, R. The economics of livestock waste and its regulation. *American Journal of Agricultural Economics*, 82(1):97–117, 2000.

Jin, D., Thunberg, E., and Hoagland, P. Economic impact of the 2005 red tide event on commercial shellfish fisheries in new england. *Ocean & Coastal Management*, 51(5):420–429, 2008.

Jin, Y., Hu, Z., and Wen, Z. Enhancing anaerobic digestibility and phosphorus recovery of dairy manure through microwave-based thermochemical pretreatment. *Water research*, 43(14):3493–3502, 2009.

Jordaan, E. M. *Development of an aerated struvite crystallization reactor for phosphorus removal and recovery from swine manure*. PhD thesis, University of Manitoba, 2011.

Jørgensen, P. J. Biogas-green energy. *Faculty of Agricultural Sciences, Aarhus University, Tjele, Denmark*, 2009.

Kalai, E. and Smorodinsky, M. Other solutions to Nash's bargaining problem. *Econometrica: Journal of the Econometric Society*, pages 513–518, 1975.

Kalaitzidou, M. A., Longinidis, P., and Georgiadis, M. C. Optimal design of closed-loop supply chain networks with multifunctional nodes. *Computers and Chemical Engineering*, 80:73–91, 2015.

Kaval, P. and Loomis, J. Updated outdoor recreation use values with emphasis on national park recreation. *Final Report, Cooperative Agreement*, pages 1200–99, 2003.

Kelly, F. P., Maulloo, A. K., and Tan, D. K. Rate control for communication networks: shadow prices, proportional fairness and stability. *Journal of the Operational Research society*, 49(3):237–252, 1998.

Kennedy, N., Evans, D. A., Kruger, C. E., Frear, C., Jensen, J., and Yorgey, G. Biogas upgrading on dairy digesters. Technical report, Washington State University Extension, 2015.

Kim, J., Realff, M. J., and Lee, J. H. Optimal design and global sensitivity analysis of biomass supply chain networks for biofuels under uncertainty. *Computers and Chemical Engineering*, 35(9):1738–1751, 2011a.

Kim, J., Realff, M. J., Lee, J. H., Whittaker, C., and Furtner, L. Design of biomass processing

network for biofuel production using an MILP model. *Biomass and Bioenergy*, 35(2):853–871, 2011b.

Kim, K., Yang, F., Zavala, V. M., and Chien, A. A. Data centers as dispatchable loads to harness stranded power. *IEEE Transactions on Sustainable Energy*, 8(1):208–218, 2017.

Kim, Y., Yun, C., Park, S. B., Park, S., and Fan, L. T. An integrated model of supply network and production planning for multiple fuel products of multi-site refineries. *Computers and Chemical Engineering*, 32(11):2529–2535, 2008.

Kondili, E., Pantelides, C. C., and Sargent, R. W. A general algorithm for short-term scheduling of batch operationsâĂŤi. milp formulation. *Computers & Chemical Engineering*, 17(2):211–227, 1993.

Krich, K., Augenstein, D., Batmale, J., Benemann, J., Rutledge, B., and Salour, D. Biomethane from dairy waste: a sourcebook for the production and use of renewable natural gas in California. *Western United Dairymen*, 2005.

Kunii, D. and Levenspiel, O. *Fluidization engineering*. Stoneham, MA (United States); Butterworth Publishers, 1991.

Lal, H., Delgado, J. A., Gross, C. M., Hesketh, E., McKinney, S. P., Cover, H., and Shaffer, M. Nutrient credit trading–a market-based approach for improving water quality. In *ASABE Annual International Meeting*, 2008.

Lam, H. L., Varbanov, P. S., and Klemeš, J. J. Optimisation of regional energy supply chains utilising renewables: P-graph approach. *Computers & Chemical Engineering*, 34 (5):782–792, 2010.

Lan, T., Kao, D., Chiang, M., and Sabharwal, A. *An axiomatic theory of fairness in network resource allocation*. Proceedings of IEEE INFOCOM, 2010.

Larkin, S. L. and Adams, C. M. Harmful algal blooms and coastal business: economic consequences in florida. *Society and Natural Resources*, 20(9):849–859, 2007.

Larson, R., Sharara, M., Good, L., Porter, T., Zavala, V., Sampat, A., and Smith, A. Evaluation of manure storage capital projects in the Yahara river watershed. *Technical Report for Dane County, WI*, 2016.

Lathrop, R. and Carpenter, S. Phosphorus loading and lake response analyses for the yahara lakes, unpublished report prepared for the yahara clean project. university of wisconsin-madison, 2011.

Leduc, S., Lundgren, J., Franklin, O., and Dotzauer, E. Location of a biomass based methanol production plant: A dynamic problem in northern Sweden. *Applied Energy*, 87(1):68–75, 2010.

Lillie, R. A., Graham, S., and Rasmussen, P. W. *Trophic state index equations and regional predictive equations for Wisconsin lakes*. Bureau of Research, Wisconsin Department of Natural Resources, 1993.

Lin, H., Gan, J., Rajendran, A., Reis, C. E. R., and Hu, B. Phosphorus removal and recovery from digestate after biogas production. In *Biofuels-Status and Perspective*, chapter 24, pages 517–546. InTech, 2015.

Lorimor, J., Powers, W., and Sutton, A. Manure characteristics, mwps-18. *MidWest Plan Service, Iowa State University*, 2004.

Lovelady, E. M. and El-Halwagi, M. M. Design and integration of eco-industrial parks for managing water resources. *Environmental Progress and Sustainable Energy: An Official Publication of the American Institute of Chemical Engineers*, 28(2):265–272, 2009.

Ma, J., Scott, N. R., DeGloria, S. D., and Lembo, A. J. Siting analysis of farm-based centralized anaerobic digester systems for distributed generation using GIS. *Biomass Bioenergy*, 28(6):591–600, 2005.

Ma, J., Kennedy, N., Yorgey, G., and Frear, C. Review of emerging nutrient recovery

technologies for farm-based anaerobic digesters and other renewable energy systems. *Report to the Innovation Center for U.S. Dairy*, 2013.

Maaß, O., Grundmann, P., and und Polach, C. v. B. Added-value from innovative value chains by establishing nutrient cycles via struvite. *Resources, Conservation and Recycling*, 87:126–136, 2014.

MacDonald, J., Ribaudo, M., Livingston, M., Beckman, J., and Huang, W. Manure Use for Fertilzer and for Energy : Report to Congress. (June), 2009.

Martín-Hernández, E., Sampat, A. M., Zavala, V. M., and Martín, M. Optimal integrated facility for waste processing. *Chemical Engineering Research and Design*, 131:160–182, 2018.

Mathers, J., Wolfe, C., Norsworthy, M., and Craft, E. The green freight handbook. *Environmental Defense Fund*, 2014.

Meers, E., Rousseau, D., Lesage, E., Demeersseman, E., and Tack, F. Physico-chemical P removal from the liquid fraction of pig manure as an intermediary step in manure processing. *Water, air, and soil pollution*, 169(1-4):317–330, 2006.

Meixner, K., Fuchs, W., Valkova, T., Svardal, K., Loderer, C., Neureiter, M., Bochmann, G., and Drosg, B. Effect of precipitating agents on centrifugation and ultrafiltration performance of thin stillage digestate. *Separation and Purification Technology*, 145:154–160, 2015.

Mele, F. D., Kostin, A. M., GuillelÀn-GosalÀlbez, G., and JimelÀnez, L. Multiobjective Model for More Sustainable Fuel Supply Chains. A Case Study of the Sugar Cane Industry in Argentina. *Industrial & Engineering Chemistry Research*, 50(9):4939–4958, 2011.

Meyer, D. and Powers, T. *Manure Treatment Technologies: Anaerobic Digesters*. University of California, Agriculture and Natural Resources (UC ANR) Publications, 2011.

Miettinen, K. *Nonlinear multiobjective optimization*, volume 12. Springer Science & Business Media, 2012.

Mihelcic, J. R., Fry, L. M., and Shaw, R. Global potential of phosphorus recovery from human urine and feces. *Chemosphere*, 84(6):832–839, 2011.

Minnesota Pollution Control Agency. Effluent Total Phosphorus Reduction Efforts by Wastewater Treatment Plants available at https://www.pca.state.mn.us. 2017. [Online; accessed 19-October-2017].

Moulin, H. *Axioms of cooperative decision making*. Number 15. Cambridge University press, 1991.

Nash Jr, J. F. The bargaining problem. *Econometrica: Journal of the Econometric Society*, pages 155–162, 1950.

National Oceanic and Atmospheric Administration (NOOA). What are HABs available at https://habsos.noaa.gov/about/. 2019. [Online; accessed 18-August-2019].

Neiro, S. M. S. and Pinto, J. M. A general modeling framework for the operational planning of petroleum supply chains. *Computers and Chemical Engineering*, 28(6-7):871–896, 2004.

Nelson, N. O., Mikkelsen, R. L., and Hesterberg, D. L. Struvite precipitation in anaerobic swine lagoon liquid: effect of ph and mg: P ratio and determination of rate constant. *Bioresource Technology*, 89(3):229–236, 2003.

Nennich, T., Harrison, J., VanWieringen, L., Meyer, D., Heinrichs, A., Weiss, W., St-Pierre, N., Kincaid, R., Davidson, D., and Block, E. Prediction of manure and nutrient excretion from dairy cattle. *Journal of Dairy Science*, 88(10):3721–3733, 2005.

North Temperate Lakes. Lake Mendota conditions available at https://lter.limnology.wisc.edu/researchsite/lake-mendota. 2018. [Online; accessed 21-December-2018].

Nunan, F. Urban organic waste markets: responding to change in Hubli–Dharwad, India. *Habitat International*, 24(3):347–360, 2000.

Nygren, E., Sitaraman, R. K., and Sun, J. The akamai network: a platform for high-performance internet applications. *ACM SIGOPS Operating Systems Review*, 44(3):2–19, 2010.

O'Shaughnessy, E., Liu, C., and Heeter, J. Status and trends in the U.S. voluntary green power market (2015 data). Technical report, National Renewable Energy Laboratory (NREL), 2015.

OVO Energy. Average electricity prices around the world available at https://www.ovoenergy.com/guides/energy-guides/average-electricity-prices-kwh.html. [Online; accessed 07-December-2017].

Page, L. Marketing manure: A value-added product for small operations. Technical report, ATTRA Sustainable Agriculture, 2014.

Papageorgiou, L., Rotstein, G., and Shah, N. Strategic supply chain optimization for the pharmaceutical industries. *Industrial Engineering Chemical Research*, 40(1):275–286, 2001.

Papapostolou, C., Kondili, E., and Kaldellis, J. K. Development and implementation of an optimisation model for biofuels supply chain. *Energy*, 36:6019–6026, 2011.

Parker, N., Tittmann, P., Hart, Q., Nelson, R., Skog, K., Schmidt, A., Gray, E., and Jenkins, B. Development of a biorefinery optimized biofuel supply curve for the Western United States. *Biomass and Bioenergy*, 34(11):1597–1607, 2010.

Paudel, K. P., Bhattarai, K., Gauthier, W. M., and Hall, L. M. Geographic information systems (GIS) based model of dairy manure transportation and application with environmental quality consideration. *Waste Management*, 29(5):1634–1643, 2009.

Pavlikov, K. and Uryasev, S. Cvar norm and applications in optimization. *Optimization Letters*, 8(7):1999–2020, 2014.

Pessino, C. and Fenochietto, R. Determining countries' tax effort. *Hacienda Pública Española/Revista de Economía Pública*, pages 65–87, 2010.

Peters, M. S., Timmerhaus, K. D., West, R. E., Timmerhaus, K., and West, R. *Plant design and economics for chemical engineers*, volume 4. McGraw-Hill New York, 1968.

Phaneuf, D. J., von Haefen, R. H., Mansfield, C., and Van Houtven, G. Measuring nutrient reduction benefits for policy analysis using linked non-market valuation and environmental assessment models: Final report on stated preference surveys. *U.S. Environmental Protection Agency*, 2013.

Prasodjo, D., Vujic, T., Cooley, D., Yeh, K., and Lee, M.-Y. A spatial-economic optimization study of swine waste-derived biogas infrastructure design in North Carolina. Technical report, Nicholas Institute for Environmental Policy Solutions and Duke Carbon Offsets Initiative, Duke University, 2013.

Pratt, C., Parsons, S. A., Soares, A., and Martin, B. D. Biologically and chemically mediated adsorption and precipitation of phosphorus from wastewater. *Current opinion in Biotechnology*, 23(6):890–896, 2012.

Pretty, J. N., Mason, C. F., Nedwell, D. B., Hine, R. E., Leaf, S., and Dils, R. Environmental costs of freshwater eutrophication in England and Wales. *Environmental Science and Technology*, 57(2):201–208, 2003.

Pritchard, G., Zakeri, G., and Philpott, A. A single-settlement, energy-only electric power market for unpredictable and intermittent participants. *Operations research*, 58(4-part-2): 1210–1219, 2010.

Qureshi, A., Lo, K. V., and Liao, P. H. Microwave treatment and struvite recovery potential of dairy manure. *Journal of Environmental Science and Health Part B*, 43(4):350–357, 2008.

Raiffa, H. Arbitration schemes for generalized two-person games. *Annals of Mathematics Studies*, 28:361–387, 1953.

Raman, R. and Grossmann, I. E. Modelling and computational techniques for logic based integer programming. *Computers & Chemical Engineering*, 18(7):563–578, 1994.

Rawls, J. *A theory of justice*. Harvard university press, 2009.

Rinaldi, S. M., Peerenboom, J. P., and Kelly, T. K. Identifying, understanding, and analyzing critical infrastructure interdependencies. *IEEE Control Systems*, 21(6):11–25, 2001.

Rockafellar, R. T., Uryasev, S., et al. Optimization of conditional value-at-risk. *Journal of risk*, 2:21–42, 2000.

RosellÃşn, J. and Kristiansen, T. *Financial Transmission Rights*. Springer, 2013.

Roth, A. E. *Axiomatic models of bargaining available at https://web.stanford.edu/~alroth/Axiomatic_Models_of_Bargaining.pdf*. Springer Verlag, 1979a. [Online accessed: 03-August-2018].

Roth, A. E. An impossibility result concerningn-person bargaining games. *International Journal of Game Theory*, 8(3):129–132, 1979b.

Rubio-Castro, E., Ponce-Ortega, J. M., Serna-González, M., Jiménez-Gutiérrez, A., and El-Halwagi, M. M. A global optimal formulation for the water integration in eco-industrial parks considering multiple pollutants. *Computers and Chemical Engineering*, 35(8):1558–1574, 2011.

RÃűmgens, B. and Kruizinga, E. Wastewater management roadmap towards 2030. Technical report, Roadmap wastewater management, 2013.

Sampat, A. M., Martín, E., Martín, M., and Zavala, V. M. Optimization formulations for multi-product supply chain networks. *Computers & Chemical Engineering*, 104:296–310, 2017.

Sampat, A. M., Martín, E., Martín, M., and Zavala, V. M. Technologies and logistics for phosphorus recovery from livestock waste. *Clean Technologies and Environmental Policy*, pages 1–17, 2018.

Sampat, A. M., Hu, Y., Sharara, M., Aguirre-Villegas, H., Ruiz-Mercado, G., Larson, R., and Zavala, V. M. Coordinated management of organic waste and derived products. *Computers & Chemical Engineering*, 128:352–363, 2019.

Sanseverino, I., Conduto, D., Pozzoli, L., Dobricic, S., and Lettieri, T. Algal bloom and its economic impact. *European Commission, Joint Research Centre Institute for Environment and Sustainability*, 2016.

Santibañez-Aguilar, J. E., González-Campos, J. B., Ponce-Ortega, J. M., Serna-González, M., and El-Halwagi, M. M. Optimal planning of a biomass conversion system considering economic and environmental aspects. *Industrial & Engineering Chemistry Research*, 50(14):8558–8570, 2011.

Schuiling, R. and Andrade, A. Recovery of struvite from calf manure. *Environmental Technology*, 20(7):765–768, 1999.

Sea-Bird Scientific. Harmful Algae Blooms (HABs) available at https://www.seabird.com/harmful-algal-bloom. [Online; accessed 06-January-2020].

Sena, M., Morris, M. R., Seib, M., and Hicks, A. An exploration of economic valuation of phosphorus in the environment and its implications in decision making for resource recovery. *Water Research*, 172:115449, 2020.

Sharara, M., Sampat, A., Good, L. W., Smith, A. S., Porter, P., Zavala, V. M., Larson, R., and Runge, T. Spatially explicit methodology for coordinated manure management in shared watersheds. *Journal of environmental management*, 192:48–56, 2017.

Sharara, M. A., Runge, T., Larson, R., and Primm, J. G. Techno-economic optimization of community-based manure processing. *Agricultural Systems*, 161:117–123, 2018.

Sheriff, G. Efficient waste? why farmers over-apply nutrients and the implications for policy design. *Review of Agricultural Economics*, 27(4):542–557, 2005.

Sherlock, M. F. The renewable electricity production tax credit: In brief. Technical report, Congressional Research Service, 2014.

Sioshansi, R., Denholm, P., and Jenkin, T. Market and policy barriers to deployment of energy storage. *Economics of Energy and Environmental Policy*, 1(2):47–64, 2012.

Spash, C. L. and Vatn, A. Transferring environmental value estimates: Issues and alternatives. *Ecological Economics*, 60(2):379–388, 2006.

State of Wisconsin - Department of Agriculture, Trade, and Consumer Protection. Facts and Figures available at http://www.wisconsindairy.org/assets/images/pdf/WisconsinDairyData.pdf. 2018. [Online; accessed 28-June-2018].

State of Wisconsin - Department of Natural Resources. Wisconsin's Healthy Watersheds Assessments available at https://dnr.wi.gov/topic/watersheds/hwa.html. 2016. [Online; accessed 28-June-2018].

Stillwell, A. S., King, C. W., Webber, M. E., Duncan, I. J., and Hardberger, A. The energy-water nexus in Texas. *Ecology and Society*, 16(1), 2011.

Stumpf, R. P. and Tomlinson, M. C. Remote sensing of harmful algae blooms. In Miller, R. L., Del Castillo, C. E., and McKee, B. A., editors, *Remote sensing of coastal aquatic environments*, chapter 12, pages 277–296. Taylor & Francis, 2005.

Szabó, A., Takács, I., Murthy, S., Daigger, G., Licskó, I., and Smith, S. Significance of design and operational variables in chemical phosphorus removal. *Water Environment Research*, 80(5):407–416, 2008.

Taskhiri, M. S., Behera, S. K., Tan, R. R., and Park, H.-S. Fuzzy optimization of a waste-to-energy network system in an eco-industrial park. *Journal of Material Cycles and Waste Management*, 17(3):476–489, 2015.

Tittmann, P. W., Parker, N. C., Hart, Q. J., and Jenkins, B. M. A spatially explicit techno-

economic model of bioenergy and biofuels production in California. *Journal of Transport Geography*, 18(6):715–728, 2010.

Tomich, M. and Mintz, M. Cow power: A case study of renewable compressed natural gas as a transportation fuel. Technical report, Energy Systems Division, Argonne National Laboratory, 2017.

Topolski, K., Noureldin, M. M., Eljack, F. T., and El-Halwagi, M. M. An anchor-tenant approach to the synthesis of carbon-hydrogen-oxygen symbiosis networks. *Computers and Chemical Engineering*, 116:80–90, 2018.

University of Wisconsin-Center for Limnology. Water sustainability and climate in the Yahara Watershed available at https://wsc.limnology.wisc.edu/about/watershed. 2018. [Online; accessed 23-July-2018].

University of Wisconsin-Extension. Dairy industry contributes 43.4 billion USD to Wisconsin's economy available at https://fyi.uwex.edu/extensioninthenews/2015/01/26/dairy-industry-contributes-43-4-billion-to-wisconsins-economy-2/. 2015. [Online; accessed 13-July-2018].

U.S. Census Bureau. Quick facts: Dane County, Wisconsin. https://www.census.gov/quickfacts/danecountywisconsin. [Online; accessed 24-December-2018].

U.S. Department of Agriculture-National Agricultural Statistics Service. 2012 census of agriculture highlights: Dairy cattle and milk production. Technical report, 2014.

U.S. Department of Agriculture, U.S. Environmental Protection Agency, U.S. Department of Energy . Biogas opportunities road map: Voluntary actions to reduce methane emissions and increase energy independence. Technical report, 2014.

U.S. Energy Information Administration. Natural Gas Weekly Update available at https://www.eia.gov/naturalgas/weekly/. [Online; accessed 06-December-2017].

U.S. Environmental Protection Agency. Trading and Offsets in the Chesapeake Bay Watershed available at https://www.epa.gov/chesapeake-bay-tmdl/trading-and-offsets-chesapeake-bay-watershed. [Online; accessed 06-December-2017].

U.S. Environmental Protection Agency. Wisconsin Integrated Assessment of Watershed Health. Technical Report March, 2014.

U.S. Environmental Protection Agency. A compilation of cost data associated with the impacts and control of nutrient pollution. Technical report, 2015.

U.S. Environmental Protection Agency. Cellulosic waiver credit price calculation for 2017. Technical report, 2016.

U.S. Environmental Protection Agency. Clean Air Act Text available at https://www.epa.gov/clean-air-act-overview/clean-air-act-text. 2017a. [Online; accessed 06-December-2017].

U.S. Environmental Protection Agency. Renewable energy certificate (REC) arbitrage. Technical report, 2017b.

U.S. Environmental Protection Agency. Landfill Methane Outreach Program (LMOP) - Methane Emissions from Landfills available at https://www.epa.gov/lmop/basic-information-about-landfill-gas#methane. 2018. [Online; accessed 28-June-2018].

U.S. Environmental Protection Agency. Polluted Runoff: Nonpoint Source (NPS) Pollution available at https://www.epa.gov/nps/nonpoint-source-agriculture. 2019. [Online; accessed 13-August-2019].

U.S. Fish and Wildlife Service. 2006 national survey of fishing, hunting, and wildlife-associated recreation. Technical report, 2008.

USDA - National Agriculture Statistics Service. Milk Production and Milk Cows available at http://www.nass.usda.gov/Charts_and_Maps/Milk_Production_and_Milk_Cows. 2018. [Online; accessed 28-June-2018].

USDA NASS (United States Department of Agriculture, National Agricultural Statistics Service). 2012 Census of Agriculture. Technical report.

USDA National Agricultural Statistics Service (NASS). 2014 Wisconsin agricultural statistics. 2014.

Varbanov, P. and Friedler, F. P-graph methodology for cost-effective reduction of carbon emissions involving fuel cell combined cycles. *Applied Thermal Engineering*, 28(16):2020–2029, 2008.

Venkatasubramanian, V. *How Much Inequality Is Fair?: Mathematical Principles of a Moral, Optimal, and Stable Capitalist Society*. Columbia University Press, 2017.

Venkatasubramanian, V. and Luo, Y. How much income inequality is fair? Nash bargaining solution and its connection to entropy. *arXiv preprint arXiv:1806.05262*, 2018.

Vesterinen, J., Pouta, E., Huhtala, A., and Neuvonen, M. Impacts of changes in water quality on recreation behavior and benefits in Finland. *Journal of Environmental Management*, 91(4):984–994, 2010.

Virginia's Legislative Information System. General Virginia Pollutant Discharge Elimination System (VPDES) Watershed Permit Regulation for Total Nitrogen and Total Phosphorus Discharges and Nutrient Trading in the Chesapeake Bay Watershed in Virginia available at https://lis.virginia.gov/cgi-bin/legp604.exe?000+reg+9VAC25-820-70. [Online; accessed 05-December-2017].

Walas, S. Selection and design chemical process equipment. *University of Kansas, USA*, 1990.

Walther, G., Schatka, A., and Spengler, T. S. Design of regional production networks for second generation synthetic bio-fuel - A case study in Northern Germany. *European Journal of Operational Research*, 218(1):280–292, 2012.

Wattenberg, M., Viégas, F., and Hardt, M. Attacking discrimination with smarter machine learning. *Google Research*, 17, 2016.

Willis, K. and Garrod, G. Electricity supply reliability: Estimating the value of lost load. *Energy Policy*, 25(1):97–103, 1997.

Wilsenach, J., Schuurbiers, C., and Van Loosdrecht, M. Phosphate and potassium recovery from source separated urine through struvite precipitation. *Water research*, 41(2):458–466, 2007.

Wisconsin Department of Natural Resources. Wisconsin outdoor recreation demand. Technical report, 2011.

Wisconsin Department of Natural Resources. Phosphorus reduction in Wisconsin water bodies: An economic impact analysis. Technical report, 2012.

Wisconsin Department of Natural Resources. Wisconsin CAFO permitted operations available at http://dnr.wi.gov/topic/AgBusiness/data/CAFO/cafo_all.asp. 2017. [Online; accessed 04-February-2017].

Wisconsin Department of Natural Resources. Lake water quality report 1950 - 2017. https://dnr.wi.gov/lakes/waterquality/Station.aspx?id=133318, 2018a. [Online; accessed 21-December-2018].

Wisconsin Department of Natural Resources. Total maximum daily load for total phosphorus in the Wisconsin river basin. Technical report, 2018b.

Wisconsin State Journal. Dane County begins 'Suck the Muck' project to remove phosphorus-laden sludge from waterways available at https://madison.com/wsj/news/local/govt-and-politics/

dane-county-begins-suck-the-muck-project-to-remove-phosphorus/article_e1ea2d61-cf27-580b-afe0-5b04cc9c01d5.html. 2018. [Online; accessed 14-April-2019].

Woods Hole Oceanographic Institution. Harmful algae: Fish kills available at https://www.whoi.edu/website/redtide/impacts/wildlife/fish-kills/. [Online; accessed 01-January-2020].

Yeomans, H. and Grossmann, I. E. A systematic modeling framework of superstructure optimization in process synthesis. *Computers and Chemical Engineering*, 23(6):709–731, 1999.

Ylivainio, K. and Turtola, E. Solubility and plant-availability of P in manure. Technical report, Baltic forum for innovative technologies for sustainable manure management, 2013.

You, F. and Grossmann, I. E. Design of responsive supply chains under demand uncertainty. *Computers & Chemical Engineering*, 32(12):3090–3111, 2008a.

You, F. and Grossmann, I. E. Mixed-integer nonlinear programming models and algorithms for large-scale supply chain design with stochastic inventory management. *Industrial & Engineering Chemistry Research*, 47(20):7802–7817, 2008b.

You, F. and Wang, B. Life cycle optimization of biomass-to-liquid supply chains with distributed-centralized processing networks. *Industrial and Engineering Chemistry Research*, 50(17):10102–10127, 2011.

You, F., Wassick, J. M., and Grossmann, I. E. Risk Management for a Global Supply Chain Planning Under Uncertainty: Models and Algorithms. *AIChE J*, 55:931–946, 2009.

You, F., Tao, L., Graziano, D. J., and Snyder, S. W. Optimal design of sustainable cellulosic biofuel supply chains: Multiobjective optimization coupled with life cycle assessment and input-output analysis. *AIChE Journal*, 2012.

Zamboni, A., Shah, N., and Bezzo, F. Spatially explicit static model for the strategic design of future bioethanol production systems. 2. multi-objective environmental optimization. *Energy and Fuels*, 23(10):5134–5143, 2009.

Zavala, V. M., Kim, K., Anitescu, M., and Birge, J. A stochastic electricity market clearing formulation with consistent pricing properties. *Operations Research*, 65(3):557–576, 2017.

Zeng, L. and Li, X. Nutrient removal from anaerobically digested cattle manure by struvite precipitation. *Journal of Environmental Engineering and Science*, 5(4):285–294, 2006.

Zhang, H., Lo, V. K., Thompson, J. R., Koch, F. A., Liao, P. H., Lobanov, S., Mavinic, D. S., and Atwater, J. W. Recovery of phosphorus from dairy manure: a pilot-scale study. *Environmental technology*, 36(11):1398–1404, 2015.

Zhang, T., Bowers, K. E., Harrison, J. H., and Chen, S. Releasing phosphorus from calcium for struvite fertilizer production from anaerobically digested dairy effluent. *Water Environment Research*, 82(1):34–42, 2010.

Zillow.com. Dane county home prices & values. https://www.zillow.com/dane-county-wi/home-values/, 2018. [Online; accessed 23-December-2018].

Zlotnik, A., Roald, L., Backhaus, S., Chertkov, M., and Andersson, G. Coordinated scheduling for interdependent electric power and natural gas infrastructures. *IEEE Transactions on Power Systems*, 32(1):600–610, 2017.

Zukerman, M., Tan, L., Wang, H., and Ouveysi, I. Efficiency-fairness tradeoff in telecommunications networks. *IEEE Communications Letters*, 9(7):643–645, 2005.